SVERIGES GEOLOGISKA UNDERSÖKNING

SER. C. AVHANDLINGAR OCH UPPSATSER N:O 560

ÅRSBOK 52 (1958) N:o 3

THE MEASUREMENT OF ROCK PRESSURE IN MINES

BY

NILS HAST

Pris 15 kronor

STOCKHOLM 1958

SVERIGES GEOLOGISKA UNDERSÖKNING

AVHANDLINGAR OCH UPPSATSER

SER. C ÅRSBOK 52 (1958) N:O 3 N:O 560

THE MEASUREMENT OF ROCK PRESSURE IN MINES

BY

NILS HAST

STOCKHOLM 1958

STOCKHOLM 1939. KUNGL. BOKTRYCKERIET P. A. NORSTEDT & SÖNER

TO

MY WIFE

Contents

Preface

The determination of the pressure acting in rock has long been one of the most urgent pursuits in mining research, since herein lies the key to the problem of increasing the stability of the mine, reducing the risk of subsidence and, hence, of promoting the safety of the workers.

In building above ground, when use is made of well tried materials, such as concrete and iron, for structures in which the stresses can be reliably calculated, there is a greater degree of safety than obtains in the mines, where neither the strength of the rock nor the loads acting on the pillars or setting up stress concentrations in the walls and roof of the rooms are known or can even be measured.

With the intensified excavation of ore over recent decades the working levels have been rapidly deepened, so that the rock pressure and, with it, the risk of caving, have increased. It is necessary today to look ahead and to plan the excavation of many mines at depths that would previously never have been considered. The problems of stability are particularly great in respect of extensive orebodies, in some cases so great that very deep excavation may be ruled out. The mining engineer must under such conditions become familiar with those forces with which he will have to contend at greater depths, so as to be able to prepare a programme of excavation suited to the prevailing conditions.

Excavation at great depth is not only a source of difficulties. The rock pressure that sets so many problems as regards safety can be turned to advantage, for it can now be exploited in the excavation of the ore to an undreamt of extent. This implies economy in labour and explosives, and more efficient mining; it can thus to some degree compensate for the unavoidable increase in expenses occurred by working at greater depths.

It has hitherto been the practice to plan the excavation according to the weight of the overburden. However, it has been found during the investigations reported in this volume that in Sweden, and probably in many other parts of the world, there are great horizontal rock pressures acting in the solid earth crust. As the stress values are often many times greater than those ascribable to the vertical load at a particular point, it would appear that the horizontal pressure is not due principally to the weight of the overburden. It is probable that they are manifestations of current geologic phenomena, which disturb the stability of the solid earth crust, and which are possibly a cause of earthquakes.

By the method described for measuring stresses in rock the absolute value and the direction of action of the principal stresses can be obtained at points 20 metres or more from the rock face in a drift. It thus provides the means for

solving many important problems, such as the stress distribution in rock around shafts, drifts and other openings; moreover, an insight can be obtained into the influence of local fissuring of the rock. For the optimal planning of the excavation of a mine a knowledge of the magnitude and direction of the pressure acting in the virgin rock is essential, to avoid setting up stress concentrations that may prove destructive in their effect. Subsidence in a drift or caving of a stope roof are often ascribed to entering "bad rock", whereas the real cause is high rock pressure the existence of which was not previously realized.

The method for measuring rock pressure was first applied in 1951 in the mines of Trafikaktiebolaget Grängesberg—Oxelösund at Grängesberg. Since this date measurements have been performed in several mines in Sweden, and some of them are described in this book. A preliminary report on the subject was given as a lecture before the Swedish Mining Association in May 1957; this was published in Swedish in Jernkontorets Annaler, 1957.

These investigations have been followed with interest by the Research Committee for "Bergtryck och Bergstyrka" of the Swedish Mining Association, and I wish to take this opportunity of expressing my appreciation of the assistance received from them in initiating the work. In particular, I would thank the Chairman of the Committee, Professor Nils H. Magnusson, Head of the Geologic Survey of Sweden, who first interested me in the problem of measuring pressure in rock. From the outset he has followed the experimental work and later the measurements in the mines, offering much advice, not least on geologic matters. I also thank him for the permission to publish this book among the memoirs of the Geologic Survey.

To Börje Hjortzberg-Nordlund, a director of Trafik AB Grängesberg—Oxelösund, I am grateful for the benefit of many discussions on the problem of rock pressure as seen by a mining engineer of wide experience.

I want to thank Dr. Markus Båth of the Seismological Laboratory in Uppsala for discussions on Part Six concerning the possible relation beetween horizontal rock pressure and earthquakes.

My thanks are due to Victor Braxton for his painstaking translation of the manuscript from the Swedish.

STOCKHOLM
MARCH, 1958 *Nils Hast*

PART ONE

THE METHOD

Introduction

Faced with the problem of determining how the stress in a wall, pillar, roof or floor of a mine is changing with the progress of excavation, one might consider using a strain gauge — a wire extensometer, for instance —, which is fastened on to the surface of the rock in which the measurements are to be made. Then, if the modulus of elasticity of the rock is known it might be regarded as a simple matter to ascertain the variation in rock pressure from the changes recorded on the gauge. Unfortunately, the problem is by no means so simple. For instance, the application of the strain gauge presents great difficulty, as the high humidity in the mine may easily give rise to flow in the adhesive by which the gauge wire is affixed to the rock surface. A more serious problem is presented by the variable state of stress that normally exists in the rock surface. The excavation of the rock adjacent to these surfaces will have been performed by blasting, and some damage to the surface zone — in the form of fissures across which forces usually cannot be transmitted — will inevitable have been incurred. This has been established by comparing the values of stresses at points near to the surface and deep in the rock obtained from several hundred measurements performed in recent years by the method described below.

In theory, the excavation of, say, a drift in stressed rock sets up greatly increased stresses in the rock near to the boundary of the opening. These stress variations may be calculated from Kirsch's and Inglis' formulae for an underground opening of circular, elliptical and square sections.

However, these calculations will give no insight into the stress distribution around the drift, since a rock wall that has been fissured by blasting does not act as a homogeneous material, and therefore the fundamental condition on which the calculations are based is not fulfilled. In all stress calculations according to the theories of Kirsch and Inglis it is necessary to assume a certain stress distribution in the virgin rock — as a rule the estimated dead weight of the overburden. However, the rock pressure measurements reported here show that in many cases the weight of the overburden is rather insignificant compared with the horizontal pressure existing in the virgin rock. The reason for this is discussed in Part VI (p. 171) and is suspected to be of a geologic or seismologic nature.

If it is required to find the absolute magnitude and direction of the principal stresses[1] — for instance in a study of the stability of a mine section — the measurements must be made at such a depth that they will not be influenced

[1] The stresses in a plane through a point may be represented in magnitude and direction by an ellipse centered on that point, the axes of which are the *major and minor principal stresses*. The stress ellipsoid gives the magnitude and directions of the *three principal stresses* at the point of measurement.

by the conditions prevailing in the surface zone, which may be several metres thick. Again, the rock is seldom free from fissures, even at places unaffected by the blasting of drifts or shafts. Stress measurements at depth have revealed sudden stress fluctuations in the vicinity of such partings. A determination of the prevailing rock pressure for a particular region requires measurements at a sufficiently large number of points along one line to enable the local effect of the fissures to be distinguished. It is therefore of vital importance that the measuring technique used should enable stresses to be recorded at points deep in the solid rock.

Description of the method[1]

Reference is made to Fig. 1 a and 1 b.

Into the rock face a hole approximately 26 mm in diameter is drilled so as to pass through and beyond the point at which the stress is to be determined. A specially designed measuring cell *c* is placed in the required position in this hole and pre-stressed to a suitable value, which is recorded.[2] Co-axial with the hole containing the cell — the cell hole — a circular channel *g* is cut (Fig. 1 a). This is taken far enough beyond the cell *c* for the material of the rock core *d* so formed to be rendered stressless at the point of measurement by virtue of its elastic expansion. The load on the cell will then be reduced simultaneously. The difference between the original load on

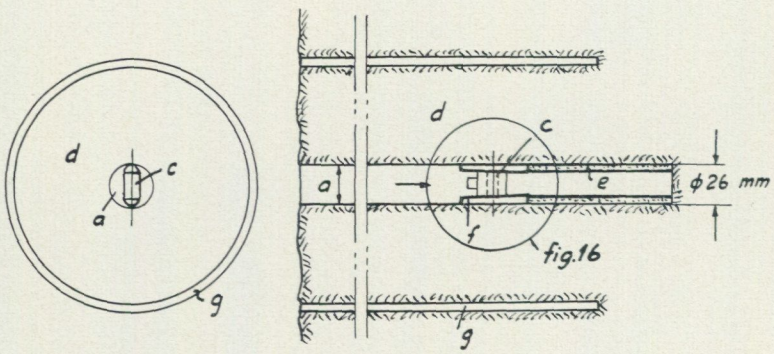

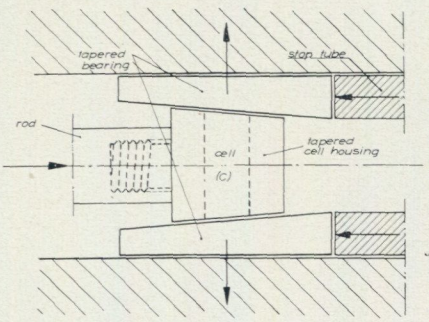

Fig. 1 a. The cell *c* in the cell-hole *a* around which the concentric stress release channel *g* has been cut.

Fig. 1 b is a detail of Fig. 1 a showing how the cell is pre-stressed according to the earliest method. The cell *c* in its housing has been inserted into the cell hole *a* until the forward motion of the tapered bearings *f* is arrested by the tubular stop *e*. The cell housing, also tapered, acts as a wedge and as it is pressed forward the cell is stressed by virtue of the normal force of reaction exerted by the bearings *f*. As the stress release channel *g* is cut, the stress in the cylindrical rock core so formed is gradually released, and with it a fraction of the load on the cell.

[1] The method described below is in principle the same as that detailed in the Swedish Patent No. 151,797 and the South African Patent No. 19,559 entitled *Method and device for measuring stresses and deformations in solid loaded materials.*

[2] The term *pre-stress* is employed here to denote the load applied to the cell prior to cutting the stress release channel, as described below.

the cell and the last value read off on completion of the stress release channel represents the absolute value of the stress acting in the rock around the cell hole. It is assumed that there is no appreciable stress remaining in the rock cylinder when the drilling is complete. Though this assumption is not always entirely justified, it can be demonstrated by practical tests that the error is extremely small. The cell records the stress in a plane perpendicular to the axis of the cell hole. It may be added that the stress field parallel to the axis also exerts some influence on the reading, a problem that is discussed later on.

By placing cells in three directions in the plane of measurement three values are obtained from which can be calculated the magnitude and direction of the principal stresses acting in the rock at the point, and in the plane, of measurement. In a homogeneous pillar, where one of the principal stresses is known to act parallel to the long axis of the pillar, it is sufficient to measure in the vertical and horizontal directions, the cell hole being perpendicular to the face. The principal stresses in three dimensions — the stress ellipsoid — may also be determined at a point in the rock, but then three holes, drilled in different directions are required. However, it is often possible to find the dominating stresses with sufficient accuracy by measurements in one vertical hole and one horisontal.

In certain cases it may be of interest to follow the stress changes in rock pillars or walls during the course of excavation without needing to know the absolute values of the stresses. The measuring procedure is then as described above except that the stress release channel *g* is not cut at all, or at least not until the existing stress fluctuations have been recorded. By cutting the channel the correction value is obtained by means of which the recorded stress fluctuations can be converted to absolute values. There is a risk that the rock will undergo plastic deformation, with consequent distortion of the results, especially when the gradual changes in the rock pressure are to be followed over a long period and when the stresses in the rock are high. Such errors may occasionally be avoided to some extent, however, by taking special measures. In any case, it would appear advisable to make absolute determinations from time to time so as to obtain a more reliable picture of the long-term stress fluctuations in the mine.

Finally, it is difficult to obtain sensitive stress recording instruments of which the calibration and the properties can be relied upon over such long periods — some years, even — as are sometimes necessary. The cells used in the method in question have no moving parts and the coil is cast entirely in material that is watertight, so that there is little risk of long-term changes of the type described.

Equipment

As far as the author is aware, no recording of absolute stress values, measured deep in the rock at a single point, has hitherto been made in a mine. As may be expected, therefore, the work in the earlier stages was somewhat experimental in character. Nevertheless, if the method of to-day is compared with that as it was first practised in Grängesberg (1951), it is seen that there has been no essential change either in the mensuration procedure or in the method of calibrating the cells. On the other hand, certain details such as the shape of the cells and the manner in which they are pre-stressed have been developed over the years so as to provide for greater ease in manipulation and higher accuracy in recording the stresses. For instance, the drilling of the stress release channel around the cell hole was earlier performed by means of a pneumatic rock drill, whereas to-day a diamond drill is used (pp. 17 and 19).

The cell

DESIGN

The pressures are recorded on the principle of magnetostriction.

The equipment comprises a cell and a recording unit. The cell consists of a nickel alloy spool (Fig. 2 a) 10 mm long; the diameter at the widest part

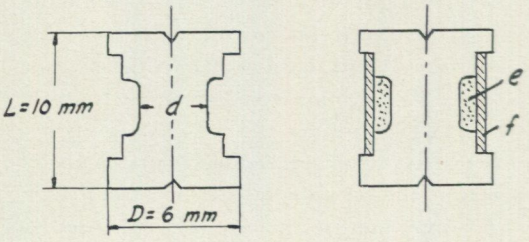

Fig. 2 a. The nickel cell spool and the spool with windings *e* and screen *f*.

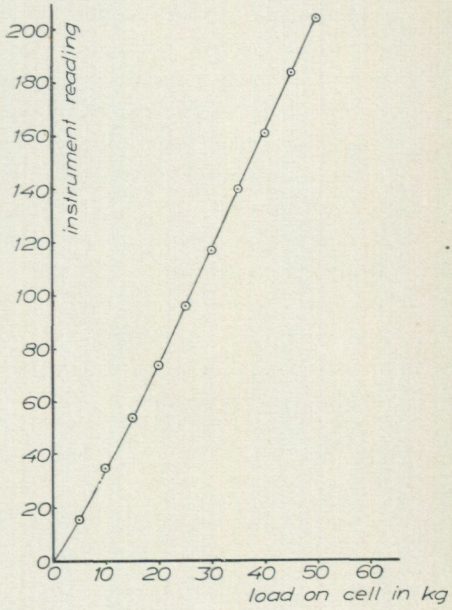

Fig. 2 b. The calibration curve of a cell.

is 6 mm and at the narrowest part, *d*, 2.5—3 mm. By varying *d* the elasticity of the cell may be changed. The external magnetic field is confined by a screen of permalloy *f*.

If a pressure is applied to the cell parallel to its axis the magnetic permeability of the nickel alloy is altered, and with it the impedance of the coil. If an alternating current is passing through the coil there is a fall in potential across it. By applying known loads to the cell a calibration curve may be drawn (Fig. 2 b). This curve is then used to convert the instrument readings to rock pressures. The cells are generally mounted in a housing of brass, aluminium or some other metal, so that fairly great loads can be applied in the pre-stressing of the cell without incurring a risk of overloading it (Figs. 3 a and b).

PRE-STRESSING PROCEDURE — FORMER SYSTEM

The cell housing has one pair of sides slightly tapered — the pair almost perpendicular to the axis of the cell (Fig. 3 a). On each of these sides is placed a metal strip — a bearing —, which is also tapered so that the cell housing and its two bearings form a unit with parallel sides. This is inserted into the cell hole by means of a special rod (Fig. 1 b). Near the bottom of the hole the bearings encounter a stop in the form of a metal tube, and their forward motion is arrested. On applying pressure to the cell housing by means of the metal rod, the housing, which acts as a wedge, is compressed by the stationary bearings. The compressive force is transmitted to the cell, which is thus pre-stressed to the required value.

The accurate orientation of the cell in the required direction of measurement may be checked by means of an indicator on the rod.

During pre-stressing the cell housing and the bearings are subjected to frictional forces acting between the contact surfaces of the housing, the bearings and the rock face. These frictional forces distort the cell readings to some extent, but the error can be kept low, provided that the pre-stress value is so high that an appreciable fraction remains after the release channel has been drilled.

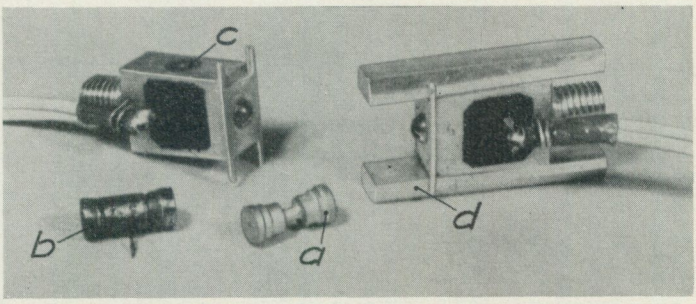

Fig. 3 a. The earlier model of cell, housing and bearings. *a* the nickel spool; *b* complete cell; *c* cell in housing; *d* one of the tapered bearings in place.

PRE-STRESSING PROCEDURE — PRESENT SYSTEM

It was found necessary in the Grängesberg mine to determine the magnitude and direction of the principal stresses at a considerable depth from the rock face. For making such deep measurements the new housing and the insertion and pre-stressing apparatus shown in Figs. 3 b and 4 a—b were designed. Fig. 3 b shows the housing, and Fig. 4 b the instrument for inserting and pre-stressing the cell, as it was developed during the mensuration work in the Grängesberg mine. The cell can be inserted, set at the required angle, and pre-stressed at the required depths with a high degree of precision. Measurements have hitherto been made at 15 metres, but even deeper recordings are possible with this new equipment.

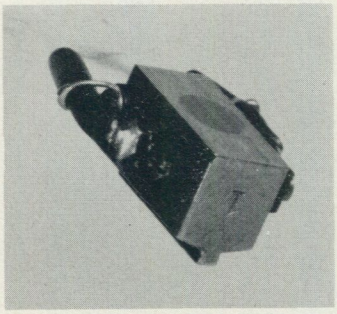

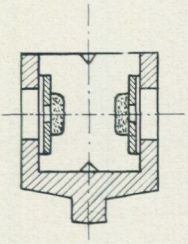

Fig. 3 b. The new design of the cell housing. One bearing and the housing are cast as one piece.

Fig. 4 a shows the cell, the T-shaped bearing and the three-part wedge system by means of which the cell is pre-stressed when it has been inserted to the required depth and set in the desired direction of measurement in the measuring plane perpendicular to the axis of the cell hole. By designing this apparatus that will enable a greater fraction of the pre-stress load on the cell to be used than in the earlier method the range of action of the cell has been widened. In the system devised the frictional forces set up on pre-stressing the cell unit act entirely within the three-part wedge system and do not load the cell, housing, bearing or hole wall.

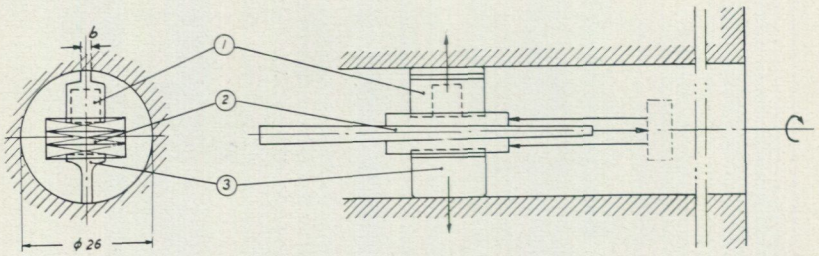

Fig. 4 a. Pre-stressing principle. (1) the cell; (2) the three-part wedge system; (3) bearing The stress is applied normal to the hole wall by rotation of a crank situated outside the cell hole. Arrows show how the frictional forces are confined to the wedge system and have no influence on the cell housing and bearing.

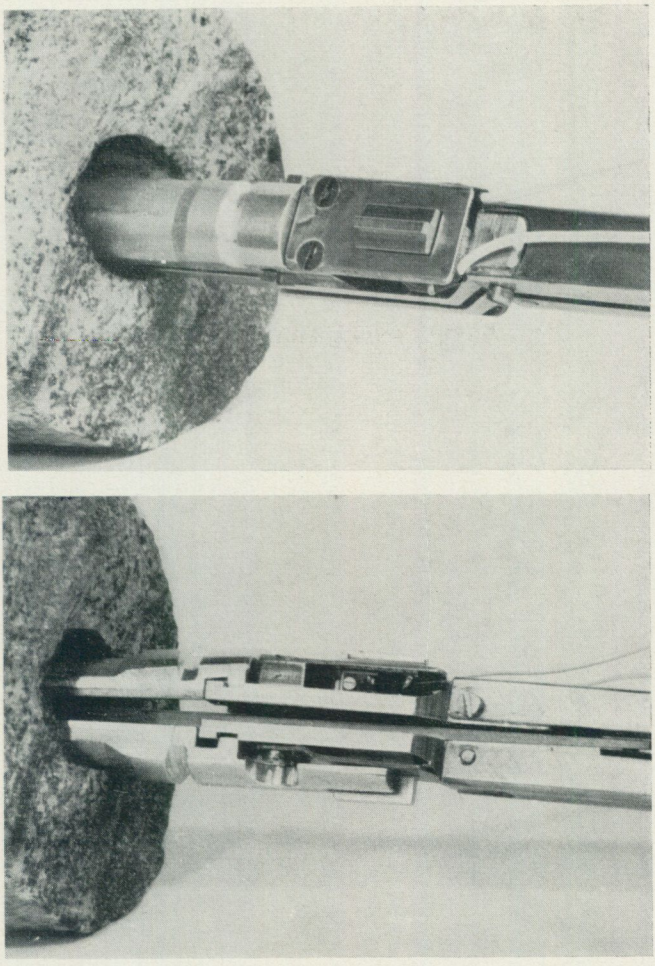

Fig. 4 b. The new arrangement for insertion and pre-stressing of the cell unit.

In the new model the housing is designed as one piece with one of the bearings, the cell being situated in a recess in the housing (Fig. 3 b). The other bearing is T-shaped. The taper of the three-part wedge system is such that it forms a parallel body. The wedges, the contact surfaces of the bearing and the housing against the wedges are precision ground.

In a recent form the T-shaped guide in Fig. 4 a can be replaced by a housing containing a measuring cell. The magnitude of the stress is then read with the aid of two cells, but the range of measurement decreases.

CALIBRATION

For the calculation of the magnitude and direction of the principal stresses directly from the values recorded by the cell it is necessary for this to be calibrated. This is performed in special prisms, and constitutes an essential

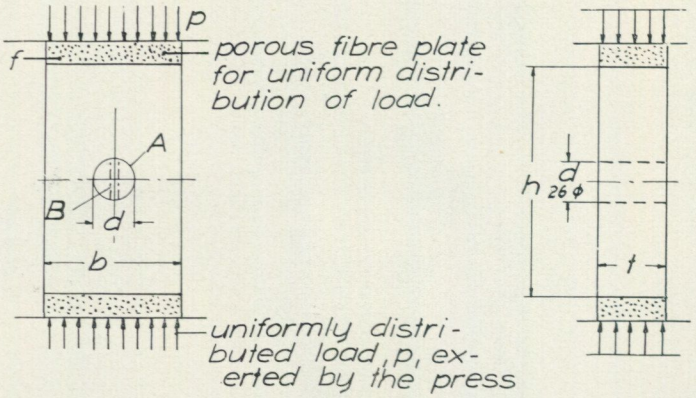

Fig. 5. The calibration prism, placed in a press, is acted on by a uniformly applied load p through friction-eliminating porous fibre plates f. The cell is inserted in the hole A and pre-stressed. The pressure p is then gradually reduced, the resulting decrease in the cell load being noted. A calibration curve is thus constructed for the cell unit in the prism or in a material of the same rigidity as the prism.

part of the mensuration procedure, greatly simplifying the calculations and increasing the accuracy of the stress determinations.

The prisms are of metal — steel, brass or aluminium, for example — or of rock of the type in which the stresses are to be measured. Fig. 5 shows such a prism. The hole A has a diameter d equal to that of the cell hole — that is, 26 mm. In the case of rectangular prisms the width b is equal to the diameter of the rock core.

The prism is placed in a press and a pressure p is applied uniformly to the end surfaces of the prism through porous friction-eliminating wood-fibre plates. The cell B in its housing is then inserted so that its direction of measurement is parallel to the axis of the prism and thus to the force p, after which the required pre-stress is applied. The load applied by the press is then reduced in steps, readings of the cell being taken until the original pre-stress load on the cell has fallen to the lowest level desirable. A calibration curve for the measuring unit in the prism is then drawn, one of the axes representing the load applied to the prism and the other the corresponding value recorded by the cell (Fig. 20).

The material of which the prism is made should have approximately the same modulus of elasticity as the type of rock in which the apparatus is to be used. Otherwise a correction must be made for the difference in elasticity. If this is small the corrections will also be small; where the discrepancy is large the correction is easily derived from curves obtained by calibrating the cell in prisms of two or more different moduli. The correction may also be calculated theoretically, but this is a more laborious procedure.

The stress release channel

Two methods have been used for drilling the stress release channel: (*a*) the seam-boring technique, with a pneumatic rock drill and (*b*) the diamond drilling technique.

SEAM-BORING TECHNIQUE. This was used in the early days. It was evolved during preliminary tests at Kantorp, Atlas Diesel's test room in Stockholm, and at Grängesberg, and used for practical work at Grängesberg and Laisvall.

The essential of this procedure is that the stress release channel is formed by drilling a series of slightly overlapping holes in a circle so that the rock cylinder so formed is completely separated from the surrounding rock, except, of course, at the end of the cylinder (Fig. 7). The diameter of the core is 20 or 30 cm, according to whether the rock has a high or a low tensile strength. The holes are drilled in turn to a distance 20 to 30 cm past the cell. The last of the holes having been cut, the absolute value of the stress at the measuring point and in the direction of the cell is obtained as the difference between the figure for the cell in its original pre-stressed state and the figure on completion of the drilling. It is interesting to study the variation in the stress in the rock core as each new hole is drilled (Fig. 6). By applying three cells in different directions in the cell hole, a few centimetres apart, it is possible to calculate the principal stresses, though only approximately as the measurements are not made at the same point.

It might be added that when the cell hole is bored with an ordinary pneumatic drill the surface must be ground smooth. This is done with a diamond reamer.

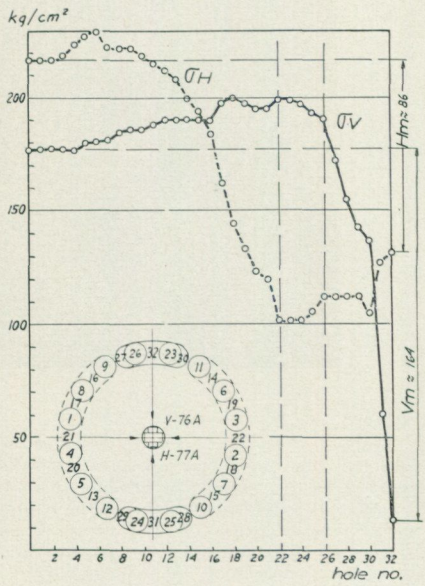

Fig. 6. Variation in vertical σ_V and horizontal σ_H stresses recorded by two adjacent and mutually perpendicular cells as the stress release channel is being cut by the seam-drilling procedure. The figures in the core indicate the order in which the holes were cut. The steep rise near the end of the curve for σ_H is due to the lateral contraction of the core with the rapid variation in σ_V; as the cutting of the stress release channel is completed V_m and H_m are the recorded stress values.

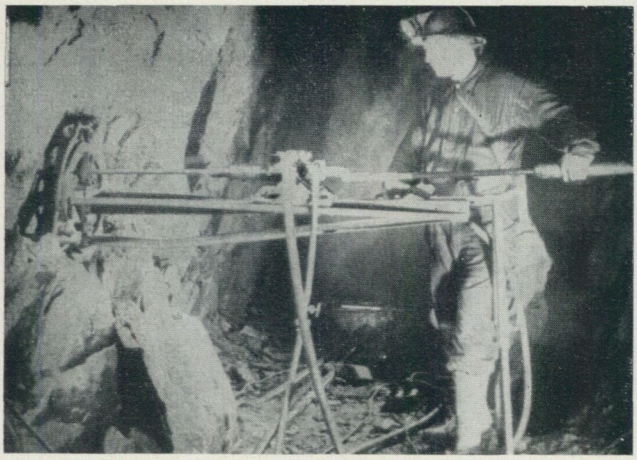

a

b

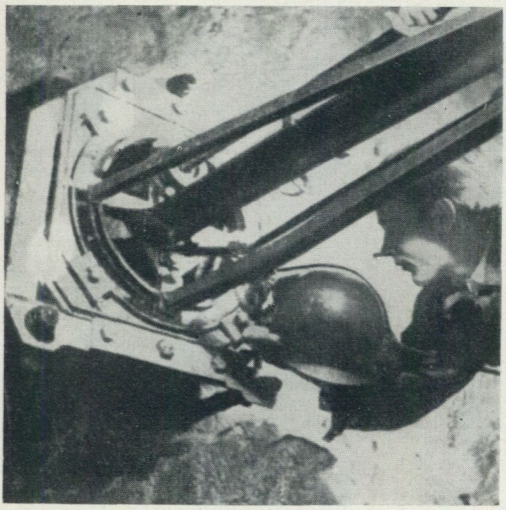

c

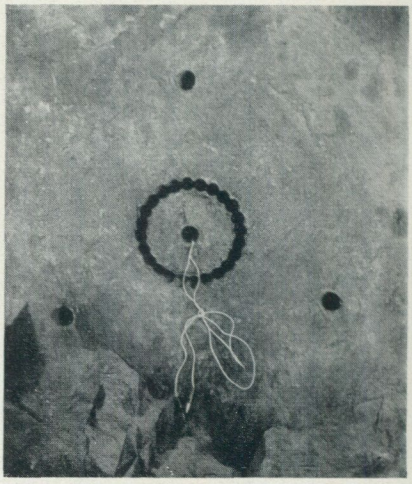

d

Fig. 7. The seam drilling apparatus. (a) The tripod support is fastened perpendicular to the rock face. The support may be rotated about its axis, and the angle read off on a scale. An ordinary pneumatic drill is used; this slides along one leg of the tripod. (b) Drilling in roof. (c) A modified form of apparatus with the possibility of lateral adjustment of the boring equipment in any direction. It is thus possible to bore a rectangular seam. (d) The stress release channel completely drilled around the cell hole. To ensure that the holes are parallel and contiguous, when one hole is being drilled an iron bar is placed in the adjacent one.

Fig. 8. The diamond drilling apparatus now exclusively used.

DIAMOND DRILLING TECHNIQUE. This procedure gives a continuous channel just as the seam-boring, though it is not drilled out as a series of holes, but gradually deepened with a circular cut. Fig. 8 shows the diamond drilling apparatus and Fig. 9 (b) the cell hole with a measuring unit. In this process the core is gradually rendered stressless as the channel A (Fig. 9 b) is deepened. The cell hole is drilled up to half a metre in advance of the channel, this being the maximum distance for which centering of the drill has been found to be sufficiently accurate. The cell is advanced in stages of 8—10 cm to positions, at which it is set in series at three different angles. The stress release channel is deepened at each stage until no further change in the load on the cell is recorded. After 3 or 4 measurements the cell hole is drilled a further half metre or so and the whole procedure repeated. If the rock pressure should be too high or the rigidity of the rock unusually low, the normal range of measurement of the cell may be insufficiently great; the cell can then be pre-stressed again during the drilling of the core. After this supplementary pre-stressing, the value of which is noted, the drilling of the stress release channel and the recording of the stress may be resumed.

If the supplementary pre-stressing is not necessary a series of cells may be inserted at one time at suitable distances along the hole. These cells are all pre-stressed and the complete stress release channel can then be drilled without interruption, the pre-stress on the cells being recorded during the drilling.

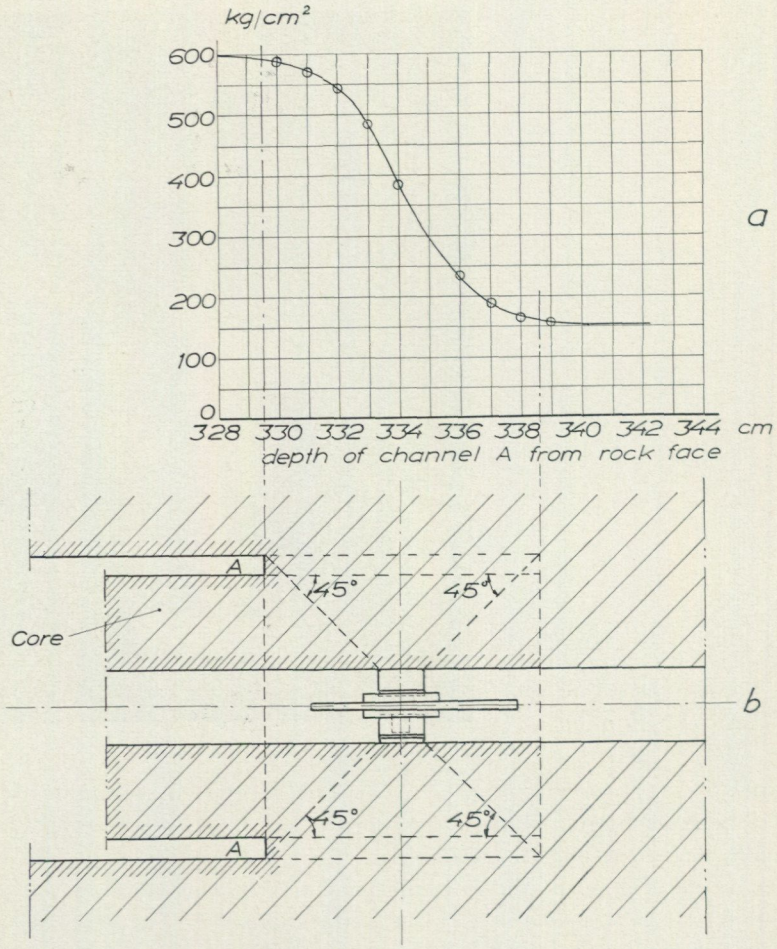

Fig. 9. (a) shows the variation in rock pressure recorded by the cell as the stress release channel is being cut by the diamond-drilling procedure; (b) is a longitudinal section through the measuring hole and the core being cut. The cell begins to record changes in the stress when the bottom of the channel is 4—5 cm from the cell, and the variation almost ceases when it is 4 cm beyond the cell.

Fig. 9 (a) reproduces the cell readings obtained during an actual diamond drilling operation. The cell is placed at a depth of 334 cm in the cell-hole drilled in a rock wall. Co-axially with the hole the stress release channel *A* is cut with a diamond bit, which thus gradually approaches the point where the cell is located. When the stress release channel has reached a depth of 329 cm from the rock face, the cell has a pre-stress value of 600 kg/sq. cm. The nearer to the cell the channel then approaches the lower does the pre-stress value fall as, during the cutting of the channel, the stress in the rock around the cell hole is gradually released. At 334 cm the cell is passed, but only when the channel front has passed the cell by about 5 cm — that is, at 339 cm — does

the value recorded by the cell remain constant. For a stress determination a total drilling distance of 339 — 329 = 10 cm — approximately the diameter of the core in this test — is required. The stress concentrations at the bottom of the stress release channel are thus distributed at an angle of about 45° to the axis of the hole.

In the diamond drilling technique there are no large temporary increases in stress of the magnitude of those set up during the seam drilling; the diameter of the cylinder can therefore be reduced; standard diamond bits with an external diameter of 101 and 140 mm are suitable, these giving core diameters of about 87 and 132 mm, respectively. As a rule the smaller one is used.

Determination of principal stresses

Calculations

A hole is drilled in the stressed rock, its diameter being small in comparison with the extent of the stress field. A cell is inserted to a certain depth in the hole and pre-stressed so that it thrusts against diametrically opposite points in the wall. The shape of the hole changes elastically with the variation of the stress in the rock. (This may occur rapidly, as during the cutting of the stress release channel, or slowly, as when the stresses in the rock itself change — for instance, during progressive excavation in the mine.) As the hole changes in shape, the load on the pre-stressed cell varies and the values are read off.

Suppose that in the unstressed rock there is a circular hole of radius a (Fig. 10 a). If a uni-axial state of tensile stress is set up in the direction $A - A$ by means of an evenly distributed load the hole becomes elliptical. When the load is removed the hole reassumes its circular form. If a cell is placed in the hole while a load p is applied, and if the cell is pre-stressed so as to thrust against diametrically opposite points of the hole — f_1 and f_2 — on changing the load p the cell will register the resultant change in deformation of the hole in the direction $A - A$; in practice this occurs when the channel is cut round the cell hole in stressed rock. If the rock is in a state of compressive stress, the load on the cell is reduced, while if the rock is under tension the stress in the cell is increased.

A stress field of unknown magnitude and direction, but which is assumed to lie in the plane of the figure — that is to say, in a plane perpendicular to the axis of the cell hole, — may be resolved into two perpendicular components A—A and B—B. In the event of a change in the state of stress in the rock a cell that is set in an arbitrary position in this plane will record the sum

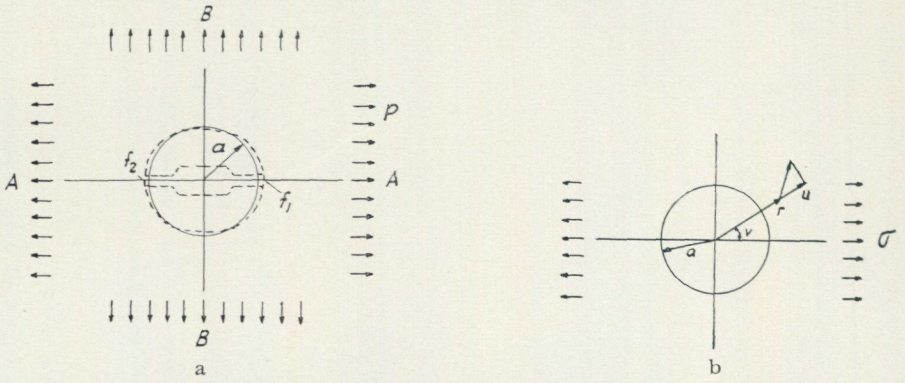

Fig. 10. (a) The stress field around a circular opening in an elastic material. A cell is placed in the hole while the material is being stressed. (b) The deformation around a circular opening in an elastic material having a uni-directional stress field σ.

of the corresponding deformations due to the component fields A and B. By placing cells in three directions in the plane of measurement the unknown stress field may be determined from the formula given below. The absolute values of the stress are obtained if the field of stress is completely released, as occurs in the case of the drilled-out core. It is possible to record changes occurring in the unknown stress field over a period simply by observing the variation in the readings of the three cells. As the cells used have no moving parts whose function may deteriorate with time, they are suitable for long-term observations. Such a form of observations may be of value where it is required to follow expected gradual changes in the stress field, say in a particular part of the rock in a mine. It may be mentioned, however, that when the observation time is very long it is preferable to make absolute determinations of the rock pressure at definite intervals, from which the stress field variations are directly evident.

The solution of the problem of the disturbed state of stress about a single opening of circular cross-section situated in a field of uniform stress is ascribed to Kirsch, and may be presented in the form:

$$\sigma_r = \frac{\sigma}{2}\left\{\left(1-\frac{a^2}{r^2}\right)+\left(1-\frac{a^2}{r^2}\right)\left(1-\frac{3\,a^2}{r^2}\right)\cos 2\,v\right\}$$

$$\sigma_v = \frac{\sigma}{2}\left\{\left(1+\frac{a^2}{r^2}\right)-\left(1+\frac{3\,a^4}{r^4}\right)\cos 2\,v\right\}$$

$$\tau_{rv} = -\frac{\sigma}{2}\left(1-\frac{a^2}{r^2}\right)\cdot\left(1+\frac{3\,a^2}{r^2}\right)\cdot\sin 2\,v$$

where σ_r is the radial stress,
σ_v tangential stress,
τ_{rv} shearing stress,
r the distance from the centre of the hole to a given point in the material,
a the radius of the hole,
and v the angle between the direction of the stress field and the direction of measurement.

From these formulae the state of deformation in the rock around the hole may be determined (Fig. 10 b). As a particular case, consider the radial deformation u of the wall of the hole — that is, the deformation recorded by the cell — if the modulus of elasticity of the cell material is taken as zero.

The radial deformation u is given by the expression

$$u = \frac{a\cdot\sigma}{E}(1+2\cos 2v)$$

E is Young 's modulus of elasticity for the material in which the hole is drilled.

If the rock in the immediate vicinity of the hole is acted on by two mutually

perpendicular unidirectional stresses such as the components of an unknown field (Fig. 10 a), the radial deformation

$$u = (\sigma_1 + \sigma_2)\frac{a}{E} + (\sigma_1 - \sigma_2)\frac{2a}{E} \cdot \cos 2v$$

where σ_1 and σ_2 are the required principal stresses of the field, and v is the angle between the direction of the principal stress σ_1 and the direction of measurement. Three measurements of u in different directions, whose angular relationship to each other is known, are sufficient for the solution of the equation.

Consider three such values of u recorded, by the cell unit. Choice of 60° or 45° as the angles between the three directions of measurement gives a simple expression for σ_1 and σ_2, and for the angle that the principal stress σ_1 makes with an arbitrary direction, from which the angle v can then be determined for each of the three directions of measurement. It is often of value to choose one of the directions of measurement as this arbitrary direction.

As the cells are to follow closely the deformations in the surface of the cell hole due to stress fluctuations in the material in which the hole is drilled the pre-stress value should be so high that it will not have vanished when the stress in the surrounding core is completely released. Should it be found while the stress release channel is being cut that the stresses at the point of measurement are higher than, or nearly equal to, the pre-stress value of the cell, the drilling may be suspended while the cell is subjected to a supplementary "pre-stress". The same procedure may be followed in cases where the stresses are higher than the value to which the cell may safely be pre-stressed.

The load applied to the cell results in a deformation not only at the points of contact f_1 and f_2 of the cell with the wall (Fig. 10 a) but also deeper in the rock around the cell hole. When, on account of change in the state of stress in the rock, the shape of the hole, and consequently the cell stress, are altered, the contact pressure at f_1 and f_2 also varies, this in turn giving rise to local deformation in the wall around these points. The cells are consequently not acting purely as deformation gauges but rather as stress metres, a fact that complicates the calculation. Account must be taken of the elasticity of the cell itself and of the secondary elastic deformation due to the contact pressures at f_1 and f_2.

This latter component may be calculated from Boussinesq 's formulae for the case when the contact surfaces at f_1 and f_2 are circular.

In addition to the above-mentioned virtue of being able to work with sufficiently large pressures at f_1 and f_2, a stress measuring gauge has the further advantage over the deformation gauge that the measuring system is less sensitive — that is to say, smaller corrections are required — where the elasticity of the material of the calibration prism is not the same as that of the actual rock around the drill hole.

Calibration of the cells in a special prism (p. 16) avoids these difficulties of calculation and simplifies the whole technique, as the deformation of the

cell and depression of the wall by the cell are automatically taken into account in the calibration procedure. By using calibration prisms of material having roughly the same modulus of elasticity as the rock in which measurements are to be made, and by making the hole the same diameter as it would be in practice, both a and E are eliminated from the above formula for u. It is then possible, moreover, to select a suitable value for the elasticity of the cell in the individual case, without the need for involved calculations of the deformation. Where a large range of measurement is required — as, for example, in the case of very high stresses in the rock, or when its modulus of elasticity is low, — the elacticity of the cell must be low. On the other hand, where a high degree of accuracy is desired, cells of greater rigidity may be used. However, as mentioned above, these objects may also be achieved by "pre-stressing" the cell again in the course of the actual mensuration procedure. This latter approach has the virtue of still allowing sensitive cells to be used while recording a state of stress over a large range.

The described method for measuring rock pressure and the associated calibration procedure greatly simplify the calculation of the stresses from the recorded values. If the moduli of elasticity for the calibration prism and the rock in which the stresses are being determined are equal very simple formulae can be derived. The following formulae are valid where the angles between the direction of measurement are 60 and 45°.[1]

Angle of 60° between directions of measurement

$$\sigma_1 = \tfrac{1}{2}\left\{\sigma' + \sigma'' + \sigma''' + \sqrt{\tfrac{1}{2}\left[(\sigma' - \sigma'')^2 + (\sigma'' - \sigma''')^2 + (\sigma''' - \sigma')^2\right]}\right\}$$

$$\sigma_2 = \tfrac{1}{2}\left\{\sigma' + \sigma'' + \sigma''' - \sqrt{\tfrac{1}{2}\left[(\sigma' - \sigma'')^2 + (\sigma'' - \sigma''')^2 + (\sigma''' - \sigma')^2\right]}\right\}$$

$$\tan 2\,\omega = \sqrt{3} \cdot \frac{\sigma'' - \sigma'''}{2\,\sigma' - (\sigma'' + \sigma''')}$$

Moreover,

$$\frac{\sin 2\,\omega}{\sigma'' - \sigma'''} > 0$$

Angle of 45° between directions of measurement

$$\sigma_1 = \tfrac{3}{4}\left\{\sigma' + \sigma''' + \sqrt{\tfrac{1}{2}\left[(\sigma' - \sigma'')^2 + (\sigma'' - \sigma''')^2\right]}\right\}$$

$$\sigma_2 = \tfrac{3}{4}\left\{\sigma' + \sigma''' - \sqrt{\tfrac{1}{2}\left[(\sigma' - \sigma'')^2 + (\sigma'' - \sigma''')^2\right]}\right\}$$

$$\tan 2\,\omega = \frac{2\,\sigma'' - (\sigma' + \sigma''')}{\sigma' - \sigma'''}$$

Moreover,

$$\frac{\cos 2\,\omega}{\sigma' - \sigma'''} > 0$$

σ', σ'', and σ''' denote the recorded cell values in three directions, where the angles between σ' and σ'' and between σ'' and σ''' are 60° (45°); ω denotes

[1] The simple form of these expressions has been derived in collaboration with Dr. Jan Hult.

the angle between the direction of the major principal stress σ_1 and the arbitrary direction of reference for the three directions of measurement.

Where there is an appreciable disparity between the moduli for the calibration prism and the rock in which the stresses are recorded it is necessary to apply a correction to the principal stress values calculated from the recorded figures. The approximate magnitude of the correction may be given by calibration of a cell in prisms of different moduli, say E_0, E_1 and E_2. A particular instrument reading will then correspond to different loads on the calibration prism, depending on which of the three moduli applies. The same load on all the prisms will give different instrument readings with the cell in question. If the cell calibrated in an E_0 prism is used in rock of modulus E_m, sufficiently accurate corrections may readily be made if it is known how much higher or lower the cell has been recording in the E_1 and E_2 prisms than in the E_0 prism, E_1 and E_2 not differing greatly from E_m.

Another method is to perform a theoretical calculation of the elasticity of a system comprising the cell unit and the secondary deformations in the wall at the points of contact of the cell unit. It is then possible to derive the change in deformation that will result from a change in the value of the rock modulus, and hence to estimate the magnitude of the correction for such cases where the cell is calibrated in a prism of modulus E_0 but applied in rock of modulus E_m. These calculations are, however, fairly complicated, and require a hypothetical stress distribution in the zone of contact between the cell guides and the wall of the hole. However, such calculations may be of value as a means of ascertaining how the variation in the elasticity of the cell unit influences the range of measurement and the sensitivity of the cell, compared with the variations in the modulus of the rock. See also page 34.

The assumption on which the formulae are based — namely, that there is a state of plane stress perpendicular to the axis of the hole — is valid with certainty only at the surface, and is approximately true for shallow holes. In the case of deeper holes, where a compressive or tensile stress may be assumed to be acting parallel to the axis of the hole, deformation or stress gauges should also be applied at several points within the hole so as to record the stress fluctuations in the rock core in an axial direction while the stress release channel is being cut. The design of these stress and deformation meters for use in holes 26 mm in diameter presents considerable, though evidently not unsurmountable, problems; such types have been tested in the laboratory and in the mines with success, though there is still room for improvement of their reliability. The axial deformation of the core between two points might be recorded simultaneously with the normal pressure at the two points.

In the evaluation of the rock pressure at a point, say several metres deep in a drift wall, it is essential to know the shearing stress at the point in question. In view of the low shearing and tensile strength but high compressive strength of rock, it is of interest to know that the magnitude of the stress along the axis of the hole does not affect the shearing stress in the plane of measurement. On the other hand, the principal stresses increase in the plane of measurement

perpendicular to the axis approximately by $\frac{1}{2}\nu \cdot \sigma_v$, where ν is Poisson's ratio and σ_v the axial load that must be applied to the rock core in a press (with the special gauge measuring in the axial direction in place) in order to record a stress variation of the magnitude occurring in the core during the complete cutting of the stress release channel.

In order to get full information of the general pressure distribution in the virgin rock in a mine the *stress ellipsoid* has to be determined at a point far below the working zone. The ellipsoid can be determined by drilling 3 adjacent measuring holes in different directions. When all the holes are at right angles to each other rather simple formulae for the magnitude of the three principal stresses and their directions can be derived, as well as for the shearing stresses and the directions of the planes along which these are acting. In most cases the 3 holes can be drilled from the end of a drift. The depth of the holes must be so great that the local influence of the drift upon the virgin rock pressure distribution at the point of measurement can be neglected.

From the 3 measuring holes we get 9 recorded stress values located in 3 planes the stress ellipses of which are determined by those values. However, only 6 values from the 3 holes are necessary for the determination of the stress ellipsoid. The 3 further values enable the accuracy of the stress ellipsoid measured to be determined.

Furthermore, in this way by drilling 3 holes and using only the standard cell unit (p. 14), it is not necessary to develop and use any instruments measuring the axial deformation of the core as was described in principle on p. 26.

Interpolation diagram for stress measurement at a point

It has been shown that, in the case of an unknown stress field acting in a plane, it is necessary to measure the stresses in three directions at a point in order to determine the magnitude and direction of the principal stresses at that point. Since this procedure is not practicable, the cell always occupying some space, however small it may be, it is necessary to take readings at three points some distance apart to get the principal stresses. This will inevitably introduce a factor of uncertainty. However, the stresses may be calculated fairly accurately from an interpolation diagram such as that reproduced in Fig. 11.

One advantage of diamond drilling over seam boring in rock pressure determinations is, as mentioned above, that the stress can be determined at a succession of points in the cell hole less than 10 cm apart. The deep bore hole thus offers the advantage of a large number of measuring points. The direction of the cell is varied from point to point so that three series of stress values are obtained, corresponding to the three required directions, which may be conveniently chosen at angles of, say, 45 or 60° to one another. In Fig. 11 the depths at the measuring points from the rock face are the axis of abscissa, while the stress values recorded are the ordinates. The values relating to each of the three directions are joined by smooth curves, from which stress values for one particular depth may be obtained in the three

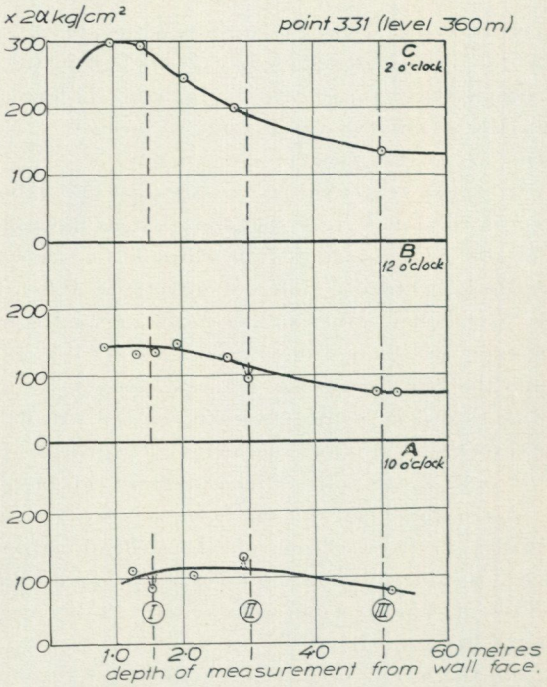

Fig. 11. Variation of rock pressure with depth at point 331 at the 360 metre level at Grängesberg. The three curves *A*, *B* and *C* relate to the three directions of measurement at angles of 60°. The broken lines indicate sections at depths of 1.5, 3 and 5 metres. This interpolation diagram is of value in calculation of the magnitude and direction of the principal stresses.

directions by interpolation. The broken lines I—III denote three such depths, and their intersections with the stress curves give the stress values for the depth in question. From these values the magnitude and direction of the principal stresses are calculated. However, since the cells in the example were calibrated in prisms of material of modulus 2,100,000 kg/sq. cm and the rock (leptite) in this case had a modulus, E_m, of 600,000 kg/sq. cm the recorded values must first be multiplied by the factor $\alpha = 0.37$. This quantity, α, is primarily dependent on the values of E_m, correction being made for the elasticity of the cell, and the form of its surfaces in contact with the cell-hole wall. See discussion on pages 35—47.

In order to reduce the discrepancy between the recorded values entered in the diagrams and the stress values calculated from them, the recorded values have been reduced in Fig. 11 and in all such diagrams in Parts II-IV by the factor $\frac{1}{2}$ but simultaneously the factor α on the ordinate axis has been changed to 2α. The factor 2α does not deviate much from unity for rock of high or rather high strength.

As a rule, the 60° system has been adopted in practice, with one direction vertical and the two others making an angle of 60° with it. In the reports and diagrams the directions of measurement are referred to as the *A*, *B* and *C* directions. The *B* direction is vertical in wall measurements, and parallel to the drift in roof measurements. In the former case the hole is viewed from the front, and in the latter case it is viewed from above; the *A* direction is 60° anticlockwise and the *C* direction 60° clockwise. Accordingly, the three directions may be denoted as 10 o'clock, 12 o'clock and 2 o'clock, respectively.

Accuracy of the method

Determination by calibration prism

From the type of values obtained by calibrating the cells in special prisms by the prescribed method (p. 16) it is possible to derive fairly simple expressions for the magnitude and direction of the principle stresses in a plane perpendicular to the axis of the hole. It is, of course, of value to know the accuracy of the method when calibration prisms and cells are used in the described manner.

Fig. 12 shows the calibration prism A of cross-section 12 by 5 cm. In the hole B, usually 26 mm in diameter, the cell C is introduced and pre-stressed against diametrically opposite points on the surface of the hole. The cell is inserted in the hole in the longitudinal direction of the prism and a calibration curve is constructed in the usual way. The actual test is then begun.

A force P is applied uniformly to the cross-section of the prism, equivalent to σ_1. The cell C is first set at an angle $\varphi = \varphi_1$ to the vertical plane through the axis of the hole. The load on the prism is released in steps and the cell readings — giving the changes in the pre-stress values — are noted. The cell is then removed, the prism is loaded to the same value as before and the cell is replaced, this time at an angle φ_2, the same procedure as before being followed. The whole is repeated a third time for the angle φ_3. From the calibration curve normally obtained the change in the stress values for the cell is derived for the angles φ_1, φ_2 and φ_3 when the load P on the prism is reduced to zero, or to a given value — in the following example from 800 to 400 kg/sq.cm. These three cell values, denoted by σ', σ'' and σ''', are inserted

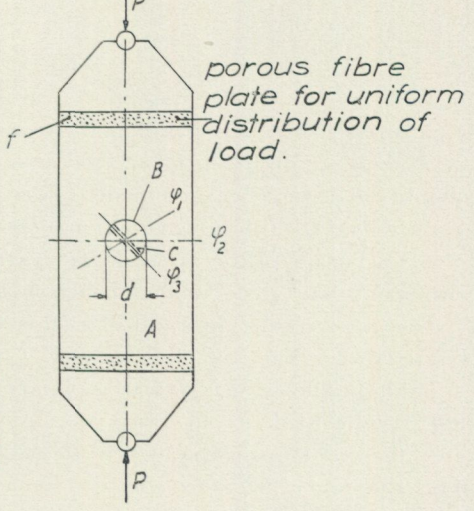

Fig. 12. The calibration prism in a press. Fibre plates f prevent the setting up of friction. When the prism has been loaded to a known value, a cell is inserted and set at an angle $\varphi = \varphi_1$. When the prism is unloaded the change in stress is recorded by the cell in the φ_1 direction. The procedure is repeated twice with the cell set at angles φ_2 and φ_3. From the calibration curve for the cell the three stress values recorded enable the load on the prism to be calculated.

TABLE I

Cell unit set at an angle $\varphi = \varphi_1$, φ_2, φ_3 etc. to the vertical (Fig. 12)	3 independent settings a, b and c for each value of φ	Stress recorded by the cell unit in the direction of measurement corresponding to a load applied on the prism		Changes in recorded stress value when load is reduced from 800 to 400 kg/sq.cm
		800 kg/sq.cm	400 kg/sq.cm	
0°	a	794	400	394
	b	800	408	392 mean 393
	c	800	408	392
30°	a	786	528	258
	b	797	533	264 m = 261
	c	789	528	261
45°	a	768	637	132
	b	792	655	137 m = 131
	c	747	623	124
75°	a	559	658	-101
	b	533	641	-107 m = -104
	c	500	604	-104
90°	a	500	641	-141
	b	474	619	-145 m = -143
	c	533	677	-144
135°	a	780	655	125
	b	800	671	129 m = 127
	c	777	651	126
195°	a	791	429	362
	b	800	437	363 m = 363
	c	794	429	365
330°	a	800	549	251
	b	797	544	253 m = 253
	c	783	528	255
345°	a	791	420	371
	b	800	437	363 m = 367
	c	797	429	368

in the formulae for the magnitude and direction of the major and minor principal stresses. The major principal stress should then be P, or the given fraction of P, and its direction should be parallel to P. The minor principal stress should be zero. The agreement between the magnitude and direction of the applied load P (or the given fraction thereof) and the recorded values is a measure of the accuracy of the method, and particularly of the calibration procedure; the results are given in the Tables I and II.

The pre-stressing procedure in this test was the later one, first used at Grängesberg (Fig. 4 a—b).

Table I shows the pre-stress values of the cell at the beginning of the test — the load on the prism in the direction of P being 800 kg/sq.cm — and the pre-stress value when the load was decreased to 400 kg/ sq.cm. The difference between the two recorded values of the cell stress repre-

sents the effect, in the direction of measurement, of the reduction in the load P from 800 to 400 kg/sq.cm. In order to increase the accuracy three independent settings and loadings, or pre-stressings, of the cell were made for each value of φ (Fig. 12). The cell was oriented so that φ had the following values: 0, 30, 45, 75, 90, 135, 195, 330 and 345°, the angle being reckoned from the vertical plane through the axis of the hole, and in a clockwise direction. The calibration prism was made of steel.

EXAMPLE I (Fig. 13).

Angles: 15, 75, 135° (at 60° to one another)

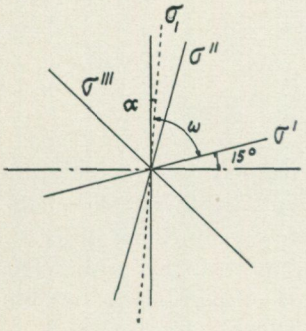

Fig. 13.

$$\sigma' = -104 \text{ kg/sq.cm}$$

$$\sigma'' = 363 \text{ »}$$

$$\sigma''' = 127 \text{ »}$$

$$\sigma' + \sigma'' + \sigma''' = 386 \text{ kg/sq.cm}$$

$$\left\{ \begin{aligned} \sigma_1 &= \tfrac{1}{2}\{386 + \sqrt{\tfrac{1}{2}(467^2 + 236^2 + 231^2)}\} \\ \sigma_2 &= \tfrac{1}{2}\{386 - \sqrt{\tfrac{1}{2}(467^2 + 236^2 + 231^2)}\} \end{aligned} \right.$$

$$\left\{ \begin{aligned} \sigma_1 &= 395 \text{ kg/sq.cm} \\ \sigma_2 &= -9 \text{ kg/sq.cm} \end{aligned} \right.$$

$$\tan 2\,\omega = \frac{236\sqrt{3}}{-208 - 490} = -0.585$$

$$\omega = 74° 50'$$

$$15° + \omega = 89° 50' \qquad \text{Hence } \alpha = 0° 10'$$

EXAMPLE II (Fig. 14).

Angles: 90, 135 and 180° (at 45° to one another)

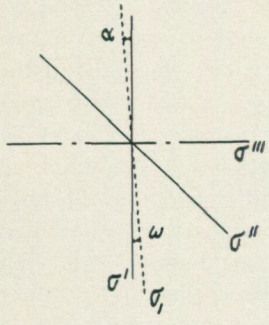

Fig. 14.

$$\sigma' = 393 \text{ kg/sq.cm}$$

$$\sigma'' = 127 \text{ »}$$

$$\sigma''' = -143 \text{ »}$$

$$\left\{ \begin{aligned} \sigma_1 &= \tfrac{3}{4}\{393 - 143 + \sqrt{\tfrac{1}{2}(266^2 + 270^2)}\} \\ \sigma_2 &= \tfrac{3}{4}\{393 - 143 - \sqrt{\tfrac{1}{2}(266^2 + 270^2)}\} \end{aligned} \right.$$

$$\left\{ \begin{aligned} \sigma_1 &= 389 \text{ kg/sq.cm} \\ \sigma_2 &= -13 \text{ kg/sq.cm} \end{aligned} \right.$$

TABLE II. *The principal stresses and their directions calculated from the measurements in Table I.*

Direction of measurement (φ in Fig. 12 and Table I)			σ_1 kg/cm² compression	σ_2 kg/cm² tension	α differences from the vertical
330°	30°	90°	386	−14	0°30′
15°	75°	135°	395	− 9	0°10′
90°	135°	180°	389	−13	−0°10′
0°	45°	90°	389	−13	0°40′
45°	90°	135°	398	−11	0°17′

$$\tan 2\,\omega = \frac{254 - 250}{393 + 143} = 0.007$$

$$\omega = 0^\circ\ 10'$$

$$\text{Hence } \alpha = -0^\circ\ 10'$$

The study of the accuracy of the mensuration method and of the stress determinations in which calibration prisms are used (Table II) shows the method to be very reliable. The major principal stress σ_1 does not differ by more than 1—3 per cent from the known load applied to the prism. The discrepancy in the direction of the principal stress is proportionally still less and does not exceed 0° 40′. The value of σ_2 should be zero, but in fact there is in all cases in Table II a small strain in the prism in a direction perpendicular to P — on an average about 12 kg/sq.cm, or 3 per cent of the load P. This effect — which is very much the same in all cases — is due to the finite width of the prism instead of the infinite width assumed by Kirsch's formulae. The quantity is probably of no practical significance. Moreover, an error in σ, of the same reason is eliminated in practice owing to the fact that the width of the rock cylinder is approximately equal to that of the calibration prism normally used.

Factors influencing the accuracy of the method in practice

The high degree of accuracy that the above tests show to be obtainable with this method presupposes measurement in metal, where the walls of the hole are reamed fairly smooth. The accuracy will be lower in rock if particular care is not taken to get the surfaces smooth. The hole that is not carefully cleaned of particles cannot be used, and the same applies if the diamond drilling equipment is not first class, or the guiding of the drill sufficiently accurate, with the result that a wavy or slightly corrugated surface is obtained in the axial direction. It has proved advantageous to use diamond bits with reaming shells, or else to polish the walls with a special diamond reamer. These procedures are neither costly nor particularly time-consuming, and they

guarantee that the walls will be sufficiently smooth for a high degree of accuracy to be attainable even in practice.

The latest types of cell and equipment for pre-stressing and inserting it in the hole have considerable increased the level of precision obtainable compared with the earliest apparatus. For example, if, in practice, the rock pressure is determined at a number of points lying in a zone of uniform stress, the recorded absolute values of the pressure in the respective directions of measurement are generally found to be similar in each group, differing by hardly more than 2—4 per cent.

Such a high degree of accuracy requires, however, that the rock be homogeneous and free from fissures — conditions that are unfortunately all too rare in those Swedish mines where the rock pressure has so far been examined. Many deep measurements have been performed, some as far as 15 metres into drift walls; it has been found that the cell hole often passes through discontinuities in the rock, these often consisting of a fissure, or a series of fissures dispersed throughout wide zones. There may also be sköls of, for instance, chlorite-mica, from less than 0.1 mm up to one-half a meter in thickness; weathered zones, crushed rock, cleavage planes and dikes may be encountered.

In such heterogeneous and fissured regions of the rock changes in the rock pressure of considerable magnitude may be expected; stress determination in the immediate vicinity of, and in, such zones would then appear to be of great importance, since their presence may well determine the static stability of the region and even of the whole mine. Knowledge of such conditions is necessary for the efficient organization of the mining from the aspects both of safety and of economy.

It is interesting to study the stress changes in the rock next to a local fissure. It is not essential that this should pass through the rock core for the stress variations in the rock around the fissure to be recordable. The location of the fissure may be determined with a reasonable degree of accuracy from the variations in the three components of the stress. The presence of the fissure is often indicated by a reduction of one component while the others are increasing. The fissure would then probably lie almost perpendicular to the first direction of measurement. The stress in this direction decreases and the lateral deformation of the rock core due to this stress will also decrease.

In the two other directions the load on the cell, which is in close contact with the wall of the hole, will consequently increase. Fig. 15 reproduces an example of rock pressure measurements performed in the Vingesbacke mine. The hole is vertical in a drift roof and the three components lie in a horizontal plane. The rock is crystalline limestone. At a depth of about 4.7 metres there is a fissure passing outside the point of measurement in the rock core.

As a rule the influence of a fissure on the curves of recorded cell values is represented in another way than in Fig. 15. Continuous curves are drawn and perpendiculars are dropped on to them from the measuring points that lie within the field of influence of the fissure (broken lines in Figs. 54a, 74b).

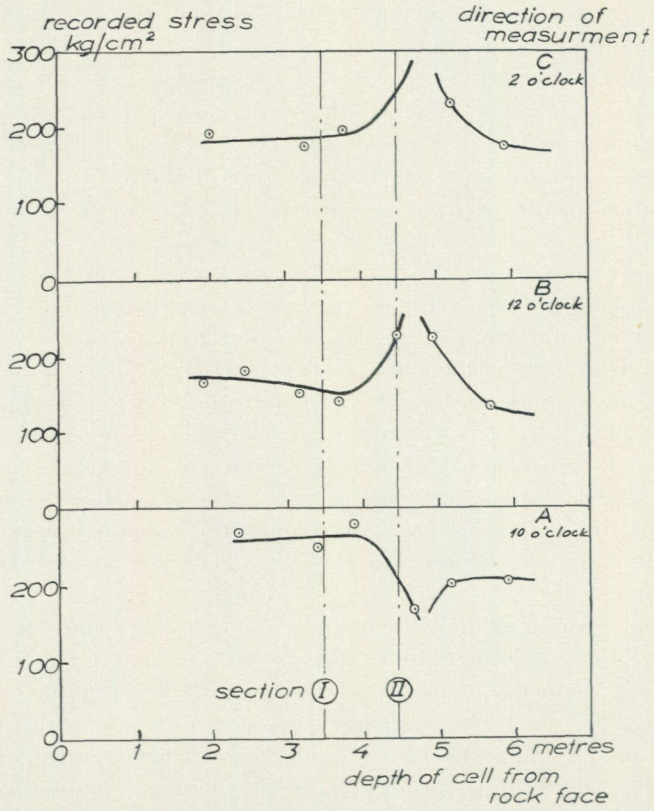

Fig. 15. Variation of stress with depth at a point in the roof at the 230 metre level in the Vingesbacke mine. All three stress components lie in the horizontal plane. Owing to the appearance of a fissure in the vicinity of, but not actually in, the rock core, one component was reduced while the two others increased. From this information the position of the fissure in relation to the cell direction of measurement may be deduced.

Sensitivity of the cell unit

The influence of the elastic properties of the cell unit and the rock on the recorded stress values

Consider a hole of radius R and located in a homogeneous material of infinite extent in which there is a unidirectional stress field σ_0 acting in a direction F—F, perpendicular to the principal axis of the hole (Fig. 16).

A cell unit C′ consisting of a housing with a measuring cell, a three-part wedge system and a T-shaped bearing (Fig. 4 a) is placed with its long axis coincident with the diameter of the hole parallel to F—F. Suppose that the cell unit C′ is replaced by a rectangular plate C of uniform cross-sectional area B. The modulus of elasticity of the material is E_C. This plate C is placed in the hole so as to make contact with the walls at the two diametrically opposite points D.

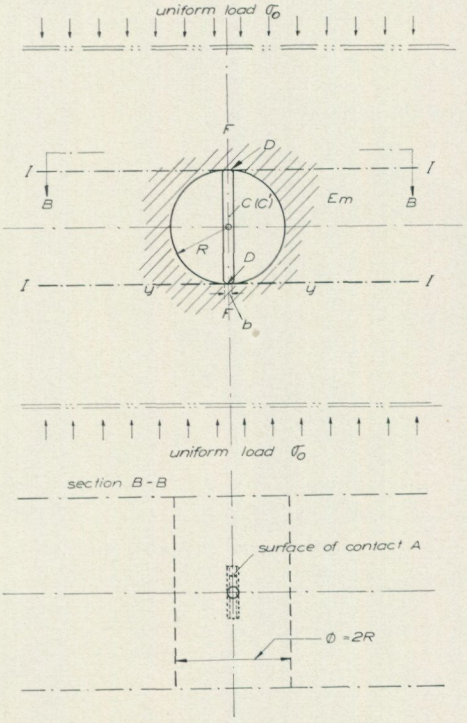

Fig. 16. A unidirectional stressfield is acting in a homogeneous material where a hole of radious R is located. In the hole a cell unit C' or a plate C is placed so as to make contact with the walls at points D.

Two imaginary planes I—I are inserted perpendicular to F—F, and tangential to the circle at the points D. The stress field σ_0 deforms the material.

At each of the two points of contact D the free wall of the hole is displaced along the line F—F and towards the centre of the hole the distance.

$$\delta_{mD} = \frac{3\,R\,\sigma_0}{E_m}$$

Putting $\sigma_0 = 1$ we have $\delta_{mD} = \frac{3\,R}{E_m}$

where E_m is the modulus of elasticity of the material.

Suppose that when the stress field σ_0 is changed by unity the load on the plate C changes by X so that there is a local deformation of the wall. Provided that the maximum width b of the surface of contact of the plate C with the wall is small compared with the radius R, the deformation will be approximately the same as if the plate were to exert an equal force on the plane surface I—I at the point D. If the plate C exerts unit force on this surface, which may be considered as the plane surface of a hemisphere of infinite radius, the point D will be displaced a distance δ_{mC} in the direction F—F. The total displacement of the point D owing to the load X is then $\delta_{mC}X$.

The elastic deformation of plate C due to the force X is

$$\delta_C = \frac{2\,R \cdot X}{B \cdot E_C}.$$

We then have

$$\frac{3\,R}{E_m} - \delta_{mC} \cdot X = \frac{R \cdot X}{B \cdot E_C}$$

$$\left(\delta_{mC} + \frac{R}{B \cdot E_C} \right) \cdot X = \frac{3\,R}{E_m}$$

Whence $$X = \frac{3\,R}{E_m \cdot \delta_{mC} + \frac{R}{B} \cdot \frac{E_m}{E_C}} \qquad \ldots\ldots\ldots\ldots\ldots\ldots\ldots\ldots \quad (1)$$

In this expression X is the recorded change in load on plate C when the uniform stress field σ_0 in the direction F—F (Fig. 16) is changed by unity.

As δ_{mC} is inversely proportional to E_m the value $E_m \cdot \delta_{mC}$ is a constant. Putting $E_m \cdot \delta_{mC} = K$

$$X = \frac{3\,R}{K + \frac{R}{B} \cdot \frac{E_m}{E_C}}$$

If the plate C were a stress-recording unit its sensitivity would be high when X is large, and small when X is small.

The value of X is dependant on two factors: the constant K and the relationship between the modulus of elasticity of the material around the hole and that of the stress recording plate C. This type of formula applies where the stress is measured by the new method of direct recording in the meter and not — as is usually the case — by recording the deformation of the material from which the stress is then calculated.[1]

From eqn. 1 it is seen that when E_C is much greater than E_m the factor $\frac{R \cdot E_m}{B \cdot E_C}$ is small compared with K; and X — the recorded stress when the change in σ_0 is unity — will be almost constant and does not vary much for different values of E_m. This is of interest *as it suggests a way of designing cell units that will give approximately correct readings independently of the modulus of elasticity of the rock*. However, the range of the instrument of measurement will then be rather small.

If E_C is much smaller than E_m the constant K is small compared with $\frac{R \cdot E_m}{B \cdot E_C}$ and the recorded value of X will be small and almost proportional to $\frac{E_C}{E_m}$, and for a particular cell inversely proportional to E_m.

The value of δ_{mC} in eqn. 1 can be calculated by Boussinesq's method. The load from the plate C that is distributed over the contact surface A deforms the wall of the hole. If the width b is small compared with R the displacement will be almost the same as that due to the deformation of a hemisphere by the force exerted by C. For the practical application of eqn. 1 in stress measurements it is necessary to determine E_C, B and the value of δ_{mC} for the particular cell unit used.

Calculation of the value δ_{mC}

To simplify the calculations suppose initially that the plate C has a surface of contact A which is circular and of radius $= r$ (I). Calculations will subsequently be made for a rectangular area of contact as in the cell unit used (II).

I. *Circular area of contact.*

If the unit load is so distributed over, and perpendicular to, the surface $A = \pi r^2$ that it remains plane and horizontal on deformation, we have according to Boussinesq,

$$w_0 = \frac{m^2 - 1}{m^2} \cdot \frac{1}{2 E_m r},$$

where w_0 is the displacement of the loaded area,
m = the reciprocal of Poisson's ratio
E_m = the modulus of elasticity of the mass.

A similar formula for direct stress recording is applied in measuring stresses in concrete by a cell cast into the mass in "*Measuring Stresses and Deformations in Solid Materials*". by Nils Hast 1943, and in Ingeniörsvetenskapsakademiens Handlingar, No. 178. Stockholm 1945.

We have

$$E_m \cdot \delta_{mC} = \frac{m^2 - 1}{2\,m^2} \cdot \frac{1}{r}$$

Putting $r = 0.15$ cm, $m = 4.5$ and $B = 0.3 \times 1.5 = 0.45$ sq.cm

$$E_m \cdot \delta_{mC} = \frac{19}{40} \cdot \frac{1}{0.15} = 3.17$$

$$\text{Then } X = \frac{3\,R}{3.17 + \dfrac{R \cdot E_m}{0.45 \cdot E_C}}$$

With the standard diameter of the hole $2R = 2.6$ cm we have

$$X = \frac{3 \cdot 1.3}{3.17 + \dfrac{1.3}{0.45} \cdot \dfrac{E_m}{E_C}} = \frac{1}{0.81 + 0.74\,\dfrac{E_m}{E_C}};$$

II. *Rectangular area of contact.*

The surface of contact of the standard cell unit is in fact not circular but rectangular; the width of the contact zone $= b$, which must be small, is 0.2 cm (Fig. 4 a) and the length is 1.3 cm.

The loaded contact area should not be too small as the contact pressure at D must not be so high that the material in the zone of contact is damaged.

The calculation of the deformation occurring when a small rectangular part of the plane boundary area of a hemisphere is subjected to a uniformly distributed unit load is not as simple as in the above case of a circle. However, in the following the problem will be simplified. The area 1.3×0.2 sq.cm. is replaced by 6 inscribed circles (nos. 1—6) each of radius $r = 0.11$ centimetre and loaded with one-sixth of the proposed unit load (Fig. 17). The displacement of area 1, for instance, is assumed to be the local deformation due to one-sixth of the unit load placed on area 1, to which is added all the displacements in area 1, when one sixth of the unit load is placed on each of the areas 2, 3, 4, 5 and 6.

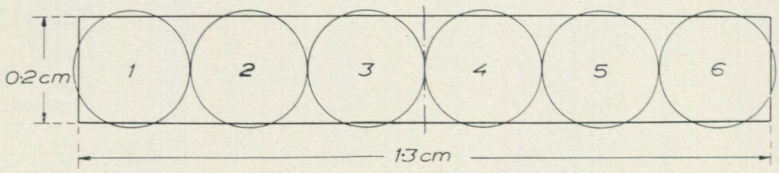

Fig. 17. In the calculations of the displacement the rectangular area of contact between the cell unit C' or the plate C and the hole wall is replaced by six circles.

The displacement w_x at a point located outside a loaded circular area on the plane boundary of a hemisphere is calculated according to Boussinesq. The area is assumed be acted on by a unit load and to remain plane during

the loading. Suppose the distance between the centre of the area and the point is x.

$$\text{then } w_x = \frac{m^2 - 1}{m^2} \cdot \frac{1}{\pi E_m r} \sum \sin^{-1} \frac{r}{x}$$

For areas 2 and 5 (Fig. 17) the displacement w_2 and w_5 is

$$w_2 = w_5 = \frac{m^2 - 1}{m^2} \cdot \frac{1}{2 E_m r} + \frac{m^2 - 1}{m^2} \cdot \frac{1}{\pi E_m r} \sum \sin^{-1} \frac{r}{x}$$

$$\text{for } \frac{x}{r} = 2,\ 2,\ 4,\ 6,\ 8$$

Putting $\dfrac{m^2 - 1}{m^2} \cdot \dfrac{1}{E_m r} = \beta$ the expression simplifies to

$$w_2 = w_5 = \beta \left[\frac{1}{2} + \frac{1}{\pi} \sum \sin^{-1} \frac{r}{x} \right]$$

$$\text{for } \frac{x}{r} = 2,\ 2,\ 4,\ 6,\ 8$$

$$\text{Similarly, } w_3 = w_4 = \beta \left[\frac{1}{2} + \frac{1}{\pi} \sum \sin^{-1} \frac{r}{x} \right]$$

$$\text{for } \frac{x}{r} = 2,\ 2,\ 4,\ 4,\ 6$$

$$\text{and } w_1 = w_6 = \beta \left[\frac{1}{2} + \frac{1}{\pi} \sum \sin^{-1} \frac{r}{x} \right]$$

$$\text{for } \frac{x}{r} = 2,\ 4,\ 6,\ 8,\ 10$$

Whence $w_1 = w_6 = 0.87\ \beta$

$w_2 = w_5 = 1.01\ \beta$

$w_3 = w_4 = 1.05\ \beta$

$0.98\ \beta$ is taken as a mean value of the displacement of the wall surface due to the unit load on each of the areas 1—6. The displacement of the rectangular area of contact loaded by unit load will then be

$$\delta_{mC} = \frac{0.98}{6} \cdot \frac{m^2 - 1}{m^2} \cdot \frac{1}{E_m r}; \quad \ldots\ldots\ldots\ldots\ldots\ldots \quad (2)$$

If we put $r = 0.11$ cm we have

$$m = \frac{10}{3} \qquad \delta_{mC} = \frac{0.98}{0.66} \cdot \frac{m^2 - 1}{m^2} \cdot \frac{1}{E_m} = \frac{1.351}{E_m}$$

$$m = 5 \qquad \delta_{mC} = \frac{0.98}{0.66} \cdot \frac{24}{25} \cdot \frac{1}{E_m} = \frac{1.426}{E_m};$$

The plate C is assumed to have a cross-sectional area $B = 1.5 \times 0.3 = 0.45$ sq.cm except at the contact surfaces where the area is 1.3×0.2 sq.cm. $R = 1.3$ cm.

In the formula $X = \dfrac{1}{\frac{1}{3}\frac{1}{R}E_m \cdot \delta_{mC} + \frac{E_m}{3B \cdot E_C}}$

we then have, when $m = \dfrac{10}{3}$ and $E_m \cdot \delta_{mC} = 1.351$

$$X = \frac{1}{0.346 + 0.741 \cdot \dfrac{E_m}{E_C}}$$

and when $m = 5$

$$X = \frac{1}{0.366 + 0.741 \dfrac{E_m}{E_C}};$$

As mentioned above the cell unit (Fig. 4 a) was replaced by the plate C of modulus E_C in order to simplify the calculations. In practice, however, it is not possible to use the plate C as a recording device as it must be pre-stressed when used to record the stress variations in a rock core.

The rigidity of the cell unit under different loads

The total deformation of the plate C (between the points D in Fig. 16) by unit load can be calculated and compared with the sum of the deformations by unit load on the various parts of the cell unit, including the cell housing, the

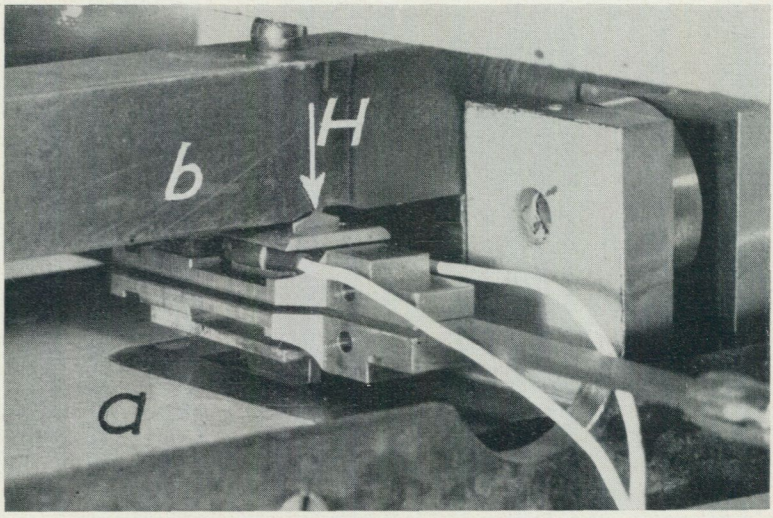

Fig. 18. An apparatus for the determination of the tota l deformation of the cell unit for various loads.

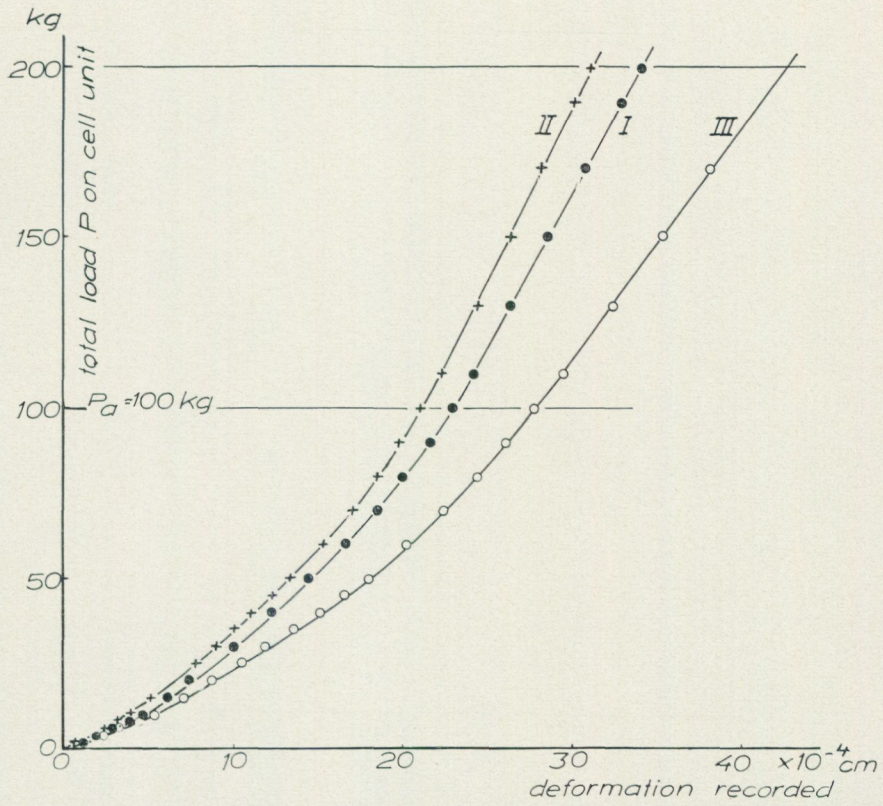

Fig. 19. The rigidity of the cell unit is a constant when the total load on the unit is > 100 kg but decreases at smaller loads. No hysteresis effect can be seen. In all cases (curves I—III) the housing and the outer wedges are of brass and the middle wedge of steel. The bearing (3 in Fig. 4 a) is of brass (I), steel (II) and aluminium (III).

three-part wedge system and the T-shaped bearing. This deformation can also be measured directly by subjecting the cell unit to unit load. In thi way the expression for X can be used to find the most suitable rigidity and area of contact A under the various conditions that prevail in stress measurements. The results of deformation measurements of this kind are given below.

Fig. 18 shows an apparatus for the determination of the total deformation of the cell unit for various loads. It consists of a base plate a and a loading arm b in such a position that b is parallel to a. At H the cell unit is applied between and perpendicular to a and b. The load P acts in the plane of symmetry of the cell unit. The decrease in distance between the steel arms a and b was recorded by means of a sensitive meter of the magnetostrictive type.[1] The recorded change in the distance separating a and b is the sum of the deformation of the cell unit (the bearing + cell housing + wedge system) and its depression in the surfaces of contact at H (steel).

[1] The design of the deformation meter is given in *Measuring stresses and deformations in solid materials* by Nils Hast, Ingeniörsvetenskapsakademiens Handlingar No. 178 1945, Stockholm.

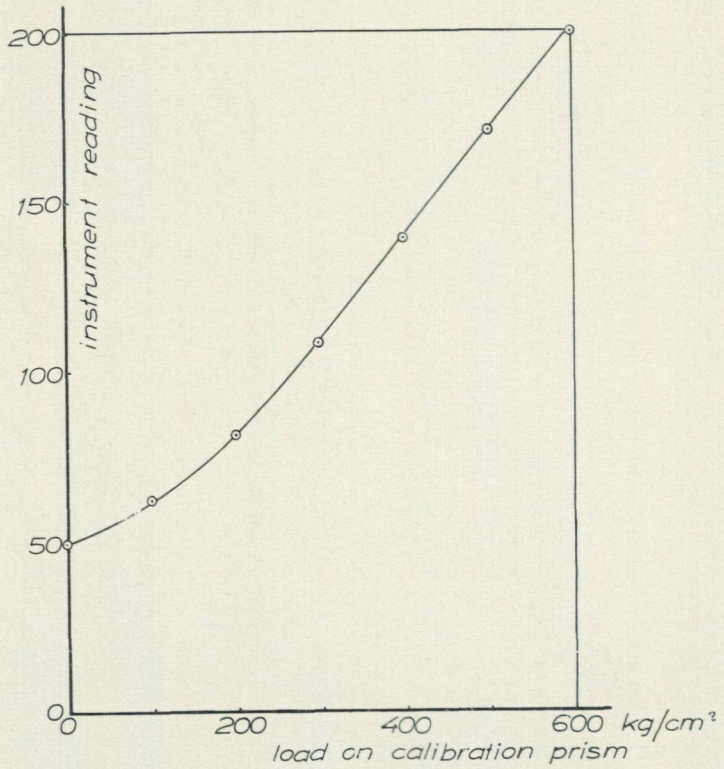

Fig. 20. Calibration curve for a cell unit pre-stressed in a 26 mm hole in a steel prism. The prism is unloaded from 600 kg/sq.cm.

As is seen from the curve in Fig. 19, the rigidity of the cell unit is low for a small load, but increases with the load until it becomes constant at $P_a = 100$ kg. This means that initially, when the load is small, the three-part wedge system is responsible for a larger part of the deformation than when the load is high. Under the increasing load the surfaces of the smoothly polished wedges are pressed together so that there is a more intimate contact. On unloading, the reverse effect occurs. It is of interest to note that there is in this case no hysteresis effect.

Curves I, II and III in Fig. 19 refer to cell units of different rigidities. In all cases the cell housing and the two outer wedges are of brass and the centre wedge of steel. The difference lies in the material of which the bearing is composed (3 in Fig. 4 a), which in curves I, II and III is brass, steel and aluminium, respectively.

Fig. 20 shows a calibration curve for a cell unit in a hole 26 mm in diameter in a steel prism; before insertion of the cell, the prism is loaded to a value of 600 kg/sq.cm. The curve shows the instrument readings obtained during a gradual reduction of the load on the prism. Except for the lower

part, the curve is straight. The curvature is due to the fact that the pre-stress level of the cell unit during the unloading procedure fell below the value P_a in Fig. 19. The cell unit then became less rigid as the unloading proceeded; that is to say, a given change in load on the steel prism corresponded to a decreasing change in stress in the cell unit. When the pre-stress value was increased, the curved part of the calibration graph was reduced, and if the pre-stress value had been high enough, the curve would have been straight. It should be added that in all cases the recording curve of the cell was straight.

In practice measurements may be performed by using such high pre-stress load that the residual load will still be greater than P_a after the stress release channel has been cut. However, as there is no hysteresis effect on unloading a cell unit, one may work with a smaller pre-stress load, and use a part of the bent curve. The sensitivity of the measurement will be lower, but the range of measurements will be greater.

The correction coefficient for a standard cell unit calibrated in steel but used in rock

The magnitude of the correction coefficient is considered here for the case where the moduli of elasticity of the rock and the calibration prism are different. An accurate expression for this coefficient considerably facilitates the calibration work.

In practice steel prisms have proved to be best since there is practically no wear or permanent depression of the surface of the hole even after long use. The moduli of the more common types of rock such as leptite and granite differ appreciably from that of steel, for which reason a high degree of accuracy is required of the correction factor.

The following cases are considered:

(i) Cell unit calibrated in a *steel* prism, stress measured in *rock*.

(ii) Cell unit calibrated in a *steel* prism, stress measured in *metal* prisms of different moduli.

(iii) Cell unit calibrated in *stone* prism, stress measured in *rock*.

In practice it is the first case that is important. Poisson's ratio is taken as 1/5 for rock and 3/10 for metal, so that $m = 5$ and 10/3, respectively. The difference in the correction coefficients from m in the three cases specified is insignificant. The last two may be regarded as special cases of the first, if the values of m for the material in which the calibration and stress measurements are made are equal.

The accuracy of the theoretically determined correction coefficients may best be checked by performing measurements also in metal prisms which are homogeneous and have known moduli of elasticity.

According to equation (1), p. 36

$$X = \frac{3\,R}{E_m \cdot \delta_{mC} + \frac{R}{B} \cdot \frac{E_m}{E_C}}$$

where

$$\delta_{mC} = \frac{0.98}{6} \cdot \frac{m^2 - 1}{m^2} \cdot \frac{1}{E_m r}$$

we have the following expressions for δ_{mC} in the case of a rectangular area of contact between the standard cell unit and the hole wall (p. 39)

when $m = 5$ $\qquad \delta_{mC} = \dfrac{1.426}{E_m}$

and when $m = 10/3$ $\delta_{mC} = \dfrac{1.351}{E_m}$

In the above expression X is the recorded change in load on plate C when the uniform stress field σ_0 in the direction $F - F$ is changed by unity (Fig. 16). E_C is the modulus of elasticity for the homogenous plate C of cross-section B, which replaces the cell unit C' in the calculations (see p. 35). C' consists of the bearing + cell housing + the three-wedge system (Fig. 4 a). In the formula for X the term $B \cdot E_C$, which represents the effect of the plate C, is replaced by another that represents the effect of the cell unit C'. This is obtained as follows.

For unit load ($P = 1$) on the whole plate C in the direction $F - F$ (Fig. 16) the deformation of the plate is

$$\Delta = \frac{1 \cdot 2\,R}{B \cdot E_C}$$

whence

$$B \cdot E_C = \frac{2\,R}{\Delta}$$

Δ was determined experimentally for the normal type of cell unit (p. 40, Figs. 18 and 19), the housing, the bearing and the outer wedges being of brass, and the middle wedge of steel. The measurements did not give Δ directly, but $\Delta + \Delta_1$, where Δ_1 is the elastic depression made by the bearings in the steel surface at H in the arms a and b.

According to eqn. (2), $r = 0.11$ cm

$$\Delta_1 = 2\,\delta_{mC} = \frac{2 \cdot 0.98}{0.66} \cdot \frac{m^2 - 1}{m^2} \cdot \frac{1}{E_m}$$

When $m = 10/3$ and steel $\Delta_1 = \dfrac{2.702}{E_S}$

From the straight portion of the curve I (Fig. 19), where the additional deformation of the wedge surfaces of contact has disappeared, the deformation for a load on the cell unit of 50 kg is $5.6 \cdot 10^{-4}$ centimetres. This gives

$$\Delta = \frac{5.6 \cdot 10^{-4}}{50} - \Delta_1 = \frac{5.6}{50} \cdot 10^{-4} - \frac{2.702}{E_S}$$

$$= 0.991 \cdot 10^{-5}.$$

In the expression

$$X = \frac{1}{\frac{1}{3R} \cdot E_m \delta_{mC} + \frac{E_m}{3B \cdot E_C}}$$

we then have

$$B \cdot E_C = \frac{2R}{\Delta} = \frac{2 \cdot 1.3}{0.991} \cdot 10^5 = 2.62 \cdot 10^5;$$

whence, for

$m = 5$ and $m = 10/3$, respectively,

$$m = 5 \qquad X = \frac{1}{\frac{1.426}{3.9} + \frac{E_m}{3 \cdot 2.62 \cdot 10^5}} = \frac{1}{0.366 + 0.127 \cdot E_m \cdot 10^{-5}}$$

$$m = 10/3 \quad X = \frac{1}{\frac{1.351}{3.9} + \frac{E_m}{3 \cdot 2.62 \cdot 10^5}} = \frac{1}{0.346 + 0.127 \cdot E_m \cdot 10^{-5}}$$

If the same cell unit is used for measurement in metal prisms of modulus E_M, and in rock of modulus E_R, we obtain, respectively,

$$X_M = \frac{1}{0.346 + 0.127 \cdot E_M \cdot 10^{-5}}$$

$$X_R = \frac{1}{0.366 + 0.127 \cdot E_R \cdot 10^{-5}}$$

When the values recorded in rock (X_R) are interpreted according to the calibration curve for metal (X_M) an error is introduced, which varies with the value of E_R and E_M. This error may be eliminated by multiplying the recorded value of X by a factor $\alpha = \frac{X_M}{X_R}$.

Then

$$\alpha = \frac{0.366 + 0.127 \cdot E_R \cdot 10^{-5}}{0.346 + 0.127 \cdot E_M \cdot 10^{-4}}$$

When $E_M = E_S = 21 \cdot 10^5$

we have for the case A when the calibration prism is of steel and the stress is measured in rock

$$\alpha_A = 0.121 + 0.0422 \cdot E_R \cdot 10^{-5} \quad \ldots\ldots\ldots \quad (3)$$

and for the case B when the prism is of steel and the stress is measured in metal of different modulus

$$\alpha_B = \frac{0.346 + 0.127 \cdot E_M \cdot 10^{-5}}{0.346 + 0.127 \cdot E_S \cdot 10^{-5}}$$

$$= 0.115 + 0.0422 \cdot E_M \cdot 10^{-5} \quad \ldots\ldots\ldots \quad (4)$$

The same cell unit was placed in a series of calibration prisms of various materials — steel, brass, aluminium, leptite. and sintered tiles. The first three experiments give control values for the curve α_B, and the last two for α_A.

When unloading the steel prism it was found that a value of X of $X_a = 50$ degrees on the cell reading instrument corresponded to a change in the load σ_0 on the prism of 117.5 kg/sq.cm. The other prisms were also unloaded until the cell unit in each case also showed a value of 50 degrees. Those recorded changes in σ_0 are given in Table III.

The coefficient $\alpha_A = \frac{X_M}{X_R} = \frac{X_S}{X_R}$ and $\alpha_B = \frac{X_S}{X_M}$

TABLE III

	E (kg/sq. cm)	Change in σ_0 when $X = X_a$ (kg/sq.cm)	Unit change in σ_0 corresponds to a value of X of	
Steel	2,100,000	117.5	$X_a \cdot \frac{1}{117.5}$	$\alpha_B = 1.000$
Brass	1,080,000	65.5	$\cdot \frac{1}{65.5}$	$\alpha_B = 0.556$
Aluminium	780,000	52	$\cdot \frac{1}{52}$	$\alpha_B = 0.442$
Leptite	620,000	45	$\cdot \frac{1}{45}$	$\alpha_A = 0.383$
Sintered tiles	380,000	35	$\cdot \frac{1}{35}$	$\alpha_A = 0.298$

The moduli of elasticity for the different prisms were measured before drilling the holes for measurement. The equations of α_A (3) and α_B (4) are linear. Fig. 21 shows the curves. The values of α_A and α_B, found by experiment, are indicated in the theoretical diagram in Fig. 21, α_A with crosses and α_B with circles.

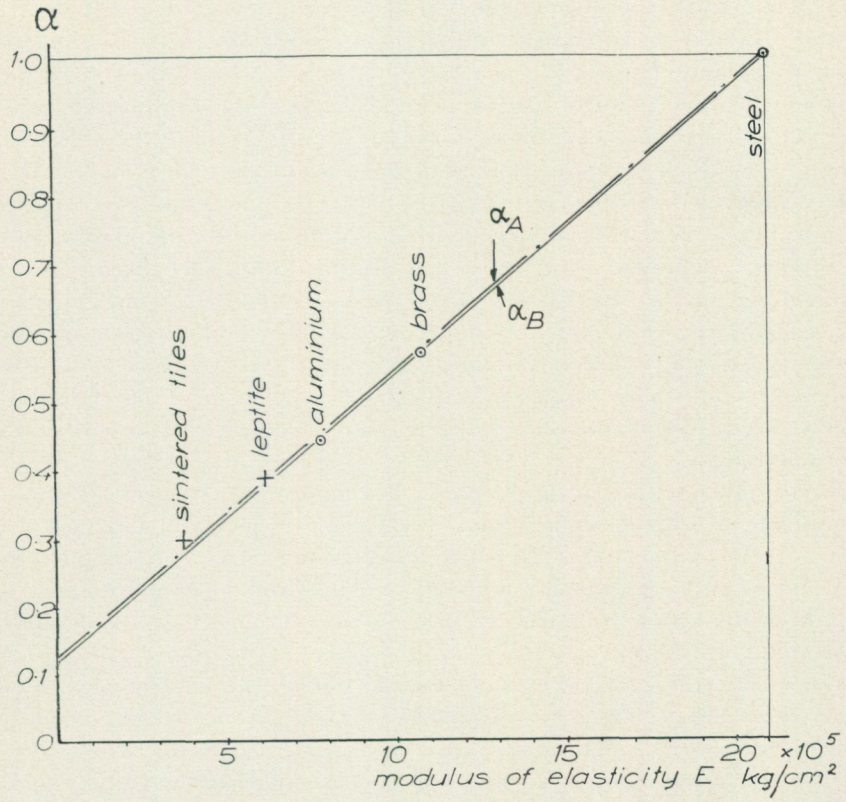

Fig. 21. *Upper curve.* Correction coefficient for a standard cell unit calibrated in steel but used for measurement in rock (α_A). *Lower curve* The same but used for measurement in metal (α_B).

The values found in the experiments lie close the corresponding theoretical curves, which are thus experimentally verified. *It is thus possible to make general use of steel prisms for calibration of the cell unit in rock pressure measurements.* As mentioned above, such a calibration procedure is to be preferred from a practical point of view.

Contact pressure between bearing and hole wall

From the above theoretical analysis of the effect of the rigidity of the cell unit it is evident that in stress measurement by the described method one may use units that are rigid, and thus record stress taken up, or units that function more or less as deformation meters. Between these extreme types are those in which the sensitivity and the range of measurement may be adapted according to the prevailing conditions. Measurements in Swedish rock have shown that a suitable maximum pre-stress value for the cell unit in practice is about 200 kg,

though it may be possible to use 150 kg or even lower, depending on the rigidity of the cell unit. When cutting the stress release channel a stress of at least 50 kg must remain so that the cell does not vibrate loose during the drilling operation. If a deformation meter is placed in the drill hole the recording unit also must be held tightly in contact with the wall of the hole. If this contact pressure is chosen too low in order to avoid too high a loading of the deformation meter, and thus to reduce its range of measurement, the meter may be displaced and the values spoiled — for instance during blasting in the rock. Plastic deformation of the rock in the hole may take place with time owing to the high pressures involved and the high moisture content of the mine atmosphere (see below). Another important factor is the fissured natural state of the rock. For a certain distance around a fissure the stress field is disturbed, and the cell units must be placed close enough together for it to be possible to distinguish the recorded values that refer to intact area from those that refer to fissured areas.

An advantage of recording stresses with a more rigid cell over deformation measurements is the lower sensitivity to variation in the elastic modulus of the rock — see, for instance, Fig. 21, where the correction curve — a straight line — does not pass through the origin. If the unit is made more rigid the line will turn upwards about the point $(21 \cdot 10^5, 1)$, and the sensitivity to differences in modulus will be still lower.

However, there is an upper limit for the rigidity, for the contact pressure under the bearings (Fig. 4 a) must not be so high as to involve damage to the wall of the hole. Of importance in this respect is not only the mean value of the contact pressure on the surface, but also the shape of the contact surface and its curvature.

When a plane area is loaded by a small body having a plane area of contact the pressure will be high along a narrow peripheral zone of the surface of contact, and consequently for the rest of the surface slightly less than the mean value for the hole. From calculations of the pressure distribution beneath a rigid plate for the case in which the plate is circular Boussinesq has shown that in theory the stress increases to infinity in an infinitely narrow marginal zone. The experiment illustrated in Fig. 21 covers 2 prisms of brittle material (natural stone and sintered tiles) and 3 of metal (steel, brass and aluminium). The cell hole in the prisms was in all cases reamed to give a smooth surface. The contact surfaces between the unit and the wall of the hole were made cylindrical, with the same radius of curvature. Although the loading conditions for the contact surface were then the same as for Boussinesq's plane surfaces, no marginal zone of high pressure was formed. The reason is given below.

There are several ways of avoiding the marginal stress concentrations, one of which is to make the radius of curvature of the cylindrical surface of contact of the unit slightly less than that of the hole. In the specific case of a plane surface and a cylindrical one of radius r in contact — the limiting case of two cylindrical surfaces — the pressure will be lowest at the boundary of the contact zone and will increase elliptically towards the centre (Fig. 22).

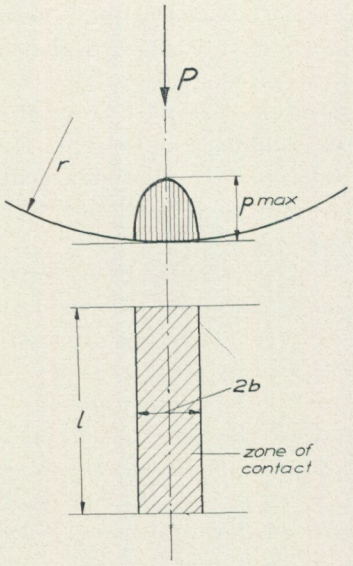

Fig. 22. The pressure in the zone of contact between two loaded cylindrical surfaces will be lowest at the boundary and increases elliptically towards the centre.

For p_{max} we have the expression

$$p_{max}^2 = \frac{P \cdot E}{2\pi\, lr(1 - \nu^2)}$$

where P is the total load on the surface of contact and l its length.

If $\nu = \frac{1}{m} = 0.2$,

we have $$p_{max}^2 = 0.165 \cdot \frac{P \cdot E}{l \cdot r}$$

If the radius of curvature of the bearing at the surface of contact is 12.5 mm, and the radius of the hole is 13 mm,

$$\frac{1}{r} = \frac{1}{12.5} - \frac{1}{13} \text{ whence } r = 33 \text{ cm.}$$

As a rule the pre-stress value for the unit does not exceed 200 kg.

Then, if $l = 1.3$ cm and $E = 500{,}000$ kg/sq.cm,

$$p_{max} = 620 \text{ kg/sq.cm.}$$

This contact pressure cannot be regarded as high for most rocks. By choosing other radii p_{max} may be further reduced.

In practice, however, the curvature of the surface of contact of the bearing is the same as that of the hole. The close agreement between the experimental results and the theoretical values (Fig. 21) shows that in practice there is no troublesome impairment of the material *providing the unit is first calibrated with a brass bearing in a steel prism.* The reason for this is the following.

In the contact surface between the hole of the steel prism and the brass bearing high marginal concentrations would in theory be set up on pre-

stressing. Owing to the difference in the strength of steel and brass there is, however, a plastic deformation of the bearing in the marginal zone as soon as the stress there exceeds the ultimate strength of the brass. The bearing is plastically deformed, and is thus no longer plane, so that in theory no appreciable marginal concentrations are set up when the unit is used in practice after calibration. This is also evident from the fact that steel calibration prisms were in almost daily use for several years without there being any marking of the wall surface.

In principle, therefore, the bearings should be plastically deformable metals such as brass and they should be overloaded in advance in steel to produce a still more marked deformation of the marginal zone.

The series of metal prisms tested (Fig. 21) included one of magnesium; the value of α_B in this case was 10 per cent higher than expected. An analysis showed, however, that on pre-loading the prism the ordinary stresses near the hole became so high that the prism was damaged locally and did not function corrrctly afterwards. The results are reported for the sake of completeness.

In absolute stress measurements by the method described above the period during which the contact surfaces are loaded is generally of the order of one hour. However, tests have been made in which the unit was pre-stressed to its maximum value for several days without any change in the pre-stress value being observed.

Rock pressure determination by deformation meters as compared with by pre-stressed cell units

The author has found from his rock pressure measurements in Sweden that the rock core with the measuring hole often is intersected by fissures, cleavage planes or thin layers of mica (or other soft materials). There is a risk that a deformation meter when placed in a bore-hole will be fastened at points where such defect rock material is located in the wall of the measuring hole. In such a case the recordings will not be reliable, but this cannot be detected. However, if a cell unit according to Fig. 14 is used at such positions the application of the pre-stress load on the cell necessitates much greater movements on the pre-stressing apparatus then in the case when the rock at the sites of the cell unit is of normal quality. In this way unsuitable locations of the recording instruments in the cell hole can be avoided.

Sometimes the inhomogeneities of fissures, cleavage planes etc. intersect the core and the wall of the measuring hole in a direction almost parallel to its axis. When such a core is being drilled out, the pre-stress load, applied on the cell unit, will give rise to movements separating the rock faces of the cleavage planes and increasing the width of the fissures. The cell readings will rapidly decrease to zero and the same will take place if the pre-stressing procedure is repeated.

To sum up: *The application of a pre-stress load on the cell unit*

1. *gives a most necessary information as regards the quality of the rock at the sites of the measuring cell units*

2. *demonstrates* — during the course of the measurements — *if the rock core is homogeneous or damaged* by the presence of cleavage planes, fissures or other defects.

When using deformation meters in the measuring hole, no such information is available and in many cases it is impossible to be sure that the recorded deformations are reliable for the calculation of the rock pressure acting at the point of measurement.

A method of stress measurement sometimes used is referring to the fastening of deformation meters (strain gauges) on to small smoothened surfaces on pillars and walls. The release of the stresses in the rock face is made by cutting a notch of sufficient depth around the gauges. However, as is evident from many diagrams of stress measurements in pillars and drift walls in this book the stresses often are very low, if any, in the rock face, due to fissuring of the rock during the blasting procedure. Even if some stress values are recorded on the meters, these readings will be of no interest *as the stress release effect of the blasting procedure is not known*. Even if the strain gauges are placed at the smoothened bottom face of a bore hole at a great depth from the rock face, say 1—2 metres, the recorded values will not be reliable. The stress in such a face is appreciably increased compared with the stress acting at some distance from the bore hole. If the rock is very hard and the virgin stress very high, there may even be strain bursts at the actual end face of the bore hole, in which case the remaining stress in this surface layer will be about zero.

As an example of this method with strain gauges fastened on to smoothened surfaces of pillars and walls, references can be given to some measurements performed in a Swedish mine.

At six points on 5 pillars the rock face was smoothened and strain gauges were carefully fastened on to these surfaces, two at each point of measurement. The recorded stresses in the pillars, obtained by cutting the stress release notch, were

on 4 gauges	0 kg/sq.cm or a small tension	
» 5 »	between 7 and 12 kg/sq.cm	
» 3 »	» 14 » 20 » » »	

The load on many similar pillars in the mine has been measured according to the author's method using cell units in bore holes. It was found that on most of the pillars the load was 150—200 kg/sq. cm.

The measurement of stress changes in rock over a long period

When following stress changes in rock over a long period by means of deformation meters placed in a drilled hole, several factors must be considered if the results are to be correctly interpreted.

1. The zero setting of the recording unit must not be altered throughout the period by the mechanical loads applied to the instrument or by the high humidity in the atmosphere of the mine.

2. Rock samples are subjected to plastic deformation on long-term loading, the magnitude of which depends on the maximum stress to which the

material is subjected and on the time the load is applied. If a hole is made in a loaded rock there will be a marked increase in stress around the hole, and these concentrations will thus increase the plastic deformation occurring with time in the wall of the hole where the instrument is applied. For a short period of one hour or less that an absolute stress determination takes in most cases there will probably be no significant plastic deformation. On the other hand, this may not be true if the recording time is extended to months or years. Limestone will probably be plastically deformed under high rock pressure, but rock salt even at a low pressure. The deformation recorded by the instrument will then no longer bear any relation to the stresses calculated from them according to the theory of elasticity.

3. As soon as the drill hole has been made the humid air of the mine comes into contact with the wall. Moisture may then diffuse into the surface layer and give rise to deformation, which will distort the values of the elastic deformation in the rock set up by stress changes during mining. There is reliable evidence from other fields of research that moisture combined with high superficial stress may result in increased plastic deformation.

4. As appears from the measurements published in this paper, the stresses generally vary from one point to another in the rock owing to the influence of fissures and sköls, which extend for a fairly large distance around the actual fissure. If the mensuration procedure is limited to the insertion of a few deformation meters in a drill hole it is not known whether they have their sites in or near fissures; the mensuration may then provide a false picture of the general rock pressure or the change in it. In absolute stress measurement, values are obtained in three directions and at many points along the hole so that the influence of the fissures passing through or near the core can be plotted. Deformation meters must be inserted along a hole in a similar manner.

5. For studying the variation in rock pressure at a point in a mine as the excavation progresses the most reliable method is to make repeated determinations of the absolute value at the point in question. *If measurements are made only of the changes in stress it is not known to which level these changes apply.* If the initial stresses are high, there is a risk that the relatively small increases in these values will provide large plastic deformation in the wall of the hole, so that, if the rock is assumed to be elastic, much too high calculated stresses will be obtained.

However, there are many instances in which it may be of great value, and cheaper, to have the pressure recording instrument remaining in the rock for continuous stress recording over a long period. In order to ensure a high degree of reliability for these recordings it would appear to be necessary to eliminate the influence of plastic deformation. An apparatus that makes possible such a procedure has been designed and has been found to function satisfactorily in practice. Such an apparatus would evidently be of value for following the stress changes in mines where block caving is practiced (Part Five, p. 162). The new instruments and results will be published in due course.

Rock of low strength and rock that is much fissured are subjected to large

deformations even when the stresses are low. However, even in such rock this apparatus promises a solution to the problem of stress measurement. In many mines this is of vital importance.

A supplementary method for measurement in highly stressed hard rock ($\sigma > 1{,}000$ kg/sq.cm)

During the drilling of the stress release channel the core may be separated into discs in places of extremely high rock pressure (1,000—1,500 kg/sq.cm) and where the rock is hard. The thickness of the discs formed is between 0.5 and 5 cm, and their surfaces are plane and smooth. Fig. 22 a shows that if the discs are piled in the order in which they are separated the fractures of the core are hardly visible. The separation of the core into discs is probably to be explained as follows.

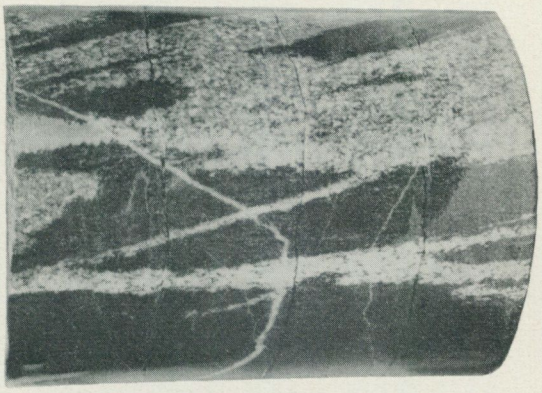

Fig. 22 a. Separation of the core into discs at right angle to the axis of the core may appear at places where the rock is hard and stresses very high ($>1{,}000$ kg/cm^2). The discs formed have plane surfaces and can be piled together.

Fig. 22 b is a longitudinal section through a bore hole where the core f is isolated from the rock by the stress release channel b. Provided that the virgin rock is strongly compressed by σ_0 in the plane $X — X$ perpendicular to the axis of the core, the rock core f tends to expand laterally. The expansion is a maximum at the end (t to t_1) but is prevented by the natural compression of the rock adjacent to section $X — X$. Moreover, this tendency is enhanced by the stress concentrations that arise around the bottom of the channels. When the core f has been cut out to a depth d the shearing forces in the surface $X — X$ are no longer able to counteract the expansive forces of the core, with the result that it is sheared off as a disc. The process is repeated as soon as the channel has been deepened a further distance d.

If the distribution of τ in the surface $X — X$ and the shearing strength of the rock are known, it should be possible to determine the magnitude of the rock pressure from the thickness of the discs. On the other hand, if the rock pressure and the τ distribution are known the shearing strength of the rock may be ascertained.

When a core is separated into discs no stress measurements can be made. However, it might be possible to avoid such fracturing of the core in the measurement procedure by the following method.

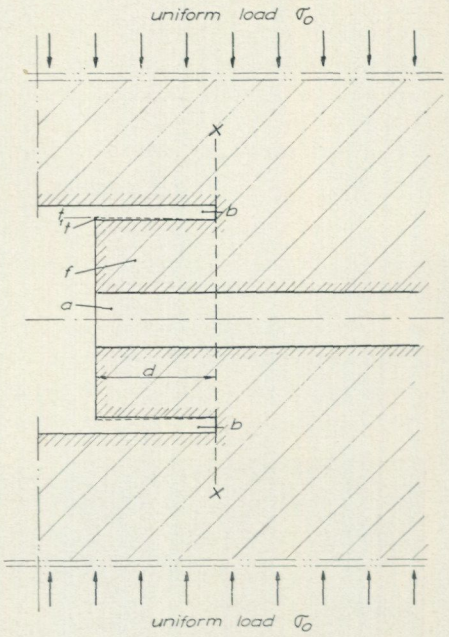

Fig. 22 b. The expansion of the core *f* is prevented at the bottom of the channel *b*. At a depth *d* the shearing forces in the plane × — × will be so high that the core will split off as a disc.

In Fig. 22 c *a* is a cell hole of diameter 26 mm and *b* the stress release channel. A cell unit — or a series of such units — is placed in the hole *a* and prestressed. Provided that an extremely high rock pressure σ_0 is acting, the core will separate into discs when the channel has been advanced a distance *d*. However, by first cutting stress release channels e_1, e_2 and e_3 remotely from the cell hole the stress field σ_0, or a part of it, is removed from the rock around the cell hole. The decrease in the pre-stress load on the cell unit is recorded during each of the operations e_1, e_2 and e_3. When the rock pressure has been

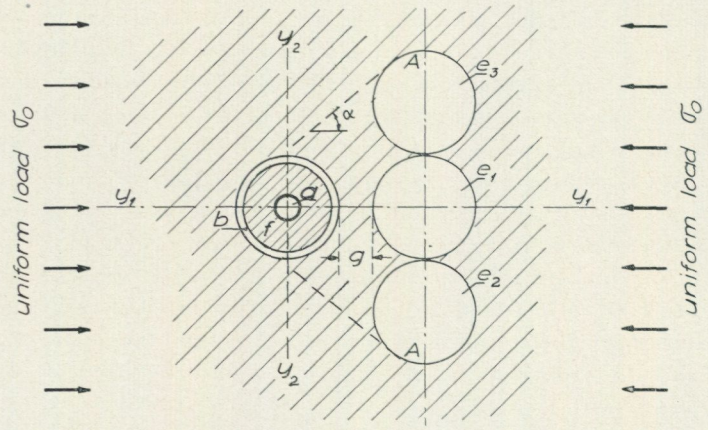

Fig. 22 c. If the rock pressure around the cell hole is so high that a separation of the core into discs may appear the stress measurements can be made in steps by first cutting stress release channels e_1, e_2 and e_3 remotely from the cell hole.

lowered in this way, the main channel b can be cut with less risk of separation of the core into discs.

The sum of the stress changes recorded on cutting e_1, e_2, e_3 and b is the pressure acting in the rock at a. It would seem best to place e_1, e_2 and e_3 in a straight line perpendicular to the direction of the highest stress component — in Fig. 22 c perpendicular to $y_1 - y_1$, the line of action of σ_0. However, the distance g must not be too small as the stresses in the direction $y_2 - y_2$ then might give rise to another unsuitable stress concentration in the rock core around a.

This method enables measurement to be made of extremely high surface stresses such as tend to cause rock bursts. Such measurements are necessary for the full interpretation of this phenomenon.

The stress-strain diagram for rock core materials

Uniaxial loading

The rock cores from points where the cell has been placed are removed in about 20 cm lengths and marked with the number of the measurement point at which the modulus of elasticity is to be determined. The length of the rock cores after the end surfaces have been planed is 15 cm, and the diameter 8.7 cm. In order to prevent friction between the cylinder and the steel plates in the press four sheets of blotting paper 0.5 mm in thickness are inserted at each end; these reduce friction and give a uniform distribution of the pressure.[1] The change in length on loading the cylinder is recorded by means of strain gauges or magnetostrictive instruments of original design; the later ones can also be used for measurement of the lateral deformation of the core.

Examples are given below of the stress-strain diagrams for rock from several Swedish mines — granite, leptite, amphibolite, limestone and magnetite ores.

The stress-strain curve for a perfectly elastic material is a straight line. When the material contains fissures the stress-strain diagram has an initial curve before becoming linear. This variation is due to the closing of the fissures on application of the load (Figs. 23 a and b).

Deformation measurements on rock cores, performed by increasing and decreasing the load through several cycles, will give the hysteresis effect for the rock as the difference between the stress-strain diagrams. As would be expected, the effect is closely related to the mechanical properties of the rock.

For values up to 700 kg/sq.cm such as were usually used rock of high modulus of elasticity displayed a very slight hysteresis effect, and as a rule no residual deformation after the removal of the load (Fig. 25 c and curve A in Fig. 24 a). The types of rock with somewhat lower moduli but rather high strength exhibited a higher hysteresis effect but insignificant residual deformation (B in Fig. 24 a). For rock with low moduli there appears in some

[1] For friction eliminating layers in compression tests see *Measuring stresses and deformations in solid materials* p. 84 by Nils Hast.

but not in all cases to be a marked hysteresis effect and large residual deformation (Fig. 23 b, c and 25 a, b).

At certain points of measurement the modulus of elasticity was between 300,000 and 400,000 kg/sq.cm for such types of rock as leptite and granite that in the same mine normally have values of 600,000 kg/sq.cm. These remarkably low values probably apply to points that have in earlier eras been subjected to great displacements (Figs. 25 a and b). On the other hand, moduli of 800,000 to 900,000 kg/sq.cm were also obtained for leptite and granite. Such points were situated near (about one metre from) the iron lens. Fig. 25 c shows such granite from Malmberget, where the iron infiltration cannot have been particularly great since the colour of the granite has not changed.

It seems probable that the hysteresis effect is related to the internal micro fissures in the material, which either are present initially or appear during loading. On change of load there is a mutual displacement of the surfaces in a fissure and since there are frictional forces acting, the material is prevented from changing its deformation on removal of the load in the same manner as when the load is applied. On complete removal of the load small grains due to rupture will remain on the fissure surfaces, especially if the internal fissuring is marked, and the fissures will be prevented from closing. This gives rise to residual deformation of the material.

The unloading member of the hysteresis loop is approximately parallel to the loading member, which indicates that the modulus of the material is about the same on loading and unloading if the region of maximum and minimum stress are disregarded. As Figs. 24 b and c and most of the stress-strain diagrams show, the rigidity of the material is higher than the mean value during the first interval of unloading, and is smaller when the load is small; this is consistent with the frictional phenomenon in internal fissures in the material.

Measurement of the absolute values of the stress by the method described involves the whole modulus range — the interval from, for instance, point *A* to the origin in Fig. 24 a. Provided that the rock is of such quality that there is no appreciable permanent deformation when the load has been removed, the stress values calculated will be correct. If the mechanical properties are not so good but there is a lateral pressure in the rock, no corrections will generally be necessary. If the longitudinally loaded core is subjected to lateral pressure the forming of the fissures and the displacements in them that give rise to the hysteresis loop in the recorded longitudinal deformation may be prevented. (Triaxial loading, see below). In rock with very low strength the corrections need be made with the guidance of load tests on the cores, which are then subjected also to a lateral load that is of the same order of magnitude as that normally acting on the core, a pressure that must be decreased as the axial load is decreased. If the rock is not stable, and plastic deformation occurs when the load exceeds a certain value, another stress measurement procedure is recommended which has been evolved by the author for use in highly fissured rock or in rock where plastic deformations occur. A more detailed treatment of this method will be given elsewhere.

Triaxial loading

Fig. 22 d is a section through an apparatus for triaxial loading of a rock cylinder (drill core).

A is a steel cylinder which is placed around a rock core *B* of standard type the outer diameter of which is 87 mm. The core is to be loaded symmetrically in lateral direction by a uniform load *t* and simultaneously in axial direction by a uniform load *p* all over its end surfaces. *C* is a cylindrical sheet of rubber 0.5 mm in thickness and persistent against oil. Its height is almost the same as that of the steel cylinder. *D* is a tightening ring of rubber which is pressed between a recess in the wall of the steel cylinder and the rubber sheet *C* by means of a steel ring *E* and 18 bolts *F* at each end. The ring *E* is cut diametrically into two parts to make it flexible and able to follow the movements taking place when the ring is pressed to obtain tightening.

The axial deformation of the core is recorded by strain gauges *I* fixed on to the surface of the measuring hole *a*.

By pumping oil through *G* the pressure *t* will act between the core and the steel cylinder, and the core will ce compressed laterally. The space *H* must be narrow so that the rubber sheet cannot expand through it. However, it must have a certain width so that no axial load will be transferred to the steel cylinder.

The measurements were performed in the following way. The rock cylinder was loaded only in axial direction with *p* ranging between 0 and 600 kg/sq.cm. The axial deformation of the core was recorded. It was also recorded in the subsequent unloading. Then a lateral load $t = 200$ kg/sq.cm was applied and another axial loading and unloading were made. Also in this case the deformation was recorded by the same strain gauges *I*. The lateral stresses inside the core are not evenly distributed. However, in principle this does not change the results recorded in the axial loadings as these are performed with a constant lateral pressure.

On pages 55—6 it has been discussed that rock materials can behave in various ways from an elastic point of view. It seems likely that this effect depends upon micro-fissuring of the material. There are (Figs. 23 a—25 c) three types observed

(1) Perfectly elastic materials the stress-strain diagram of which is a straight line; small or no hysteresis appears in the diagram in unloading the material.

(2) Elastic materials. The magnitude of *E* is lowest at small loads and increases with the load. In unloading hysteresis appears; no residual deformation appears after unloading the material.

(3) Rock materials as in (2) but residual deformation appears after unloading the material being stressed.

In the stress-strain diagram in Fig. 25 d, the curve A_0 represents the axial deformation of the core of rock of the type (1) recorded when $t = 0$ and the curve A_{200} the same when $t = 200$ kg/sq.cm. In this case (perfectly elastic material) the presence of the lateral load seems to be of no influence with respect to the value of *E*.

Fig. 25 e illustrates the effect of lateral loads on rock materials of the type (2) curves B_0 and B_{200}. It is evident that the value of E increases — the rock material will be more rigid — when a lateral load t is applied. When $p = 600$ kg/sq.cm and $t = 200$ kg/sq.cm the value of E for the rock material used increases about 7 %.

The effect of lateral loads on rock material of the type (3) is that the value of E is increasing as in the type (2). Moreover there are no residual deformations after unloading as in the case when no lateral forces are applied. It tells us that the lateral load prevents the micro-fissures from extending when the stress in the rock material increases as they would do in the case when no lateral forces were acting.

Fig. 25 f shows that the maximum magnitude of the hysteresis effect in unloading an axially stressed rock cylinder, type (2) or (3), is decreasing with increasing lateral loads t. In the case of unloading sample A_{200} almost no hysteresis effect appears until the axial load has been lowered to 400 kg/sq.cm. With increasing lateral load the hysteresis affect seems to decrease and probably disappear altogether when the magnitude of the lateral load is high enough.

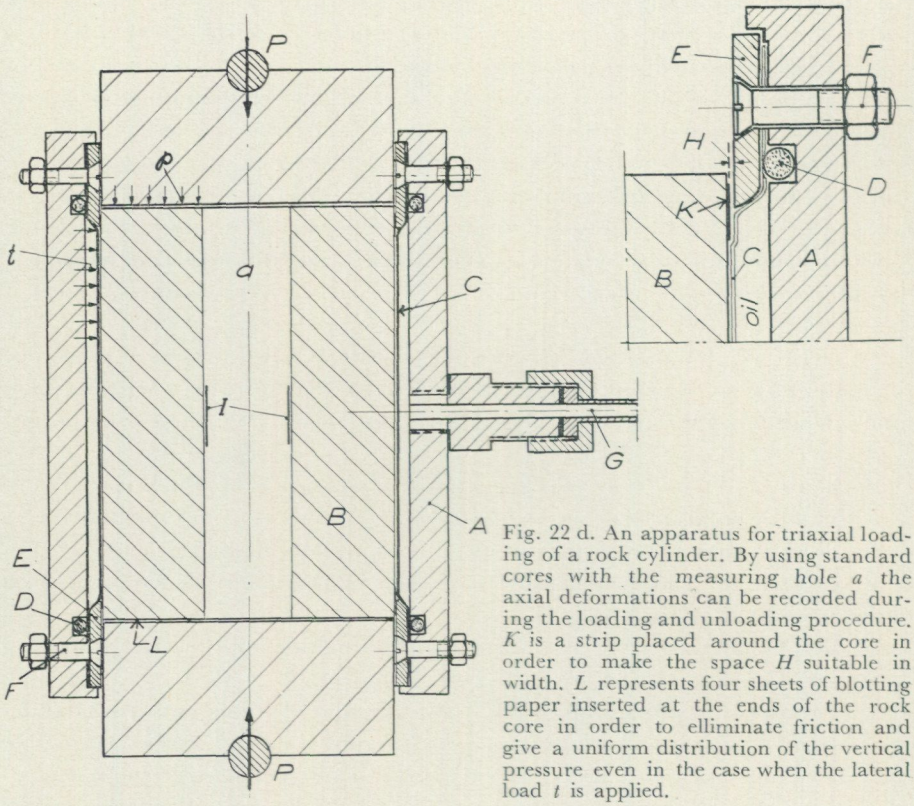

Fig. 22 d. An apparatus for triaxial loading of a rock cylinder. By using standard cores with the measuring hole *a* the axial deformations can be recorded during the loading and unloading procedure. *K* is a strip placed around the core in order to make the space *H* suitable in width. *L* represents four sheets of blotting paper inserted at the ends of the rock core in order to elliminate friction and give a uniform distribution of the vertical pressure even in the case when the lateral load *t* is applied.

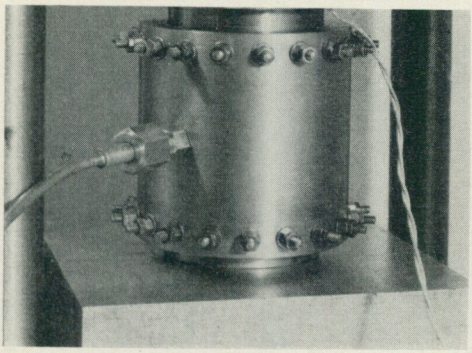

Fig. 22 c. A photo of the apparatus in Fig. 22 d.

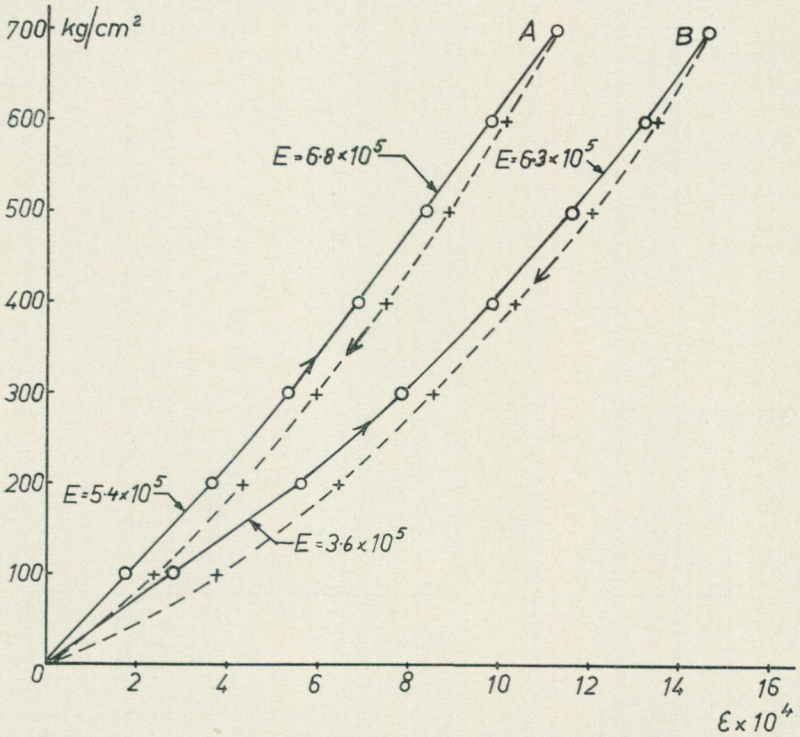

Fig. 23 a. Curve A is for red leptite and curve B for red granite from Malmberget. The broken lines show the deformation during unloading and the existence of a hysteresis effect. Repeated loading cycles gave the identical curves. For high loads the stress-strain diagram tends towards a straight line.

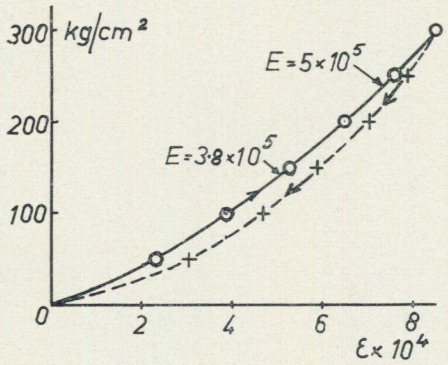

Fig. 23 b. Limestone from Ställberg.

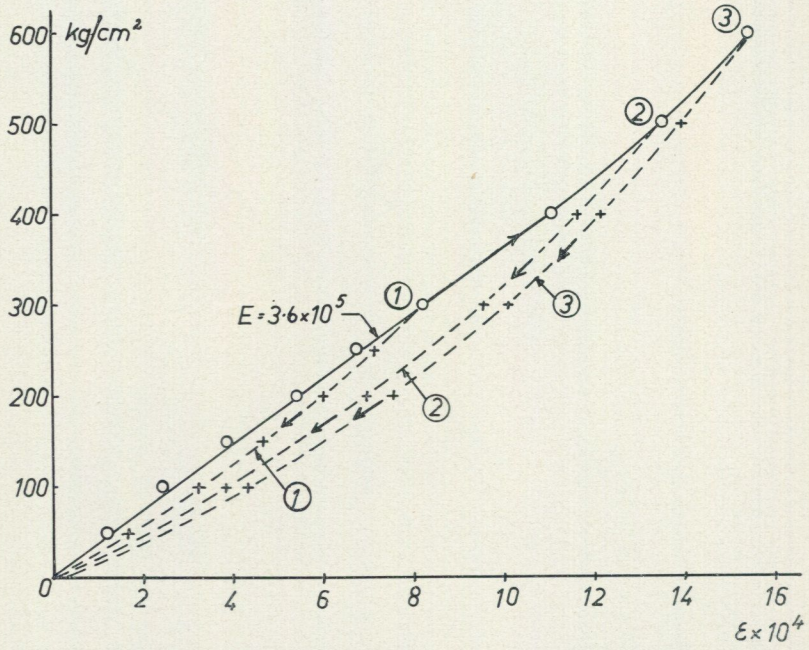

Fig. 23 c. Leptite from Ställberg having a low modulus of elasticity. The prism was loaded to 300, 500 and 600 kg/sq.cm in turn. In all cases the deformation on unloading was measured. It is evident that the residual deformation was of appreciable magnitude only for the highest load, and that the hysteresis effect increased markedly with the maximum load on the prism.

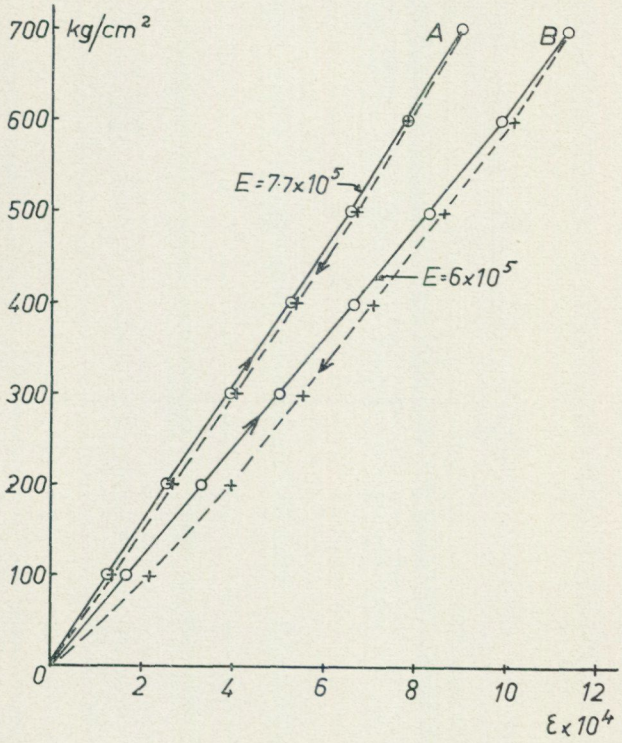

Fig. 24 a. Curve A represents leptite from Ställberg and curve B red leptite from Malmberget. On re-loading to 700 kg/sq.cm the increased deformation for material A was nil and for B about 2.5 per cent.

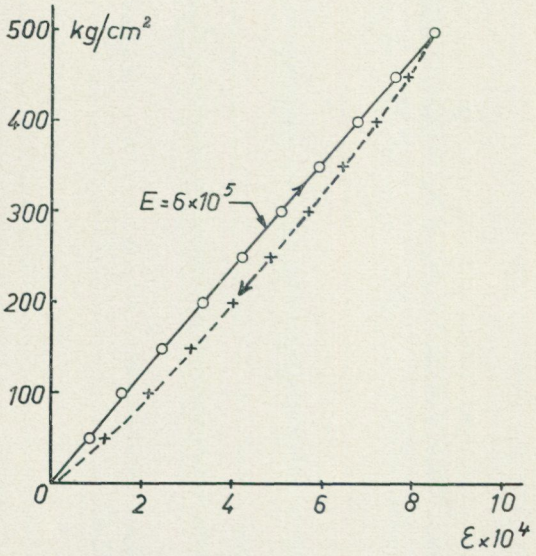

Fig. 24 b. Red granite from Malmberget. The modulus of elasticity was — as normally is the case — the same for the loading and unloading of the prism, except for the extreme ends of the curve.

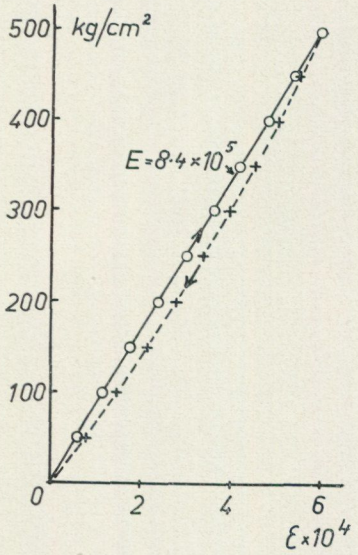

Fig. 24 c. Amphibolite from Vingesbacke.

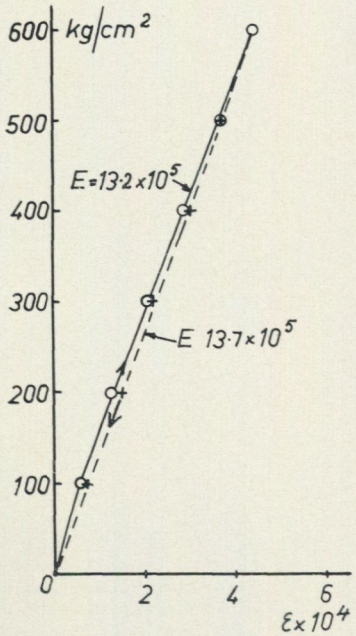

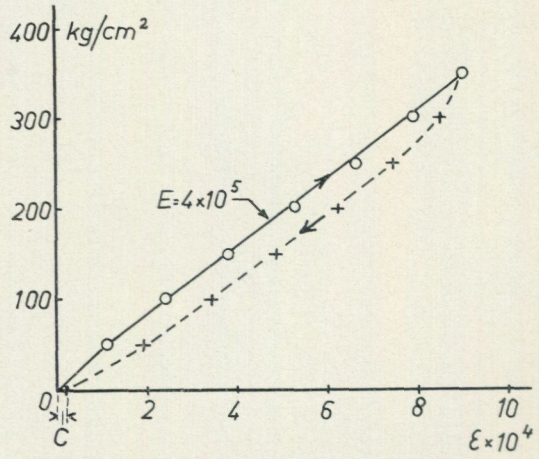

Fig. 25 b. Leptite from Ställberg with a low modulus of elasticity. Depth 460 cm from drift wall face. There is a marked hysteresis effect but small residual deformation.

Fig. 24 d. Magnetite ore from Ställberg.

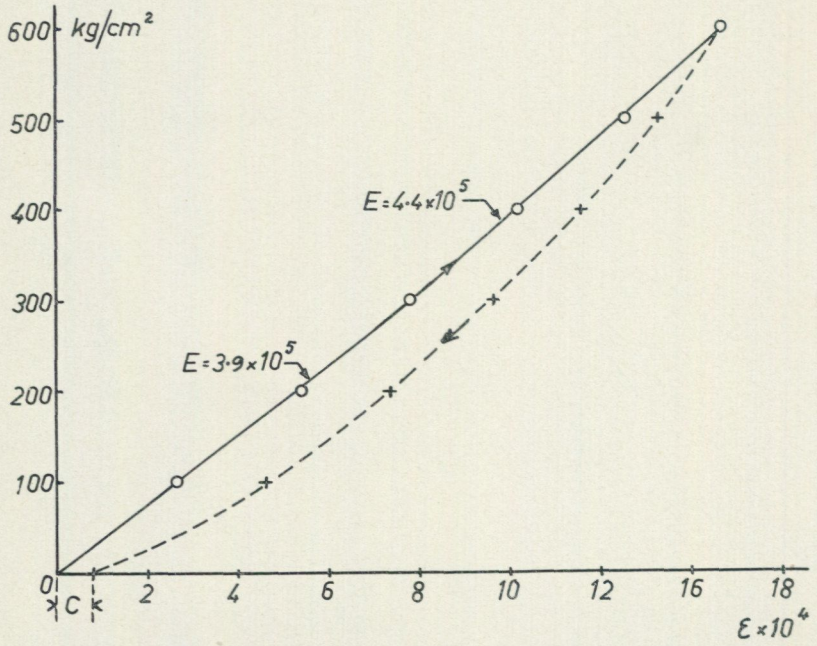

Fig. 25 a. Red granite from Malmberget. Depth 270 cm from the roof face of a drift. The modulus of elasticity is exceptionally low. A marked hysteresis effect and residual deformation of the prism are evident. The material of the core is probably fissured in its micro structure due to overloading during earlier eras.

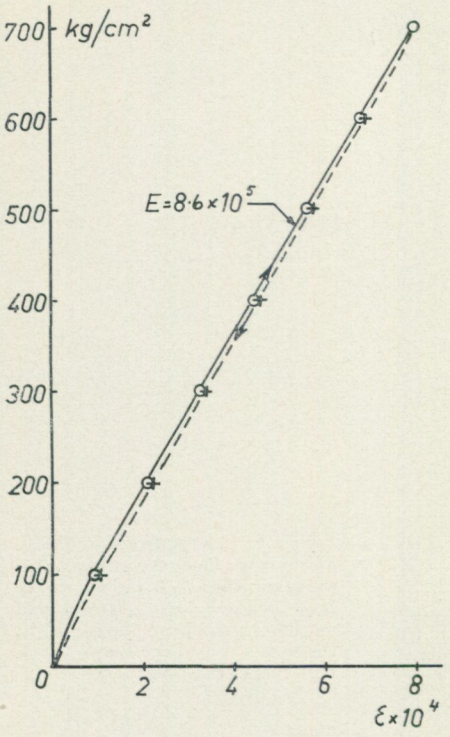

Fig. 25 c. Red granite. Sample taken at a depth of 120 cm from the roof face and 100 cm from the contact surface between the granite and the ore lens. The modulus of elasticity is about 50 per cent higher than the normal value for granite. The difference between the deformations on first and second loading is small.

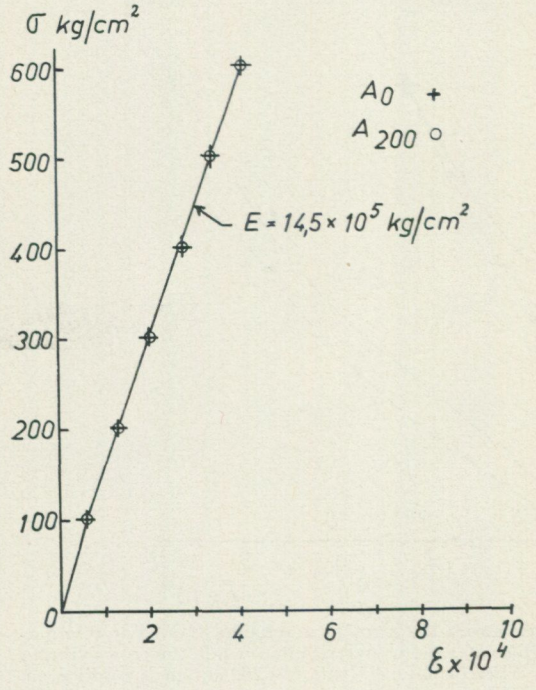

Fig. 25 d. Iron ore from Ställberg. The stress-strain diagram is a straight line and identical in uniaxial loading (A_0) and triaxial loading (A_{200}, t = 200 kg/sq.cm).

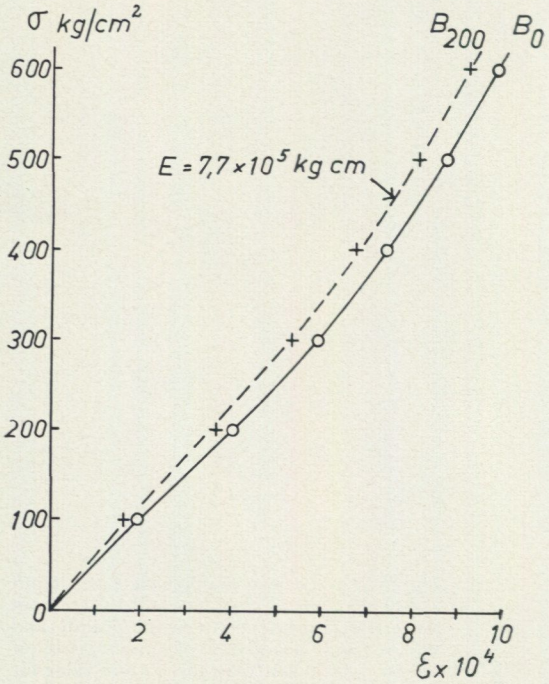

Fig. 25 e. Leptite from Ställberg. The curve B_0 is the stress-strain diagram when $t=0$ and the curve B_{200} the same when a lateral load $t=200$ kg/sq.cm is applied. In the latter case the value of E will increase about 7 %.

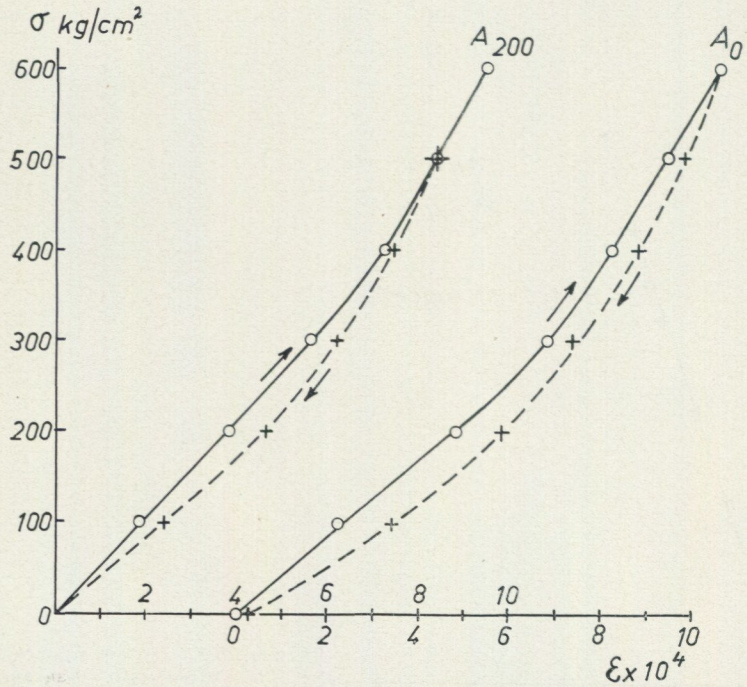

Fig. 25 f. Curve A_0 represents the stress-strain diagram fo a uniaxial loaded leptite material from Ställberg. The dashed line illustrates the hysteresis effect when the rock cylinder is unloaded. Curve A_{200} shows that when a lateral load $t=200$/sq.cm is applied no hysteresis effect excists in the beginning of the unloading procedure.

PART TWO

APPLICATION OF THE METHOD AT THE LAISVALL MINE

Geology

A typical profile of the Central Mine at Laisvall is the following: a soil stratum of several metres; mica schist and quartzite schist, 30 metres; various types of mylonite, 20 metres; more schist, 5 metres; various strata of sandstone, 36 metres; arkos, 3 metres, this lying directly on solid granite. Some of the sandstone strata are impregnated with PbS the content of which varies considerably from one stratum to another as well as laterally. The richest deposits are in the eastern corner, where the mining was first begun. The sandstone strata are generally mined to a depth of 10 metres, although in places this figure has been appreciably increased.

The sandstone is generally strong and hard. The rock strata are, however, interrupted in places by horizontal layers of clay, often no more than a few millimetres in thickness, although they may be several centimetres. These are of great lateral extent; as they become thinner they are often overlapped by others. The homogeneous sandstone strata may be several metres in thickness

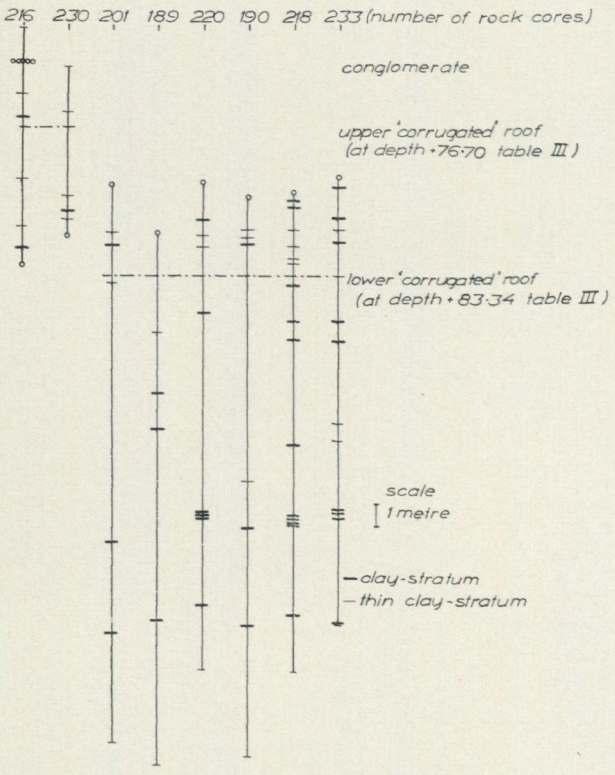

Fig. 26. Levels of the clay layers found in some rock cores.

TABLE III. *Geologic formation at Laisvall*

Borehole: Laisvall no. 246. Position: L 2000 N, p 191.0 E. Diam. 46 mm. Vertical.

Proof no.	Analyzed	Depth	Strata	Pb %	Length m	
					Section	Core
		0.00– 0.75	Above ground level			
		0.75– 6.09	Soil stratum			
		6.09– 26.10	Mica schist			
		26.10– 34.75	Quartzite schist			
		34.75– 39.50	Ultramylonite			
		39.50– 42.60	Sparagmite and arkos mylonite			
		42.60– 56.40	Syenite mylonite			
		56.40– 56.80	Dark schist		0.40	0.12
		56.80– 61.55	Clay schist		4.75	4.32
		61.55– 62.30	Upper sandstone (schist conglomerate)		0.75	0.74
		62.30– 64.19	» »		1.89	1.89
1584	A	64.19– 67.21	» » with PbS	2.68	3.02	3.00
		67.21– 73.81	Middle sandstone		6.60	6.47
1585	A	73.81– 76.13	Lower sandstone with PbS (at a depth of 76.13 clay stratum)	3.63	2.32	2.29
1586	A	76.13– 78.55	Lower sandstone with PbS (at a depth of 76.70 upper "corrugated" roof)	1.95	2.42	2.32
1587	A	78.55– 79.45	Lower sandstone with PbS	18.7	0.90	0.90
1588	A	79.45– 83.45	» » , yellow colored, with PbS (at a depth of 80.80 and 81.00 clay stratum) (at a depth of 83.34 lower "corrugated" roof)	2.87	4.00	3.97
1589	A	83.45 86.76	Lower sandstone with PbS	11.4	3.31	3.31
1590	A	86.76– 89.45	» » » » (at a depth of 86.84 and 89.45 clay strata)	2.05	2.69	2.67
1592	A	89.45– 92.57	Lower sandstone, dark with a small content of PbS	0.84	3.12	3.12
1591	A	92.57– 93.65	Lower sandstone, with PbS (at the lower end many clay strata)	4.03	1.08	1.08
		93.65– 95.50	Lower sandstone with clay		1.85	1.81
1593	A	95.50– 97.50	» » with PbS	1.96	2.00	2.00
		97.50–100.40	Arkos			
		100.40–101.44	Granite			
		Slut.				

though in places they are hardly one-half a metre. In a mine such as Laisvall, with plane roof spans of 15 metres, the stability of the roof is reduced to a serious extent if a clay stratum happens to lie too near the face.

In the Laisvall mine there are two characteristic levels in the sandstone strata; they are known as the upper and the lower "corrugated" roof. In the profile report reproduced in Table III the depths are given as 76.70 and 83.34 metres, respectively. The region around the deeper of these contains an unusually dense series of thin, horizontal strata of clay (Fig. 26).

In the Central mine there are two main directions of fissuring, which are roughly perpendicular to one another. The larger of two systems runs in a N—S direction and includes continuous sköls and open fissures, often water-bearing — a feature by means of which their presence is readily detected.

The fissure systems are practically vertical. As will be shown below, there is a clear relationship between the main direction of fissuring and the direction of the major principal stress in the roof and floor. Accurate knowledge of the fissure system is necessary, since there are often fissures in the pillars that may seriously reduce their strength. A system of spacing the pillars is discussed below in which the risk of their strength being diminished by the fissure systems is reduced to a minimum.

Stress measurements in pillars and walls

The rock pressure measurements in the Laisvall mine described in the following were performed during the years 1952—53.

Vertical loads on pillars and walls

The pillars in the Laisvall mine are spaced at 20—25 metres (measured from centre to centre), and the free span of the plane, horizontal roof between adjacent pillars is 15—18 metres (Fig. 27). The proposed diameter of the pillars is 7 metres, and their distance apart 22 metres, with a corresponding

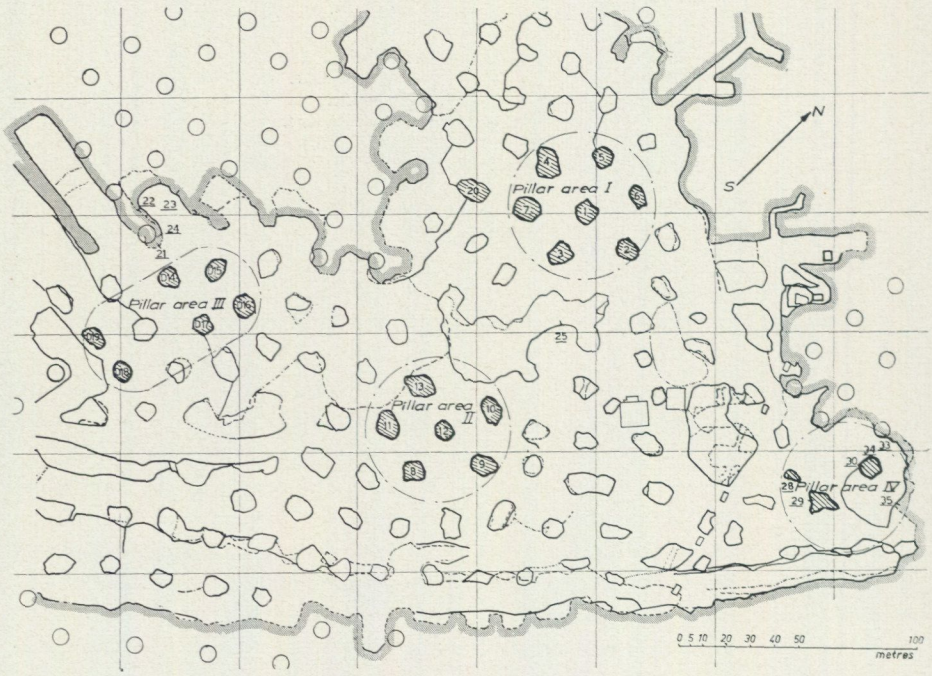

Fig. 27. Plan of the Laisvall mine showing location of pillars. The pillars in which stress measurements were made form four groups — areas I—IV — of different ages. The circles indicate proposed positions of pillars.

minimum free span of 15 metres. The cross-sectional areas vary widely owing to the breaking off of the rock along existing fissures and cleavages during blasting operations. This has also resulted in an uneven spacing of the pillars, and in a considerable variation in the thickness of the individual pillars between roof and floor. The load-carrying capacity of the pillars is thereby reduced. On first consideration, it might seem fairly obvious that the accidental narrowing of a pillar during the excavation might be compensated for by making the neighbouring pillars correspondingly wider. The problem is not so simple, however, for there is a risk of overloading the narrow pillars, as will be shown.

The pillars are generally 8—9 metres in height, but in some areas further excavation of ore has subsequently been made in the floor, as a result of which the height of some of the pillars has been increased to about 18 metres.

Both in the region already excavated and in the proposed extension, the size and spacing of pillars are such that they will occupy one-tenth of the total area. Since the overburden is generally almost 100 metres deep the dead weight may be responsible for a load of about 250 kg/sq.cm on the pillars. This, however, assumes that the pillars are evenly spaced, of equal cross-sectional area, of uniform thickness from roof to floor, and homogeneous — with no fissures or other zones of weakness.

It was obvious that the pillars in the Laisvall mine satisfied none of these four conditions. Consequently, an estimate of the safety of the pillars called for careful measurements of the individual pillars, a task that was undertaken by the management. The position of the pillars was accurately measured and from this data the roof spans were found. Moreover, the cross-sectional areas were measured, the pillar contours on the floor and roof, with any narrowing between these levels, being inserted in the plan. From these drawings it is possible to determine the area of the roof that represents the load on a certain pillar by virtue of its position in relation to the others (supported roof area, Fig. 28); from this quantity the corresponding load on the individual

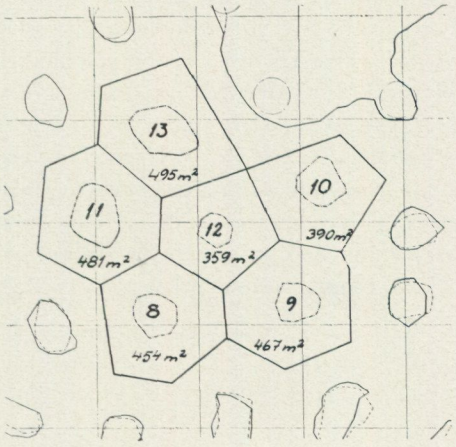

Fig. 28. The polygons around the pillars represent those areas of the roof for the support of which the pillars are individually responsible — the supported roof areas. Area II.

pillars due to the overburden is obtained. The loads so calculated may then be compared with those obtained from a direct measurement of the rock pressure. The measurements and calculations provide a picture of the actual stress distribution in the mine — for instance, the manner in which the total weight of the overburden is distributed between the pillars and the walls of the room. Moreover, it is possible to judge how the roof load is shared between a small pillar and an adjacent larger pillar.

Other fundamental problems to which the answers may be obtained from the described procedure are: Is a fissured pillar able to carry an appreciable load? How does the age of the pillar, counted from the time of its cutting, affect its strength over a number of years?

Of more than one hundred pillars in the mine, four groups have been chosen by way of illustration, these being denoted on the map (Fig. 27) by the roman numerals I—IV.

I. One of the earlier excavated areas consisting of 8 pillars situated near the shaft.
II. A somewhat younger part, consisting of 6 pillars, situated roughly in the centre of the mine.
III. A group of 6 pillars situated near the then working face.
IV. A group of 3 columns and 2 parts of the wall situated in the first part of the mine to be excavated.

The difference in age of the pillars in areas III and IV was about 15 years.

Measurements were also made in 2 pillar walls in the working face near area III (points 21—24) and in the large centre pillar (point 25).

CALCULATED PILLAR LOADS

Area II is taken by way of example. Fig. 28 shows the supported roof areas for the individual pillars, obtained by drawing in the perpendicular bisectors of the lines joining the centres of adjacent pillars. The continuous and broken contours of the pillars indicate the section of the pillar at the floor, and roof, respectively. The area of the polygon so formed multiplied by the dead weight of the overburden per unit area gives the load on the pillar. If the cross-sectional area of the pillar is known then the vertical stress thereon may be obtained. Tables IV—VII give the cross-sectional area, supported roof area, total load, and calculated vertical stress for the pillars in areas I—IV. These stress values relate to the cross-sectional areas of the pillars at the height above the floor at which the stresses were determined by direct measurement. These cross-sectional areas vary widely:

Area I	Variation in cross-sectional area	43	to 107	sq. metres
II		43	94	
III		43	64	
IV		28	72	

TABLE IV. *Pillar area I*

Pillar no.	Cross-sectional area A of pillar at level of measurement (sq.m)	Supported roof area on pillar (sq.m)	Total load on pillar in tons. Roof load 250 tons/sq.m	Vertical stress σ_V in pillar		$\frac{\sigma_V\text{-rec.}}{\sigma_V\text{-calc.}}$ (per cent)	Remarks	Smallest cross-sectional area A_s of pillar (sq.m)	$\frac{A}{A_s}$ (per cent)
				Calculated	Recorded				
1	64	500	125,000	195	79	40	Open fissure	45	70
2	51	440	110,000	216	126 255	59 118	Fissure	41	80
3	78	540	135,000	174	150[1] 224	86 128		59	75
4	107	450	113,000	106	119	112	70° Fiss.	79	74
5	61	475	119,000	195	64 191	34 98	Fissure	42	69
6	43	440	110,000	255	41[1]	16		28	65
7	89	550	137,000	156	194[1]	124	Closed fissure	67	75

TABLE V. *Pillar area II*

Pillar no.	Cross-sectional area A of pillar at level of measurement (sq.m)	Supported roof area on pillar (sq.m)	Total load on pillar in tons. Roof load 250 tons/sq.m	Vertical stress σ_V in pillar		$\frac{\sigma_V\text{-rec.}}{\sigma_V\text{-calc.}}$ (per cent)	Remarks	Smallest cross-sectional area A_s of pillar (sq.m)	$\frac{A}{A_s}$ (per cent)
				Calculated	Recorded				
8	55	454	113,500	206	204	99		45	82
9	57	467	117,000	205	240[1] 168[1] 108	117 82 53		50	88
10	72	390	97,500	135	106[1] 144[1]	Depth 100 cm 79 170 cm 107		62	86
11	88	481	120,000	137	125	91		88	100
12	43	359	90,000	209	180	86		32	74
13	94	495	124,000	132	111	84		94	100

[1] The stress release channel was made by the diamond drilling technique; in all other cases the seam-boring technique was used.

The total loads on the various pillars, calculated from the supported roof areas, range as follows:

Area I	Variation in pillar load	110,000 to	137,000 tons
II		90,000	124,000
III		87,000	110,000
IV		60,000	130,000

If area IV, the first of the areas excavated, is disregarded, the pillars there being very unevenly spaced, the calculated pillar load does not vary greatly. On the other hand, owing to large differences in the cross-sectional areas of the pillars, the calculated vertical stress would be much greater for the narrower than for the wider pillars. That this was so is evident from Tables

TABLE VI. *Pillar area III*

Pillar no.	Cross-sectional area A of pillar at level of measurement (sq.m)	Supported roof area on pillar (sq.m)	Total load on pillar in tons. Roof load 250 tons/sq.m	Vertical stress σ_V in pillar		$\frac{\sigma_V\text{-rec.}}{\sigma_V\text{-calc.}}$ (per cent)	Remarks	Smallest cross-sectional area A_s of pillar (sq.m)	$\frac{A}{A_s}$ (per cent)
				Calculated	Recorded				
14	43	440	110,000	255	70	28	Influence from wall	21	49
15	55	430	107,000	188	81	43	»	37	67
16	54	360	90,000	167	162	97		38	70
17	52	370	92,500	178	156	88		34	65
18	64	440	110,000	172	140	82		54	84
19	52	350	87,500	168	140 212	83 126		35	67

TABLE VII. *Pillar area IV*

Pillar no.	Cross-sectional area A of pillar at level of measurement (sq.m)	Supported roof area on pillar (sq.m)	Total load on pillar in tons. Roof load 250 tons/sq.m	Vertical stress σ_V in pillar		$\frac{\sigma_V\text{-rec.}}{\sigma_V\text{-calc.}}$ (per cent)	Remarks	Smallest cross-sectional area A_s of pillar (sq.m)	$\frac{A}{A_s}$ (per cent)
				Calculated	Recorded				
28	28	240	60,000	214	35	16	Fissure	24	85
29	72	520	130,000	180	—	0	Fissured rock	72	100
33	Wall	—	—	—	62 71				
34	63	360	90,000	142	33 87 114	23 61 80	Fissure	48	76
35	Wall	—	—	—	42 69				

In area III and IV the stress release channel was made by the diamond drilling technique

IV—VII. The problem of the extent to which a large pillar with a small load can relieve a small pillar that is carrying too high a load is of fundamental importance when estimating the required accuracy of pillar spacing. This is discussed below.

DEPRESSION OF THE ROOF AND FLOOR BY THE PILLAR AND ITS INFLUENCE ON THE BEARING CAPACITY

The function of the pillar is to transfer the roof load to the floor and the underlying strata. The total deformation that occurs in the system consisting of the roof, pillar and floor is the sum of the compression of the pillar and its depression of the roof and floor. With a knowledge of the area of contact between the pillar and the roof, and between the pillar and the floor, the

pressure per unit area of contact and the modulus of elasticity of the roof and floor material, the depth of the depression and its form around the head and foot of the pillar (funnel-shaped) may be calculated from expressions given by Boussinesq for a force that loads a hemisphere of infinite radius. The calculation of the deformation may be simplified by considering only the area immediately around the pillar. As is seen from Boussinesq's formulae given below, the deformation increases not only with the load per unit area but also with the diameter of the loaded surface — in this case the area of contact of the pillar with the roof and floor. In other words, a large pillar with a small load per unit area may give rise to as deep a depression in the roof face as a narrow pillar with a higher load per unit area. The deformation of the actual pillar is proportional to the vertical stress in it, but the total deformation may be as great for a larger pillar carrying a smaller load as for a small and heavily loaded pillar. The results of the following calculations relating to pillars in area II show the extent to which the neighbouring pillars may assist one another.

If the load σ_V from the pillar is assumed to be uniformly distributed over the surface of contact with the floor or roof (Fig. 29), then, according to Boussinesq, for a total unit load uniformly distributed over the whole contact surface the depression δ_0 at the centre of the surface is given by the expression

$$\delta_0 = \frac{1.57\ \alpha}{R} \quad \ldots\ldots\ldots\ldots \quad (5)$$

α being the factor $\frac{4}{\pi^2 E_r} \cdot \frac{(m^2 - 1)}{m^2}$

where R = semi-diameter of the pillar
E_r = modulus of elasticity of the roof material
m = the ratio between the axial deformation and the lateral elongation of the material in the body.

If the distribution of the load between the pillar and the roof and between the pillar and the floor is assumed to be parabolic, with $\sigma_V = 0$ at the boundary and a maximum at the centre, we have

$$\delta_0 = \frac{2.09\ \alpha}{R} \quad \ldots\ldots\ldots\ldots \quad (6)$$

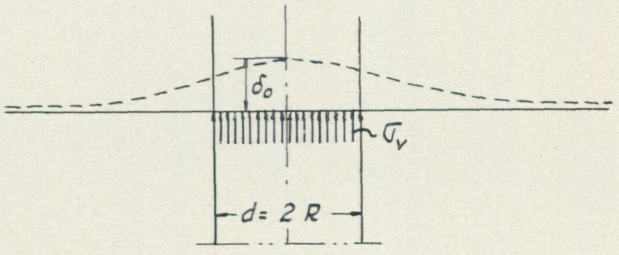

Fig. 29. Depression of the roof due to uniformly distributed pressure exerted by a pillar.

In fact, the actual distribution of the load is probably intermediate between parabolic and uniform. In one case measurements of the vertical stress showed increasing values from the face to the centre of the pillar. In the following it is assumed that there is a depression in the roof or floor of magnitude

$$\delta_r = \delta_f = \frac{1.8\,a}{R}, \quad \ldots\ldots\ldots\ldots \quad (3)$$

measured at the centre of the pillar.

The depression in the roof and floor at the boundary of the pillar will be less than this. However, the surface of the pillar is generally fractured, with the result that the stresses are lower in this zone. It would therefore be more correct to consider the deformation at the centre of the pillar.

The deformation of the pillar itself during the excavating process under the load of the overburden will be

$$\delta_p = \frac{0.9\,h \cdot P}{E_p \cdot A}, \quad \ldots\ldots\ldots\ldots \quad (4)$$

where h = height of the pillar
A = cross-sectional area of the pillar
P = total load on the pillar, of which about 10 per cent is inherent in the pillar material before its excavation
E_p = modulus of elasticity for the material of the pillar.

As mentioned above, the height of the pillar is generally 8—9 metres. In view of the large horizontal forces acting at the head and foot of the pillar, which render it more rigid, it may be considered justified to reduce the length of the pillar slightly in the following calculations — to, say, 7 metres. The presence of large horizontal forces in the roof and floor is dealt with below.

The total deformation, δ, in the vertical system of support — consisting of the roof, pillar and floor — is $\delta_r + \delta_p + \delta_f$.

Assuming that $\delta_r = \delta_f$ we have for a total load P,

$$\delta = P \cdot 2\,\delta_r + \delta_p.$$

Inserting the values from eqns. (3) and (4), we have, for the total deformation,

$$\delta = P \left[2 \cdot \frac{1.8\,a}{R} + \frac{0.9\,h}{E_p\,A}\right]. \quad \ldots\ldots\ldots\ldots \quad (5)$$

In this expression a may be replaced by

$$\frac{4}{\pi^2 E_r} \cdot \frac{m^2 - 1}{m^2}$$

It has been found from rock cores from the measurements that the homogeneous quartzite in pillars and roof has an elastic modulus of about 400,000 kg/sq.cm. The material in the floor is an arkos which has probably a lower ultimate strength than quartzite. As the bore profiles show, there are a large number of thin horizontal layers of clay between the sandstone strata in the rock that forms the roof of the mine. In view of the occurrence of the arkos and clay the modulus of elasticity $E_f = E_r$ is taken as 250,000 kg/sq.cm.

Then, substituting the appropriate values

$m = 4$
$h = 7$ metres
$E_p = 400{,}000$ kg/sq.cm
$E_r = 250{,}000$ »

we obtain

$$\delta = P\left[\frac{1.57}{1000\ A} + \frac{0.55}{100{,}000\ R}\right] \quad \ldots\ldots\ldots \quad (6)$$

The calculation of the value of δ has been performed for all the pillars in area II — that is, Nos. 8—13. In practice a pillar is not of uniform width and the contact areas at the roof and floor are generally unequal. This is taken into consideration in the calculation by denoting the cross-sectional area at the level of measurement by A and the mean value of the areas at the roof and floor by A_m.

The pillars of Area II will be considered in turn, and the appropriate values inserted in eqn. 6

Pillar 8

$P = 113{,}500$ tons
$A = 55$ sq.m

$$R = \sqrt{\frac{A_m}{\pi}} = \sqrt{\frac{53.5}{3.14}} = 4.1 \text{ metres.}$$

The total deformation of the system is then
$\delta_8 = 0.35 + 1.51 = 1.86$ cm

Pillar 9

$P = 117{,}000$ tons
$A = 57$ sq.m

$$R = \sqrt{\frac{55}{3.14}} = 4.2\text{m}$$

$\delta_9 = 0.32 + 1.53 = 1.85$ cm

Pillar 10

$P = 97{,}500$ tons
$A = 72$ sq.m

$$R = \sqrt{\frac{68}{3.14}} = 4.65 \text{ m}$$

$\delta_{10} = 0.22 + 1.15 = 1.37$ cm

Pillar 11

$$P = 120{,}000 \text{ tons}$$
$$A = 88 \text{ sq.m}$$
$$R = \sqrt{\frac{88.5}{3.14}} = 5.3 \text{ m}$$
$$\delta_{11} = 0.22 + 1.25 = 1.47 \text{ cm}$$

Pillar 12

$$P = 90{,}000 \text{ tons}$$
$$A = 43 \text{ sq.m}$$
$$R = \sqrt{\frac{38.5}{3.14}} = 3.5 \text{ m}$$
$$\delta_{12} = 0.33 + 1.41 = 1.74 \text{ cm}$$

Pillar 13

$$P = 124{,}000 \text{ tons}$$
$$A = 94 \text{ sq.m}$$
$$R = \sqrt{\frac{94}{3.14}} = 5.5 \text{ m}$$
$$\delta_{13} = 0.21 + 1.24 = 1.45 \text{ cm}$$

Of the pillars in Area II the largest and smallest cross-sectional areas are 94 and 43 sq.m for Nos. 13 and 12 respectively. The corresponding stresses, calculated on the basis of the supported roof areas, are then 132 and 209 kg/sq.cm. In spite of the difference between these values the vertical deformation of the supporting system at the centre of the pillar is roughly the same in both cases, 1.45 and 1.74 cm. This means that if the load on pillar 12 is reduced by 9 per cent and that on pillar 13 is increased by the same percentage the deformation of the two pillars will be the same; that is to say, there can no longer be a transference of load from one to another. The relief of pillar 12 at the expense of 13 or any other neighbouring pillar will therefore be insignificant, even were it possible to neglect the elastic deformation of the roof due to the redistribution of the load. This deformation has, in fact, a very marked influence and practically rules out a transference of load from one pillar to another *via* the roof, even where the pillars are fairly close to one another.

By way of illustration (Fig. 30), consider an instance where a part σ_1 of the carrying capacity of the pillar *A* may be available to support the load that according to the supported roof area, should be borne by pillar *B*. How great a part of this available capacity σ_1 can be assumed by pillar *B*? The problem may be expressed in another way: suppose that the effect of applying σ_1 directly to pillar B is represented by the depression *a* and that if the same

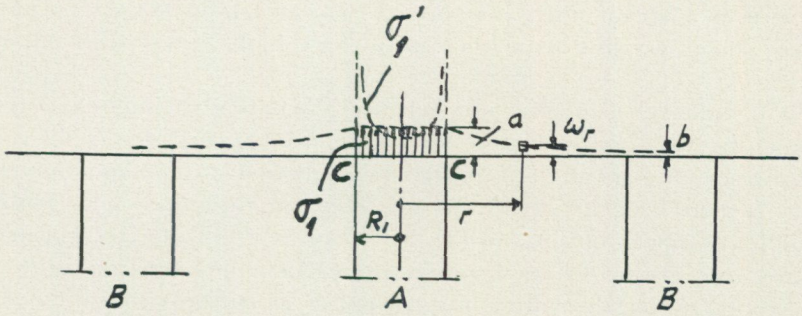

Fig. 30. Sharing of load between pillars having high and low vertical stresses.

σ_1 is applied to pillar A the deformation is b. The ratio $\frac{b}{a}$ is a measure of the potential transference of the load from A to B.

According to Boussinesq the form of the depression can be calculated for a roof such as the one in this example if the following data are known: the absolute value of σ_1, its distribution, the dimensions and spacing of the pillars, and the elasticity constants. However, these calculations will be complicated even when σ_1 is assumed to be uniformly applied to the area $c - c$ (Fig. 30). Only for the case where the area $c - c$ is assumed to remain plane, σ_1 then assuming values in accordance with the broken line of load distribution (σ_1') over pillar A, is a simple expression obtainable for the form of the depression. Denoting the depression for points outside the boundary of the pillar by ω_r we have

$$\omega_r = \frac{m^2 - 1}{m^2} \cdot \frac{1}{ER_1\ \pi} \cdot \sin^{-1} \frac{R_1}{r}$$

When $r = R_1$,

$$\omega_r = \frac{m^2 - 1}{m^2} \cdot \frac{1}{2\ ER_1},$$

and when $r = 6\ R_1$,

$$\omega_r = \frac{m^2 - 1}{m^2} \cdot \frac{1}{19\ ER_1}$$

The magnitude of b will be no more than approximately 10 per cent of a. Even if 50 per cent of the load-carrying capacity of A could be surrendered to pillar B, only one-tenth, and in favourable cases perhaps one-fifth, of this capacity could actually be assumed by B owing to the elastic behaviour of the roof. As a rule, the available fraction is much smaller than one-half. (See above calculation of the values of σ_V for pillars 8—13.) It is apparent, therefore, that *a narrow pillar that is over-loaded, with too high a value of* σ_V, *and located at a normal distance from a large pillar with a lower value of* σ_V *is not relieved to an appreciable extent by the presence of the larger pillar.*

In the case of adjacent pillars of roughly the same cross-sectional area but which are unequally loaded — owing, for example, to differences in their

supported roof area — there may be some re-distribution of the vertical load between them; but this is not the case as regards the over-loaded pillars at Laisvall.

This question of load distribution between pillars is of importance when planning the form and spacing of the pillars to be applied during the course of excavation at Laisvall. The pillars should be made approximately equal in size. If there is in the virgin rock a marked natural tendency for fissuring, the risk that a pillar will be fissured to the detriment of its load-carrying capacity is appreciably greater for smaller pillars than for larges ones (see below). If only for this reason, the cutting of small pillars should be avoided.

In the above argument it is assumed that the pillars behave elastically. If there should be a tendency for them to rupture and if marked plastic deformation has occurred, there will be a different re-distribution of the load, the intact pillars then assuming a higher proportion of the load.

However, the safety requirements will then not be fulfilled and the risk of roof failure will increase. These aspects cannot therefore be regarded as being of practical significance.

MEASURED AND THEORETICAL PILLAR STRESSES

Since the minimum cross-sectional area of the pillar is generally not more than 65—75 per cent of the area at the level of measurement, the maximum stress σ_V on the material in the pillars will be 50—30 per cent greater than the values given in the tables.

All the values obtained in the field work in areas I—IV have been included in Tables IV—VII except those relating to seam boring tests in which the rock core fractured during the drilling operation — generally owing to local tensile stresses set up in the rock of rather low tensile strength. Owing partly to this property of the rock, seam boring was replaced by diamond drilling. In Tables IV and V these values are indicated by an asterisk. In Tables VI and VII all data relate to the diamond drilling technique. Comments are made below on a number of pillars in each area. The presence of fissures in the pillars is entered in the table under the heading *Remarks*.

AREA I

From the column *Recorded* stress it is seen that $\sigma_{vert} = \sigma_V$ may vary widely within the individual pillar. No. 6, a small pillar — cross-sectional area 43 sq.m at measurement level and minimum area 28 sq.m higher up — had a vertical load of only 41 kg/sq.cm, compared with the calculated 255 kg/sq.cm. In general, the pillars of area I are very badly fissured, and the stresses vary widely from one to another; even more important, in the individual pillar the stress may be high in one place but practically zero in another. This is discussed below in connection with the significance of the age of the pillar.

Of No. 20, which is just outside area I, a part near the top was removed by error during the extension of a ventilation shaft, leaving a narrow section

in which the stresses are seriously high — considerably higher than in any other pillar in the mine. There is thus a risk of rupture at this point, and reinforcement is indicated. However, as is generally the case with weakened pillars this would be an extremely difficult and expensive measure.

AREA II

Pillar 9 is the only one of this group to have a non-uniform internal stress distribution. The pillars seem to be strong and fissures do not appear to the extent that they do in area I. The minimum area does not differ greatly from the area at the measurement level; No. 12 is an exception, with a percentage ratio of 74. However, the variation in the cross-sectional area from one pillar to another is large — 43 to 94 sq. metres — in spite of the fact that the range of the roof load area is no more than 359—495 sq. metres, with corresponding calculated loads of between 90,000 and 124,000 tons.

The theoretical stress is high — a little more than 200 kg/sq.cm for the small pillars 8, 9 and 12; it is least in the large pillars 10, 11 and 13, where σ_V is about 130 kg/sq.cm. The measured pillar stresses agree fairly well with the theoretical values, being about 90 per cent of them. The heavily loaded pillar 9 is an exception; the stress varies from one part of this pillar to another owing to the presence of cracks, measurements at three points giving values of 108, 168 and 240 kg/sq.cm. The theoretical value is 205 kg/sq.cm.

AREA III

Most of the pillars in area III are higher than those of area II, whereas their cross-sectional areas are on an average appreciably smaller. These longer pillars are not of such uniform thickness as are the shorter pillars in area II. The minimum areas range from 49 to 84 per cent of the area at measurement level, though this dimension does not vary greatly from one pillar to another — four of them being between 52 and 55 sq. metres, one 64 and one 43.

At the time the measurements were made, area III was near the working face. Pillars 14 and 15 had only recently been cut out from the rock wall. It is of interest to note that these two pillars were still not bearing their full load. The rock wall at the working face still carried a large part of the roof load that later on was to be transferred to the pillars. It is probable that 14 and 15 will not carry their full load until another room has been excavated. Time seems to be a major factor in this redistribution of the load.

If these two pillars are excepted, the measured pillar stresses are in fairly close agreement with the calculated values, being on an average about 90 per cent of them, as was the case for most of the pillars in area II.

AREA IV

This area being the site of the earliest excavation in the mine, the pillars are among the oldest. Measurement of the stress was performed in three of them, 28, 29 and 34, with cross-sectional areas of 28, 72 and 63 sq. metres respectively. All three pillars were much damaged by fissuring. Calculated

from the supported roof area, the stress in 28 and 29 is about 200 kg/sq.cm and on 34 about 140 kg/sq.cm. However, the first two pillars were found to be practically stressless; the stress in the third pillar varied, but the average was very much lower than the calculated value. It may be inferred, then, that the roof in this area is probably supported mainly by the adjacent boundary wall of the mine. For respective cell depths of 70 and 120 cm at point 33 in the wall the values of σ_V were 62 and 71 kg/sq.cm, and for depths of 30 and 70 cm at point 35 they were 42 and 69 kg/sq.cm. The load on the boundary wall was thus roughly twice as great as could be ascribed to the dead weight of the wall itself and the related parts of the roof. The reason that the pillars in this zone of excavation are not carrying their full load is discussed below (p. 81).

Horizontal rock pressure in the mine

HORIZONTAL STRESS AT THE PILLAR HEAD AND FOOT

In all 21 pillars of areas I—IV and in pillar 20 close to area I stress measurements were made at the foot of the pillar at a level of 1.2 metres above the floor. The stress was recorded in the vertical and at 60° on either side of the vertical; the major and minor principal stresses, σ_1 and σ_2, were then calculated. The values of σ_1 $(= \sigma_V)$ are given in Tables IV—VII. The values of σ_2, expressed as a percentage of σ_1, are given in Fig. 31. The figures for the vertical stress should in fact have been increased slightly owing to the existence of a stress acting parallel to the axis of the rock core, and deriving from the horizontal rock pressure in the floor. However, owing to technical difficulties these axial stresses in the core were not recorded while it was being drilled. The seam boring measurements and most of the other stress determinations in the pillars were performed at a depth of 40—80 cm from the face of the pillar. As the stress perpendicular to the face is zero in and near the pillar face the horizontal pressure cannot have attained its full value in this direction at only 40—80 cm. Measured perpendicular to the axis of the cell hole the

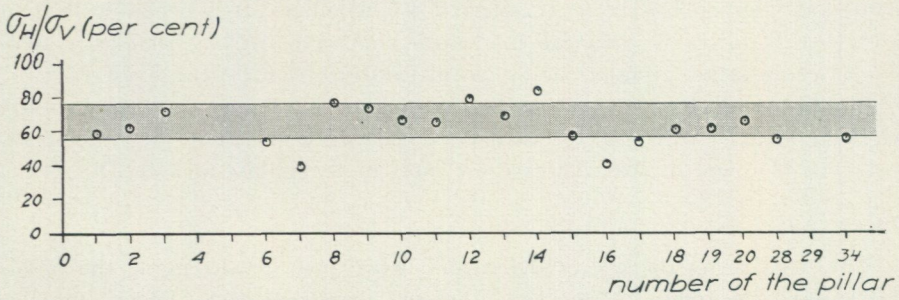

Fig. 31. Horizontal stresses in pillars expressed as a percentage of the vertical stress (measured at 1.2 metres above floor level). The values of σ_H lie in the region of $\sigma_H = 2/3\ \sigma_V$, indicating high horizontal pressure at the foot and head of the pillars.

horizontal stress, σ_H, is approximately equal to two-thirds of the vertical stress σ_V. Measured perpendicular to, and a short distance from, the face the horizontal stress ought then to be considerably less. Approximately, $\sigma_H = 0.3\ \sigma_V$. As no correction for this unmeasured horizontal stress was made in Table IV an error may have been introduced. This is estimated at $\frac{1}{2} \cdot 0.3\ \nu\sigma_V$ where ν is Poisson's ratio for the material; the error is thus about 4 per cent of σ_V, and is small enough to be included in the general margin of uncertainty.

Fig. 31 refers to pillars 1—20, 28, 29 and 34. No values of σ_H/σ_V are given in the diagram for pillars 4, 5 and 29. The two first had such large fissures that the natural lateral pressure conditions were completely changed (Fig. 33), and 29 was practically stressless.

It is evident from the diagram that at the foot of the pillar there is a natural horizontal pressure that originates in the floor. The same will apply to the head of the pillar and the roof. As the pillars are generally about 7 metres in diameter, and as the measurements were performed about 1.2 metres above floor level there are natural horizontal forces acting even at the level of measurement. As Fig. 31 shows, $\sigma_H \backsim 2/3\ \sigma_V$. With a margin of uncertainty of $\pm$ 0.1 σ_V — that is, for values of σ_H between 0.57 σ_V and 0.77 σ_V, — all pillars are included with the exception of 7, 14 and 16. Pillar 7 has large internal fissures (Fig. 33), and the floor in the vicinity of 16 is very badly damaged by fissuring (Fig. 35). In the cases where several stress measurements were made in the same pillar the mean is given.

A possible explanation of the horizontal rock pressure, the presence of which is confirmed by the measurements, is discussed below (p. 90). The rock pressure, which is perhaps of geologic origin, is acting throughout the area of excavation. There should then be a horizontal pressure in the roof, the floor and the adjacent part of the pillars. The same is true for the boundary walls — that is to say, in all new or old working faces. The roof and floor stresses are treated in greater detail below (p. 82).

HORIZONTAL STRESS IN WALLS AND WALL PILLARS

Points 21—24 are situated at the working face, all but point 23 being in a wall pillar at that time being cut; it lies in an E-W direction — that is, perpendicular to the main fissure system. At points 22 and 24 the horizontal stress was determined in an E—W direction — that is, parallel to the longitudinal dimension of the wall pillars —, but at point 21 in the N—S line, parallel to the narrowest dimension of the wall pillars (Fig. 27). The stresses determined are at

Point 21:	$\sigma_H =$	101	142	162 kg/sq.cm	at a depth from wall face of
	$\sigma_V =$	127	112	122	80, 115 and 145 cm resp.
22:	$\sigma_H =$	105	80		55 and 100
	$\sigma_V =$	77	105		

23:	σ_H = 186	152	116	50, 90 and 130
	σ_V = 154	113	70	
24:	σ_H = 94	82	73	130, 165 and 200 cm
	σ_V = 180	160	139	

Owing to superficial damage to the pillars and walls inflicted during blasting operations there will normally be a superficial zone of released stress. If this zone is disregarded, it is generally true that the stress in the wall of the working face is highest near the surface, and diminishes with depth. In principle, the conditions are much the same as in a drift wall. The rate at which the stress falls is dependent on the dimensions of the room. The existence of high stresses in both the horizontal and vertical directions is evident from the values given above. The deviation in respect of point 21 is probably to be ascribed to its position in the rounded end of the pillar wall, where a more homogenous stress distribution would be expected.

For a depth of about 130 cm the approximate values of σ_H are:

Point 21: σ_H = 152 kg/sq.cm Point 22: σ_H = 70 kg/sq.cm
23: = 116 24: = 94

There is thus an average E—W horizontal stress at points 22, 23 and 24 of less than 100 kg/sq.cm, while in the N—S direction, as recorded at point 21, it is about 150 kg/sq.cm, in spite of the fact that the stresses from the roof and floor should be more easily transmitted parallel to, than at right angles to the length of the pillar.

It would thus appear that the head and foot of all the pillars are subjected to directional horizontal forces. Those acting in the roof and floor appear to be roughly 50 per cent greater in the main direction of fissuring than at right angles thereto. At 6 points in the roof and 2 in the floor the horizontal stresses and their directional distribution in the horizontal plane were measured. As appears from the following, these measurements are in close agreement with the above estimates.

Measurements of the vertical and horizontal stresses at two points, 33 and 35, in the boundary walls around the first area of the mine to be excavated revealed that there, too, large horizontal stresses are acting. The vertical and horizontal stresses are almost equal.

Point 33	σ_H = 90	87 kg/sq. cm	at 70 and 120 cm, resp.
	σ_V = 62	71	
Point 35	σ_H = 54	63	30 and 70 cm
	σ_V = 42	69	

HORIZONTAL STRESS IN THE CENTRAL PILLAR, POINT 25

In the Laisvall mine there is a large pillar measuring in places about 70 metres in length and some 20 metres wide. This pillar, the ore content of which does not warrant its excavation, constitutes an important factor in the

stability of the room. Measurements have shown the presence of a stress concentration in this pillar, the values being high in both vertical and horizontal directions, and roughly equal in magnitude (Fig. 27).

Point 25 $\sigma_H = 324$ 326 kg/sq.cm
$\sigma_V = 332$ 320
} at 80 and 130 cm, resp.

From the comments on the stress measurement in areas I and II it is clear that the loads on the pillars are smaller than would be expected from the supported roof areas — for area II about 10 per cent and for area I even lower. It is probable that an essential part of these "lost" stresses is located in the central pillar. By virtue of its large cross-sectional area the pillar also absorbs large horizontal forces. It may be shown that σ_H in the pillar is of the same magnitude as the major principal stress a short distance from the rock face of the roof (Figs. 37a, b and c).

Fissures and pillar strength

The rock in the Laisvall mine is traversed by several fissure systems, the largest of them lying in a N—S direction, with another roughly perpendicular to it.

The fissures appear in many of the pillars and constitute an important factor in determining their strength, for which reason an inspection of the state of each pillar was made at the same time as the stresses were measured.

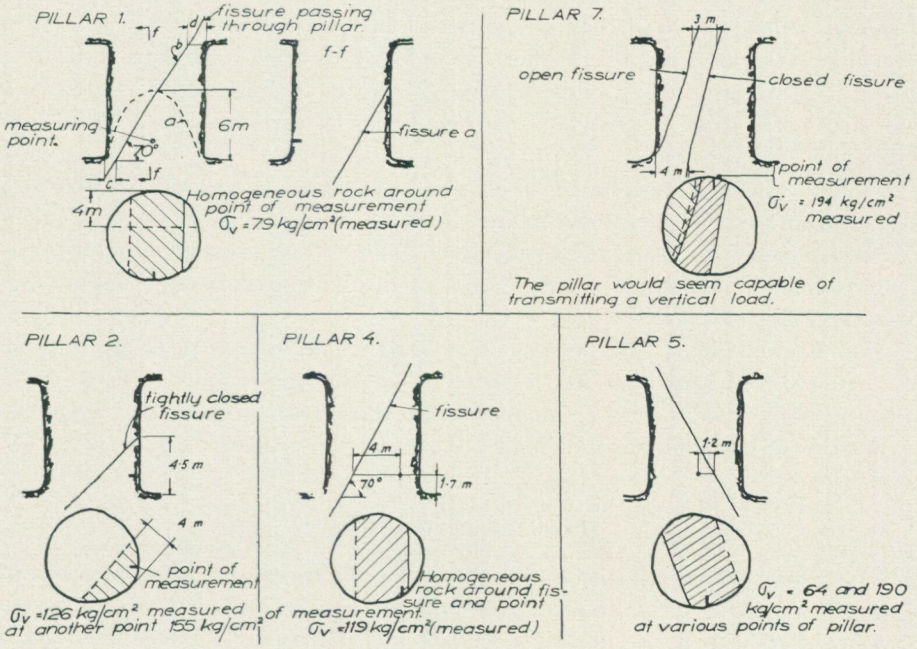

Fig. 33. Examples of fissures in pillars of area I.

The inclination of the fissures was found to be roughly the same throughout the whole mine. In the case of a high and narrow pillar there is the risk that the fissures will pass through the pillar far enough seriously to reduce their strength.

By way of illustration Fig. 33 shows conditions of pillars 1, 2, 4, 5 and 7, all of which are in area I, where the fissures are more numerous than in the other areas that were excavated more recently. Fissuring in areas II and III is appreciably less pronounced than in I, whereas that in area IV, the oldest of them, appears to be worse. Pillar 1 has two fissures that are approximately perpendicular to one another. Fissure *a* extends about half-way through the pillar, while *b* passes from the head to the foot. Owing to the great width of this pillar the oblique crack lies wholly within it, but it is evident that the strength of the pillar must be appreciably diminished by the presence of these two fissures. The stress values for the pillar would normally be about 250 kg/sq.cm but at the point illustrated only about 80 kg/sq.cm was recorded. For the vertical load to be transferred down through the pillar to the floor the fissure surfaces must be pressed tightly together so that there is friction between them; moreover, the distances *c* and *d* must be large enough to provide the shearing stresses in these narrow sections and thus to ensure stability.

Pillar 2 also contains an oblique fissure. This is closed and passes through the lower part of the pillar, so that there is a greater likelihood of stabilization of the forces acting in the fissure. Measurements showed that the vertical stresses in the part of the pillar just below the fissure are comparatively high, though still lower than they would be in an intact pillar.

Pillars 4 and 5 provide further examples of fissuring and sköls. It is true that the cracks do not pass right through the pillar, but the intact parts are probably too small for the pillar to be capable of carrying appreciable loads for long.

Pillar 7 has an open fissure that reaches the face at the foot. No load can be transmitted by the wedge-shaped part of the pillar so formed. There is also a closed fissure, across which forces might be transmitted provided that the horizontal component of the forces can be stabilized by shearing stresses at the head and foot.

In fissured pillars such as Nos. 1, 4 and 5 there is a fairly large internal stress variation, and therefore a danger that the pillars will gradually split. In the long run, therefore, such fissured pillars will probably be unable to carry their share of the roof load.

Age and pillar strength

The influence of age on the strength of the pillars, expressed as the relationship between the age of the pillar and the ratio of the recorded to the calculated value of the stress, is shown in Fig. 34 and Tables IV-VII. As mentioned above, the age of the pillars is reflected by their group, the order of age being

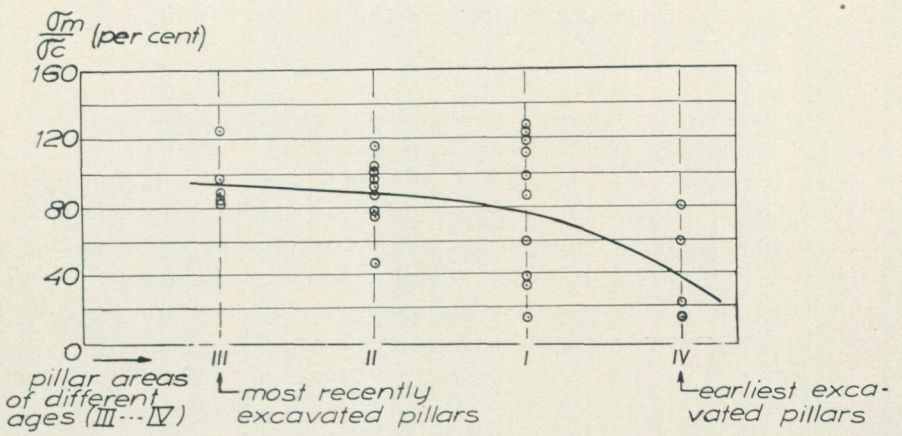

Fig. 34. The load-bearing capacity of a pillar decreases with time. The pillars of area III are the youngest and those of area IV the oldest ones. The ratio of the measured to the calculated vertical stress is constant at about 90 per cent in the youngest group, but varies widely with increasing age of the pillars.

III, II, I and IV, where III is the youngest group and IV the oldest. The difference in age between the pillars in areas III and IV is about 15 years. Pillars 14 and 15 have been omitted from the diagram, these being so near the working face, the massive boundary wall, that they could not assume their full share of the roof load.

For the pillars of area III the ratio is about 90 per cent, the figures for the individual pillars being rather similar. In area II the ratio is fairly consistent at about the 90 per cent line, but for the two oldest pillar groups, I and IV, an appreciably greater dispersion is evident.

The load-carrying capacity of the pillars changes with age in two ways:

1. The load on the pillars gradually decreases with time.

2. In the individual pillar the stress distribution tends to become less uniform, which implies that certain areas of the pillars are relieved of stress while in others the stress is increased. This redistribution in the brittle rock probably occurs through the formation and extension of fissures from the internal stress concentrations, which in many cases will have been set up at the time the pillar was being cut out. The marked dispersion of the stress and the low residual loads on the pillars of area IV seem to represent a final phase in the stress flow with the passage of time.

The possibility cannot be ruled out that the pillars of areas I and IV may originally have been more severely fissured than those of the other areas, though this does not appear to have been the case in respect of the fissuring existing in the roof or the walls in the areas. It is still possible, however, that the tensile strength of the sandstone is lower, and the stress flow with the passage of time greater in I and IV than elsewhere, since in these areas the quartzite has the highest lead content — 10-12 per cent, against the normal 3-5 per cent in the parts of the mine now being worked.

Stress measurements in the roof and floor

The stability of the roof

The plane roof over the room in Laisvall presents difficult problems from the aspect of strength and safety. The main risk is that the roof will fracture in places and fall. Rock bursts in some parts of the mine further increase this danger.

According to the current system the pillars are generally placed not more than 15 metres apart, the minimum distance compatible with the use of machines for loading. An increase to 18 or 20 metres would permit greater mobility of these machines, but would result in an increase in the tensile stress in the roof span and thus enhance the risk of subsidence.

The study of the distribution of stress in the roof is therefore of major importance, chiefly as a means of ascertaining the condition of stability of the roof, and how it may be affected by the passage of time. For a calculation of the effect of an increase in the free span it is necessary to know the present magnitude and direction of the roof stresses and how they may be influenced by such an increase in the span.

The roof material is sandstone or quartzite, which borings have shown to be interrupted by clay layers. These are nearly horizontal and sometimes less than one metre apart. They are between one and ten millimetres in thickness and are of great lateral extent. In places, however, they thin out and disappear, only to be replaced almost immediately by others. They are generally plane, though they may be slightly curved or corrugated.

Even if the roof were homogeneous the overburden would set up tensile stress in the face. In view of the low ultimate tensile strength of rock, and especially sandstone, there will be a risk of a roof caving. The presence of clay layers greatly prejudices the stability of the roof. The roof plates, which in places are hardly more than one metre thick, will then act as beams or slabs supported by the pillars, and loaded by the overlying clay stratum, which in turn is loaded by the rest of the overburden. The tensile stresses in the roof face are then much greater than if the roof were solid for an appreciable depth. It is evident, then, that measurement of the roof stresses constituted an important part of the programme for the study of the Laisvall mine.

Large horizontal compressive stresses were found to be acting in the roof. Measurements at two points in the floor confirmed the presence there too of high compressive stresses. The magnitude and direction of the principal stresses were calculated from the figures obtained for the 5 roof and 2 floor points (pp. 85—8). The horizontal stresses in the boundary walls and the central pillar have been dealt with above (points 21—24, 25, 33 and 35, pp. 77—9).

Compressive stresses in the roof and floor

Stress measurements described above (pp. 76—7) revealed large lateral forces acting at the ends of the pillars. The presence has also been shown of large horizontal forces acting at the central pillar and in the boundary walls. At

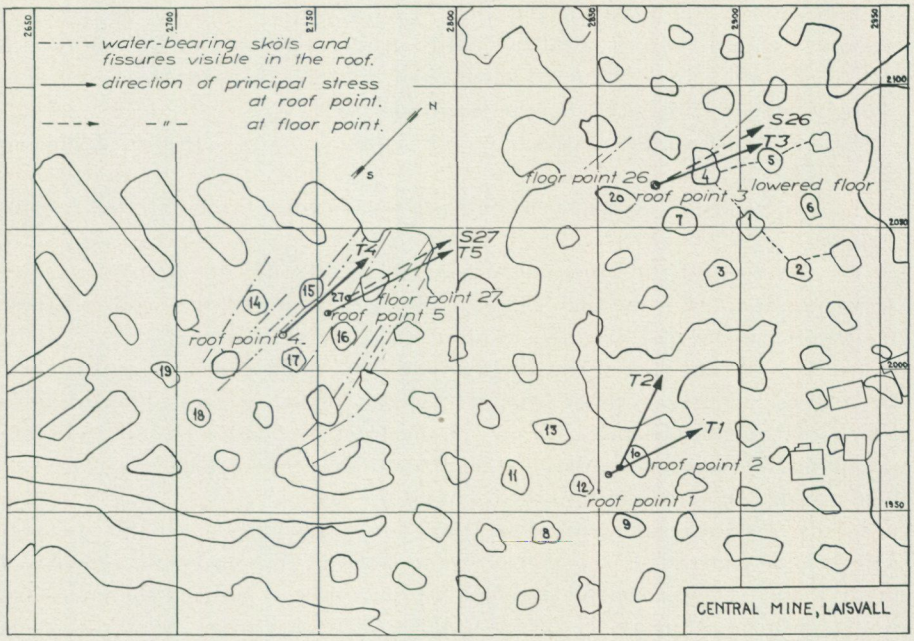

Fig. 35. Location of the five roof points and two floor points. T_1-T_5 and S_{26} and S_{27} indicate direction of the measured major principal stress at these points, and its position in relation to the main direction of fissuring.

point 25 in the central pillar the stresses are greater than at any other part of the mine. It is probable that the rock in the roof and the floor is subjected to large horizontal forces in all directions, and that it is chiefly these forces that give rise to the reactions in the pillars and walls.

The compressive stresses in the roof were measured at 5 points. They are situated as follows:

Point 1	halfway between pillars	10 and	12	in area II
2	halfway between point 1 and pillar		10	II
3	halfway between pillars	4 and	20	I
4		14	17	III
5		15	16	III

The positions of the points are shown in Fig. 35, in which the fissures and water-bearing sköls have also been entered. The fissures are seen to be very numerous in area III.

The stress determinations in the floor were performed at two points:

Point 26		immediately	below	roof	point	3
27	almost	»	»	»	»	5

The stresses were measured at several points down to a depth of 2—2.5 metres from the rock face. Owing to the fissured state of the floor that was

probably due to the blasting operation, reliable values could not be obtained at point 27 until a depth of 80 cm had been reached. At point 26 one or two low stress-values were recorded fairly near the face, but the readings were probably much influenced by the neighbouring fissures.

The roof and floor determinations were carried out so as to give the following information:

(1) The variation of the horizontal principal stresses from the roof face to a depth of 2—2.5 metres.

(2) The form of the horizontal stress ellipse and the direction of its axes at various depths from the roof face. It was required to know whether the stresses in the roof and floor exhibit a directional variation.

For the roof and floor points the diamond rock drilling technique was used. By drilling the stress release channel a series of values was obtained from which the magnitude and direction of the horizontal principal stresses were calculated for various depths by the method detailed in Part one. The cell hole was drilled vertically into the roof and the floor.

As the stress measurements show, there are disturbances near the roof face. These would generally be due to fissures and sköls but, as is seen in the case of roof point 1, the proximity of the larger pillars or projecting parts of the boundary walls appear to influence the direction of the principal stresses. At all the points the direction of the major principal stress at fairly great depth in the roof is approximately N-S — that is, near the general direction of the fissures in the mine; the direction is approximately the same for all the roof and floor points (Fig. 35). It is evident that the horizontal stresses in the roof and floor vary considerably with direction. At a depth of 1.5 metres the ratio between the minor and major principal stresses, σ_2/σ_1, is between 0.4 and 0.6 for all except point 5 in the roof and 26 in the floor, for which the values are 0.3 and 0.7, respectively. Since the minor principal stress σ_2 is roughly perpendicular to the main direction of fissuring and many fissures could be

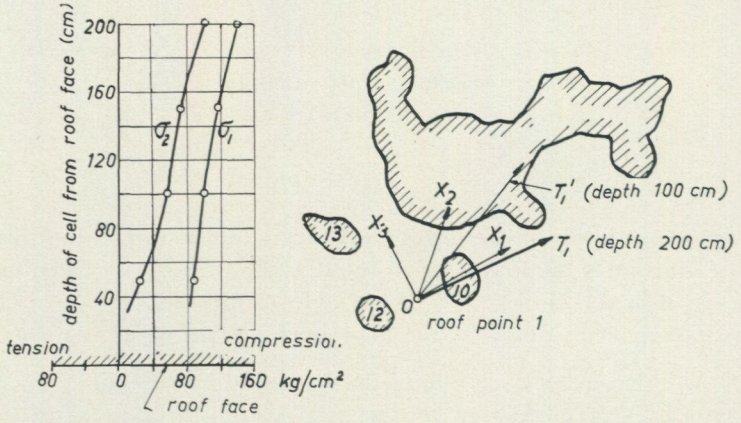

Fig. 36 a. Roof point 1. Magnitude of principal stresses at varying depths from the roof face; cell hole vertical. Direction of the major principal stress T_1' at a depth of 100 cm, towards the large central pillar. At greater depth the direction changes until it is parallel to those of the other roof points.

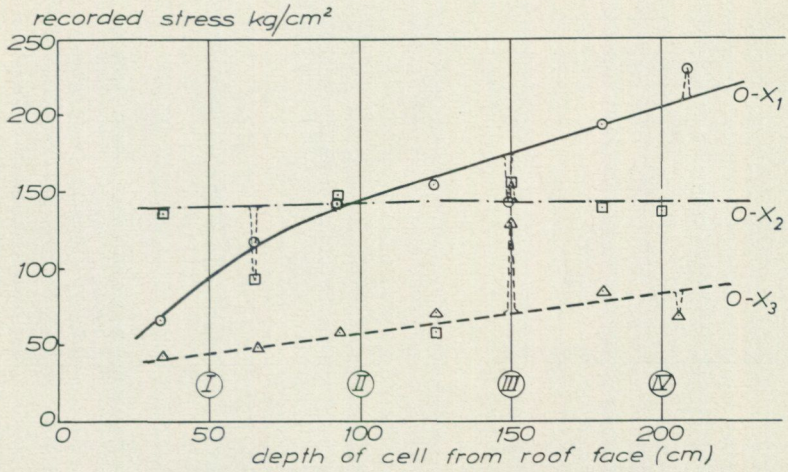

Fig. 36 b. Interpolation diagram for calculation of the magnitude of the principal stresses at various depths from the roof face (Sections I—IV). Roof point 1. Fissures are appearing in the core at a depth of 150 and 210 cm (p. 33).

observed near the measurement points it is hardly surprising that the values of σ_2 are rather inconsistent for the different depths and points.

Each of the roof and floor points will be commented on briefly.

ROOF POINT 1 — situated mid-way between pillars 10 and 12.

The interpolation diagram for this point (Fig. 36 b) shows the variation of the stress with depth in the three directions OX_1, OX_2 and OX_3, the angle between OX_2 and the other two being 45°. The magnitude and direction of the principal stresses have been calculated for depths of 50, 100, 150 and 200 cm and they are reproduced graphically in the stress diagram (Fig. 36 a).

The major principal stress σ_1 deviates only slightly from the direction OX_1, which lies in a vertical plane through the centres of pillars 10 and 12. This direction of σ_1 is true, however, only at fairly great depths from the rock face (2 metres). At a depth of about one metre the direction of the principal stress is roughly midway between OX_1 and OX_2. It is evident from this that the direction of the principal stress near the surface of the roof is influenced by the presence of the central pillar.

It is seen from the diagram that at geater depth the major principal stress σ_1 is about 50 per cent greater than the minor stress σ_2, and that it increases almost linearly with depth from the roof face. On account of difficulty in guiding when drilling the cell hole near the rock face no measurements were made closer to the surface than 50 cm.[1]

The most interesting problem with respect to the roof point 1 is: What is the stress acting near the surface of the roof? A state of tension would be expected in the roof midway between the supporting pillars. Such tensile

[1] This difficulty has since been overcome and it is now possible to record the stress at points 10 cm from the rock face.

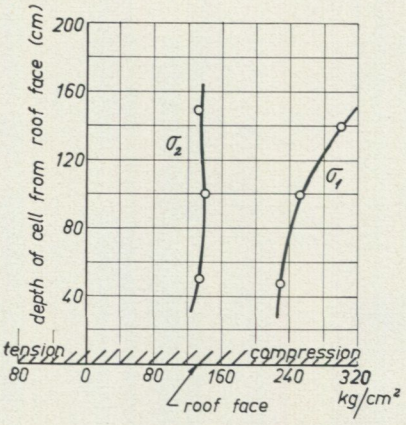

Fig. 37 a. Roof point 2. Magnitude of principal stresses at varying depths from roof face.

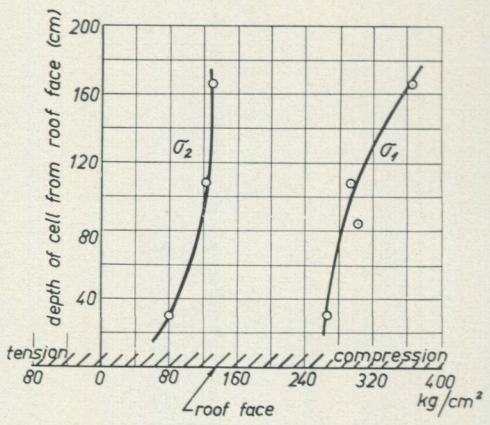

Fig. 37 b. Roof point 3. Magnitude of principal stresses at varying depths from roof face.

stresses would, however, imply a serious risk of a caving of the roof. It is therefore important that the measurements, in fact, indicate a compressive stress. In the case of roof point 1 the prolongation of the σ_1 curve in Fig. 36 a would suggest that there is a state of compressive stress in the actual roof face.

It is assumed, however, that the stress curve remains almost linear up to the rock face. The presence of compressive stress seems even more certain at the other roof points. The only state of horizontal tensile stress in the roof face at the points of measurement would seem to be at roof point 1, where the minor principal stress σ_2 is possibly some 20 kg/sq.cm.

ROOF POINT 2 — situated in the line of the pillars 10—12, but lying midway between point 1 and the face of pillar 10. The tensile stress in the roof face due to the overburden will always be less at point 2 than at 1. Both σ_1 and σ_2 are large compressive stresses, apparently even near the surface of the roof. σ_2 is about 130 kg/sq.cm, and σ_1 is nearly twice this value (Fig. 37 a). There is practically no risk of tensile stress acting in the actual roof face. However, these high compressive stresses also imply a risk of caving of the roof.

ROOF POINT 3 — situated midway between pillars 4 and 20. The compressive stresses are very high, σ_1 being about 360 and σ_2 about 120 kg/sq.cm at a depth of 1.7 metres (Fig. 37 b). Nearer the surface the stresses are apt to be lower, but at only 30 cm σ_2 is still about 80 kg/sq.cm. The directions of the principal stresses are fairly constant at depths greater than 30 cm.

ROOF POINT 4 — situated midway between pillars 14 and 17. Near the roof face the stresses fluctuate, apparently owing to the influence of the large fissure and sköl zone in area III (Fig. 35). Deeper in the roof the stresses are high and display a tendency similar to those at roof points 1—3. The directions of the principal stresses are about the same as for the other points.

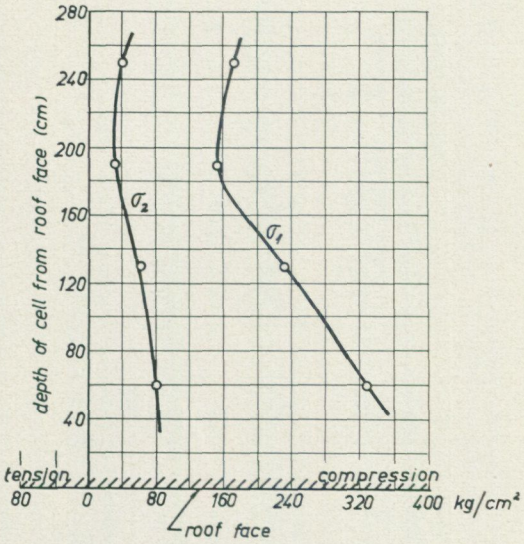

Fig. 37 c. Roof point 5. Magnitude of principal stresses at varying depths from roof face. Fissures rather near the cell hole relieve the stress in the surrounding rock at a depth of about 2 metres.

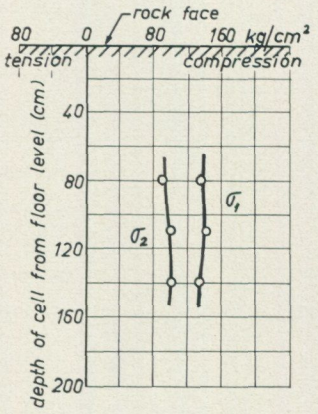

Fig. 37 d. Floor point 27. Magnitude of principal stresses at varying depths in the floor.

ROOF POINT 5 — situated midway between pillars 15 and 16. Near the roof face both σ_1 and σ_2 are large horizontal compressive stresses but they diminish with depth (Fig. 37 c). While the roof is rather free from cracks at the rock face in the region of the hole, the inclination of the fissures that intersect the roof face near pillar 15 suggests that at a depth of 2 metres they approach rather near the cell hole and relieve the stress in the surrounding rock. It is probably this state that was recorded by the cells.

FLOOR POINT 26 — situated immediately below roof point 3 (Fig. 38). The rock was found to be fissured to a considerable depth; this complicated the drilling operation. Penetration of water into the cell hole rendered stress measurements a little more difficult. At depths of less than one metre the principal stresses are fairly constant, with $\sigma_1 = 170$ and $\sigma_2 = 70$ kg/sq.cm. At 30 cm the respective values are only 30 and 20 kg/sq.cm; these low figures suggest that the stresses in the rock around the point have been released owing to fissuring, which probably occurred in connection with excavation work. The directions of the principal stresses are rather constant at various depths in the floor.

FLOOR POINT 27 — situated near pillars 15 and 16. No stresses could be recorded until a depth of 80 cm was reached owing to numerous fissures in the surface zone of the floor. The values of σ_1 and σ_2 are 140 and 100 kg/sq.cm, respectively (Fig. 37 d). The directions of the principal stresses are in close agreement with that for the other floor point 26, and with the directions for the roof points 1—5.

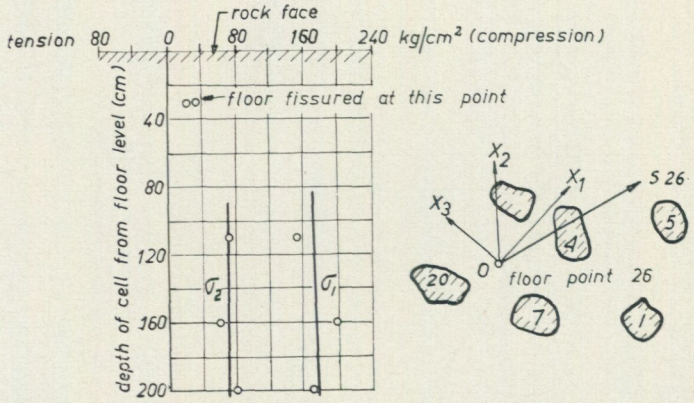

Fig. 38. Floor point 26. Magnitude of principal stresses at various depths in the floor. The surface is much fissured so that compressive forces there are low at the face.

ASPECTS OF THE HORIZONTAL STRESSES

The stress measurements suggest the following conclusions.

High horizontal compressive stresses are acting:

(a) in the roof and floor of the mine, and

(b) in the pillars and the boundary walls — even as high above floor level as 1.2 metres, where the measurements were made.

These horizontal stresses display a directional variation, being at their maximum in the main direction of fissuring (N—S), in which they are 1.5 times to twice as great as at right angles thereto.

The horizontal stress in the large central pillar measured in a direction almost the same as T_1 (Fig. 35) is about 300 kg/sq.cm — that is to say, of the same order as in the roof. The stress in the floor (the surface of which has been damaged by blasting) appears to be somewhat lower than in the roof, perhaps owing to the fact that here the sandstone strata changes to an arkos of lower strength, or that the horizontal stresses are absorbed by the harder granite bedrock. From the aspect of the stress distribution the level at which the measurements were made in the pillars — 1.2 metres above floor level — should be reckoned not from floor level but from the intact part of the floor that lies about one metre lower. That greater horizontal stresses were found by measuring parallel to the smallest dimension at point 21 than in the longitudinal direction at, say, point 22 seems a clear indication that the horizontal stresses in the pillar vary with direction.

Two theories are advanced below on the origin of the horizontal stresses (p. 90). It is evident, however, that the reason for the directional variation may possibly be that the horizontal force is prevented from full action perpendicular to the principal plane of fissuring by the very existence of these fissures. The horizontal stresses would then tend to assume the character of a uniform field in which the penetration of the stress is opposed more in one direction than in another.

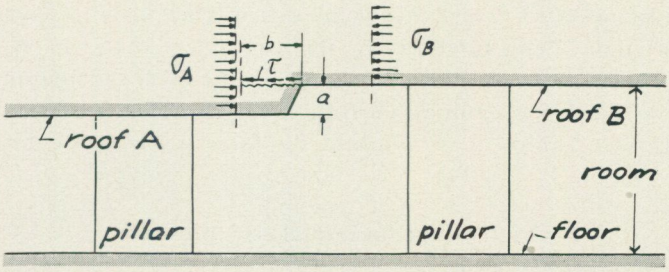

Fig. 39. Stress conditions around a difference in level in the roof.

SHEARING STRESSES AND ROOF SUBSIDENCE

The situation will be considered in which the roof is at two levels, one part in the excavated room being higher or lower than that of the adjacent part of the mine (Fig. 39).

The compressive stresses σ_A and σ_B may be regarded as balancing one another except at the difference in level a between roofs A and B. The transmission of the force $\sigma_A \cdot a$ is then effected through the development of shearing stresses τ along the line represented by prolongation of roof B into the rock of roof A — say, for a marginal zone of the width b. Consequently, the presence of a marginal zone such as that shown in Fig. 39 would seem to increase the risk of a roof fall. It is probable that there are horizontal strata

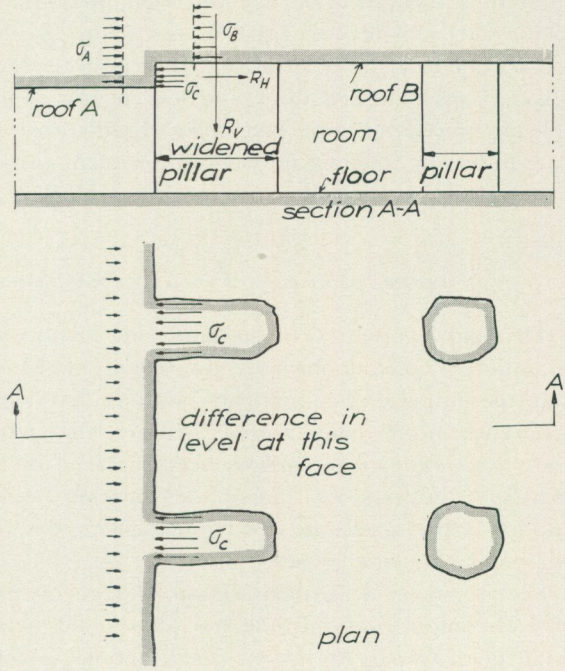

Fig. 40. Wide pillars introduced to provide stable conditions against roof subsidence near the difference in level of the roofs.

in the sandstone that, though not composed of clay, have a lower ultimate shearing strength than is generally the case, and that roof *B* represents a plane of weakness, as does the zone width *b*. If a step in the roof cannot be avoided, the resulting shearing forces should be taken up by strong pillars (Fig. 40), which must transmit the force $\sigma_A \cdot a$ to the floor and to roof *B*.

Origin of the horizontal rock pressure

Two theories will be advanced on the origin of these horizontal forces. The solution of this problem would throw light on the nature of the horizontal stresses — their direction and, perhaps above all, their variation. Do they disappear with time from an area that has been fully worked, with a consequent threat to the stability of the roof?

As the measurements in the roof and floor have shown, the horizontal stresses display an appreciable directional variation. The major principal stress lies slightly E of N (Fig. 35). The ratio σ_1/σ_2 of the major and minor principal stress varies due to the fissures not only from one point of measurement to another but with depth in a particular cell hole.

GEOLOGIC ROCK MOVEMENTS

The possibility that the directional properties and the magnitude of the stresses may be due to movements in the earth strata is found in the geographic situation of Laisvall in the Scandinavian mountain range; the stresses may be set up through movements in the nappes in this area. To test the validity of this explanation it would be necessary to perform stress determinations in the ground outside Laisvall. Parts three and four of this book give such examples of rock pressure measurements. There are considerable horizontal rock pressures in several mining regions in Central Sweden and Norrland and also Norway. The problem is discussed more in detail in Part six.

THE PRESENCE OF LEAD SULPHIDE IN THE SANDSTONE

The lead compounds in the sandstone strata were probably added eras ago in liquid or gaseous form by impregnation. Microscopic examination shows that the impregnation of lead sulphide has changed the original cohesive properties in the contact zone between the individual quartz grains where the quartz has to some degree been replaced by lead sulphide. The tendency that lead displays for plastic deformation under quite small loads may impart to the sandstone mechanical properties of a plastic nature that the pure rock does not possess.

Fig. 41 shows a vertical section through the ground in which a stratum *A* of lead-containing sandstone has above and below strata of unimpregnated sandstone. Owing to plastic deformation under the dead weight of the

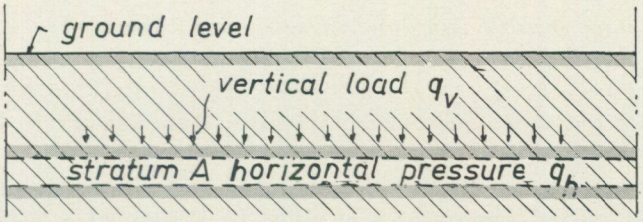

Fig. 41. Vertical section through strata, including one stratum A of lead-sulphide-impregnated sandstone. The plastic nature of the lead compound will probably give rise to a horizontal stress, q_h, which tends to stabilize the stratum A during the transmission of the weight of the upper strata.

overburden to which the stratum A has been subjected over long eras there has been a flow of stress. Since this stratum is totally enclosed by non-plastic rigid ground strata, there can be no appreciable lateral flow. However, the plasticity of the lead sulphide interspersed between the silica grains can result in a certain hydraulic lateral pressure q_h in the stratum; this pressure constitutes a stabilizing factor in the transmission of the vertical load q_V to the underlying rock.

The state of stress illustrated in Fig. 41 has been set up over geological ages. If the stratum A is suddenly excavated and the roof is supported by narrow pillars, the situation shown in Fig. 42 will arise. The force q_h in the rock around the stope in the stratum A will not disappear as it is still serving to maintain the lateral equilibrium of the unexcavated parts of the stratum. To compensate for the horizontal forces in the unexcavated part A compressive forces of reaction are set up in the roof and floor.

This explanation may be regarded as fairly acceptable and it seems probable that some horizontal stresses in the roof and floor have been set up in the manner described. However, these stresses seem to be greater than would be expected. At a depth of 2 metres from the roof face the horizontal stresses still tend to increase at certain points. This may be a local variation, and have its origin in fissures or horizontal strata of clay in the sandstone. Just as the reduction in the stress near the roof face is probably due to bending tensile stresses acting there, so the increase in stress at greater depth might be attributed to the bending compressive stresses in the upper

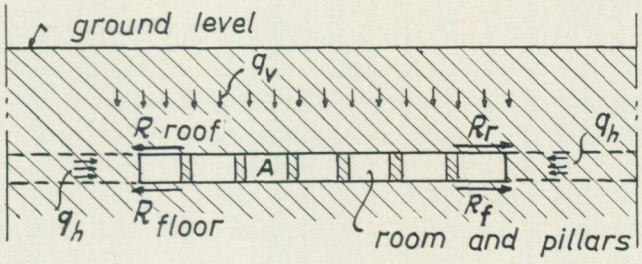

Fig. 42. Stress conditions around a room when excavation of stratum A has begun.

part of the same bearing roof slab. However, in the light of what is said in Part six it seems most likely that the horizontal stresses are of geological — tectonical nature.

For a reliable determination of the stress distribution in the roof very deep measurements are required. Unfortunately, at the time the roof measurements were carried out the development of the measuring apparatus was not sufficiently advanced for stress measurements to be performed at greater depths than 2—2.5 metres. It may be added that the apparatus has since been improved to the point where stress determinations can be made at a depth of 20 metres or more in the roof or wall.

Summary and conclusions

There follows a brief survey of the conclusions relating to the form and location of pillars with respect to their strength and to the stability of the roof in the Laisvall mine.

PILLAR LOAD

Accurate measurements show the cross-sectional area of the pillars to be extremely variable, owing, it would seem, to breaking off of the rock along open or closed fissures during blasting operations.

The variation in the cross-sectional area of the pillars in area I is 43—107 sq. metres, in area II 43—94 and in area III 43—64 sq. metres the measurements being made 1.2 metres above floor level. The pillars generally become narrower with the distance from the floor, and as a rule also from the roof. The effect is most clearly evident in the case of the most slender pillars; for instance, pillar 6 in area I diminishes from 43 to 28 sq. metres, pillar 12 in area II from 43 to 32 and pillar 14 in area III from 43 to 21 sq. metres (Tables IV—VI). The total load, calculated on the basis of the supported roof area for the individual pillars, does not vary over so wide a range, however; in area I it was 110,000 to 137,000 tons, area II 90,000 to 124,000, and area III 87,500 to 110,000 tons. It follows that the stress σ_V in the various pillars must vary by a large margin.

A large pillar with a low stress cannot to an appreciable extent relieve a narrow pillar that is heavily loaded. The stress in several small pillars in the four areas is too high. Unfortunately, these pillars are also more precariously penetrated by fissures. In the Laisvall mine the main direction of fissuring is so nearly vertical that such a fissure may pass through the pillar and leave at the head and the foot intact portions wide enough to ensure lateral stabilization of the forces in the plane of fissuring, and thus enable the pillar to support its share of the roof. When the pillar is narrow and tall this favourable situation is less likely to occur. The presence of open fissures

in the pillar is generally an indication that movement of the rock around the fissure has already taken place. In this case forces can no longer be transferred across the fissure. Measurement of the internal state of stress about closed fissures showed that they function quite differently from open ones. In order that a closed fissure shall remain closed and transmit forces when the pillar is loaded over a long period the presence of stabilizing horizontal forces within the pillar head or foot is necessary.

However carefully the spacing of the pillars is planned, as it evidently was in area III, one cannot be certain that after the blasting operations all the pillars will be able to support their share of the roof with a satisfactory margin of safety. However, the situation is improved if, instead of single pillars, wall pillars are left that have the same thickness as the existing pillars. These pillar walls should be cut so that they are pendicular to the general direction of the fissures. Then, when the wall has been examined for fissures, the damaged ore-bearing parts should be excavated so as to leave the more intact and stronger portions as free pillars. This procedure has, in fact, now been introduced. Such pillar walls are shown in the west corner of Central Mine (Fig. 27, upper left corner).

The presence of the high horizontal stresses revealed by the measurements in the roof, floor and ends of the pillars is of great significance from the aspect of the strength of both roof and pillars. The strength of the pillars is increased by the lateral compression of the rock at the roof and floor, which tends to close the fissures and hold the head and foot of the pillar together. By cutting the pillar walls so that they lie perpendicular to the main direction of fissuring the maximum value of the horizontal stress will tend to hold the pillar together in a direction parallel to its smallest dimension.

It should be ensured that when the pillar walls are being cut down to pillars only unfissured parts are left. It is, however, essential that if any fissure exists in the residual part the intersection of the fissure with the plane of the roof or floor should be far enough from the face of the pillar to leave a wide undamaged portion sufficient for the stabilization of the lateral forces set up by the appearence of the fissure.

Stress measurements show that the pillar with an exceptionally large cross-sectional area will serve as a reliable long-term support for the roof. Narrow pillars, on the other hand, have a tendency to lose their load-carrying capacity with time. At present a large part of the roof in the Laisvall mine would seem to be carried by the boundary walls and the large central pillar, which was fortunately left unexcavated owing to its low ore content. The prime essential as regards the safety of a worked zone of a mine is that the haulage ways should be safe from roof subsidence. In this case these ways pass just outside the central pillar (point 25). In general the safest place for the haulage ways in old mine rooms is probably along the walls; here they are likely to be more independent of the effect of time on the individual pillar. A study of the variation of the roof stresses near the walls with time would clearly contribute to greater safety in the mine.

The sandstone in the Laisvall mine seems to be homogeneous and strong, values of 1,600—1,800 kg/sq.cm having been obtained in tests performed on homogeneous cores 87 mm in diameter and about 15 cm in length; pressure-distributing porous plates were used. When present in a pillar the sandstone or quartzite will be subjected to loading over a long period, and the breaking strength will be considerably lower than under the test conditions of rapid loading. In this case a minimum safety factor of 6 must be adopted.

According to data from the management the spacing of the pillars was planned on the basis of a permissible load of 250 kg/sq.cm on the pillar material. However, this assumes (1) uniform thickness of each pillar (2) no fissuring and (3) equal spacing of the pillars, so that the roof load is uniformly distributed.

In general, none of these requirements is fulfilled, with the consequence that seriously high local stresses are set up. For instance, in pillar 20, from the upper part of which a portion was detached by careless blasting of a ventilation duct, the values exceed 700 kg/sq.cm. Here some reinforcement is called for. As appears from Table IV, the calculated stress in the narrowest part of the pillars is in some cases too high — between 250 and 300 kg/sq.cm — and this is often aggravated by fissuring. It is then impossible to avoid high stress concentrations around the fissures, especially their ends, and in time the pillar will gradually split.

The pillars of the whole of area I, and probably those just outside, are being deprived of their load-carrying capacity in this way, and the area should for this reason be kept under strict observation. This redistribution of the stress means that the weight of the roof in the area is gradually being transferred to the boundary walls and the large central pillar. It would seem to be a matter of time before the roof subsides. It must be observed in this connection that the sandstone in the roof is not homogeneous but is interrupted by horizontal strata of clay.

In the part of the mine that was the first to be opened — the east corner of the room — the pillars differ very much in shape, and are badly fissured. The stress measurements have shown clearly that the pillars are carrying a very small load, and it is possible that if the sandstone there is interrupted by clay layers they are at present doing little more than support the sandstone strata located near the roof face. Even if their load is small and is decreasing with time it would therefore probably be inadvisable to remove the pillars.

STABILITY OF THE ROOF

In the Laisvall mine the stability of the roof is a very important factor, especially as regards the risk of caving. It is also important to obtain the maximum permissible free span in order not to restrict the manoeuvrability of the mechanical loading equipment.

The quartzite in the roof seems to be of very fine grain and homogeneous in structure, and to have a fairly high compressive strength. However, a

disturbing factor is the occurrence of horizontal clay strata, generally up to one centimetre in thickness.

In the surface of the horizontal roof spans the dead weight of the overburden will set up tensile stresses; these, however, will not be very great if the roof is homogeneous to an appreciable depth. If on the other hand, as is the case here, there are horizontal clay layers only a metre or two from the face, quite a different situation will exist. The roof below the clay will then be suspended as a beam between supports, and it may, by virtue of its dead weight, be acted on by bending forces — positive moments at the centre and negative at the supports — and shearing forces. Owing to the partings and fissures along which slipping may occur, other forces may act on the roof face through the agency of the clay layers. As a precaution it should be ascertained, as soon as a room has been excavated, whether there is a sufficient thickness of homogenous rock up to the first layer of clay to carry at least its own weight with a reasonable margin of safety.

However, rock has low tensile and shearing strength, which means that the roof may subside even when only low tensile stresses are acting in the face. From the aspect of safety in the excavation work it is therefore essential that there should be no tensile stresses in the roof face. Measurements have shown this to be the case, and moreover that appreciable horizontal compressive stresses are acting. The difference between the maximum and minimum values σ_1 and σ_2 of the principal stresses is great, however. The major stress σ_1 has a tendency to increase with depth from the roof face, and is usually between 200 and 300 kg/sq.cm but at some points only about 100. On the other hand, the values of the minor stress, σ_2, do not tend to increase appreciably with depth, except at roof point 1, where σ_1 and σ_2 show a parallel variation. σ_2 at a depth of 2 metres is generally about 100 kg/sq.cm. The σ_2 curve for roof point 1 shows that the face of the rock is probably under tension, but at no other point of the roof where measurements have been made does this appear to be the case.

At roof point 4 and, deeper, at point 5 the presence of dikes and fissures seems responsible for wide variations in stress. Both points are situated in a much fissured rock (Fig. 35). The great variation in the stress field suggests that the risk of subsidence of the roof in this area is probably greater than for the unfissured roofs of the central parts of the mine.

In area IV, the first to be excavated, the stresses in the pillars have now practically disappeared. The question whether the roof stresses are also affected by the passage of time cannot be answered in the absence of such measurements at this site; nor is it known whether the roof stresses at the boundary walls of the room are greater or smaller than at the centre of the mine; this information would indicate whether the safest haulage ways in the old part of the mine are those along the boundary walls.

The risk of subsidence of the roof is particularly great in the working zones having a stepped roof. Free boundary zones between the two levels should be avoided. If this cannot be done, buttressing pillars should be left. The

problem of shearing stress arises also in the blasting of drifts and headings with vaulted roofs. For the reasons stated above, the plane roof should be the most stable in areas where horizontal stresses are acting, at least in sandstone strata.

In the central parts of the Laisvall mine the roof is probably less stable in the E—W direction than perpendicular thereto. A somewhat shorter span in the former direction than in the latter would therefore seem indicated. It should be possible to take this into account when planning the spacing and distribution of the pillars, at the same time giving due regard to the manoeuvrability of the excavating machines.

PART THREE

APPLICATION OF THE METHOD AT THE GRÄNGESBERG MINE

Introduction

The first practical experiments in rock pressure measurement by the method described in Part One were performed in the mine of Trafikaktiebolaget Grängesberg—Oxelösund in 1951. Inevitably they were at first experimental in character, but with the accumulation of experience of the most suitable design for the measuring cell, the type of amplifier and the drilling technique the results of the measurements began to prove of value. During 1953—54 stress measurements were performed according to a programme, the chief object being to determine the absolute value of the stresses at a large number of points in the mine where there was reason to believe that they were high. Measurements demonstrated, however, that whereas the vertical stress was in fact generally small — no greater than could be accounted for by the dead weight of the overburden — the horizontal stress was high — at some points ten times as great as the vertical component. This horizontal stress was tentatively ascribed to the residual part of the hanging wall. Owing to overhang and fissuring, parts of the wall may tend to slip towards the orebody, and thus give rise to lateral forces thereon. However, it can be shown theoretically that the hanging wall cannot be responsible for such high horizontal pressures as were revealed, even if some form of lever action could be assumed to be acting. At quite an early stage measurements showed that the horizontal stress was as high as 500 kg/sq.cm in places.

These findings put an entirely new face on the problem. Whereas the measurements had formerly been concerned chiefly with finding the vertical load at various points in the pillars and walls, there were now quite different and still more important problems to be resolved, namely:

(1) What is the origin of the high horizontal pressure?

(2) How is the stability of the foot wall and the whole stope affected by this horizontal pressure?

(3) How will the horizontal pressure vary as the depth of excavation is increased? Will the pressure increase still further?

(4) If the horizontal pressure increases with depth, which excavation procedure should be chosen with a view to minimizing the risk of subsidence, of cutting out an undue amount of rock with the ore, and ensuring the continuation of selective mining at greater depths?

(5) Can an excavation procedure be devised such that the great horizontal forces may be exploited for crushing the ore, with resultant economy in the consumption of explosives?

These questions cannot be answered unless there is a detailed knowledge of the state of stress in the orebody itself and in the country rock for a considerable distance from the orebody. It is also necessary to know how the

stresses will be affected by removal of ore, especially those acting near, or in, the actual zone of excavation.

The former practice of measuring the stress in pillars, roofs and walls at the most two metres deep will no longer be adequate. For an accurate determination of the stress in the rock around the orebody deep cell holes are necessary, which enable stress determinations to be made at depths of 10 to 15 metres, or even more, from the rock face.

It is necessary to penetrate the high stress zone — the zone of disturbed natural stress — that surrounds an opening such as a drift or a shaft. Knowledge of these stresses is essential for an accurate estimate of the stability of the strata, and for getting an impression of what is to be expected from excavation at greater depths. These requirements of stress measurements in deep bore-holes have necessitated intensive research on instruments and the evolution of methods for performing this new type of measurement.

The Grängesberg mine

Location of orebodies

The Grängesberg deposit consists of very long series of orebodies (Figs. 43, 44, 51 and 52); there are two shafts — the Jakobina and the Central. One of these series, comprising the Lönnfallet, Müller, Mellanfältet, Karl-Johan and Strandberg bodies, is about 1.5 km long. Parallel to this runs another series composed of the Timmergruvan and Mossgruvan lenses. The width of the lenses is greater than is usual for Swedish mines, and varies with depth. For instance, at the 310 metre level the maximum width of Lönnfallet is normally 60 metres, Müller 40—50, Mellanfältet 50, Karl-Johan 70 and Strandberget 30—50 metres. Between Müller and Mellanfältet, and between this body and Karl-Johan the deposit is constricted and even interrupted. The rock bands separating the lenses are so narrow and irregular in shape that they cannot be kept intact during the excavation of the bodies.

The deposit consists chiefly of magnetite ores with a small fraction of haematite ores and some skarn. The country rock is principally leptite. Chlorite-mica sköls are common in this leptite as are dikes of leptite of dacitic and andesitic composition, pegmatite and quarts. The magnetite ores varies widely in its physical properties. Tests with 87 and 132 mm rock cores 15 cm in length

Fig. 43. The orebodies at Grängesberg. There are series of connected bodies, the largest of them being Lönnfallet—Müller—Mellanfältet—Karl Johan—Strandberget (about 1.5 km long) and Timmergruvan—Mossgruvan.

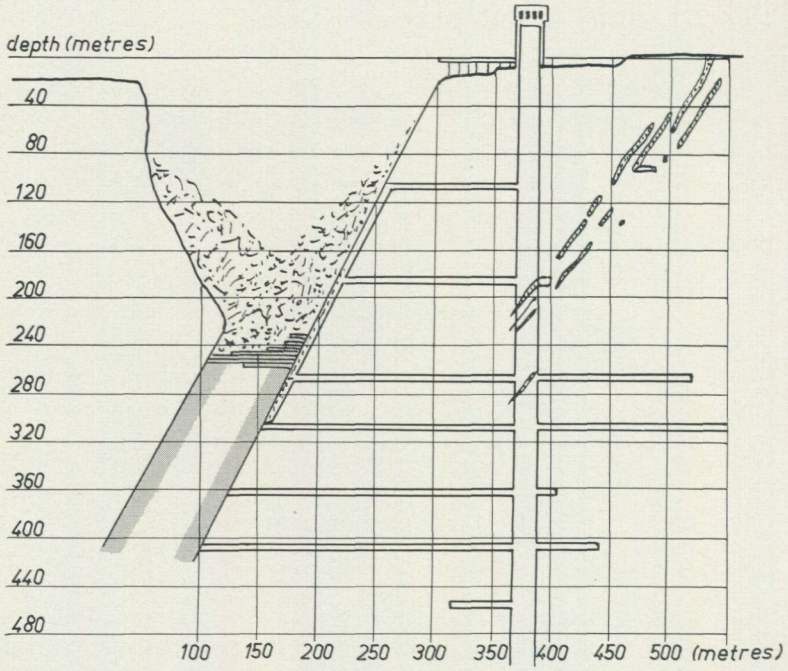

Fig. 44. Vertical cross section through the Central Shaft and Lönnfallet lens. The dip of the lens is 63°. The lenses in the top right-hand corner are the excavated Västra Ormberget (Fig. 43). The main drifts at the various levels are inserted.

revealed ultimate strengths of 600—1,500 kg/sq.cm. The strength is even less in some places, and in others the ore has split along the natural planes of cleavage, owing probably to high shearing stresses to which the ore is, or has in the past been, subjected. A core obtained by diamond drilling may in this case often be broken apart in the hands, each small piece however appearing to be quite strong.

The longitudinal section through Lönnfallet and Müller shows the levels as they were in 1953 when stress measurements were in progress (Fig. 45). Since then the excavation has been taken considerably deeper (about 8 metres annually). Moreover, an attempt is being made to increase the rate of excavation in the Lönnfallet area so that the 60—70 metre difference in the height of the working face in profile 38 will soon be eliminated.

The stability around the stopes is threatened by the presence of several largely parallel lenses (Fig. 43). The Östra Ormberget and, particularly, the Timmergruvan bodies have been worked down practically to the level of the larger deposit consisting of Lönnfallet — Karl-Johan (Fig. 51). The plunge of the excavated Timmergruvan body causes it to cut into the foot wall of Mellanfältet opposite the Jakobina Shaft. Similarly, the excavated Västra Ormberget body cuts into the foot wall of Lönnfallet behind the Central Shaft.

The foot wall contains numerous chlorite-mica sköls, the presence of which lowers its stability, as do the stopes of the parallel bodies when they cut into the foot wall of the main orebody.

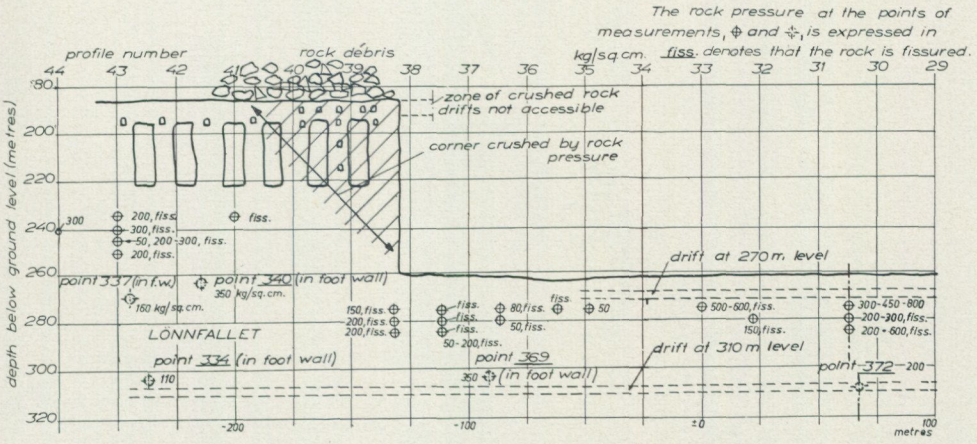

Fig. 45. Longitudinal section through the orebodies in the Lönnfallet—Müller region, showing the 60—70 metre difference in level near profile 38. The figures at the points indicated by small circles are the stresses measured in the lens in the direction hanging wall—foot wall. These points generally lie one over the other at 3 or 4 different levels, and thus show how the stress varies with depth in the zone of excavation. The measurements were performed in pilot drifts (Fig. 48). Measurements made at a number of points in the foot wall and located near the lens have also been inserted (larger, broken circles).

The problem of the stability of the walls bounding the stopes is a complicated one; to clarify the situation it was deemed necessary to determine the absolute values of the stress concentration at a number of selected points in the mine.

Evidence of high horizontal rock pressure

Before measurements were begun an inspection was made of the drifts and levels where the rock pressures were presumed to be highest. A number of observations were made and note was taken of incidents during recent excavation work and that might be regarded as evidence of high rock pressures. The explanation of a number of such incidents that had been obscure at the time of their occurrence was immediately revealed by study of the rock pressure values. Among these the following may be mentioned by way of illustration:

(1) Fig. 46 shows a cross-section through profile 29 at the 270 metre level. It intersects four parallel haulage ways. The excavation of the orebody had reached the stage where the roof over the drifts consisted of a 7 metre thick slab in which chutes had been blasted. Two horizontal open fissures were found in the wall of no. 3 drift; they were 2—3 cm wide and visible for a considerable length of the wall. According to the mining engineers these fissures had been observed some months previously, since when they had shown a tendency to widen.

(2) No. 2 drift had an unstable roof, from which loose rock had from time to time been removed, with the result that the drift had become much higher than the adjacent ones. As this cleaning was of no avail the whole drift was timbered.

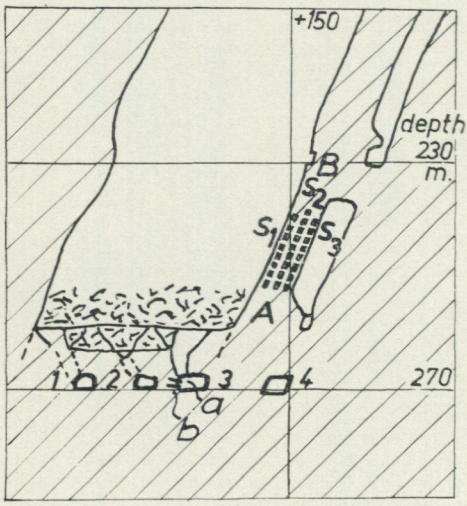

Fig. 46. Vertical cross-section through four parallel drifts at the 270 metre level, profile 29. The rock pressure has caused horizontal fissures *a* and *b* of great length in the drift wall. It has damaged also the shafts S_1 and S_3 and caused subsidence in the roof in drift 2.

(3) In the Lönnfallet block (Fig. 45) it was observed that the level of the floor of a drift at the 200 metre level had suddenly risen by about one-half a metre.

(4) Between the large ore lens and the narrow parallel lens (Galtstrecket) there are three climbing shafts S_1, S_2 and S_3 (Fig. 46). S_1 and S_3 lie very near the face of the rock wall separating the stopes and are so badly fissured that it is impossible to use them. Shaft S_2 in the centre of the wall, on the other hand, seems to be intact.

Stress measurements revealed the existence of a high horizontal pressure throughout the area — for the most part perpendicular to the orebody; that is to say, in the plane indicated in Fig. 46. The horizontal stress in the orebody is greatest in the upper part, and falls off with depth. Near the upper face the stresses have been so high that the rock has been crushed, the fractured zone of it being forced upwards, in spite of the weight of the ore and overlying rock débris. The fissures following the wall in no. 3 drift bear witness to the progressive upward movement of the roof. There is thus no question of any sagging of the floor of this drift, as has hitherto been supposed.

A similar explanation applies in the case of the above example of the upward movement in the floor level (3).

The caving of the roof of no. 2 drift, where blast cleaning was of no avail (2), is also readily explained. The rock in the roof was being crushed by the enormous lateral pressure, and the upward movement of the roof slab — probably still greater than that occurring in no. 3 drift — resulted in the continuous breaking away of rock.

The wall *A*—*B* in (4) has been damaged by high bending forces apparently simultaneously with the lateral compression of the rock roof of drifts 1—3. One side of the wall is damaged by tensile and the other by compressive stresses, the intervening rock being intact.

Stresses and undesirable local concentrations in stope walls

As the rock constituting the stope walls will have been deprived of its natural lateral support, there is a risk of subsidence as the mining is continued downwards, especially when the strength of the rock is low, or when it is penetrated by sköls, fissure zones or earlier excavated footwall ore lenses parallel to and near the main ore. It must be pointed out that if the rock around a stope is acted on by horizontal pressures exerted by the surrounding terrain, the stability of the boundary walls is reduced. In areas where there are many sköls containing chlorite-mica, which acts as a lubricant, cylindrical slips may occur such as those in road and railway embankments. The cylindrical surface may gradually link up with the various sköls, and so form a slip face with the least resistance to rupture of all possible such faces.

There is, however, a stabilizing factor that reduces the likelihood of caving. Where the difference between the length and the width of the excavated room is not large extensive subsidence of part of the walls is generally prevented by the arch thrust that acts around the opening, stabilizing the walls and preventing any appreciable lateral movement of the strata. It is desirable, therefore, that the horizontal section of the orebody be circular, or in any case not much longer than it is wide. The arch thrust may also be set up around the extensive orebodies, but this state of stress occurs only beyond a certain distance from the lens and stabilizes only the area beyond the hypothetical arc joining the extreme ends of the lens (Fig. 47). The stability of the rock located between the lens and the arc will not be increased to the same extent. Where the lens is long certain strata may therefore be so situated that the arch thrust cannot be relied upon to stabilize them.

The various orebodies of the Grängesberg mining area are closely situated so as to form series of lenses. After the ore has been removed there remains a cavity, which is one kilometre in length, of varying width, depending on the thickness of the orebody, and whose depth increases with the progress of the excavation. The present working level is slightly more than 200 metres in the southern part of Lönnfallet and slightly less than 300 metres in Müller and Mellanfältet. The stope along the orebody is partly filled with rock débris, but from the aspect of stability this material is of little significance and the stope must be regarded as empty. In the case of a long stope, such as that at Grängesberg, there is little likelihood of an arch thrust forming in the

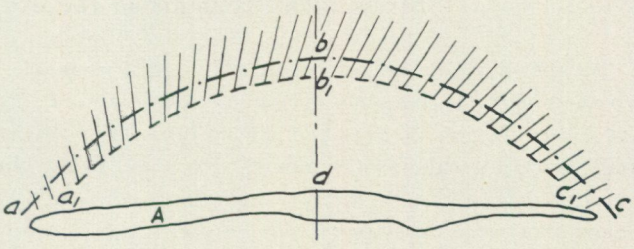

Fig. 47. An arch thrust a—b—c forming in front of a lens A and stabilizing the region outside the zone and preventing slipping of the outside material.

surrounding rock. The walls must be stabilized section by section. If the hanging wall is strong there may be a pronounced overhang, but sooner or later part of this section will break off.

The numerous sköls in the foot wall at Grängesberg largely follow the dip of the ore lens — about 63°. As the measurements show, a horizontal rock pressure of considerable magnitude is acting in the foot wall. As a rule this is now regarded as the safer side of the mine, where lifts and the main haulage ways are usually located, though it is not necessarily so, especially if the wall be penetrated by numerous sköls.

In such cases it is extremely important to follow the fluctuations in rock pressure during the course of excavation, a measure that will ensure the maximum safety and allow the removal of the ore to be planned in such a way as to exploit the stabilizing forces to the full, while the risk of introducing destructive forces in important sections of the mine during the work is minimized.

It will be shown below that in the foot wall the rock plates between the chlorite-mica sköls undergo a plastic and elastic deflection, as a result of which roughly uniform shearing stresses are set up throughout the wall. This unexpected situation has come to light through rock pressure measurements. They have shown, moreover, that at a certain depth, rather near the surface of the working zone, there is a point, no. 337 (Fig. 53), where shearing stresses of about 60 kg/sq.cm exist — about four times greater than elsewhere in this part of the foot wall. The evidence suggests that this stress concentration will move downwards as the excavation proceeds, and will become still greater as the rock pressure increases with depth. There is a danger that the foot wall material in this zone will then be crushed, as a result of which the excavated ore will be mixed with rock; there will also be a risk of overloading in the underlying part of the foot wall.

The only means of detecting this danger before demolition had taken place in the marginal zone of the foot wall was by rock pressure determinations. These have shown, moreover, that if this zone is kept under observation and suitable measures are taken for the subsequent excavation of the ore it may be possible to avoid an undesirable situation which might prejudice the continued working of the mine.

Stress measurements in the ore lens

In the first major programme for rock pressure determinations in the Grängesberg mine the measurements were confined only to the actual orebody. At the beginning of 1952 the ore in Lönnfallet down to the 185 metre levef had practically all been removed (Fig. 45). Below this, there was a zone ol crushed ore about 5 metres thick. Between the 190 and 220 metre levels magazines were excavated, and between them a number of drifts. The stress

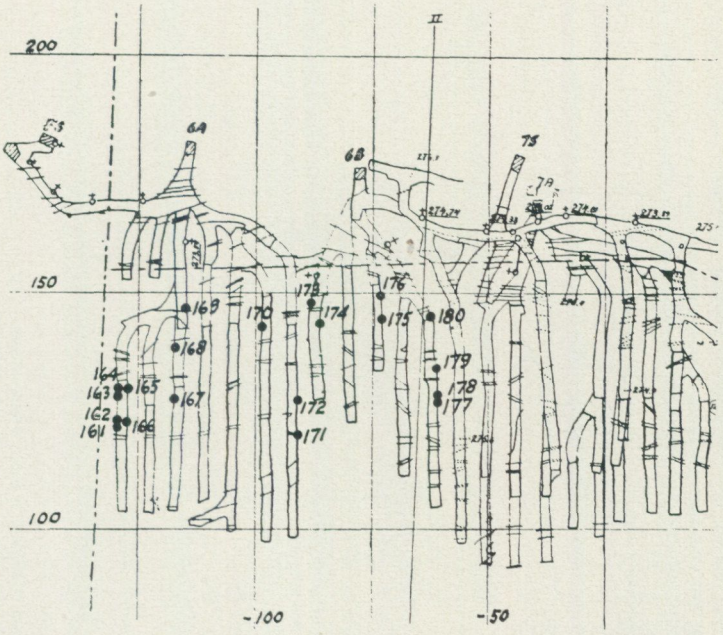

Fig. 48. Pilot drifts in the zone of excavation; the stresses are measured in the walls between the drifts.

determinations in these walls were among the first measurements to be undertaken in the mine. The stress release channel was cut by the seam drilling method (p. 18). At 190 metres the stresses were greatest at points nearest the difference in level adjacent to profile 38, and diminished with distance therefrom. In the free corner the maximum stresses were 500 kg/sq.cm or more but at profile 41 they had already fallen to about 200 kg/sq.cm. The horizontal stresses were the greater, but the vertical ones, too, seem to have increased; this suggests the presence of a hydraulic state of stress in the ore body in the heavily compressed region at the step between Lönnfallet and Müller — except, of course, in the surface zones. The major principal stress is inclined at an angle of about 30° to the horizontal, and is thus almost perpendicular to the hanging wall. Next to this wall there is a certain stabilization of the highly stressed parts of the orebody.

Soon after the above measurements had been carried out, there were subsidences in the drifts in the free corner. All the cross-cuts up to profile 41 (Fig. 45) became inaccessible for varying distances, but the worst affected were those on each side of profile 39, which were totally destroyed. At the same time as the free corner at profile 38 ceased to function as a rigid support between the foot and hanging walls the large horizontal stresses were automatically transmitted to greater depths. To ascertain the magnitude and distribution of these stresses and to study their effect on the orebody, a series of stress determinations was carried out in 1953—54 in cross-cut — in Lönnfallet

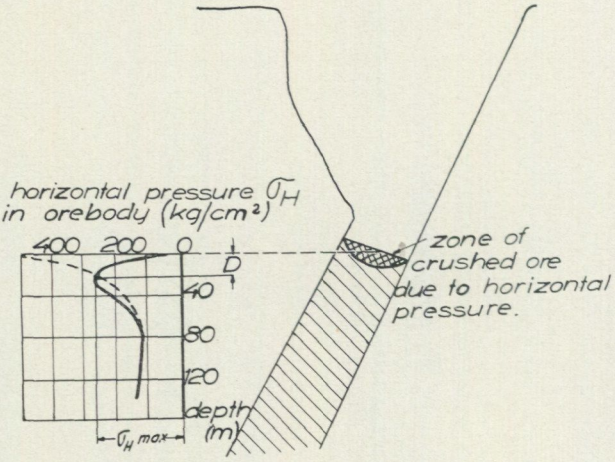

Fig. 49. Variation of the almost horizontal stress with depth in the zone of excavation. The broken line represents the pressure that would have acted had there been no crushing of the ore.

at levels between 235 and 250 metres and in Müller at 275, 280 and 285 metres.

Fig. 48 shows these drifts between profiles 29 and 38 at the 275 metre level as they were on about 1st January, 1954. The width of the drifts was from 2 to 2.5 metres and the pillars between 2.5 to 5 metres thick. The walls appeared to offer very good prospects of successful stress measurements, they being perpendicular to the hanging and foot walls. By drilling the cell hole perpendicular to the wall face the stresses were measured in the plane of the wall, in which direction the rock pressure is probably greatest. The material in the walls is magnetite, with a Young's modulus of about 1,300,000 kg/sq.cm, and the ultimate strength is fairly high at those places where the ore has not been crushed by the rock pressure. These tests were performed by the diamond drilling technique (p. 19). As a rule a 146 mm diamond bit was used for measurements in magnetite instead of the 102 mm usually used in rock. The diameter of the core after cutting was 132 mm. This increase was made chiefly in an attempt to reduce the tensile stress in the core adjacent to the cutting zone of the channel. It has been shown that the overburden covering the four longitudinal drifts at the 270 metre level is gradually being crushed through the effect of the predominantly horizontal rock pressure.

Fig. 49 illustrates how pressure probably affects the upper, still unexcavated, parts of the orebody. It might be expected from the theory that there would be extremely high stresses in the surface zone. However, this high pressure crushes the ore in the marginal zone, so that the stress is approximately zero at the surface, and then fluctuates as illustrated in the sketch.

In view of the proximity of the pilot drifts to the 270 metre level, they probably fall within this crushed zone; they would consequently be unsuitable sites for determining the maximum value of the rock pressure. On the other hand, it is also important to know the variation of the rock pressure with depth (Fig. 49). Moreover, the pilot drifts are probably the only ones being available with the exception of the main haulage ways at the 310 and 360

metre levels. These are probably too deep to provide any information on the actual crushed zone and, owing to the continuous traffic, are rather unsuitable for measurement work.

The measurements in the working drifts were thus necessary, although it was realized that at some of the points they might give no indication of the stress, the walls in many places being so badly crushed that there did not remain an intact piece of ore large enough for the core to be cut from it. This fact is, in itself, interesting evidence of the efficiency of the crushing of the ore through the agency of the prevailing rock pressure. Measurements in Müller revealed complete crushing at the 275 and 280 metre levels (Fig. 45). In the cases where the cell hole happened to be placed in a piece of ore large enough for a whole core to be obtained, horizontal stresses of about 50 kg/sq.cm were recorded. This suggests that at those levels there is a general horizontal stress of about 50 kg/sq.cm. In some of the inclined drifts at the 275 level it seems as if the strength of the ore has been much lowered by high shearing stresses. Where measurements were performed at 285 metres horizontal stresses of 200 kg/sq.cm were generally encountered. It is interesting to note that in profile 38 — that is to say, below the 60 metre wall bounding the higher Lönnfallet region — horizontal stresses of about 200 kg/sq. cm were measured at the 285 metre, but this stress value applies also to the 275 and 280 metre levels. The vertical stresses also differ considerably from those at the other measuring points. It is evident that the upward movement and fissuring of the roof at these levels has been prevented by the weight of the wall (Fig. 45, 46). The same situation is recognized in profile 30 1/2, where the stresses at 280 metres were 200—300 kg/sq.cm, and at 285 nearly 600 kg/sq.cm. It is clear that the vertical load from the remaining parts of the Müller block constituted the stabilizing factor. For the major horizontal stress recorded in this profile at the 275 metres level, values as high as 800 kg/sq.cm were found in a few cases, with several readings of 300—450.

As the corner next to profile 38 was crushed, increased rock pressures would be expected at deeper levels. Measurements made in Lönnfallet between profiles 41 and 44 then showed the presence of stresses of about 200 kg/sq.cm at a few points at the 235 metre level; at 240 metres they had risen to 300, but by 245—250 metres they had fallen to 200 (300 kg/sq.cm in a few cases).

In Fig. 45 a number of points in the foot wall are marked with broken circles, these being outside the actual orebody. The distance between the ore lens and these points is, in the case of Lönnfallet, not more than 10—30 metres at the 270 metre level (points 337 and 340 in Fig. 51), and 20 metres at the 310 metre level (points 334 and 369 in Fig. 52).

Such points outside the Müller and Mellanfältet lenses are also marked, point 372 at the 310 metre level, for instance, lying 10 metres from the orebody.

Stresses in the foot wall between the Central and Jakobina Shafts

Zones of increased stress around drifts

The thickness of the wall between the drifts in Fig. 48 is roughly the same as the width of the drifts. The walls act as horizontal pillars, which transfer the horizontal forces between the hanging and foot wall. The stresses may be assumed to be rather homogeneous within the cross-section of the wall when this is parallel to the horizontal forces. Where the stress field is not parallel to the axis of the drift higher stresses will then prevail, there being a zone of increased stress around each such drift.

The magnitude of the stresses at a circular opening is given by Kirsch's formulae (Fig. 50).

Depth in the roof:	o	$\frac{a}{2}$	a	$2a$	$3a$
Value of $\sigma = \sigma_0 \times$	3.60	1.52	1.21	1.06	1.03

where a is one-half the height of a circular drift and σ_0 the stress at a point remote from the drift.

Measurement of the horizontal stress in a vertical cell hole in the roof must therefore be made at a fairly great depth in order to clear the high stress zone surrounding the drift. A horizontal cell hole in the wall of the drift must also be taken to a considerable depth before the undisturbed vertical stress can be measured. Accordingly, the stress measuring technique must permit recording at great depth. It is usual to find the rock fissured to a certain depth around the drift from blasting during excavation. This zone is generally unstressed, as has often been confirmed by means of the measurements. In the first one-half to one metre from the face of the drift little if any stress is recorded; then high values appear, these gradually falling to a constant value, which can be taken as the normal stress for the virgin rock in that region. Fig. 54 b illustrates such a stress distribution at point 329 deep in a wall at the 360 metre level in Lönnfallet.

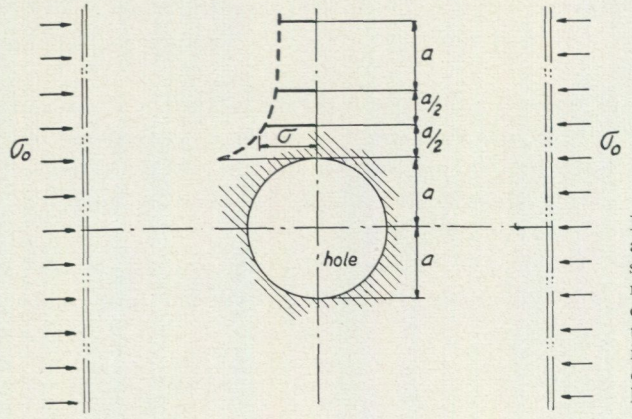

Fig. 50. Increase in stress near a hole of radius a in a plate subjected to a load σ_0, the radius of the hole being small compared with the width of the rod or plate. The diagram illustrates also the stress conditions around a circular drift located in a stress field.

Horizontal stress measurement in the roof

A cell hole is drilled vertically in the roof of a drift, and the cell inserted, oriented and pre-stressed at the required depth. By placing the cell in three directions in a plane perpendicular to the axis of the hole, the magnitude and direction of the principal stresses are obtained for that point and plane.

270 metre level. The stress ellipses for the roof points were calculated from the values generally obtained at a depth of between 3 and 5 metres (Fig. 51). At points 352 and 353 in the Jakobina area the depth was only 1.5 metres. The depth of 3 metres corresponds approximately to the height of the drift — that is, 2 *a* in Fig. 50 —, at which depth the increment in the horizontal load on the pressure zone around the drift probably does not exceed 6 per cent. At point 344 the values vary appreciably with depth. The two ellipses at this point show that not only the magnitude of the principal stresses but also their direction varies with their distance from the roof face. The measuring point was situated near a diabase dike and the stress fluctuations were probably due to fissuring in the rock contiguous with the diabase, which fissures originate in the intrusion of the diabase into the leptite formation.

The maximum stresses are high in the foot wall in Lönnfallet — about 300 kg/sq.cm — except at point 344, which at 5 metres does not indicate more than about 170 kg/sq.cm (see above). The direction of the principal stresses at points 340 and 344 shows that in a horizontal projection the lateral pressure on the ore lens is not perpendicular to the axis of the lens, but about 60° to it. This is probably ascribable to the excavated rooms in the Västra Ormberget. These old open stopes, marked on the plan in Fig. 51, lie south of the main drift from the Central Shaft. As the level rises, the north end of this excavated part of the lens turns still more northward, to reach the ground level 150 metres behind and north of the shaft the Central Shaft (Fig. 53). The major principal stress at point 340 is directed towards the place where the foot wall, which is intersected also by the Östra Ormbergsgruvan body, encounters the rock behind.

For point 343 the directions of the principal stresses diverge from those for the other points. It is situated next to the 60—70 metre high wall constituting the difference in level between the Lönnfallet and the Müller regions (Fig. 45). As mentioned above, there had been crushing of the rock in this part of the wall, and the accompanying movement probably also involved the 270 metre level, where point 343 is situated. The directions of the principal stresses changes from point to point. As point 344 is passed the stress ellipse is practically a circle, and that at 343 assumes a flatter shape, with a new direction of the major axis.

The horizontal stresses at the 270 metre level in Lönnfallet are generally higher than those at the same level around the main drift of the Jakobina Shaft — that is, opposite the Mellanfältet body. This is consistent with the fact that the 270 metre level in the Lönnfallet region lies some ten metres below the working face — that is, at a level where a high lateral pressure is acting in the ore (Fig. 49), whereas the main drift of the Jakobina Shaft at

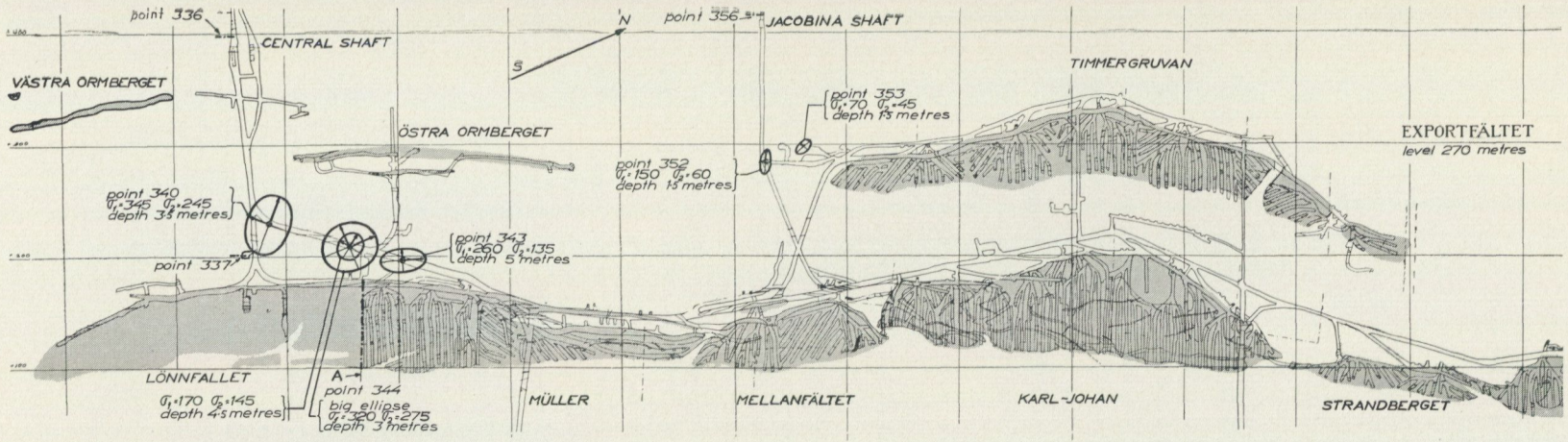

Fig. 51. The 270 metre level at Grängesberg, showing the results of stress measurements in the roof. The stress ellipses refer to the horizontal pressure at the indicated distance from the rock face. The rock pressure is highest at the level in the region of the Central Shaft where the zone of excavation is at 270 metres or less; it is much lower in the region of the Jakobina Shaft where the excavation is below this level.

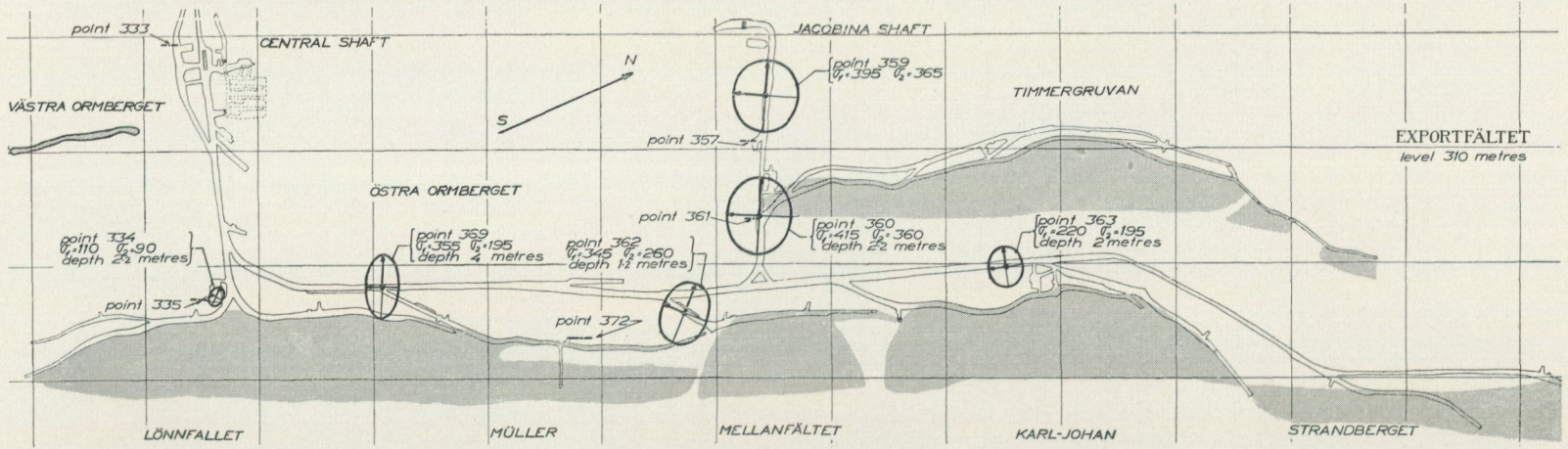

Fig. 52. The 310 metre level at Grängesberg. The stresses are greater in the region of the Jakobina Shaft than of the Central Shaft. The zone of excavation is above this level.

270 metres lies at the same level as, or above, the excavated levels of Mellanfältet; there will therefore be no high stress concentrations at, for instance, point 352 (Fig. 51).

310 metre level (Fig. 52). In contrast to the findings relating to the stress distribution in the various regions of the 270 metre level, at 310 metres the stresses around the main drift from the Jakobina Shaft are very high, and these values remain fairly constant up to the 60 metre step between Lönnfallet and Müller. At points 369 and 362 stresses of about 350 kg/sq.cm were measured, and at points 360 and 359 about 400 kg/sq.cm. It is evident that the 310 metre level is so far below the present excavation level in Mellanfältet and Müller that it clears the crushed zone and is perhaps not far from the level of the maximum horizontal stress (Fig. 49). In the vicinity of the orebody, as at point 369, the major principal stress is roughly twice as great as the minor.

However, around the main haulage way from the Jakobina Shaft roof measurements revealed very high stresses also acting parallel to the ore body. These recorded values may, to some extent, be due to the zone of increased pressure around the drift, and especially in the case of point 359, at a depth of only 70 cm, but the basic cause lies elsewhere. In 1955, sköls and fissures were mapped in practically all accessible drifts and levels throughout the Grängesberg mine (p. 117) and many such features were found that contained chlorite-mica. It is to be expected that a rock pressure with a definite direction will gradually assume a hydraulic character in a rock containing numerous fissures and sköls in different directions just as it would if the material were gravel, for instance.

Owing to its overhang the rock between the hanging wall of Timmergruvan and the foot wall of Karl-Johan is gradually being broken away as the excavation advances to a lower level. The long foot wall of Lönnfallet—Müller—Mellanfältet will then have a free corner between Mellanfältet and the south end of Timmergruvan (Figs. 51 and 52). The high stresses acting perpendicular to the Müller and Mellanfältet bodies will set up concentrations is the rock corner at the end of Timmergruvan. If Timmergruvan is further excavated its stope will cut into the high stressed foot wall of Lönnfallet—Müller—Mellanfältet and give rise to dangerous stress concentrations and influence the stability of the foot wall opposite the Jacobina shaft.

Stress measurement in the walls of the haulage ways from the Central and Jakobina Shafts

The values entered in Fig. 53 for the various points refer to the stresses in the plane of section. They were measured in cell holes that were perpendicular to the walls of the haulage ways (Figs. 51 and 52). At each of the levels 270, 310 and 360 metres two cell holes were made: one rather near the orebody and the other near the Central Shaft. The measurements were all performed deep in the rock (deep stress determinations), and the calculated principal stresses refer to points in the rock located 5—10 metres from the

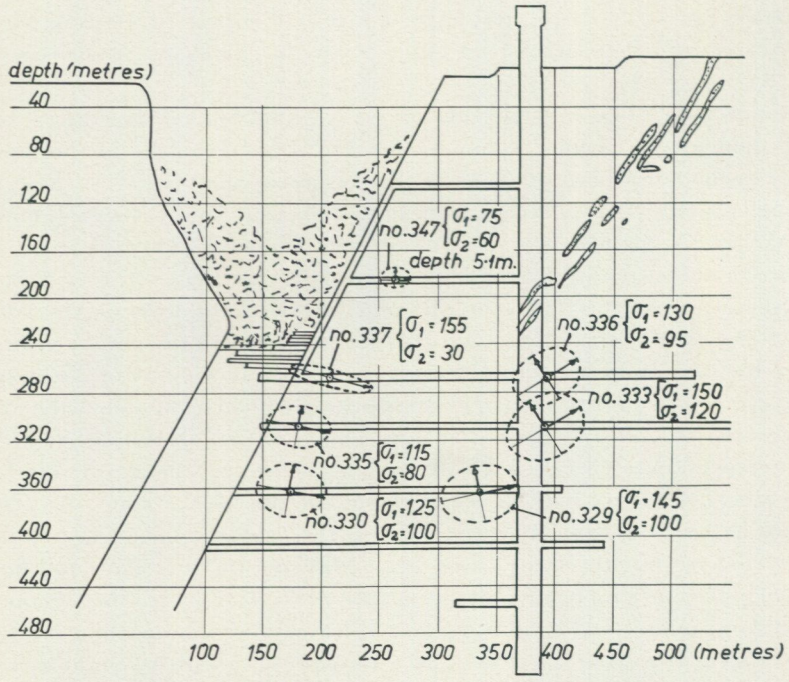

Fig. 53. Vertical cross-section through the Central Shaft and main drifts. The stress values inserted were obtained from deep measurements in the drift walls.

face of the drift wall. The values were in all probability uninfluenced by the high stress zone around the drift — an important point in this connection, as accurate data on the direction of the principal stresses are essential.

Fig. 54 a shows the stress components at point 337 in three directions at 60° to each other. In Fig. 53 the stress ellipse for this point refers to a section 5 metres deep in the drift wall. The vertical component is zero and deeper in the rock there is a tendency for tensile stresses to occur. At about 5.7 metres there is apparently a fissure, passing the core at some distance, that gives rise to an increase in the vertical value, while the two other components are lower. The position of the fissure is dealt with above (p. 33). Other fissures are passing the core at 4.3 and 6.9 metres.

The stress components at points 329 at the 360 metre level are shown in Fig. 54 b. It is interesting to note that the drift walls here are less badly damaged by blast than is generally the case in this mine, so that the stress measurements could be made nearer the face of the wall than usual. All the curves, and particularly the one relating to the vertical components, clearly reflect the presence of the high stress zone around the drifts and shafts.

The flattened form of the ellipse for point 337 is to be observed. As the point is situated below the excavated orebody a fairly small vertical load would be expected. However, the ellipse demonstrates that the shearing stress is high (60 kg/sq.cm). The major axis of the ellipse is inclined upwards towards

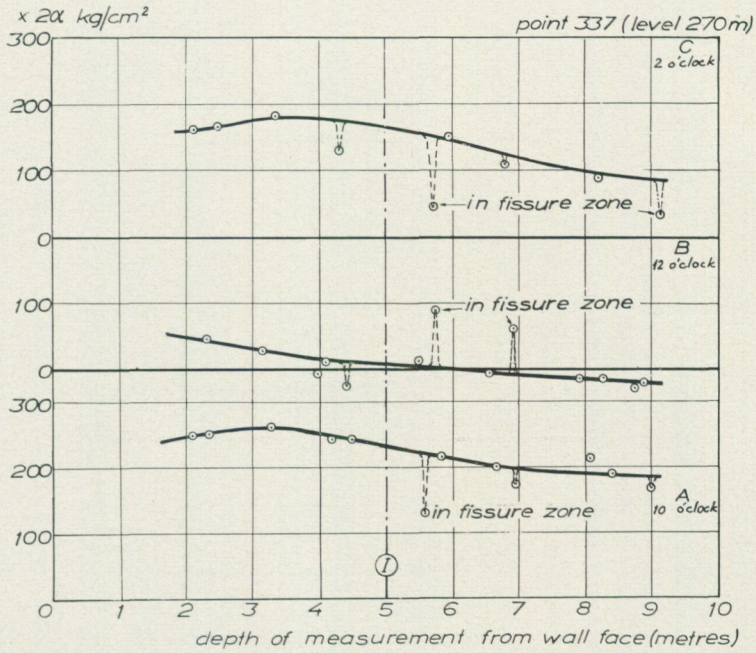

Fig. 54 a. Stress components in the A, B and C directions for point 337 at the 270 metre level. The interpolation diagram shows that the section for determination of the principal stresses at this point according to Fig. 53 is at a depth of 5 metres. At 5.7 metres the values are influenced by a fissure passing the point of measurement, but not encountered by the rock core. Deeper in the rock the measured vertical component B represents tensile stresses.

the hanging wall, and probably tends to become perpendicular to it as the point of measurement approaches and enters the orebody. This contains a marginal zone of chlorite sköls, so that there will be hardly any frictional forces acting between the surfaces. For the points in the foot wall that are situated 25—50 metres from the orebody the vertical stresses increase with depth below the zone of excavation (Fig. 53). Point 337 at the 270 metre level, where a horizontal stress of 155 kg/sq.cm was measured, is clearly not situated near that zone of Lönnfallet where the maximum horizontal stress prevailed. The recorded horizontal stress, however, is greatest at the higher levels, first falling off with depth and then increasing slightly. Whether this is a general state or whether it is due to local conditions around the measuring points cannot be decided on the basis of the rather small number of values available.

At all the levels the horizontal stress displays no marked tendency to fall off with distance from the orebody; on the contrary, it may even increase, as it does at 310 and 360 metres. This suggests that the horizontal stress is not due to the pressure of the hanging wall, for then the horizontal stress would fall off with distance from the orebody. Except near the working zone the shearing strength of the rock, most of which is leptite, is about 15—20 kg/sq.cm at points in the foot wall. This is not a very high value.

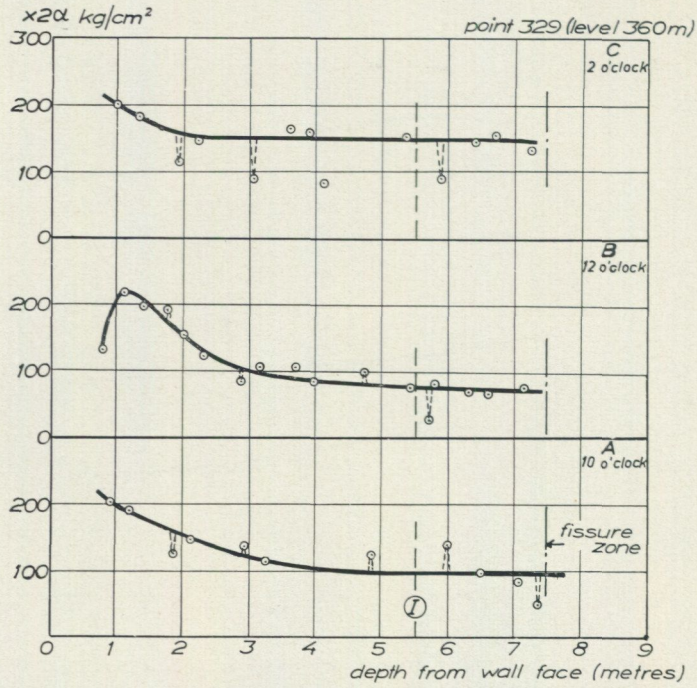

Fig. 54 b. Stress components in the A, B and C directions for point 329 at the 360 metre level. The wall was less damaged by the blasting procedure than usual so that the stress values could be obtained rather near the rock face. The zone of increased stress around the drift (Fig. 50) is clearly represented. At a depth of 5.8 metres a fissure is passing near the core and another one at 1.8 metres.

A most interesting point is that the rock between the sköls in the part of the foot wall in which measurements were made (some 250 metres from the orebody) is apparently acted on by equally high shearing stress. This suggests that in the foot wall around the Central Shaft there is elastic and plastic deformation, mainly in the chlorite-mica sköls, by virtue of which the shearing stresses are uniformly distributed throughout the foot wall — a significant factor as regards its stability. This does not apply to the foot wall in the vicinity of the working zone in the orebody, where disturbingly high shearing stresses are acting.

Fig. 55 shows a vertical section passing through the Jakobina Shaft and the main drifts at various levels, and perpendicular to the Mellanfältet body. This section shows point 105 in profile $30\frac{1}{2}$ and the adjacent point 372, neither of which actually fall in the plane of the section, however. The stresses at roof point 369, situated roughly half-way between the Jakobina and Central Shafts, are also inserted. Point 374 is in the north wall. The stress ellipses for points 357 and 361 in the south wall of the drift at 310 metres are very flat. The shearing stresses are extremely high at these points. It is interesting to note that here and at point 356 — at the 270 metre level — the inclination of the major principal stress is 20° to the horizontal. The plane through the

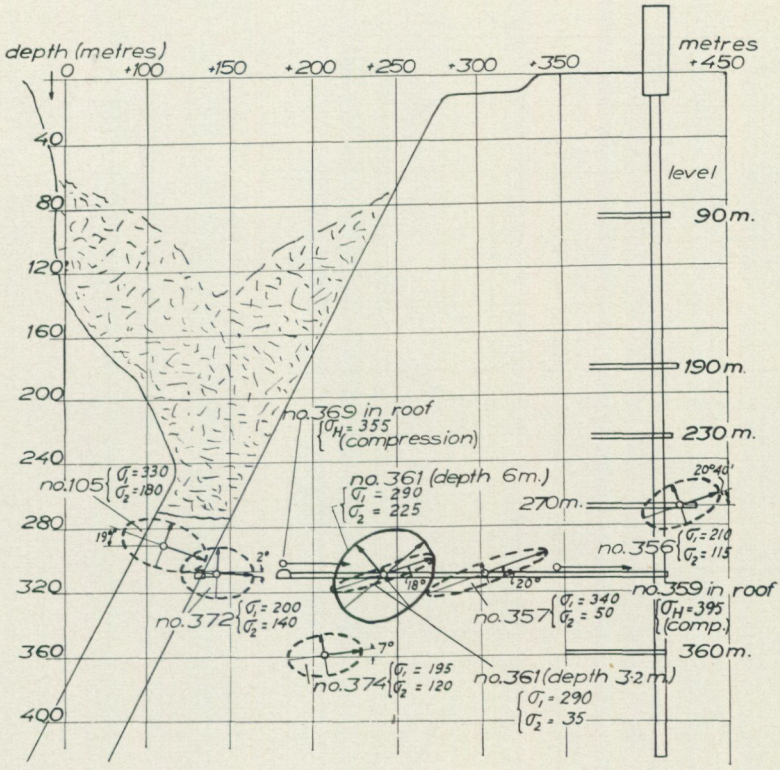

Fig. 55. Vertical cross-section through the Jakobina Shaft and main drifts. Deep measurements.

point where the maximum shearing stress prevails is thus inclined at $45 + 20 = 65°$, or approximately the direction of the sköls in this area, and also perpendicular to surface itself. It is possible that the presence of the sköls, which are probably of limited length (overlapping each other) and interrupted by homogeneous rock, sets up parallel zones of weakness in the rock, without fissures actually forming. Measurements in uncrushed zones would then reveal very high shearing stresses in the direction of the sköls.

The stress ellipse for point 361 is also given for a greater depth in the wall than that to which the flattened ellipse refers. At this point, the shearing stress is much smaller and the inclination of the axes of the ellipse different. Fig. 56 gives all the stress values for point 361, and the positions I and II of the sections where the principal stress has been calculated. The flattened stress ellipse of section I refers to a depth of 3.2 metres. Here, $\sigma_1 = 290$ and $\sigma_2 = 35$ kg/sq.cm; that is to say, $\sigma_1 > 8\sigma_2$. Section II refers to a depth of 6 metres, where $\sigma_1 = 290$ and $\sigma_2 = 225$ kg/sq.cm. The value of τ_{max} at this point is much lower than at 3.20 metres. This marked change in stress would appear to be ascribable to the presence of a sköl zone about one metre thick in the direction of the measuring hole at a depth of about 4 metres (Fig. 56). The vertical component, B in the diagram, is 40 to 50 kg/sq.cm and tensile before the

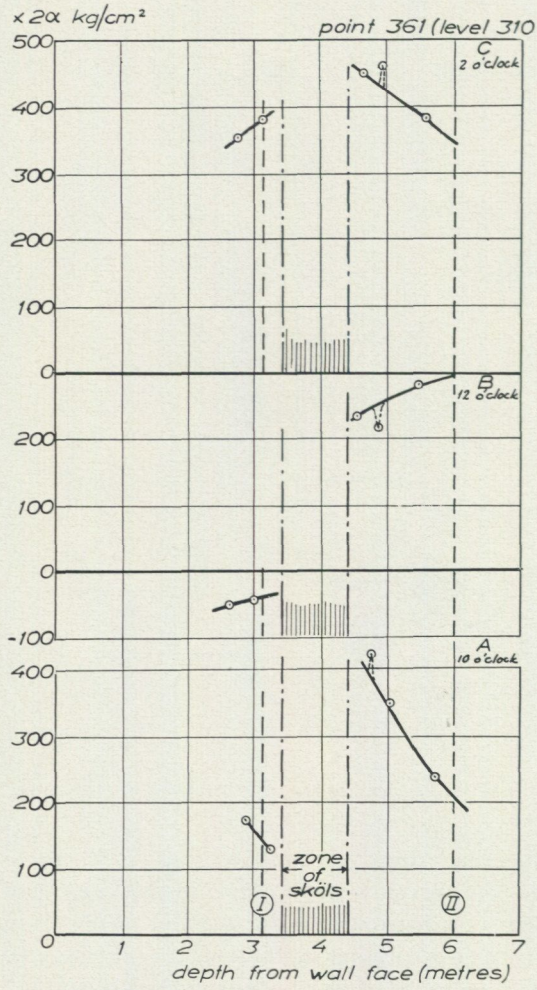

Fig. 56. Stress fluctuations at point 361 at the 310 metre level, apparently due to the appearance of a wide sköl and fissure zone. Before this zone the vertical component (B direction) is 40—50 kg/sq.cm, tensile, whereas after the zone it is over 200 kg sq.cm compressive.

sköl zone, but immediately after it the stress is a compressive one of more than 200 kg/sq.cm. This zone may be the cause of the almost hydraulic state of stress at point 361 at the depth of 6 metres. In fact, there are great fluctuations in stress field in the heavily loaded section through the Jakobina Shaft, which indicates a degree of instability at the free corner of the foot wall above mentioned. The stresses measured in the main drift of the Jakobina area are much higher than those acting in the main drifts from the Central Shaft (Figs. 53 and 54), a situation that may have its general explanation in the proximity of the Central Shaft to one end of the long stope of Lönnfallet, Müller, Mellanfältet, Karl-Johan and Strandberget, where the fairly undisturbed rock begins, whereas the Jakobina Shaft and its main drifts are roughly in the middle of the stope (Fig. 52). The existence of the deep stopes of Västra Ormberget (Figs. 51, 52 and 53) also lowers the transmission of horizontal forces in this region.

The horizontal stress in the drift walls at the 310 and 360 metre levels is high — 300-350 kg/sq.cm — and is largely consistent with the horizontal values in the roof of the main drift (Fig. 52). The differences are probably due to the stress zones around the drifts.

Sköl formation in the foot wall

General aspects

The study was prompted by the pronounced occurrence of sköls at all levels in the mine, and by the fact that they consisted of chlorite and mica. This means, in fact, that the fissure surfaces and the contact zones are covered by a lubricant, as a result of which only normal forces are transmitted across the discontinuities in the rock. There is reason to believe that there are large lateral movements around the sköls, where they are wide and consist partly of chlorite and mica.

There can be no doubt that the presence of numerous sköls considerably weakens the foot wall. From the aspect of stability the most serious weakening

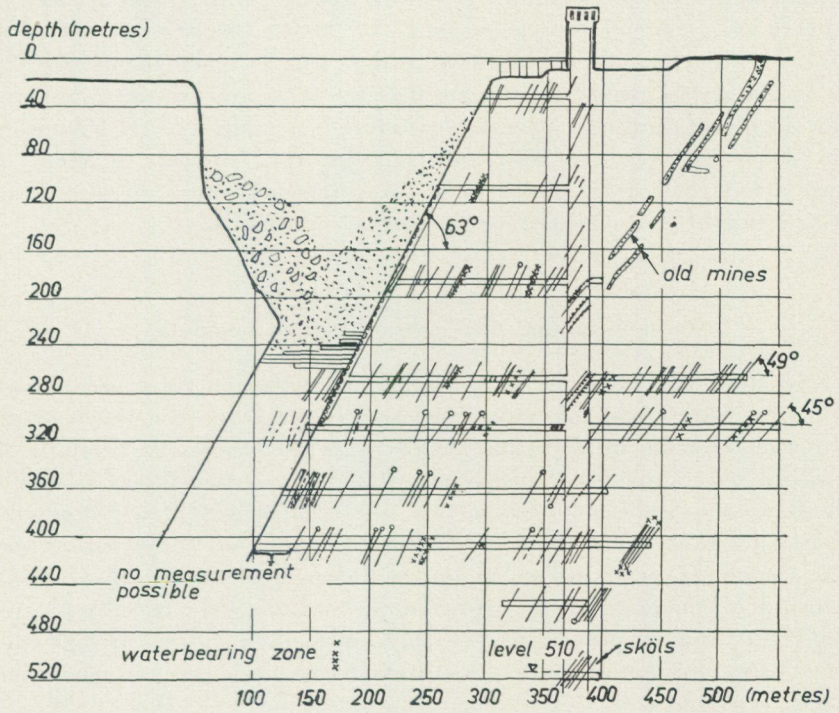

Fig. 57. Vertical cross-section through the Central Shaft and main drifts, showing occurrence of sköls and their dip. Their intersection with the horizontal is perpendicular to the main drifts (parallel to the ore body). Their width and mineralogic composition were also noted. It is observed that the sköls nearest the ore lens are parallel to it — dipping at 63° —, whereas at a distance their dip decreases. At the inner end of the main drift the angle is still 49° and 45° at the 270 and 310 metre levels, respectively.

occurs if the sköls are very extensive — for instance, if they pass from one level to another. This is to some extent the situation as the number of sköls is almost the same at the various levels at 190 metres and below. However, it is only some water-bearing zones that are continuous (Fig. 57). Other types of sköls tend to become thinner and eventually die out, only to be replaced by others a short distance away. In such cases of alternating sköl and rock, or of overlapping sköls there will also be a considerable weakening of the foot wall. This will be so frequently intersected in the direction of the sköls that a section through the foot wall in this direction will pass through a considerable area of chlorite and mica — materials incapable of transmitting shearing forces. Such forces in the surface of the section will then be absorbed by intact rock, with the result that the stresses will be appreciably greater than they would normally be in homogeneous rock under similar loading conditions. As a result, the stability of the foot wall is lowered by the possibility of slipping parallel to the sköls.

Figs. 53 and 55 show the major and minor principal stresses σ_1 and σ_2 and their direction at a number of points in sections through the foot wall. The maximum shearing stress, τ_{max}, is $\frac{1}{2}(\sigma_1 - \sigma_2)$. The surface over which this maximum stress value applies lies in the bisector of the angle between the directions of σ_1 and σ_2. For points not too close to the orebody this is the same as the inclination of the sköls (points 356, 357 and 361 in Fig. 55). This is not unexpected, and suggests that the sköls are probably numerous in the foot wall, although they are usually not actually observed elsewhere than where they intersect the drifts. However, their presence is often confirmed during the course of the stress measurements, when the appearance and direction of thin ones can be studied in the rock core.

The sköls around the Central Shaft in Lönnfallet

The position and direction of all the sköls in this region have been entered in Fig. 57. They could, of course, be observed only between the floor and the roof of the main drift but their slopes have been measured carefully. To emphasize their direction the sköls have been represented in the section by lines that are considerably longer than the scale length of the observable stretch of the sköl within the drift. The stopes that, west of the Central Shaft in the section, appear down to 200 metres belong to Västra Ormberget. The downward continuation of its corresponding thin ore veins may be followed in the shaft and deeper drifts. The surfaces of these bodies are generally covered with chlorite-mica, so that as regards shearing strength and tendency to slip they resemble sköls.

The sköls usually intersect the horizontal plane in a line perpendicular to the main drift of the Central Shaft, and are thus roughly parallel to the ore lens. Throughout the foot wall, from the ore lens to the Central Shaft, they have the same dip as the lens — that is, about 63°. It is interesting to note

that the inclination of the sköls on the other side of the shaft tends increasingly to the horizontal — at the extreme end of the main drift at the 270 metre level the inclination has decreased to 49°, and at 310 metres to 45°. Where the intersection of the sköls and the horizontal plane is not perpendicular to the main drift the sköls marked in the figure are indicated by a line terminating in a small circle. In some instances the sköls lying in a continuation drift close to the main drift have also been entered. They are indicated by broken lines.

The sköls are at certain places grouped into bands or zones; for instance, at 410, 460 (at the end of the main drift) and 510 metres — the bottom of the shaft. Water-bearing zones have been entered in the appropriate section (Fig. 57). There is one of them at a constant distance of about 150 metres from the large lens at all levels from 270 down to 410 metres — the deepest of the more fully excavated main drift. The water-bearing zone thus follows the dip of the lens and may be connected with the excavated mines of Västra Ormberget.

There are sköls also at the 35 and 100 metre levels, though they are rather sparse. At 190 metres and below they become more numerous, and at 360 metres there is a dense area extending from the large orebody about 60 metres into the foot wall. Whether there is a similar area next to the one at 410 metres cannot be decided until the main drift from the Central Shaft has been taken down to the lens at this level. With the exception of this zone the high density of the sköls does not decrease, but may even increase, with distance from the lens. There is a group of these structures in, or west of, the Central Shaft — for instance, at the 270, 410 and 510 metre levels (Fig. 57). Along such well-defined sköl zones there is a greater likelihood of slipping than along single overlapping sköls separated by intact rock.

The foot wall must have a sufficiently high degree of stability against slip along circular cylindrical surfaces, which may follow the old stopes of Västra Ormberget and at deeper levels gradually link up with various sköls. It is then the shearing strength of the slabs of homogeneous rock between the sköls that represents the stabilizing forces against slip. As the depth of mining increases it becomes more important to calculate the possible surfaces of slip.

The sköls around the Jakobina Shaft in Mellanfältet

A similar study has been made for the Jakobina region and the main drifts leading therefrom. As regards their density a cross-section with the sköls drawn in would have much the same appearance as in Fig. 57.

The width of the sköls or sköl zones varies from one millimetre or so to 30 centimetres, the most common ones being from one to 5 centimetres. The sköls can appear as clayey contact surfaces between different types of rock, such as diabase, leptite, granite and pegmatite. Many of the sköls consist of chlorite-mica layers on each side of thin ore veins.

The origin of the horizontal rock pressure in the Grängesberg mine

Measurements in the ore lens and foot wall revealed the presence of a predominantly horizontal pressure in the Lönnfallet, Müller, Mellanfältet and Strandberget regions. The state of horizontal stress in the other parts of the Grängesberg mines has not been determined.

The rock pressure measurements suggest the following conditions.

(1) The stresses are low in the uppermost part of the working zone, below which they attain a maximum in a distance that is probably about the same as the width of the ore lens; they then diminish until there appears to be another increase (Fig. 49).

(2) The horizontal stresses are highest roughly perpendicular to the plane of the lens.

(3) Even at great depth (Figs. 53 and 55) the horizontal stress is about one and a half times as great as the vertical stress at the same point.

(4) The horizontal stresses in the foot wall at the deep levels are constant for considerable distances from the ore lens, and would seem to be greater rather than smaller than the stresses at the adjacent points in the ore lens.

(5) Even at some points at the 190 metre level that lie 50—60 metres above the ore level in the large orebody there are high horizontal stresses (point 347, Fig. 53).

(6) Horizontal stresses act in the whole foot wall from the Central to the Jakobina Shaft. They are between 50 and 100 per cent higher in the latter area than in the former at corresponding levels.

In both long and short term planning of the excavation of ore in the Grängesberg mine account must be taken of the origin of these horizontal stresses, and not only for reasons of safety and the stability of the mine, but as much to achieve the most economic methods of production. It is important that the available rock pressure should be exploited as a cheap method of crushing the ore prior to excavation. It has been demonstrated that in these areas high stresses are acting even at the present levels of excavation; the horizontal pressure is likely to increase with depth, and will thus be a still more effective means of crushing the ore.

A study of the horizontal pressures suggests three possible origins:

A. Pressure from the hanging wall.

B. A horizontal pressure in the virgin rock that from the beginning may not be very high but as the ore is removed becomes concentrated around the bottom of the stope, as a result of which great stresses are set up in the working zone. It is assumed that the rock in the foot wall is acting as a homogeneous material and that the stress is distributed in accordance with elastic theory. This form of stress concentration is referred to below as type *B*.

C. Horizontal pressure due to the weight of the foot wall may appear in the

working zone but the stress concentration differs from type *B* in that elastic and plastic deformation and deflections take place in the sköls and sköl zones of the foot wall. This form of stress concentration will be called type *C*.

A. Pressure from the hanging wall

Since the hanging wall consists of strong types of rock, there is a natural overhang above the working face. The wall will thus subject the ore to a certain horizontal pressure, especially if parts of it tend to slip down towards the orebody owing to internal fissuring. Calculation shows, however, that these forces from the hanging wall are only a small fraction of those due to the horizontal pressure in question.

If the hanging wall were to subject the foot wall to horizontal forces *via* the ore these would be greatest at the part of the foot wall nearest to the orebody, the stresses in the wall then falling off with distance therefrom. As is evident from the transverse sections in Figs. 53 and 55, this is in fact not the case. According to Fig. 55 horizontal pressures at least as great as those in the immediate vicinity of the hanging wall have been measured at points up to 300 metres away in the foot wall. It is clear, then, that the horizontal stresses do not originate in the hanging wall to any appreciable extent.

B. Stress concentrations set up by horizontal rock pressure in the virgin rock in accordance with elastic theory

The study of this possibility is divided into three sections:

(i) Types of lateral stress in virgin strata; (ii) the manner in which these stresses in homogeneous rock may in the course of mining become concentrated around the orebody, particularly at the working zone; and (iii) the decrease in this stress concentration with depth below the working zone.

This last factor is important. Even if the measured distribution of the horizontal stresses near the working zone prove consistent with (ii) the pressure acting in the ore lens cannot be regarded as a concentration of stresses in homogeneous adjacent rock in accordance with elastic theory, as is assumed in *B*, unless the decrease in the stress concentration with depth is also consistent with (iii). If this is not the case the third possible origin of the horizontal rock pressure (*C*) must be considered.

(i) *Types of lateral stress in strata of virgin state*

Measurement has shown that such stresses occur in many mines in Sweden. At some places they may be of geological origin. It would appear unlikely, however, that in the Grängesberg region these stresses will be permanent, owing to the presence in the foot wall of numerous fissures and chlorite-mica sköls; however, *they would most probably persist if the geologic or tectonic forces were still acting*.

The presence of inclined sköls is another possible natural origin of the horizontal stresses. The foot wall at Grängesberg is cut by numerous

oblique sköls and several water-bearing zones passing from one level to another. The sköls have the same dip as the orebody. Since they cannot transmit tangential but only normal forces a lateral pressure will be set up by the weight of the overburden. The magnitude of this pressure is difficult to determine theoretically, but from the dip of the sköls it may be estimated at about 60 per cent of the vertical stress at the same point.

(ii) *Stress concentration in the working zone*

An approximate theoretical treatment of the stress concentration may be of interest, even if it can demonstrate only the tendency of this concentration in and around the orebody owing to the lack of information on the magnitude of the general horizontal stresses in the virgin rock.

In his paper entitled *Stresses in a plate due to the presence of cracks and sharp corners*, Inglis has solved the problem of stress concentrations at the end of internal cracks in a stressed material. The same formulae apply in the case of a crack penetrating from the surface. His solution of the problem is based on the case of the distribution of stresses about an elliptical opening, the crack being considered as a very flat ellipse.

Consider a homogeneous plate, which is subjected to a uniformly distributed tensile or compressive stress σ_0 parallel to its main axis (Fig. 58). In one edge of the plate and perpendicular to its long axis there is a slit D — for instance, an open crack. Around the bottom of the slit there will be a stress concentration that will in some respects resemble that existing around the bottom of a stope on excavation of the ore. In the diagram, e—e may be assumed to represent the ground level in an open mine, and the slit D the stope.

The stress σ_b acting in the material around the end of the slit is given by the expression

$$\sigma_b = \left[1 + 2\sqrt{\frac{a}{\varrho}}\right]\sigma_0$$

where ϱ = radius of curvature of the bottom of the slit

σ_0 = stress acting in the material at a great distance from the slit
σ_b = stress acting in the material around the end of the slit
a = depth of the slit from the edge of the plate

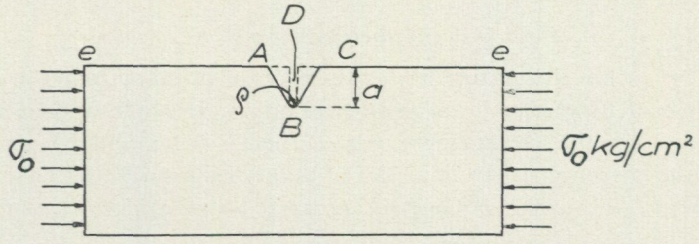

Fig. 58. A plate in which there is a notch ABC, at the bottom of which the radius of curvature is ϱ. The plate is compressed by σ_0. The broken line represents the slit D for which Inglis' formulae strictly apply. BC represents the inclination of the foot wall at Grängesberg.

According to Inglis the stress distribution will not differ appreciably if the slit is replaced by a notch having sloping sides.

Comparing Figs. 58 and 44, it is seen that

the surface BC corresponds to the foot wall, and
» » AB » » » destroyed part of the hanging wall
the point B » » » depth of excavation
the radius ϱ » » one-half the width of the lens.

A part of the hanging wall remains intact; this, however, does not appreciably influence the stress concentration at the point C.

1. Inserting in the above formula the values from actual excavations in Lönnfallet, viz

$$a = 270 \text{ metres } \varrho = \frac{70}{2} = 35 \text{ metres}$$

we obtain

$$\sigma_b = \left[1 + 2\sqrt{\frac{270}{35}}\right] \sigma_0$$

$$= 7\ \sigma_0 \text{ approx.}$$

2. For the Müller region

$$a = 300 \text{ metres, } \varrho = 50/2 = 25 \text{ metres}$$

so that

$$\sigma_b = \left[1 + 2\sqrt{\frac{300}{25}}\right] \sigma_0$$

$$= 8\ \sigma_0 \text{ approx.}$$

3. At places in Strandberget where the ore lens is narrow

$$a = 270 \text{ metres, } \varrho = 8/2 = 4 \text{ metres}$$

so that

$$\sigma_b = \left[1 + 2\sqrt{\frac{270}{4}}\right] \sigma_0$$

$$= 18\ \sigma_0 \text{ approx.}$$

What is the magnitude of the general natural lateral pressure? If this pressure σ_0 is assumed to be 60 per cent of the vertical load — the overburden —,

$$\sigma_0 = \frac{60}{100} \cdot 270 \cdot 2.7 = 44 \text{ kg/sq.cm}$$

Inserting this value of σ_0 in the above expressions for σ_b, we have

for Lönnfallet $\sigma_b = 7 \times 44 = 300$ kg/sq.cm
Müller $8 \times 44 = 350$
Strandberget $18 \times 44 = 800$

Inglis found that the stress concentration at B (Fig. 58) is not so much dependent on the slope of the sides of the notch as on the value of the horizontal stress σ_0 acting at the bottom of the notch.

Inglis' formula assumes that σ_0 is constant over the width of the plate. If the horizontal rock pressure is assumed to bear a constant relationship to the vertical pressure, being zero at ground level and increasing linearly with depth, the calculated values of σ_b are too high. However, the stresses at B are not appreciably influenced by a decrease in the value of σ_0 near the surface e—e (Fig. 58). Moreover, it is improbable that high horizontal stresses can act around the lens near ground level, even in strong rock.

The values of the stress thus calculated for the bottom of the slit for Lönnfallet, Müller and Strandberget are, at least for some points, in agreement with the stresses measured in the ore body. In Lönnfallet a maximum pressure of 200—300 kg/sq. cm was obtained for the 240 metre level; in Müller it was 200—300 kg/sq. cm at the 290 metre level, and more than 600 kg/sq.cm at 285 metres. In the narrowest part of the Strandberget orebody the stresses exceeded 800 kg/sq.cm.

The uppermost part of the working zone was crushed for the length of the orebody, and nowhere did the stress exceed 50 kg/sq.cm, forces acting near the surface apparently being transmitted downwards as the crushing of the surface advanced.

The presence of such high pressures as 600 kg/sq.cm in profile $30\frac{1}{2}$ in the wide Müller body is not consistent with the values calculated from Inglis' formulae. These pressures may, however, be local.

There will, of course be closer agreement if the natural horizontal stress σ_0 is greater than has been assumed — namely, 60 per cent of the vertical load. But then there would be a greater discrepancy in respect of the other values in Lönnfallet and Müller.

As mentioned above it is not possible only on the basis of the calculations under (ii) to ascertain whether the stress concentration existing around the ore lens is due to the prevailing natural horizontal rock pressure. However, this would appear *not* to be the case in view of the absence of any fall in the magnitude of the horizontal stress with depth from the working zone, as is proved in (iii).

(iii) *The decrease in stress with depth below the working zone*

With the notation of Fig. 59 the normal stress σ_x in the section $A' - A''$ is given by the expression[1]

$$\sigma_x = \sigma_0 + \sigma_0 \frac{b}{2\,(y^2 - b^2 + a^2)} \cdot \alpha$$

$$\alpha = 2(a+b)^2(2a-b)\,\frac{1 + \dfrac{y}{2\sqrt{y^2 - b^2 + a^2}}}{(y + \sqrt{y^2 - b^2 + a^2})^2} + \frac{b \cdot y}{\sqrt{y^2 - b^2 + a^2}}$$

[1] Neuber: Kerbspannungslehre, pp. 48—51.

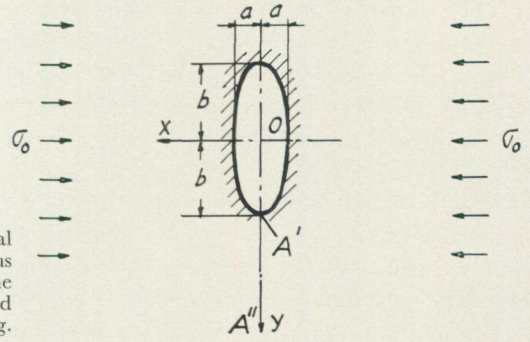

Fig. 59. Calculation of the horizontal stress for the section A′ — A″ at various depths from the elliptical bottom of the opening which is located in a stress field $= \sigma_0$ at a large distance from the opening.

where a = one-half the width of the orebody
b = » height » » »
y = the depth of the point A'' below the ground level that is below point 0 in Fig. 59.

The quantity σ_x is calculated for different values of $\frac{a}{b}$. Putting $\frac{a}{b} = 1$, the values of σ_x in the section $A' — A''$ are obtained for the case of a circular opening. If $\frac{a}{b} = 0$ the values refer to the case in which the opening is in the form of a vertical slit.

In Fig. 60, C denotes the lowest point of the ellipse or slit, which corresponds to the bottom of the stope (A' in Fig. 59). The distance from point 0 (Fig. 59) down to the point where the value of σ_x is required is denoted by y. At a depth of 300 metres below C the value of σ_x is only 1.1 σ_0 but at a depth of 20 metres — roughly one-third the width of the Lönnfallet orebody — σ_x is approximately 2.7 σ_0.

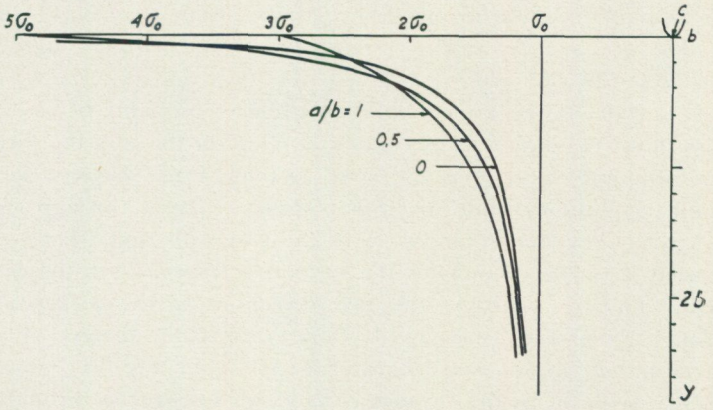

Fig. 60. Calculated stress for the case where the ratio a/b between half the width of the lens and its excavated depth underground is 1, 0.5 and 0. In the last instance it will be a very narrow lens or a deeply excavated lens of fairly small width.

The increase in the horizontal stress in a vertical section through the bottom of the slit or the stope thus diminishes very rapidly with depth therefrom. The stress measurements (Fig. 45) consistently indicate that the stresses decrease rapidly in a strata just below, and within, the zone of excavation, but at greater depths they are rather high and even show an increase (Fig. 53).

It is thus evident that the high horizontal stresses in the Grängesberg mines cannot be ascribed to the type B concentration of a natural horizontal pressure in the virgin rock, in which case it is assumed that the rock in the foot wall is homogeneous and conforms to elastic theory.

It remains to examine whether the horizontal stress concentrations may be of the type C, in which case the requirements of an elastic behaviour of the foot wall are to some degree modified.

C. Stress concentrations due to the weight of the foot wall and influenced by the presence of sköls

The horizontal forces in the foot wall, which is cut into rock slabs by the numerous sköls, are stabilized in such a way that the shearing stress τ is almost uniform throughout the rock plates for large parts of the foot wall (Fig. 53).

Fig. 61 shows a section through the Central Shaft in which the stress ellipses have been inserted for six points. In all cases the readings used in the calculation of the principal stresses and directions were made at depths of about 5 metres, so that it may be assumed that the high stress zone around the drift exerted no appreciable influence.

Along the axes of the principal stresses $\tau = 0$, and at an angle of 45° to them, τ is a maximum. It is then possible to draw an arc $x_1 - x_2$ that passes through the points 335 and 336 at 310 and 270 metres, respectively, so that the major axis of each ellipse is tangential to the arc at the two points. The direction of the major principal stress differs insignificantly at the three points 337, 335 and 330, which lie one above the other and rather close to the orebody. The arcs $y_1 - y_2$ and $z_1 - z_2$ may also be drawn through, or near, the points 333, 329 and 330.

Without introducing an appreciable error it may probably be assumed that in the case of all the points in the foot wall lying on the arcs the direction of the major principal stress σ_1 is the same as that of the tangent to the arc at the point in question, while the minor stress σ_2 passes through the centre O of the circle. The maximum stress in the foot wall thus passes along the arcs in question, while σ_2 denotes the normal pressure along the same lines or surfaces. Since $\tau = 0$ along the two directions of the principal stresses $\tau = 0$ along the arcs or surfaces. If O is taken as the centre of moments of the forces acting, say, on unit length of the foot wall (Fig. 61), the influence of the normal stress σ_2 in the circular surface (all forces pass through O) and of the shearing stresses in the circular surfaces $x_1 - x_2$, $y_1 - y_2$ and $z_1 - z_2$ ($\tau = 0$ for these surfaces) disappear.

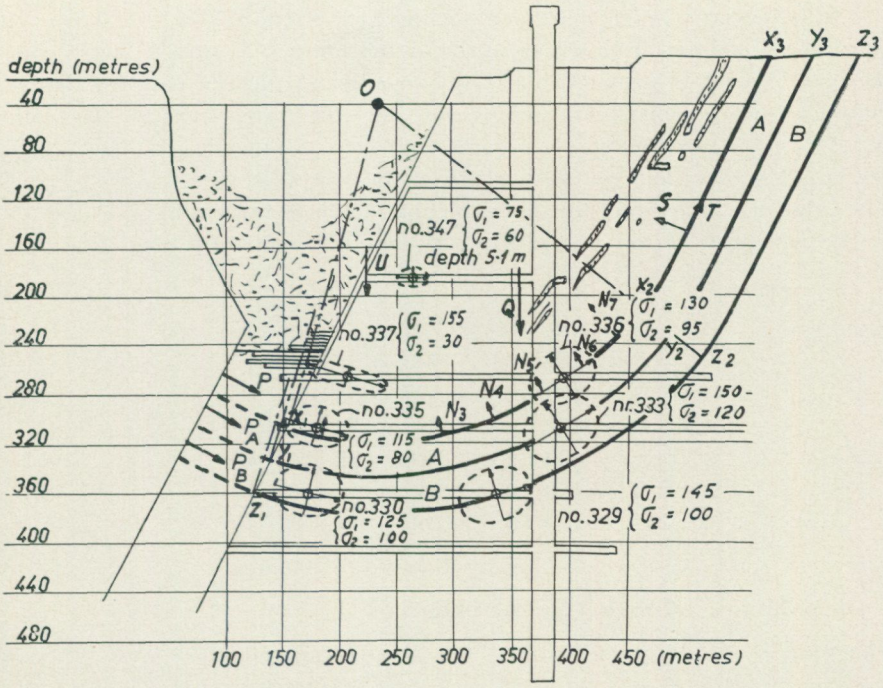

Fig. 61. Vertical cross-section through the Central Shaft (as Fig. 53) in which have been inserted three lines or surfaces $x_1 - x_2 - x_3$, $y_1 - y_2 - y_3$ and $z_1 - z_2 - z_3$, along which the shearing stress is zero — that is to say, along this surface the rock slabs intersected by the chlorite sköls are not subjected to shearing forces. In fact they are not circulo-cylindrical surfaces of slip, but, on the contrary, surfaces where the danger of slip is least in the foot wall, the τ value being about 0.

There remain then the following forces:

Lateral force P in the lens

Normal force S in the surfaces $x_2 - x_3$, $y_2 - y_3$ and $z_2 - z_3$

Shearing force T in the surface $x_2 - x_3$ etc.

The weight of the foot wall Q above the surface $x_1 - x_2 - x_3$ etc.

Weight U of the material within the area between the line $x_1 - 0$ and the foot wall.

An estimate of the magnitude of the shearing stresses along $x_2 - x_3$ is obtained by projecting the forces acting on to this line, which has the same inclination as the foot wall.

The forces acting are:

The weight Q of the foot wall = 75,000 × 2.7 = 203,000 tons per metre, (1 metre = unit length, measured in the direction of the orebody.)

The normal reaction P from the body acts roughly perpendicular to the hanging wall; this was shown by measurements at certain points in the body and was, moreover, suggested by the presence of chlorite sköls on the surface of the hanging wall, which prevent frictional forces from acting there. The distance $x_1 - x_2$ is divided into 7 parts by the resulting normal forces $N_1 - N_2 - N_3$

... N_7, the width of each element being 48 metres. As Fig. 61 shows, the value of σ_2 changes from 80 kg/sq.cm at the point 335 to 95 kg/sq.cm at the point 336. It is assumed that this change occurs linearly with the distance between these points. The expression for the projection of the forces N_1, N_2 ... on the direction $x_2 - x_3$ is

$L = 48\ \sigma_2 \cdot 10\ c$ tons per unit length of the foot wall.

The value of c varies according to the inclination of the normal forces N_1, N_2 ...

The weight U of the material on the foot wall is 10,000 tons.

The magnitude of T

$$
\begin{aligned}
L_1 &= 480 \cdot 80 \cdot 0.964 = 37{,}100 \text{ tons} \\
L_2 &= 480 \cdot 83 \cdot 0.900 = 35{,}800 \text{ »} \\
L_3 &= 480 \cdot 87 \cdot 0.810 = 33{,}800 \text{ »} \\
L_4 &= 480 \cdot 90 \cdot 0.716 = 30{,}900 \text{ »} \\
L_5 &= 480 \cdot 93 \cdot 0.570 = 25{,}300 \text{ »} \\
L_6 &= 480 \cdot 95 \cdot 0.436 = 19{,}800 \text{ »} \\
L_7 &= 480 \cdot 95 \cdot 0.260 = 11{,}800 \text{ »} \\
\text{Total} &\quad 191{,}500 \text{ tons}
\end{aligned}
$$

On projecting on to $x_2 - x_3$ we obtain:

$$
\begin{aligned}
\text{The sum of the downward forces} &= 0.89\ Q + 0.89\ U \\
&= 190{,}000 \text{ tons} \\
\text{The sum of the upward forces } L_1 + L_2 \ldots\ldots\ldots + L_7 + T &= 191{,}500 + T \text{ tons}
\end{aligned}
$$

It follows that shearing force T is small compared with the other forces in this comparison and may therefore be neglected. The assumption that for the points between 335 and 336, too, the major principal stress is tangential to the circle with centre O will probably not involve any appreciable error, in view of the close agreement between the major axes of the ellipses for all the points of measurement in the arc system. The flatter form of the ellipse for point 337 than for the other points is due to the local state of stress prevailing in the crushed zone. It may be added that the shearing force T in the surface $x_2 - x_3$ acts in the direction of the sköls and is zero at all parts of this surface where sköls may occur.

Considering the moment about O, the effect of the normal force S due to the surface $x_2 - x_3$ disappears, since its moment arm about O is small.

In the surface $x_1 - x_2 - x_3$ $\tau = 0$. The normal forces at the arc surface $x_1 - x_2$ pass through O. Thus the two remaining forces, the weight Q of the unit length, of the foot wall and the resulting reaction P in the ore lens, give

$$P \cdot a = Q \cdot b \quad \text{or} \quad P = Q \cdot \frac{b}{a},$$

where

a = the moment arm of P about O

b = the moment arm of Q about O

Inserting known values

$$a = 256 \text{ metres}$$
$$b = 120$$

we have

$$P = 95{,}000 \text{ tons}$$

If the height of the pressure zone in the ore lens is 55 metres (Fig. 61) the mean stress on the ore in this zone will be

$$\sigma_{mean} = \frac{95{,}000{,}000}{550{,}000} = 170 \text{ kg/sq.cm}$$

It is probable that the reaction P from the orebody, which at point 337 is 155 kg/sq.cm, increases with depth and then decreases to 115 kg/sq.cm at point 335.

An estimate of the variation of the force P with depth is obtained as follows. The major axes of stress ellipses for points 330 and 329 are tangents to the arcs $z_1 - z_2$, as are the axes of the ellipses for the points 336, 335 on the arcs $x_1 - x_2$. The same is true for the point 333 and $y_1 - y_2$. The distance between the x and y lines and between y and z is 35 metres.

If the part of the foot wall bounded by $x_1 - x_2 - x_3$ is prolonged to $y_1 - y_2 - y_3$, a similar relationship between the weight Q and the reaction P can be found for that greater part of the foot wall.

Denoting the reaction of the former ring A by P_A and that of the latter ring B by P_B, we have:

$$P_A \cdot a_A = Q_A \cdot b_A$$
$$P_B \cdot a_B = Q_B \cdot b_B$$

Inserting known values

$$Q_A = 54{,}000 \text{ tons}$$
$$Q_B = 59{,}000$$

we have

$$P_A = 34{,}000 \text{ tons}$$
$$P_B = 36{,}000$$

As a mean value for the height 35 metres we then have

$$\sigma_A = 96 \text{ kg/sq.cm}$$
$$\sigma_B = 102$$

Thus, σ_B is greater than σ_A; that is to say, the stresses increase with depth. This follows directly from the fact that Q increases as the square of the distance.

Near the zone of excavation, for a depth down to 55 metres, the mean stress $\sigma_m = 170$ kg/sq.cm; 35 metres deeper it is 96 kg/sq.cm, and a further 35 metres down, 102 kg/sq.cm.

If it is assumed that the contact zone of the foot wall bears on the orebody at a smaller height than 55 metres, say at 20 metres, the pressure on the orebody will be much greater. The stress distribution will be as shown in Fig. 49. The surface zone of the ore is crushed, so that the increase in stress indicated by the broken curve cannot occur, there being instead a more widely distributed increase in stress in the upper zone of the lens. The maximum stress in the body depends on the compressive strength of the ore.

The estimates show that P in the ore lens automatically constitutes a support that prevents large movements of the foot wall. That this may occur to the extent indicated by the stress measurements is due to the fact that, owing to the presence of many chlorite-mica sköls, the foot wall is plastically and elastically deformable. The separate rock plates dipping at 63° with sköls between them probably constitute a system where deflections of the separate plates take place at increasing load. This implies the advantage that the shearing stresses acting on the rock plates may be equalized over large parts of the foot wall. This is directly evident from the measurements performed in the section through the Central Shaft.

As a rule $\frac{1}{2}(\sigma_1 - \sigma_2) = \tau_{max}$ is 15—20 kg/sq.cm at the measuring points, values that cannot be considered high for the rock in question. In the neighbourhood of the level of excavation, as at point 337, there are high local shearing stresses. It would appear advisable to follow these stresses during the course of the excavation in the mine.

The arcs $x_1 - x_2$ etc. *are not cylindrical surfaces of slip. On the contrary, a slip along these surfaces is impossible, since* $\tau = 0$. τ_{max} occurs at planes 45° to the σ_1 and σ_2 axis. On this basis it is possible to estimate the form of the surfaces where τ_{max} prevails in the foot wall.

Summary

Three possible explanations A, B and C of the source of the high horizontal rock pressure in Grängesberg have been examined (p. 120). Pressure due to the hanging wall (A) as well as to the concentration of horizontal stresses in the virgin rock, arising on the assumption that the foot wall consists of homogeneous rock that behaves in accordance with the elastic theory (B), are probably not acceptable. On the other hand, if the latter assumption is rejected and account is taken of the high deformability of the foot wall intersected by sköls the third explanation (C) would seem the most likely.

PART FOUR

MEASUREMENT OF STRESSES IN A PILLAR IN KAPTENSLAGRET AT MALMBERGET

At Malmberget in northern Sweden there is one of the largest known ore deposits in the country. It consists of a number of orebodies forming an arc some four kilometres in length (Fig. 62) and, in places, 60 metres in width.

Adjacent to the main orebody there is a separate deposit — Kaptenslagret — about 800 metres long and 30—40 metres thick, of which a horizontal section at the 360 metre level is shown in Fig. 63.

The ore deposit, which consists of magnetite, is situated in primary rock. The lenses dip at 60—75°. The rock of the hanging and foot walls is red or grey leptite and red granite, the latter in particular containing bodies of pure quartz. Remarkably enough, whilst the foot wall of the long arc of lenses contains numerous sköls, generally of chlorite, the foot and hanging walls of Kaptenslagret are practically free from them, although thin veins of volcanic rock and clayey cleavage planes are found in places. At the surface of contact between the country rock and the ore in both foot and hanging walls, there are clayey surfaces. In the Kaptenslagret area the rock is alternately granite and leptite and generally has good mechanical properties. The fissuring of these rocks is here unusually slight. Strain bursts have occurred in the area — which suggests strong, rigid rock and high stresses. There are three chief planes of cleavage.

The pillar between hanging and foot walls

The Kaptenslagret lens has been mined out down to the 410 metre level and for the whole of its length, with the exception of about 50 metres denoted by *A* in Fig. 63, this part remaining as a pillar or a horisontal support between the hanging and foot walls (Fig. 64). The pillar has a uniform width of 50 metres at the 280 metre level and below. Small areas of the pillar are left between the 240 and 280 metre levels.

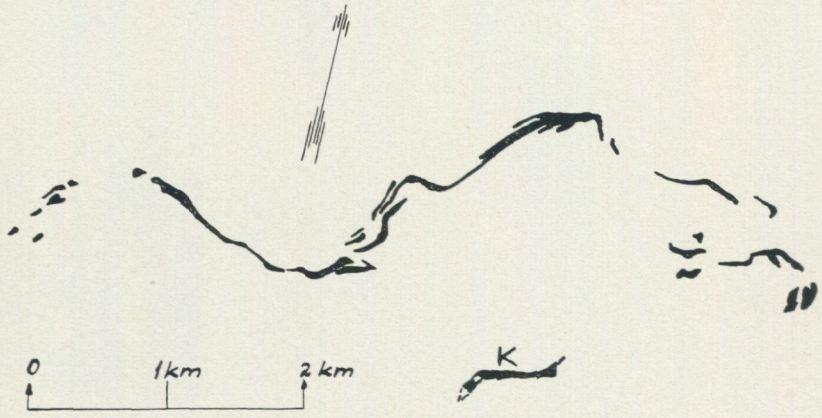

Fig. 62. Iron ore deposits at Malmberget.

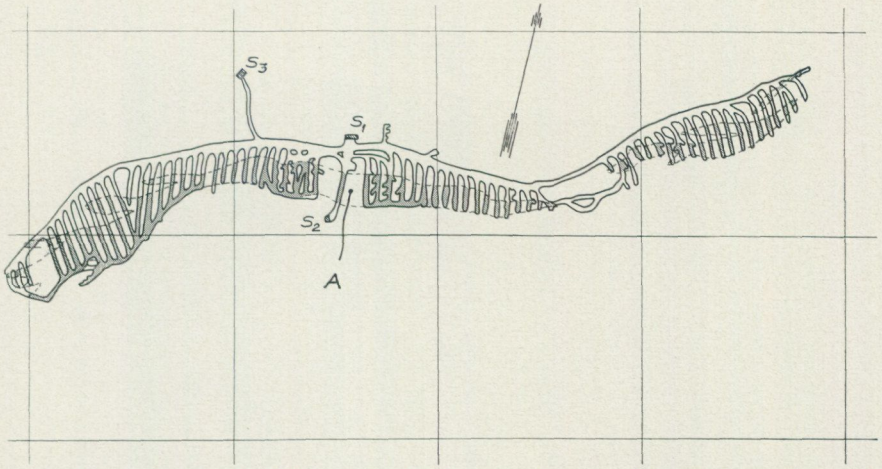

Fig. 63. Kaptenslagret at the 360 metre level. *A* is a pillar between the hanging and foot walls, remaining from the 240 to 410 metre level. (Figs. 64 and 65). Scale 1 : 7,400.

As is seen from Fig. 65 and the plans of the various levels of the pillar (Figs. 70—74), there is an inclined shaft in the foot wall and a vertical Hertig shaft in the hanging wall. Opposite the shaft the foot wall is practically vertical between the 280 and 320 metre levels. It contains a narrow orebody, which probably has clayey boundary surfaces. The Hertig shaft is located near the hanging wall and will suffer damage when the adjacent hanging wall caves. It is to stabilize the foot and hanging walls as well as the shafts that the 50 metre pillar has been left. However, it soon became evident that the pillar was highly stressed. The pillar was stabilizing the foot and hanging walls and was transmitting great pressures from the country rock — probably for the most part horizontal — which were acting in the virgin rock. The concentration of these horizontal forces became so great that fissures, mostly longitudinal, appeared in the inclined shaft, which consequently had to be reinforced with concrete.

A new shaft has recently been constructed in Kaptenslagret (S_3 in Fig. 63). Since pillar A contains much high-grade ore it is intended to mine it out as soon as possible. Any damage to the Hertig shaft caused by the removal of the pillar between the foot and hanging walls will be of no significance, since the shaft will no longer be required. The inclined shaft, on the other hand, should be preserved — at least until the pillar has been removed down to the 360 metre level.

In order to make it possible to forecast the fate of the shaft and the surrounding region of the foot wall when the pillar has been removed the following information is required.

(1) The magnitude and direction of the forces transmitted to the foot wall *via* the pillar.

(2) The magnitude and distribution of the stresses in the part of the foot wall next to the pillar and around the inclined shaft.

(3) The magnitude and direction of the virgin rock pressure in the area.

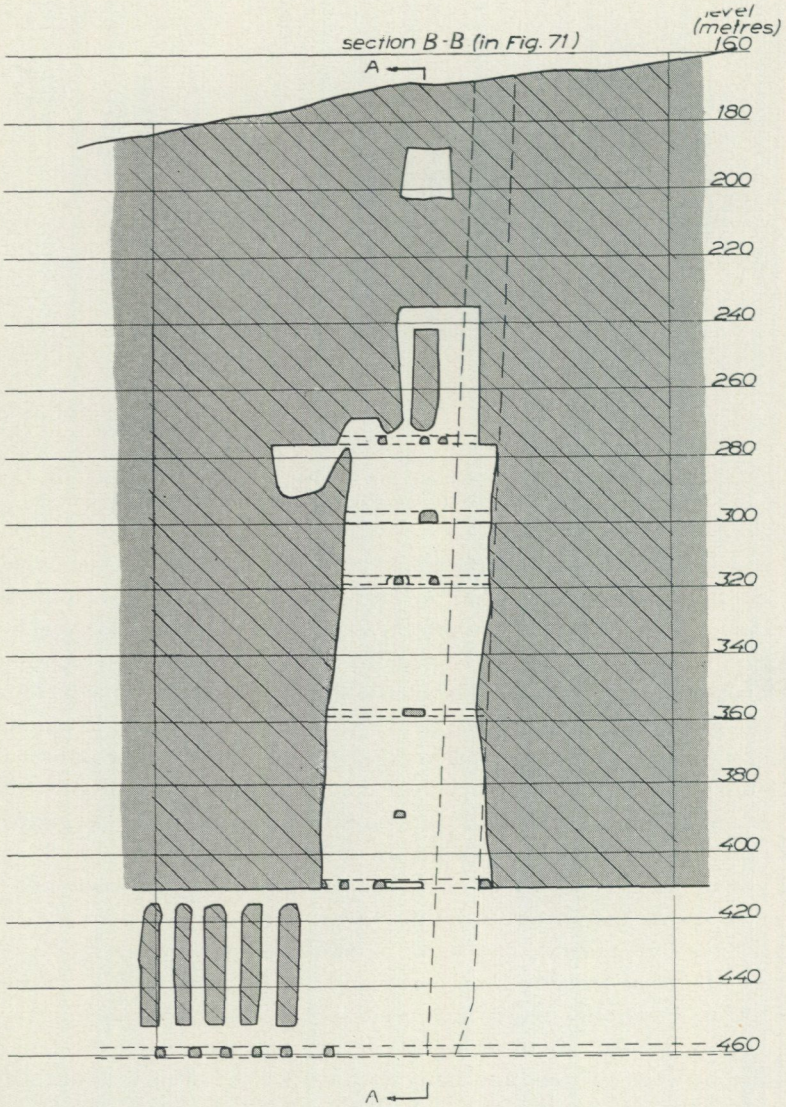

Fig. 64. Cross-section B—B of the pillar remaining in Kaptenslagret. Fig. 71 shows the location of section B—B. For the longitudinal section A—A see Fig. 65.

The forces to which the foot and hanging walls are subjected by the pillar tend to stabilize them. Should the pressure be only slight, the risk of caving through slipping of the foot wall in the near of the inclined shaft would not be great if the pillar were removed. On the other hand, if the pressure is very high, or if there should be in the area a high rock pressure that is acting in an unfavourable direction, careful planning of the removal of the pillar would be necessary. This should be done in stages, level by level, the horizontal stresses in each part to be removed first being released by cutting vertical slits.

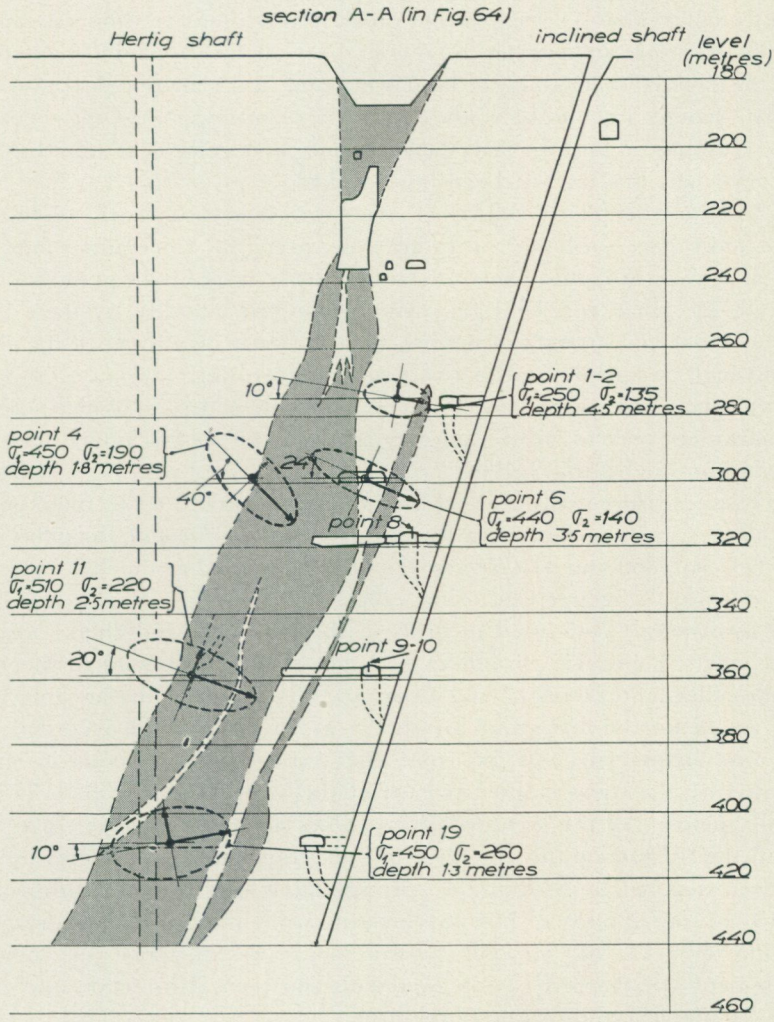

Fig. 65. Longitudinal section through the pillar *A* in Fig. 63. The stress ellipses give the principal stresses and their directions at points of measurements located in the foot and hanging walls near the site of the pillar.

The measurement of the magnitude and distribution of stresses in the part of the foot wall around the pillar and the inclined shaft (point 2) will give the actual magnitude and direction at various points in the foot wall. If the foot wall is regarded as an infinite hemisphere and the pillar pressure as a load on its plane surface, calculation of the stresses at various points in the foot wall should be possible when the magnitude and direction of the forces exerted by the pillar on the foot wall are known. If the measured and the calculated values and directions of the stresses are found to agree, it may be deduced that the foot wall is functioning as if it were of homogeneous material, and hence that the wall has not been fissured or crushed under the

concentrated pressure exerted by the pillar. If the pillar is removed carefully it should therefore be possible to retain the wall intact, and the continued use of the inclined shaft would be largely ensured. If the measured stresses in the foot wall should prove to be considerably higher or lower than the theoretical values, crushing or fissuring may be suspected, and great care would then be indicated when this level is being approached.

The ore in the pillar consists of magnetite that is of coarse texture and for the most part probably of rather low strength. Since uniformly thick bands of granite or leptite penetrate the ore body in the pillar, parallel to the foot wall, the pillar will be rigid, being reinforced laterally by these layers. In spite of the low strength of the ore in the pillar it may then still be able to transmit high compressive stresses without disintegrating.

All the stress measurements were made in granite or leptite of high strength; this guarantees correct stress values even when the rock is under such high stresses as prevail in this region.

The stress measurements in the following account fall into two main groups:

Wall measurements performed in the cross-cut passing through the pillar at the levels 275, 300, 360 and 410 metres. Point 23 is situated at the 460 metre level in the foot wall 70 metres west of the pillar.

Roof measurements performed in drifts in the foot wall, and chiefly near the inclined shaft. Points 15, 16 and 21—22, however, are situated further away from the pillar, and points 12 and 18 are in the pillar near the hanging wall.

The results for the first group are shown in Fig. 65 and the recorded stress values are entered in Figs. 66—69. The results for the second group are illustrated by the stress ellipses at each of the levels 275, 300, 320, 360, 410 and 460 metres. All the recorded stress values are given in Figs. 70 a—75 c.

In all the stress diagrams the three 60° directions of the stress measurement have been denoted by *A*, *B* and *C*, corresponding approximately to the directions 10, 12 and 2 o'clock. For wall measurements the operator is assumed to be facing the wall, and for roof measurements he is above the point of measurement. In the first case *B* represents the vertical direction and in the second one the length direction of the drift.

See also p. 28.

Wall measurements

At each level 275, 300, 320, 360 and 410 metres there is a cross-cut passing through the pillar, these cross-cuts connecting the Hertig and the inclined shafts (Figs. 70—74). By drilling the cell holes perpendicular to the wall face pillar stresses were measured in a plane parallel to the longitudinal dimension of the pillar; that is to say, the stresses measured were those acting on the foot and hanging walls.

In Fig. 65 the stress ellipse is drawn for five such points, two of which are situated in the foot wall and the other three in the hanging wall. It is

interesting to note that as deep as pillar exists the major principal stress is roughly perpendicular to the hanging wall — apparently owing to the presence of clayey boundary surfaces, which prevent the transmission of forces parallel to the surfaces between the ore and the wall. The hanging wall is inclined at 70° to the horizontal, and the major axis of the stress ellipse dips at 24° and 20° at the 300 and 360 metre levels (points 6 and 11, resp.). At the 275 metre level the inclination of the major axis is less, probably owing to local conditions around points 1 and 2, in the neighbourhood of which there is the end of a narrow footwall ore lens. Point 11 is situated a short distance lateral to the longitudinal section of the pillar through the inclined shaft shown in Fig. 65. The hanging wall is somewhat further forward at point 11, and the point is actually situated in granite (the broken line of the hanging wall). The same is valid for point 19.

The principal stress σ_1 at the 275 metre level was 250 kg/sq.cm, but had increased to 450 at the 300 metre level. The stress is further increased to about 510 kg/sq.cm at the 360 metre level. The minor principal stresses for the upper points 1, 2 and 6 were 135 and 140 kg/sq.cm, respectively, and for the point 11,220 kg/sq.cm. The direction of σ_2 approximates to that of the hanging wall.

Wall points 1—2

Fig. 66 gives the results for points 1 and 2 at the 275 metre level. At point 1 measurements were made at depths of from 70 to 480 cm in granite. As the stresses near the surface of the drift wall was not recorded, another hole was drilled at point 2, and the stress measured at depths of from 12 to 130 cm. The stresses were measured for various distances from the rock face in the verti-

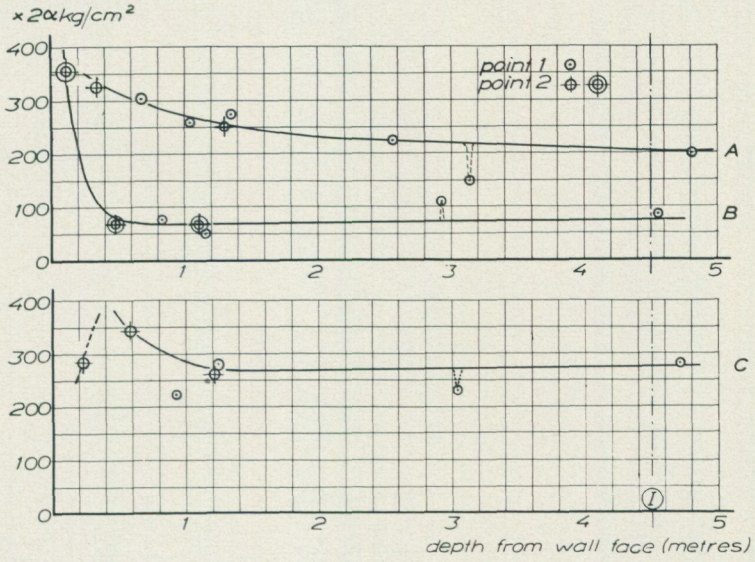

Fig. 66. Stress values recorded at wall points 1 and 2 at the 275 metre level. At a depth of 3 metres the core approached a fissure in the rock, *A* and *C* values decreased and *B* increased. $2\alpha = 0.7$.

cal direction (B) and at 60° on each side (A and C). Near the face there were recorded high B-values — at 12 cm $355 \times 2\alpha = 355 \times 0.7 = 250$ kg/sq.cm, and nearer the surface probably still higher values. The presence of increased values in the surface zone in the case of the 60° components, too, suggests the influence of the high vertical component. Moreover, at a depth of 3 metres the rock core approached a fissure in the rock as the curves show — one value increasing and the two other adjacent values decreasing. For the section at 4.5 metres the values of the calculated major and minor principal stresses were

$$\sigma_1 = 250 \text{ kg/sq.cm}$$
$$\sigma_2 = 135 \quad »$$

The inclination of the major axis of the ellipse is 10° to the horizontal. Principal stresses near the wall face were higher than at the depth of 4.5 metres.

Wall point 4

Fig. 71 shows the location of point 4 in the hanging wall at the 300 metre level. The rock is granite. Fig. 65 illustrates the stress ellipse which is calculated for a depth of 1.8 metres. The principal stresses were

$$\sigma_1 = 450 \text{ kg/sq.cm}$$
$$\sigma_2 = 190 \quad »$$

The direction of the major principal stress was 40° to the horizontal. This is about 15° more than at the points 6 and 11, owing probably to local conditions around point 4.

$$\tau_{max} = \frac{450 - 190}{2} = 130 \text{ kg/sq.cm}$$

Wall point 6

Fig. 67 shows the values recorded for point 6 at the 300 metre level on the foot wall side. The stresses could not be measured near the surface. The

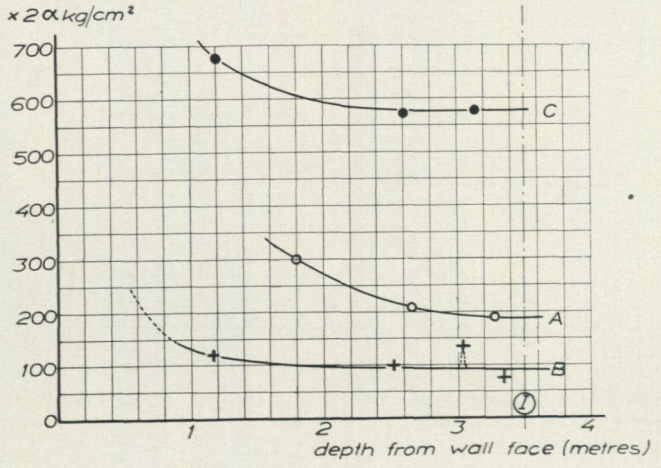

Fig. 67. Stress values recorded at wall point 6 at the 300 metre level. The stresses could not be measured near the wall surface, owing to fissures in the rock. $2\alpha = 0.7$.

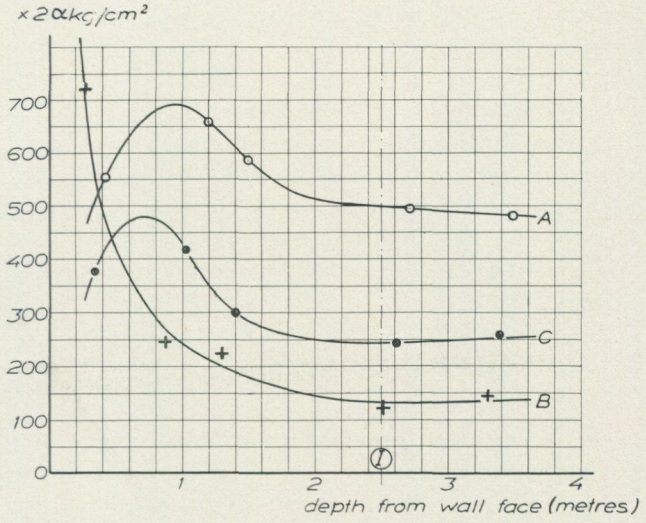

Fig. 68. Stress values recorded at wall point 11 at the 360 metre level. The vertical *B* component shows the tendency for high surface stresses which rapidly decrease with depth from rock face. There is a marked influence also on the *A*- and *C*-components but their maximum appears deeper in the rock, a phenomenon also observed at other points. Hard granite. $2\alpha = 0.8$.

vertical component near the surface was evidently very high, as it exerts a marked influence on the 60° values. In the *C*-direction, which is almost perpendicular to the hanging wall, values of about $700 \times 2\alpha = 490$ kg/sq.cm were measured. For a section 3.5 metres from the rock face the principal stresses were

$$\sigma_1 = 440 \text{ kg/sq.cm}$$
$$\sigma_2 = 140 \quad »$$

The inclination of the major principal stress was 24° to the horizontal. $\tau_{max} = 150$ kg/sq.cm.

Wall point 11

The rock in which the measurements at point 11 at the 360 metres level were performed was hard, strong red granite, with veins of pure quartz. Two rather thin sköls appeared in the rock core at depths of between 47 and 93 cm. Down to 3.5 metres the rock was then intact, no fissures being encountered, which is remarkable.

Fig. 68 (the curves *A*—*B*) shows the stresses recorded at point 11 in the hanging wall. For the location in plan, see Fig. 73. As at point 6 the vertical stress (the *B*-component) is high near the wall face, the two 60° values (*A* and *C*) being clearly influenced thereby. It is interesting to note that the maxima of these values refer to points some distance from the face.

The determination of the stress in a vertical direction in the drift wall, made at a depth of 25 cm, revealed a recorded value of $720 \times 2\alpha = 575$ kg/sq.cm. If the vertical stress had been measured still nearer the wall face, for instance at a depth of only 10 cm, a higher value would probably have been obtained. At 250 cm the stress had fallen to about one- sixth of the 25 cm value.

The *B* component in Fig. 68 illustrates this tendency for high surface stresses. Where the rock is unfissured these might be so high that the surface zone is

separated with such rapidity as to sound like a shot. *This sudden increase in stress towards the surface reveals the mode of origin of the strain bursts.* It can be added that at points 9 and 10 and at many other places in Kaptenslagret there is also visible evidence of such damage in the walls and roof.

Further investigation with recording of stress concentrations very near the rock face and in various directions might well throw light on the general mechanism of the strain and rock bursts and hence indicate ways of avoiding them, or at least of reducing their effect.

For point 11 at a depth of 250 cm the calculated principal stresses σ_1 and σ_2 were

$$\sigma_1 = 510 \text{ kg/sq.cm}$$
$$\sigma_2 = 220 \quad »$$

The direction of the major principal stress is 20° to the horizontal — that is, almost perpendicular to the hanging wall. The direction is approximately the same as for point 6. $\tau_{max} = 145$ kg/sq.cm, which is a very high value.

Wall Point 19

Fig. 74 shows the location of point 19 on the hanging wall side in granite. Fig. 69 shows the stresses recorded at various depths. Near the wall face the stresses in all directions were rather low. At a depth of about 35 cm high values in the *B* direction (vertical) were obtained, which indicates the existence of even higher vertical stresses at, say, 25 cm. At a depth of 1.3 metres the principal stresses were

$$\sigma_1 = 450 \text{ kg/sq.cm}$$
$$\sigma_2 = 260 \quad »$$
$$\tau_{max} = 95 \quad »$$

This τ value was lower than for points 4, 6 and 11 (Fig. 65), where τ_{max} was 130, 150 and 145 kg/sq.cm respectively. The pillar was free only down to a depth of 410 metres. Beyond that level the ore lens was not mined out, and it would be expected that the τ values between the hanging wall and the pillar would decrease there as is the case.

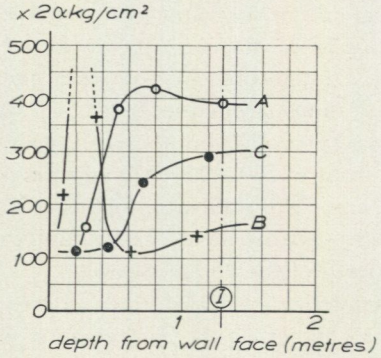

Fig. 69. Stress values recorded at wall point 19, which is located at the 410 metre level (Fig. 65) where the pillar merges the fully unmined ore lens. $2\alpha = 0.85$.

As is seen from Fig. 65, the stresses in the remaining pillar are almost perpendicular to the hanging wall for the distance that the pillar has been cut out. At the 410 metre level, where the ore is not mined out, the stress conditions in the virgin rock and ore must exert an influence. The major principal stress at point 19 acts 10° above the horizontal whereas at points 1—2, 4, 6 and 11 it acts below the horizontal.

Roof stresses

General aspects

Fig. 65 shows that the forces due to the pillar act roughly perpendicular to the foot and hanging walls except at point 19. This applies to a vertical section through the pillar. To ascertain these forces projected on a horizontal plane stress measurements were performed in the roof at the levels 275, 300, 320, 360, 410 and 460 metres — the cell holes being perpendicular to the roof face. The results are given in Figs. 70—75. The magnitude and direction of the principal stresses have been calculated for some depths, and the stress ellipses entered in plans of the levels. Points for the pillar measurements are located near the boundary of the hanging and foot walls but the roof points were generally deeper in the foot wall. As the plans show, the foot wall contains not only the inclined shaft, but also local ore bins which are about 15 metres in depth, for use in tipping broken ore into the skip. Stress concentrations surrounding these shafts and bins influenced the measurements at the roof points placed in their vicinity. On the hanging wall side the roof measurements were performed in granite immediately adjacent to the orebody. The points in the foot wall are in granite or grey or red leptite.

The value of the major horizontal principal stress in the foot wall is about 300 kg/sq.cm at 275 metres and increases to 600 kg/sq.cm at 320 metres and 700 or even higher at 360 metres; at 410 metres, where the pillar ends (Fig. 74), the stress falls to about 550 kg/sq.cm; at the 460 metre level — that is, 50 metres below the upper face of the zone of excavation — a stress with a horizontal component of about 350 kg/sq.cm is acting in the virgin rock in a direction about 10° to the direction of the lens.

It is interesting to note that the pressure, exerted by the pillar perpendicular to the foot wall face (Fig. 65), is lower than the pressure acting at the points of measurement in the foot wall opposite the pillar. The pressure in the pillar is only one of the perpendicular components of the pressure prevailing at the face of the foot wall. The other stress components are parallel to the surface. Owing to the forces from the pillar and the spaces in the foot wall constituted by the inclined shaft and the ore bins there is a stress concentration in remaining parts of the foot wall. However, one of the most important reasons for the high stress in the foot wall is probably that in the bed rock at the out-mined levels there exists a natural stress field which is large — its σ_1 value about 350 kg/sq.cm acting almost parallel to the foot wall.

The results of all the measurements performed in the foot wall are repro-

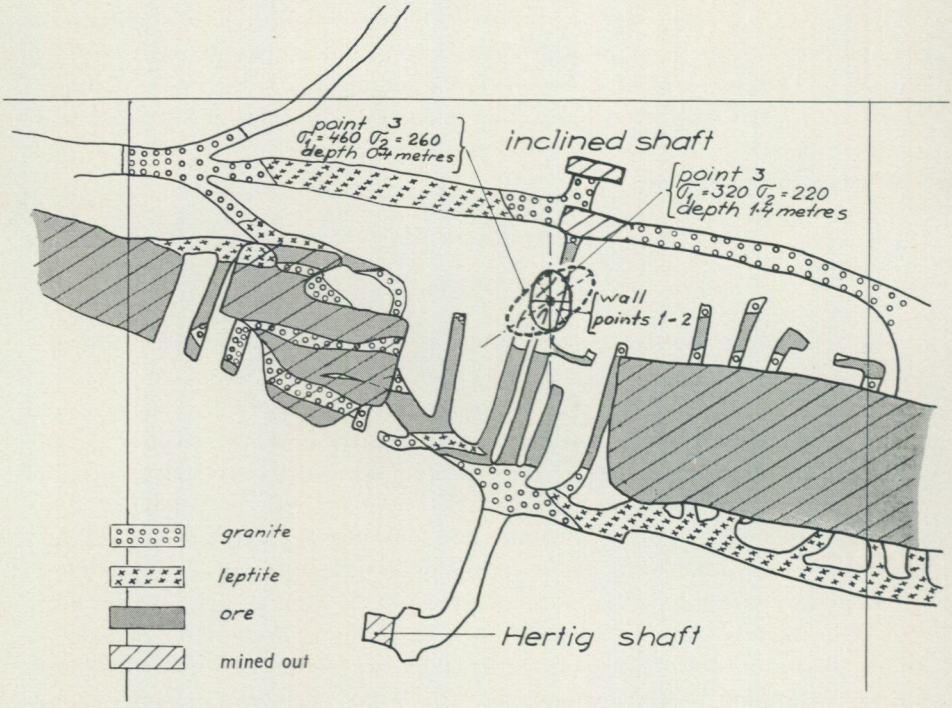

Fig. 70. 270 metre level. Points 1 and 2 are located in the cross-cut wall, point 3 in the roof. The scale for all the Figs. 70—75 is 1 : 2060.

duced below — in the form of diagrams containing the recorded values, and as calculated principal stresses.

275 metre level

Roof point 3

Fig. 70 a shows the horizontal values recorded at point 3 in the roof. Measurements made parallel to the drift are denoted by *B* and those at 60° thereto by *A* and *C*. The measurements were performed in hard granite, near

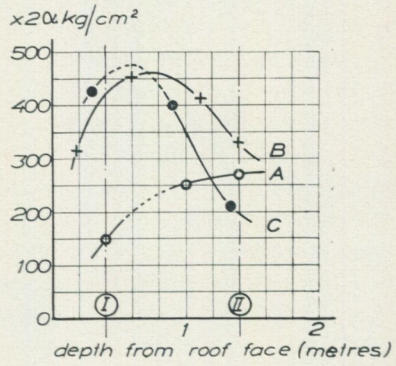

Fig. 70 a. Stress values recorded in the directions *A*, *B* and *C* in the cell hole of roof point 3. $2\alpha = 0.7$.

points 1 and 2 (Fig. 70). Near the roof face high stresses are acting, especially in the B and C directions — about $450 \cdot 2\alpha = 315$ kg/sq.cm at a depth of 60 cm; these then fall off with depth. The principal stresses at a depth of 40 cm were

$$\sigma_1 = 460 \text{ kg/sq.cm}$$
$$\sigma_2 = 260 \quad »$$

and at 140 cm:

$$\sigma_1 = 320 \text{ kg/sq.cm}$$
$$\sigma_2 = 220 \quad »$$

The direction of the major principal stress deviates by 18 and 33°, respectively, from the longitudinal direction of the pillar.

300 metre level

Roof point 7

As elsewhere in the Kaptenslagret lens, the bed rock at this point consists of rigid, hard leptite with 10—20 per cent quartz. The leptite is penetrated by veins of hornblende, which follow roughly the direction of the axis of folding (the direction of dip). The fissures observed in the leptite during the drilling of the stress release channel are probably due, as far as point 7 is concerned, to the presence of planes of cleavage in the leptite or of veins of other materials of low strength. The planes of cleavage may have originated geologic eras ago when

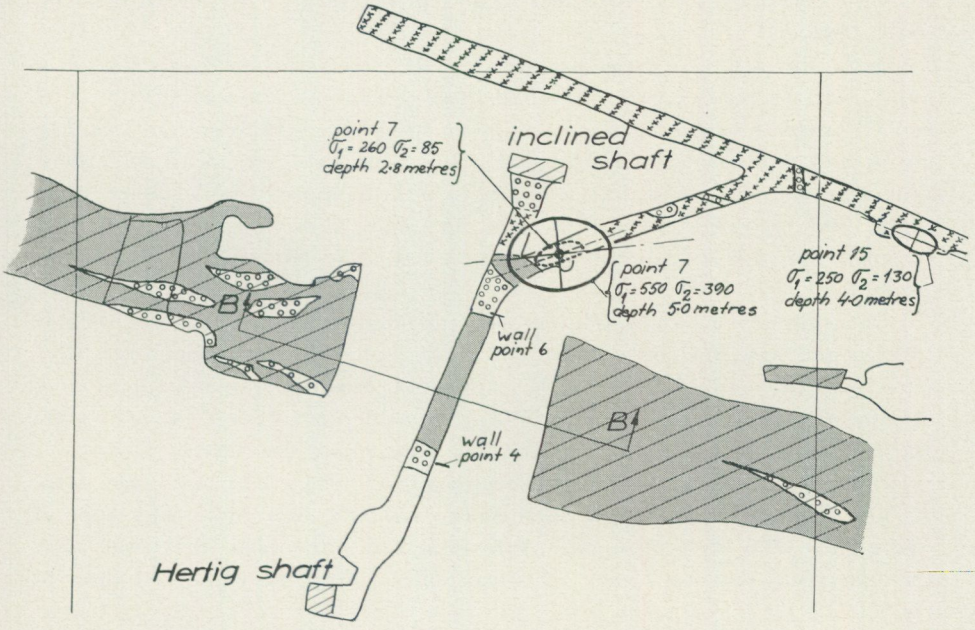

Fig. 71. 300 metre level with roof points 7 and 15. For cross-section B—B of pillar see Fig. 64.

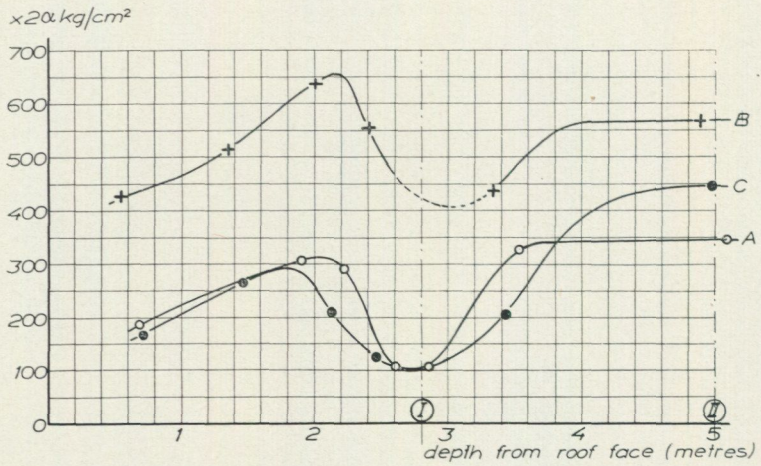

Fig. 71 a. Stress values recorded at roof point 7 in Fig. 71.
$2\alpha = 0.54$ at section I and 0.72 at a depth of 1.5 metres from roof face and at section II.

the ore deposit underwent folding and great changes in position. In plan they are practically perpendicular to the axis of folding and are transverse cleavage planes typical of Kaptenslagret. They are probably due either to tension acting during the main folding or to shearing during the transverse folding. The cleavage planes have in places a thin film of chlorite mineral, but they are generally extremely thin zones of crushing, sometimes with some clay mineralization. In both cases they are planes of weakness in the rock, along which the rock cores often tend to break.

Fig. 71 shows the location of point 7 at the 300 metre level and Fig. 71 a shows that the recorded stresses in all three directions of measurement (*A*, *B* and *C*) increase with the depth from the rock face. At a depth of 2 metres the stresses suddenly decrease by $200 \cdot 2\alpha = 140$ kg/sq.cm in all directions. This zone of low stress has a width of a little more than 1 metre, after which the recorded stresses increase to their former maximium values, except in the case of *C*, for which direction it is about 50 per cent higher than originally.

It is of interest to know that fissures and veins appeared between 80 and 130 cm and between 360 and 480 cm in the high stress zones, but in the low stress zone the rock seemed to be unfissured. However, an investigation of the modulus of elasticity of the rock at different depths at point 7 gave 590,000 and 380,000 kg/sq.cm in the high and low stress zones, respectively.

In the former case the loading interval was 0—500 kg/sq.cm, and in the latter 0—300, but here the value of *E* increased to 440,000 when the loading interval was higher (300—600 kg/sq.cm). When these differences in the value of *E* are taken into account, the low stress zone is even more marked than in Fig. 71 a.

The stress ellipses were calculated for depths of 2.8 and 5 metres (Fig. 71 a).

These ellipses are inserted in the plan in Fig. 71. The principal stresses at the greater depth were

$$\sigma_1 = 550 \text{ kg/sq.cm}$$
$$\sigma_2 = 390 \quad »$$

In the low stress zone at 2.8 metres the corresponding values are 260 and 85 kg/sq.cm. The major principal stress differs at the depth of 2.8 metres by 2° and at 5 metres by 15° to the direction of the main drift, as Fig. 71 shows. The maximum shearing stress at the measuring point is represented by the planes that constitute the bisector of the angle between the directions of σ_1 and σ_2, and at depths of 5 and 2.8 metres is 80 and 87 kg/sq.cm respectively.

The shearing stress is thus about the same in the low and high stress zones. τ_{max} appears in a plane that in a horizontal section deviates by only 15° from the direction of the hanging wall, and seems to be parallel to the small orebody located near point 7 in the foot wall. The other plane of τ_{max} is 90° to the first one (Fig. 71).

Roof Point 15

The roof point 15 is located in a widened part of the main drift running the length of the ore lens. The rock is predominantly leptite, with some calcite and mica. The rock surface was fissured down to about 45 cm.

The recorded value for the *B* direction, which is parallel to the main drift, was $310 \cdot 2a = 200$ and for the *A* and *C* directions about $140 \cdot 2a = 90$ kg/sq.cm. At about 90 cm the cell hole passes near a fissure, with the result that the *B* value falls while the *A* and *C* values increase. At about 2.3 metres another fissure is approached in another direction. The principal stresses at a depth of 4 metres were

$$\sigma_1 = 250 \text{ kg/sq.cm}$$
$$\sigma_2 = 130 \quad »$$

The major principal stress acts parallel to the foot wall (Fig. 71).

Point 15 lies about 80 metres east of the inclined shaft. At the 320 metre level the stresses were measured at another point, 16, situated up to 70 metres west of the shaft. In both cases the points lie so far from the pillar that there

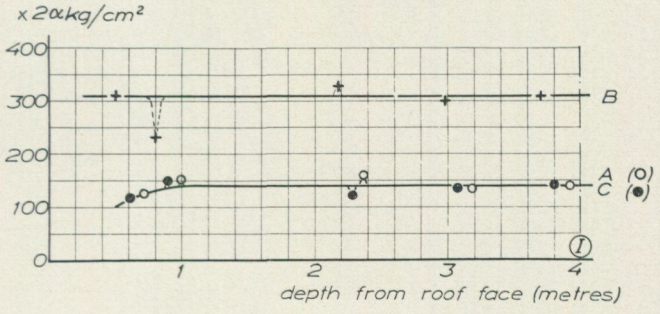

Fig. 71 b. Stress values recorded at roof point 15 in Fig. 71. The values show no changes with depth. As the *A* and *C* values are equal the direction of the major principal stress is the same as that for B. $2a = 0.65$.

it is unlikely to exert any appreciable influence on the values. At point 16 the horizontal stress field resembles that at point 15 in magnitude and direction.

The stress concentrations around the shaft in the foot wall would thus appear to be the resultant of three stress fields acting in the region of the shaft:

(1) the pressure exerted on the foot wall by the pillar, and acting roughly perpendicularly to the wall;

(2) the compressive stress of the foot wall parallel to the lens; and

(3) the weight of the foot wall.

The origin of the very high stresses found to be acting in the foot wall around the shaft is evident only when these three points are known. It may be added that the presence of the small orebody immediately adjacent to point 7 and separated from the main orebody by a plate of granite (Fig. 71) implies a lowering in the stability of the foot wall. The surface of contact of the lenses with the country rock is covered throughout the whole of Kaptenslagret by layers of clay-like material, which are often very thin; these prevent close adhesion between the ore and the country rock. At present the foot wall opposite the shaft at the 300 metre level seems to be strong and capable of bearing and distributing the pressure exerted by the pillar. However, if the pillar is removed there is some danger that the forces acting along the foot wall will cause slipping along the boundaries with the two orebodies, unless the granite (Fig. 71) between them is strong enough to prevent it.

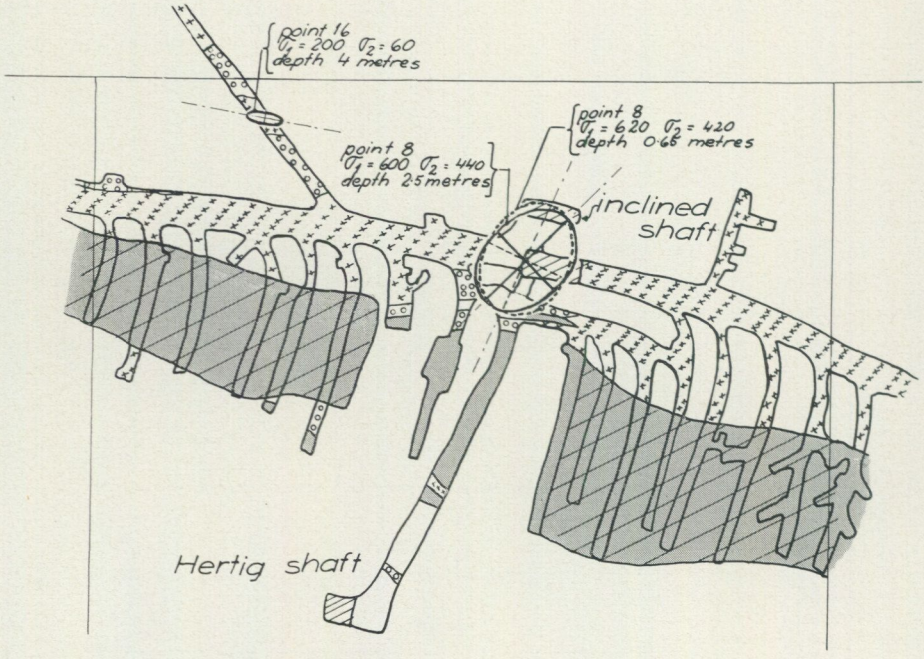

Fig. 72. 320 metre level with roof points 8 and 16.

320 metre level

Roof point 8

Point 8 is situated roughly opposite the inclined shaft. The other shaft depicted in Fig. 72, and which lies next to the inclined shaft is an ore bin going down from the 320 metre level about 15 metres for tapping into the skip. The roof of the main drift in which point 8 is located thus passes intact over the ore bin (Fig. 65). To a depth of 30 cm from the face the rock in the roof is fissured, and between 95 and 185 cm it consists of pure quartz with numerous planes of cleavages and a clayey fissures. Otherwise the rock is leptite, practically intact and strong. It was necessary to discontinue drilling at 3 metres however, when a large water-bearing fissure was encountered.

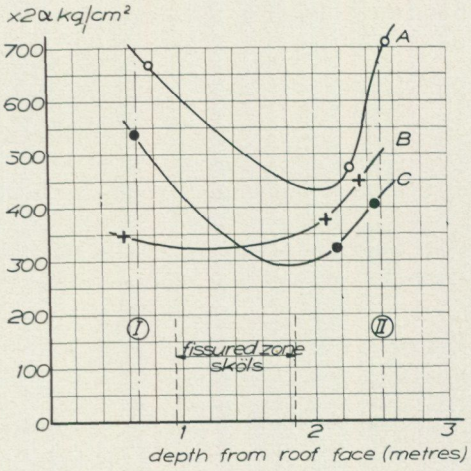

Fig. 72 a. Stress values recorded at roof point 8 (see Fig. 72). $2\alpha = 0.65$.

The principal stresses have been calculated for the 70 and 250 cm depths. The values of σ_1 for the two cell positions do not differ much, whereas the direction of the axes of the stress ellipse varies by about 20° (Fig. 72). The reason for this, as Fig. 72 a shows, is that the recorded B value increases until it is larger than that for the C direction. At 2.5 metres from the face the principal stresses were

$$\sigma_1 = 600 \text{ kg/sq.cm}$$
$$\sigma_2 = 440 \quad »$$

The shearing stress, τ_{max}, is then 80 kg/sq.cm. The direction of one of the surfaces, where the greatest shearing stresses are acting, is parallel to the foot wall. Similar stress conditions as regards τ_{max} were found at the 300 and 410 metre levels.

Roof Point 16

Point 16 is located in granite in the foot wall (Fig. 72), about 35 metres from its face at a place where there is no marked influence of the stresses

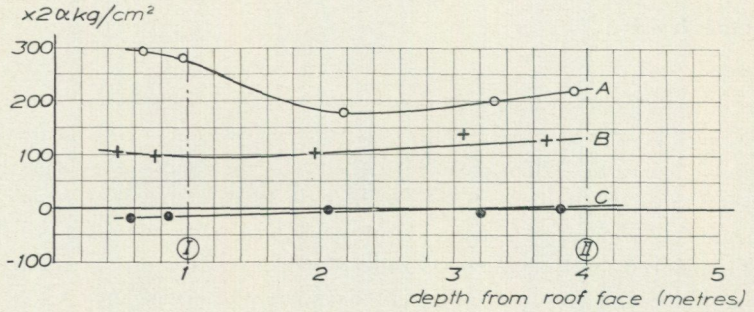

Fig. 72 b. Stress values recorded at roof point 16 in Fig. 72. $2\alpha = 0.72$.

from the pillar. Fig. 72 b shows that the recorded value in the *C* direction is tensile and about zero at a depth of 4 metres, where the principal stresses were

$$\sigma_1 = 200 \text{ kg/sq.cm}$$
$$\sigma_2 = 60 \quad »$$

σ_2 is exceptionally small compared with σ_1.

At both the points 15 and 16 the major principal stress was parallel to the ore lens, and had a maximum value of about 200 kg/sq.cm.

360 metre level

Roof points 9 and 10

The points 9 and 10 are located in the main drift (Fig. 73); this is roughly parallel to the free surface of the foot wall, and between this and the inclined shaft. The distance of the drift from the shaft is only about 5 metres. An ore bin is situated as at the 320 metre level and complicates the stress distribution in this part of the foot wall.

The stresses at point 9 are higher than at any other point in Kaptenslagret — 1,000 kg/sq.cm, and probably reaching 1,500 kg/sq.cm in places. The stresses at point 10 are also very high. The rock in the vicinity of point 14 seems to be seriously damaged and a part of the forces from the pillar must find their way over to the still intact part of the foot wall west of the inclined shaft; this may explain the directions of the axes of the stress ellipse at point 9. Points 9 and 10 in the roof are complementary. The former was the first to be drilled but this was discontinued at 145 cm owing to obstruction by a quartz zone. The hole at point 10 was also vertical to the roof face, at about 3 metres from point 9. Fig. 73 a shows the recorded values for the two points on the same diagram. At point 9 a value of $281 \times 2\alpha = 160$ kg/sq.cm was recorded in the *B* direction at a depth of 21 cm. Only 30 cm deeper the value had risen to about 1,000 kg/sq.cm. At 112 cm it was down to 500 kg/sq.cm. Between 60 and 100 cm apparently still higher stresses were acting in the very homogeneous and hard rock; as a result, during the cutting of the stress

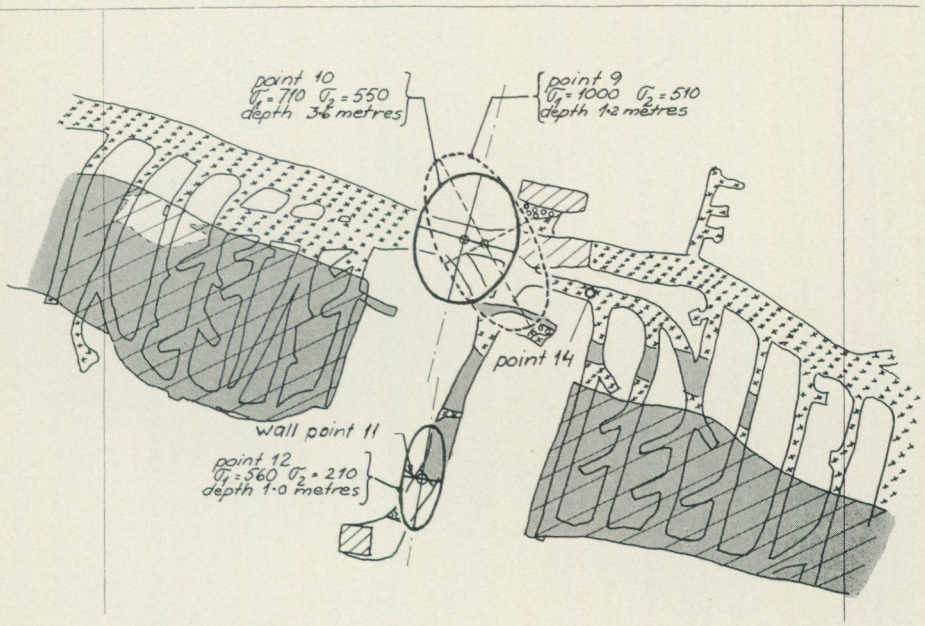

Fig. 73. 360 metre level with roof points 9, 10, 12 and 14 and wall point 11.

release channel, the rock core was cut off perpendicular to the axis in a series of parallel discs, each about 2 cm in thickness. Near these two extreme depths the discs were slightly thicker. The reader is referred to pages 51—53 where this phenomenon is explained. As the maximum B value (Fig. 73 a) could not be determined owing to the shearing effect it is indicated in the diagram by a broken line. The same applies to the C component, for which a maximum value of $1{,}170 \times 2a \cong 800$ kg/sq.cm was read at 121 cm and $785 \times 2a \cong 450$ at 32 cm. The values for the A direction are much lower. Between 220 and 340 cm there is a zone of cleavage planes in which no determinations were made. All the A and C components are about $650 \cdot 2a = 450$ kg/sq.cm at greater depths than 1.5 metres. The values of the B component are considerably lower, a little more than one half — as would be expected, in view of the fact that this direction is perpendicular to the line of action of the load exerted by the pillar.

It is to be noted that up to a depth of about one metre, the A component is much lower than the C, but then increases to about the same magnitude. This change is reflected in the form and position of the stress ellipse. The principal stresses at a depth of 1.2 metres were

$$\sigma_1 = 1{,}000 \text{ kg/sq.cm}$$
$$\sigma_2 = 510 \quad »$$

and at a depth of 3.6 metres

$$\sigma_1 = 710 \text{ kg/sq.cm}$$
$$\sigma_2 = 550 \quad »$$

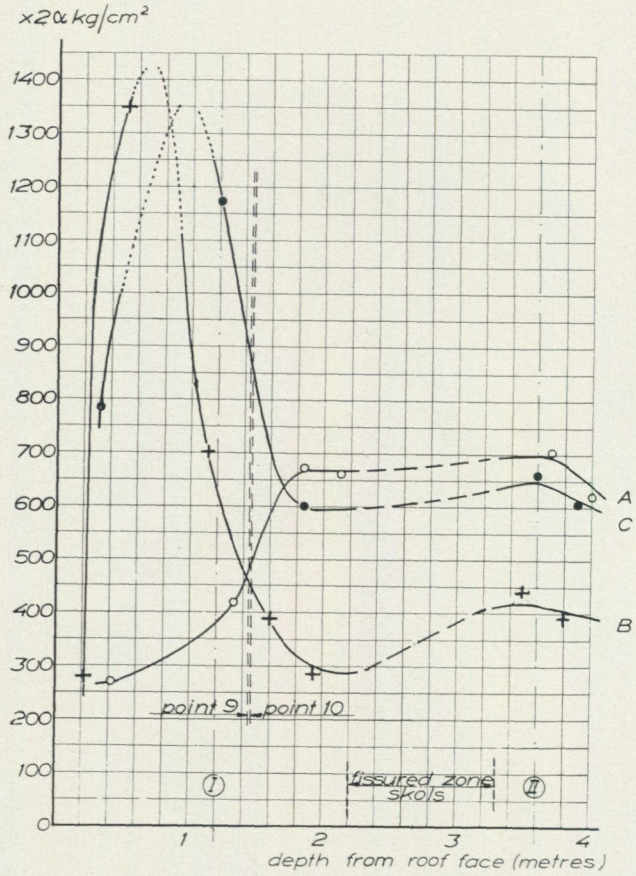

Fig. 73 a. Stress values recorded at roof points 9 and 10 (see Fig. 73). $2\alpha = 0.7$. Near the rock face, at a depth of 20 cm, $2\alpha = 0.55$.

In the former case σ_1 was acting at 45° to the direction of the pillar, while in the latter case it was parallel to the pillar. τ_{max} for the two depths was 240 and 80 kg/sq. cm, respectively, the former being a very high value.

No stress readings were obtained at point 14 owing to the large number of fissures and planes of cleavage, the rock core disintegrating into small pieces some centimetres or so wide. It is probable that the large forces exerted by the pillar have fractured the foot wall just east of the shaft, where point 14 is situated. The rock was probably weak from the outset, owing to many cleavage planes and the presence of a smaller lens parallel to the large orebody. Under these conditions it is to be expected that forces in the north part of the pillar would pass obliquely to the parts of the foot wall lying west of the shaft. This would set up large stress concentrations around the shaft, as the values of τ and σ at point 9 confirm. It may be added that, according to points 15 and 16 at the 300 and 320 metre levels, there is a fairly high pressure of about 250 kg/sq.cm acting parallel to the foot wall. The ore bins to the skip in front of the inclined shaft begins on a level with the drift floor. On this account high stress concentrations would be expected for some distance above

the roof face. Herein, too, may lie an explanation of the high values of the stress ellipse for point 9.

Roof point 12

The cell hole at point 12 was drilled vertically into the roof near wall point 11, and in the same granite, which was very hard. Fig. 73 b shows the recorded values in the *A*, *B* and *C* directions. At a depth of only one metre the stress seems to have stabilized. The concentration towards the surface zone is most noticeable in the *A* and *C* directions, and is probably due to a prevailing rock pressure in the region that acts roughly parallel to the ore lens. The cross-cut represents a space in this stress field, to which the stress concentrations in its roof and floor are due.

The *B* component is almost independent of the depth from the roof face, since the maximum stress in the pillar passes practically parallel to the drift itself — that is to say, in the direction of the *B* component. However, the transverse rock pressure that gave the high surface stresses for the *A*- and *C*-directions also influenced the *B*-recording but deeper in the rock than in the former cases. Reference is made given to point 11 (Fig. 68). The principal stresses were

$$\sigma_1 = 560 \text{ kg/sq.cm}$$
$$\sigma_2 = 210 \quad »$$

From these values we have $\tau_{max} = 170$ kg/sq.cm.

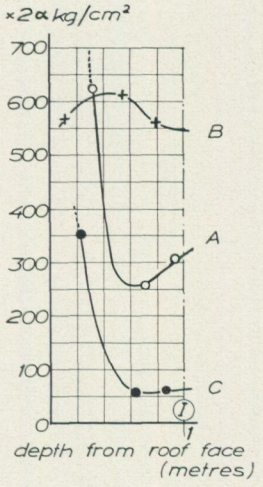

Fig. 73 b. Stress values recorded at roof point 12 in Fig. 73. $2\alpha = 0.85$.

410 metre level

Roof point 17

This point is located in a cross-cut entering the foot wall (Fig. 74). To a depth of about 2 metres the rock is hard banded granite, with some mixture of mica and hornblende. Between 2 and 3 metres deep in the rock there are many fissures and planes of cleavage. From 3 to 4.2 metres the mica content

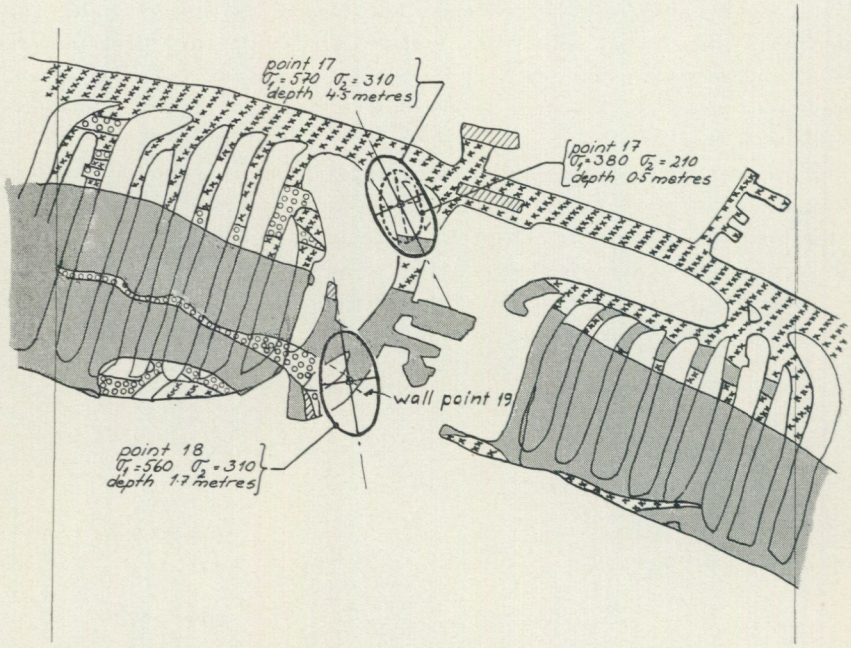

Fig. 74. 410 metre level with roof points 17, 18 and wall point 19.

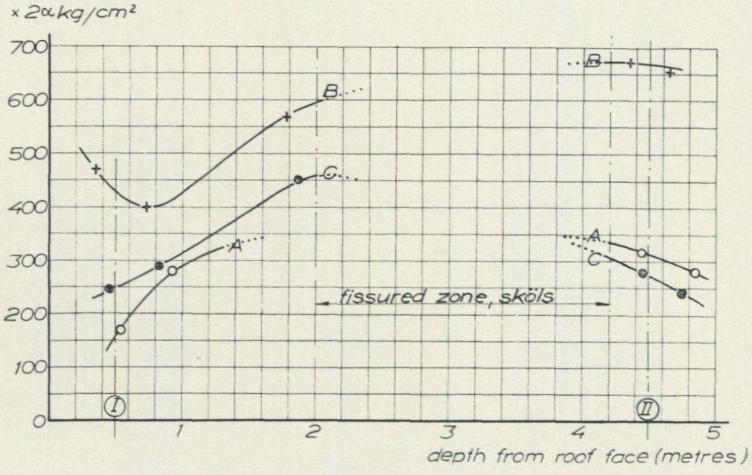

Fig. 74 a. Stress values recorded at roof point 17 in Fig. 74. $2\alpha = 0.7$.

is very high and the rock assumes the character of breccia, with hollows containing pyrites. Deeper than 4.2 metres the rock becomes homogeneous again. No stress determinations were performed between 2 and 4.2 metres.

The principal stresses were calculated for sections 0.5 and 4.5 metres from the roof face. The values are higher at the greater depth where they were

$$\sigma_1 = 570 \text{ kg/sq.cm}$$
$$\sigma_2 = 310 \quad »$$

τ_{max} at the point is high, 130 kg/sq.cm, which indicates that the foot wall there is still strong. τ_{max} appears in surfaces parallel to the foot wall and the small ore body.

Roof point 18

This point is located in the hanging wall quite near the ore and point 19 (Fig. 74). The horizontal principal stresses were

$$\sigma_1 = 570 \text{ kg/sq.cm}$$
$$\sigma_2 = 310 \quad »$$

At the corresponding points 12 and 18 at the 360 and 410 metre levels, the values of σ_1 were equal but σ_2 was about 50 per cent higher at the lower point 18 than at 12, owing to the influence of the unexcavated orebody on each side of the pillar up to the 410 metre level. This means that the τ_{max} value is not so extremely high as in point 12. The principal stresses at points 12 and 18 differ slightly in direction at the two points. The lower value for the A component near the surface than deeper in is due to the presence of fissures

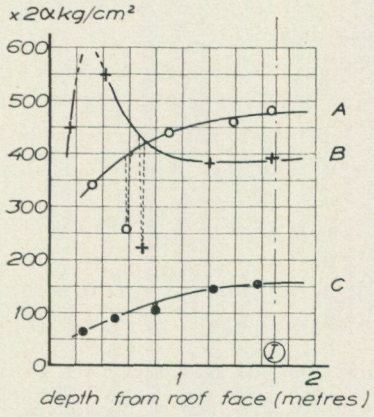

Fig. 74 b. Stress values recorded at roof point 18. At a depth of 0.6 metre there is a fissure outside the core. $2a = 0.85$.

in the rock (Fig. 74 b). The deviation of the recorded values at about 60 cm from the normal curves shows that the point of measurement is approaching a fissure but this does not pass through the rock core near the point. This fissure was in fact noted in the report. The low C component is probably due to the intersection of its line of action with the Hertig shaft, which is located only 7 metres from the point (Fig. 74).

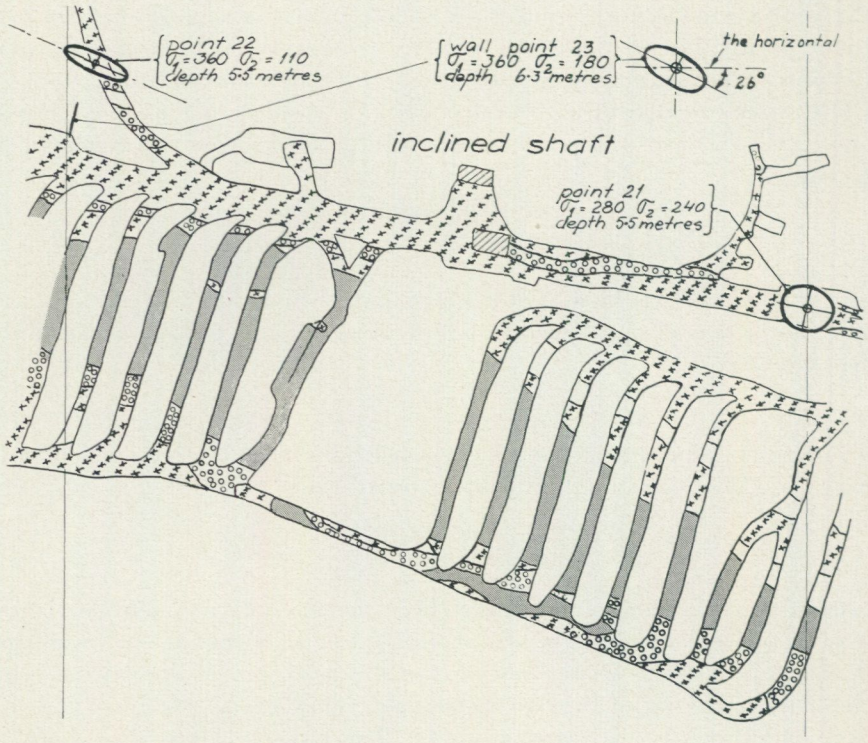

Fig. 75. 460 metre level with roof points 21, 22 and wall point 23.

460 metre level

Roof point 21

Point 21 is located 70 metres east of the inclined shaft in leptite, which is banded at places (Fig. 75). Fig. 75 a shows the recorded stresses. At a depth of about 2 metres there is a fissure with clayey surfaces, which disturbs the stress conditions around the core. The principal stresses at a depth of 5.5 metres were

$$\sigma_1 = 280 \text{ kg/sq.cm}$$
$$\sigma_2 = 240 \quad »$$

which indicates an almost hydraulic stress distribution. This might be due to crushing of the rock in the neighbourhood of, but not at, this point.

Roof point 22 and wall point 23

Point 22 is located 80 metres west of the inclined shaft and in homogeneous granite (Fig. 75). The recorded stresses are shown in Fig. 75 b. A fissure in the rock is passing the core at a depth of about 2.5 metres. The stress component in the C direction is $200 \cdot 2\alpha = 140$ kg/sq.cm at a depth of 60 cm but decreases gradually until at 5 metres it is zero. A similar situation obtains at the corresponding point 16 at the 320 metre level, where the C value indicates a low tensile stress which becomes zero at a depth of 4 metres.

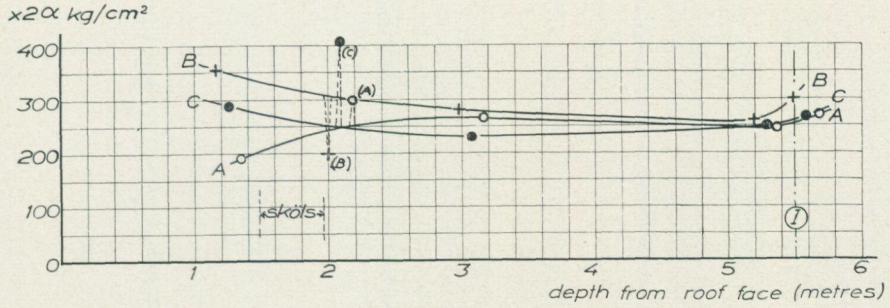

Fig. 75 a. Stress values recorded at roof point 21. $2\alpha = 0.65$.

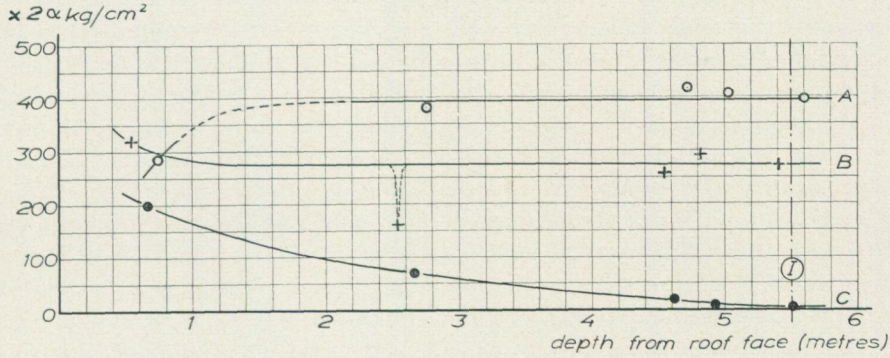

Fig. 75 b. Stress values recorded at roof point 22. $2\alpha = 0.7$.

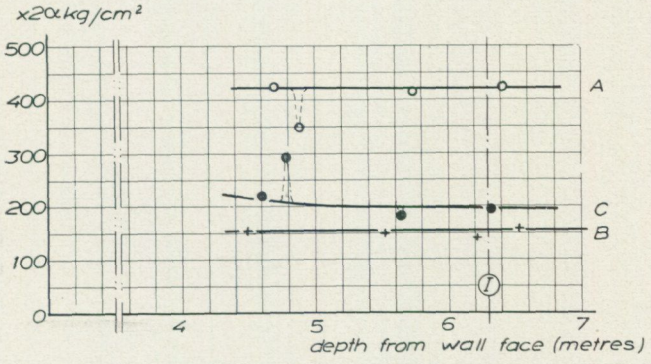

Fig. 75 c. Stress values recorded at wall point 23. $2\alpha = 0.7$.

The principal stresses at a depth of 5.5 metres were

$\sigma_1 = 360$ kg/sq.cm
$\sigma_2 = 110$ »

For points 16 and 22 $\sigma_2 : \sigma_1$ is in both cases 0.3.

Point 23 is located in the drift wall near point 22 (Fig. 75). The measurements were made at depths between 4.5 and 6.5 metres. The rock is hard granite and

unfissured except at a depth of 4.8 metres (Fig. 75 c). The recorded values show no changes with depth. The principal stresses at a depth of 6.3 metres were

$$\sigma_1 = 360 \text{ kg/sq.cm}$$
$$\sigma_2 = 180 \quad »$$

The σ_1-axis is 26° to the horizontal.

Deformation of the foot and hanging walls by the pillar

As pointed out above, the stresses in the pillar act on the foot and hanging walls as a uniformly distributed load of about 450 kg/sq.cm, directed perpendicular to the wall face. The area of load is band-shaped, just as the area of contact of the pillar and the foot wall. For an accurate determination of the deformation due to this load in or near the surface to which it is applied the band-shaped area of loading must be of finite length and symmetrically located on an infinite hemisphere. However, in this case there is no symmetry because the lower end of the pillar merges with the unexcavated ore lens.

An approximate estimate of the deformation is obtained if the whole pillar is replaced by a series of touching circular pillars of the same diameter as the width of the pillar and having the same load per unit area. The deformation caused by such a pillar in the foot and hanging walls may be calculated for unit load from Boussinesq's formulae (see Part I, Fig. 17, p. 38 and Part II, p. 70). If the same assumption is made regarding the distribution of load over the surface of the pillar the required subsidence in the foot and hanging walls for a unit load distributed over an imaginary circular pillar is

$$\delta = \alpha \cdot \frac{1.8}{R}$$

in which $\alpha = \dfrac{m^2 - 1}{m^2} \cdot \dfrac{4}{E\pi^2}$

The radius R of the pillar is 25 metres

Poisson's ratio, $\dfrac{1}{m} = 1/5$ and the modulus of elasticity E of the rock is 550,000 kg/sq.cm.

Then, for a pillar load of $\pi \times 2{,}500^2 \times 450$ kg, the deformation for the whole pillar load

$$\delta_p = 4.5 \text{ cm}$$

Taking into account the deformation effects of the underlying imaginary circular pillars, the total deformation, measured at the centre of the uppermost pillar, may be estimated at 7 cm. This means that by excavating the whole pillar in Kaptenslagret the surface of the foot wall will move outwards about 7 cm at the site of the pillar at the upper levels.

General remarks on the pillar in Kaptenslagret

The stress measurements have revealed that the pillar in Kaptenslagret transmits large forces between the foot and hanging walls; at all levels the forces are perpendicular to the walls. At the uppermost level (275 metres) the stresses in the pillar were about 250 kg/sq.cm, but below this level a figure of 450 kg/sq.cm seemed to apply. At a depth of 410 metres the ore lens was not mined out; the stresses and directions changed, since they were influenced by the virgin rock pressure at deeper levels.

The reason for the recorded horizontal stress concentrations in the pillar and the connected parts of the foot and hanging wall is probably to be found in the general rock pressure — a stress field in the region around Kaptenslagret —, the maximum value of which is directed about E—W — that is to say, about 10° to the longitudinal direction of the foot wall. However, as is seen from point 23 the major principal stress in the virgin rock at Malmberget is about 25° to the horizontal.

Owing to the excavation of the ore lens on each side of the pillar the rock pressure has been concentrated in the pillar itself. As stress measurements have shown, the stress in the pillar is high in its longitudinal direction. As both the foot wall and the hanging wall consist of strong red granite or leptite the walls in question should be able to absorb the pressure exerted by the pillar, and there should be no appreciable risk of caving in the foot wall on removing it. However, there are three reasons why the conditions are not so favourable in practice:

(1) In the foot wall there is a shaft (opposite the pillar), which gives rise to a local concentration of the high stresses deriving from the pillar.

(2) Parallel to the orebody there is a smaller lens, the presence of which results in the destruction of the good granite or leptite area of which the foot wall would otherwise be constituted. In addition, there are at places in the rock veins of weaker material and clayey joints — often just near the small foot wall orebodies; within certain parts of the foot wall the rock contains numerous planes of cleavages and zones of crushing — often very thin, sometimes with and sometimes without superficial clay mineralization.

(3) The natural lateral pressure in the ground is very high, and because its direction of action in a horizontal plane is almost parallel to the ore lens it might when the pillar is removed cause bulging of that part of the foot wall corresponding to the small orebodies. The high shearing forces acting in the foot wall and near the pillar in planes parallel to the wall face indicate the risk of such a slip.

The stress measurements provide evidence that the rock in the foot wall at most levels functions as a homogeneous body. It may be inferred that the pillar has still not set up local crushing of the foot wall and that this is thus still capable of carrying its load. This is the prime essential for retaining the stability of the foot wall after the pillar has been removed. The other condition

is that the removal of the pillar shall be so performed that the now high stresses — such as the high shearing stresses acting in planes parallel to the foot wall — are not increased by dynamic forces set up on removal of the pillar.

It must be emphasized, however, that the stresses acting around the shaft at the 360 metre level constitute an unstable situation that is not found at the other levels. In September, 1957, measurements at points 9 and 10 revealed stresses of about 1,200 kg/sq.cm in the roof of the main drifts immediately west of the climbing shaft. This high value suggested that there was a risk of rock bursts. As Fig. 73 a shows, though these stresses fell off with depth they were still quite high. The top of the pillar was removed down to the 300 metre level during the autumn of 1957 and a check measurement was performed in February, 1958. This showed that the stresses at points 9 and 10 had definitely increased. The maximum principal stresses were probably higher than 1,500 kg/sq.cm, but owing to their magnitude no accurate determination was possible at that time. During the drilling operation the rock core was sheared off into a series of thin plates about one centimetre thick, owing to the occurrence of high shearing stresses (pages 51—3). It was found that the stress distribution had changed: the stresses no longer decreased with depth.

At point 14 (Fig. 73) and in the surrounding area, between the stope of the ore lens and the ore bin, it was impossible to drill a cohesive core. Pieces about one centimetre across and of irregular shape were obtained, as evidence that crushing had already set in. The oblique direction of the principal stresses at point 9 illustrates that the horizontal forces from the east side of the pillar tend to be transmitted to the still intact parts of the foot wall west of the inclined shaft. Even if the pillar were removed with extreme care at this level and the parts of the foot wall west of the shaft were to remain, there might still be a local slip in the foot wall around point 14. This would incur a risk of local damage to the shaft at this level.

PART FIVE

BLOCK CAVING AND ROCK PRESSURE

General discussion

One method of excavation in a mine is that in which large portions of an orebody — blocks perhaps 50 metres long and 50 metres high — are under-cut; that is to say, a horizontal zone is cut beneath the block, which is then left to disintegrate from the under face upwards over a period, the loosened pieces of ore then falling and breaking up still further. From the economic aspect the advantage of this system is that the crushing of the ore is effected with no use of explosives, and the number of workers required is small. The cost of the preparatory work on the block includes the undercutting and the blasting of chutes and drifts for the transport of the crushed ore. The disadvantage of the method is that a long time generally elapses between the preparation of the block and the actual onset of the disintegrating or crushing process. This time, the maturing period, is moreover difficult to forecast, as it varies appreciably from one case to another. If it is too long, the production of the mine may be prejudiced.

The block caving method is used in some mines in the world where the strength of the ore is low, so that the block will disintegrate under the action of its own weight and possibly a low rock pressure. However, the method of block caving is also used in many mines where the ore has good mechanical properties. In this case the disintegration of the block seems to be effected by the agency of a high horizontal rock pressure acting in the mine. The existence of such a pressure in the rock has been demonstrated in several Swedish mines, and its magnitude and direction have also been determined. It therefore seems possible that an insight into the mechanism of the block caving process and the factors regulating the disintegration of the ore and the maturing period might be obtained by analyzing the effect on the block when it is acted on by rock pressure with a distribution of the type shown in Fig. 49, p. 106.

In this case very high stresses may generally be expected in the upper levels of the ore lens under excavation; these stresses will gradually decrease appreciably in magnitude down to a depth perhaps equal to the width of the lens; they may then increase again, though slowly. This horizontal pressure in the upper part of the lens may be looked upon as a stress concentration originating from a general horizontal rock pressure prevailing in the virgin rock in the region in which the lens is situated, its distribution perhaps being distorted near the lens by a dense series of sköls in the foot wall (see Part III). The stresses near the working face in the upper part of the lens will often be so great that the ore is crushed, the stresses in the uppermost part of this zone then being almost zero, and increasing rapidly to a maximum value, as shown in Fig. 49.

The principle of block caving is illustrated in Fig. 76 a, which shows a cross-section through a block. By mining out the horizontal zone *A* the block is

The concentration of the horizontal rock pressure in the working face of the orebody.

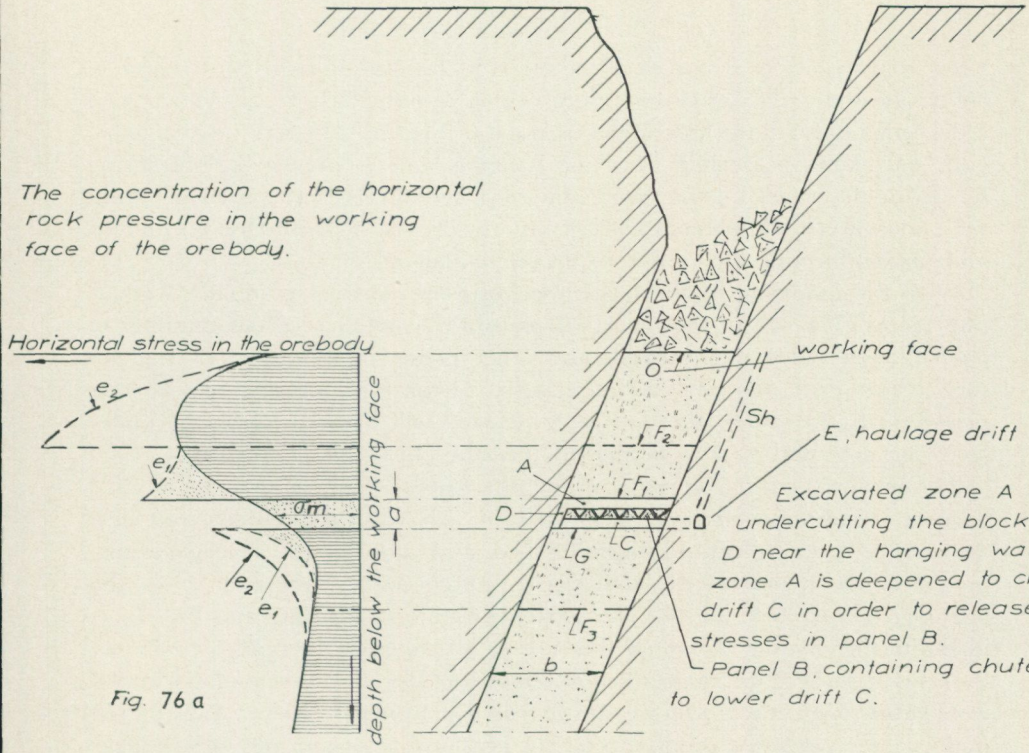

Fig. 76 a

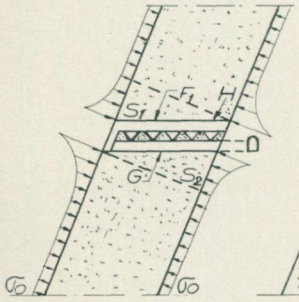

Fig. 76 b

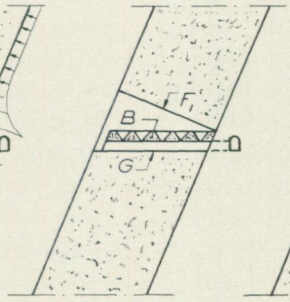

Fig. 76 c

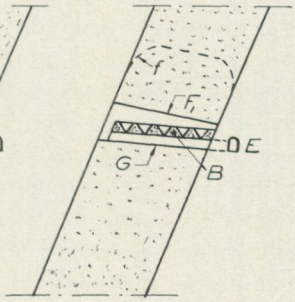

Fig. 76 d

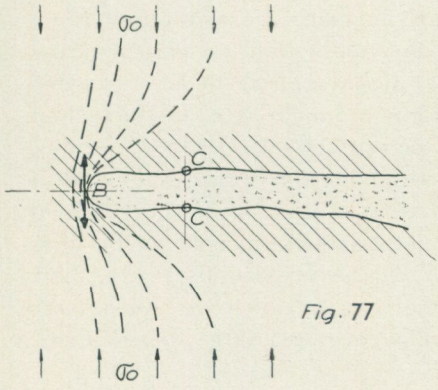

Fig. 77

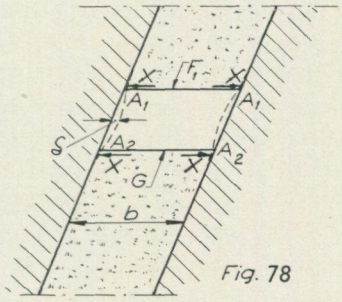

Fig. 78

freed from the under lyingpart of the ore lens. B is an ore panel with a serie of chutes located over a cross-cut C and issuing into the drift E. At D the zone A is deepened down to the floor of the cross-cut C (Fig. 76 a), so that the rock panel with the chutes is isolated from the hanging wall to prevent stresses being set up in the panel by the horizontal rock pressure. Disintegrated ore from the under face F_1 of the block will fall into the chutes, from which it is removed and carried through the cross-cut C to the haulage E.

With the maturing of the block the horizontal stresses gradually work it into pieces. The ore in the block will naturally contain a certain number of cracks, often tightly compressed, and other planes of weakness. Even if no such cracks exist, the block when exposed to the rock pressure over a long period with the under surface F_1 unsupported will disintegrate at the under face, the ore splitting and falling off into the chutes.

The meaning out of the room A and the stope D implies that the original horizontal compressive stresses in the ore lens at a vertical distance a and with an average stress σ_m can no longer be absorbed, the force $a \cdot \sigma_m$ being transmitted to the region of the ore lens — mostly just above and below the opening, that is, to F_1 and G. The broken curves e_1 in the diagram (Fig. 76 a) illustrate the manner in which this stress redistribution probably occurs. At the level F_1, where the stresses before removal of the ore in the rooms A and D were rather high, there are greatly increased marginal stresses, which should imply more favourable conditions for the crushing process in the surface layer F_1. At G, too, the stresses increase, but owing to the lower initial values the final stresses are not so high. After the crushing process has begun and the surface F_1 moves upwards, the rate of crushing is accelerated — as may often be observed in practice. The process is illustrated in principle by the changes in the form of the stress curves at the new position F_2 of the front. Since the new stressless zone has increased in height to $F_2 - G$ the horizontal forces transmitted from the zone to the surface stratum at F_2 and G increase appreciably, and the curves e_1 change to the curves e_2.

The study of the stress distribution in the Kaptenslagret body at Malmberget (Fig. 65) and at Grängesberg show that the rock pressure in and near the orebody is perpendicular to the surface of contact between the rock and the ore. This is probably due to the presence along these surfaces of chlorite or of other clay minerals, across which only normal forces may be transmitted. If it is assumed that the rock pressure acts in this direction within the lens, the usual horizontal under-cut of a block (Fig. 76 a) would appear to be unsuitable for an inclined orebody. Fig. 76 b illustrates a similar face in which compressive forces are acting perpendicular to the ore lens. The wedges S_1 and S_2 in the ore will be subjected to shearing forces along the broken lines, and at first there will be no highly concentrated stress-bearing underzone such as that in Fig. 76 c, where the angle of the under-cut is changed to the most convenient one. The whole wedges S_1 and S_2 are not broken off at once, there probably being a gradual process of destruction in which the wedges are broken off by the shearing forces as a number of rather large pieces of ore.

Instead of the ore at F_1 gradually splitting off under the rock pressure, as is desirable, large pieces of ore from the wedge S_1 will probably at first fall into the chutes in the ore panel B over the cross-cut C, where they will need to be blasted in order to facilitate smooth discharge. Experience has also shown that in many instances the disintegration of the block does not progress satisfactorily until the surface zone has been worked.

By making the under-cut of the block perpendicular to the hanging and foot walls as in Fig. 76 c the continuous crushing process will start soon after the cut is made. The removal of the ore through the cross-cut C to the haulage way E would probably be facilitated by having the floor of the cross-cuts inclined when the scraping method is practised. When mechanical loading is used it is not convenient to have a sloping floor in C. In cases where the angle of the lens to the vertical is large it may be difficult to have the under face F_1 at right angles to the foot and hanging wall as in Fig. 76 c. However, it seems likely that from the ore-crushing point of view great advantages are to be gained, even if the under-cut angle is changed from the horizontal by only one-half of that in Fig. 76 c.

In order to ensure a continuous crushing process over the whole front F_1 and to avoid the complications incurred by the shearing of forces acting on the wedge S_1 Fig. 76 b, the whole of the wedge S_1 may be removed immediately after the under-cut has been made. This is performed by using deep drilling.

This measure avoids the danger of pieces of the wedge S_1 choking the chutes of B and interfering with the natural discharge of the crushed ore near the foot wall. Moreover, the frontal zone at H near the foot wall may be the only part of F_1 where the crushing can properly set in before the wedge S_1 is broken off.

It is seen from the stress curve in Fig. 76 a that if the level F_1 is made too low — for example at F_3 when the block will have the height O-F_3 instead of O-F_1 — the stress in the under face of the block due to the under-cut would, according to the adjacent stress curve, not be sufficiently high for crushing in F_3 to set in. The block will remain intact until the stress conditions are changed by excavation of the ore in a zone of greater height beneath F_3 than in the case of the F_1 position ($=a$), or by mining out a vertical band-shaped zone sufficiently wide on each side of the block. There would then be a stress concentration in the block acting against these free fronts and the stresses might increase to such a magnitude that crushing of the ore would take place.

The foot and hanging walls of the rock facing the under-cut will be deformed elastically — often several centimetres, depending upon the height of the under-cut — into the stope, as soon as the forces of reaction in the ore against the prevailing lateral rock pressure have disappeared on removal of the ore from the under-cut zone. A similar deformation of the rock will occur at places where the ore has been ruptured. The relatively large lateral movement of the walls is significant from the aspect of crushing, for the ore may then still be subjected to continuous pressure after the first fissures have appeared, which in itself, implies some yield in the ore. The expanding foot and hanging walls exert a pincer

action on the fronts G and F_1. An approximate calculation of the lateral movement of the country rock walls on disappearance of the horizontal rock pressure in the zone D is simple, but it is more difficult to ascertain the magnitude o the stresses in the orebody in a horizontal direction set up at the fronts F_1 and G — the forces X in Fig. 78. It seems probable that these forces are distributed over the whole width of the lens, with a maximum near the fronts F_1 and G, and falling off rapidly with distance from this face. Moreover, it seems likely that this superficial concentration of crushing forces is most marked in the parts of the front F_1 located near the hanging and foot walls, and that they decrease with the distance therefrom. An essential of efficient crushing of the ore is that the adjacent country rock be strong and that the force X large.

A few words may be in place regarding the maximum value of these surface stresses X and their location on F. Fig. 79 shows a square hole with rounded corners of radius ϱ in homogeneous rock that is stressed in the direction y—y by σ_0 acting at a great distance from the hole. The maximum stress will appear near the corners, as has been calculated by Inglis in the case of a hole in a stressed plate. The hole can be made by cutting two elliptical holes as in Fig. 79. The stresses in the corners of the square can be calculated from Inglis' formula for the elliptic hole. To get the square hole the cutting process has to be extended, but the error in the formulae below is small.

$$\sigma_A = -\sigma_0 \cdot \sqrt{\frac{l}{\varrho}}$$

$$\sigma_B = -\sigma_0 \left[1 + \sqrt{\frac{l}{\varrho}} + \sqrt{\frac{\varrho}{l}}\right]$$

$$\sigma_C = \sigma_0$$

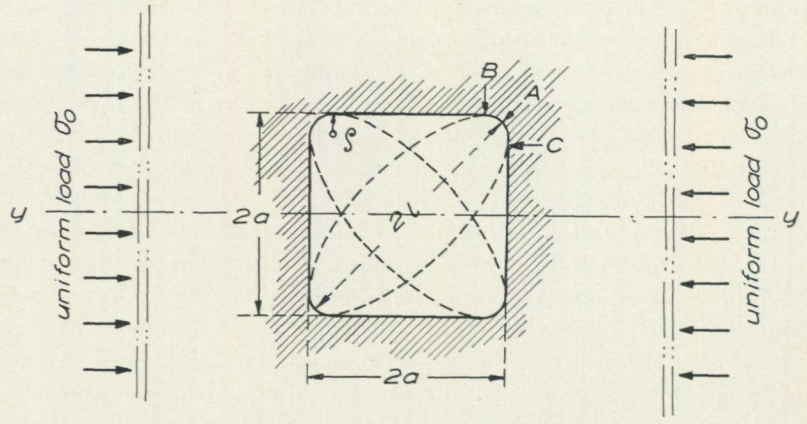

Fig. 79. A square hole in a loaded plate, replaced by 2 elliptical holes according to Inglis in the calculation of surface stresses at A, B and C.

σ_A, σ_B and σ_C are the surface stresses at points A, B and C in Fig. 79. If σ_0 is compressive, σ_A and σ_B are also compressive and σ_C tensile. The width and height of the hole is $2a$ and its diagonal is $2l$.

The greatest compressive stress along the rounded corners occurs at a point between A and B, and, if ϱ is small compared with l, its approximate value is

$$\sigma_{max} = -\frac{\sigma_0}{2}\sqrt{\frac{l}{\varrho}}\left[1 + \frac{\sqrt{2\,l + 2\,\varrho}}{\sqrt{l} - \sqrt{\varrho}}\right]$$

By putting $l = 10$ metres, we have, for various values of ϱ,

$\varrho = 0.5$ metres	$\sigma_{max} = 6.6\ \sigma_0$
1.0 »	$= 4.4\ \sigma_0$
2.0 »	$= 3.8\ \sigma_0$

If σ_0 is compressive σ_{max} is also compressive.

From these calculations it is evident that the stresses at face F_1 in Fig. 78 (forces X) are highest at a small distance from A_1. It is probable that they are lowest in the middle of F_1. If the corners are retained sharp at A_1, the stresses at F_1 will be higher than when the corners are rounded. It seems likely that the disintegrating process of the ore will be at its greatest intensity uear A_1, and from the point of view of running mining the rate of removal of the ore should then be sufficiently high at these points.

Where there is friction-eliminating material on the contact surface between the ore and the country rock, the crushing front F_1, which is continuously moving upwards during the disintegration of the block, for the most part remains plane, possibly with somewhat larger falls of ore in the centre. If the friction-eliminating layers or covering are absent at the boundary surfaces, the front F will be built out with end pieces that are friction- bound against the rock wall, say, along the line f in Fig. 76 d.

A block should not be placed at the end of a lens as from B to C in Fig. 76 d. In this case the removal of the ore will result in an increase in pressure in parts of the rock at the end of the lens (B). The crushing forces available at C will be small since the original rock pressure, σ_0, is taken up mostly at B as soon as the ore is mined out — this being done without any appreciable expansion of the walls at points C, located not far from B.

From the above it would appear that a knowledge of the direction and magnitude of the rock pressure is desirable when planning block caving. If much experience has been gained in a mine in the application of this mining technique, the dimensions of the block will be a matter of judgement. But this does not mean that the shape of the block will always be the most suitable from the aspect of productivity; it will then be advisable to place reliance on the rock pressure curve (Fig. 76 a) and on knowledge of the ultimate strength and crushing properties of the rock. Where block caving

is being introduced in a mine for the first time it is practically essential to plan the disposal of the block on the basis of the pressure curve. A suitable place to perform rock pressure determinations would be the climbing shafts, which are generally located some fifty metres apart in the foot wall (*Sh* in Fig. 76 a). It is true that the stresses are not measured in the ore itself, but if the shaft does not lie too deep in the foot wall the measurements will probably be acceptable. The rock pressure curve (Fig. 76 a) must be measured and constructed for all those parts of the mine where blocks are to be cut, as the rock pressure has been found to vary much from one part of a mine to another.

The crushing forces and the width of the ore lens

As shown above, the crushing force in the zones F_1, F_2 and G is dependent on the elastic deformation of the walls (δ in Fig. 78) as the supporting pressure exerted by the ore is removed. If the ore at F_1 and G no longer resists the elastic movement of the walls, no stresses will act at F_1 and G. The greater the resistance offered the greater will be the forces X (Fig. 78), until they prevent almost any movement in the wall at points A_1 and A_2. In this case, too, the portion of wall between A_1 and A_2 moves inwards elastically. If the orebody is wide the longitudinal deformation of the face F_1 over the whole width of the body (from A_1 to A_1) will be appreciable compared with the elastic movement of the wall itself at A_1 and A_2. The same is true if the modulus of elasticity of the ore is low. A large fraction of the force X will then disappear through the low resistance of the frontal zones to the elastic movements of the walls.

Consider one narrow and one wide orebody in which the prevailing horizontal rock pressures are equal. Mining out of rooms of equal length and height will result in equal elastic deformation of the wall if the points A_1 and A_2 are assumed to be fixed. On the other hand, the elastic deformation of the frontal zones F_1 and G for the whole orebody of width b will increase with the value of b. It follows that the forces X will be greater for the narrower than for the wider orebody. This situation has in fact been observed at the Grängesberg mine. The narrow orebody at Strandbergsfältet is acted on by an appreciably greater horizontal rock pressure than wider bodies in the vicinity. It should be observed, however, that the mensuration values in this example do not relate to blocks but to levels in, or near to, the working face of an orebody.

It might be added that in the instance of narrow lenses a permanent vaulting may occur, in which case the flat part of the curve f will disappear (Fig. 76 d). Where there is much friction between the ore and the country rock very high pressures may be transmitted across the body and the ore will not be forced down. If the rock is weak, however, there is a risk that the wall will rupture.

Fig. 80 is a vertical section through the working zone of the ore lens in the mine of Ställbergsbolagen at Ställberg in Central Sweden. Although the horizontal rock pressure is very great the block caving method cannot be used owing to a small width of the ore lens. The width is only 4 metres; the length of the lens is about 1 km. The mine is the deepest one in Sweden and the horizontal rock pressure acting at a depth of 915 metres reaches a magnitude of 550 kg/sq.cm in a direction 60° to the lens. This stress-value is greater than that measured in any other mine in this country.

The ore has been mined out down to a depth of 650 metres. During the last years the working face has been lowered to levels where very high horizontal pressures are acting. The broken ore is mixed up with rock and the percentage of

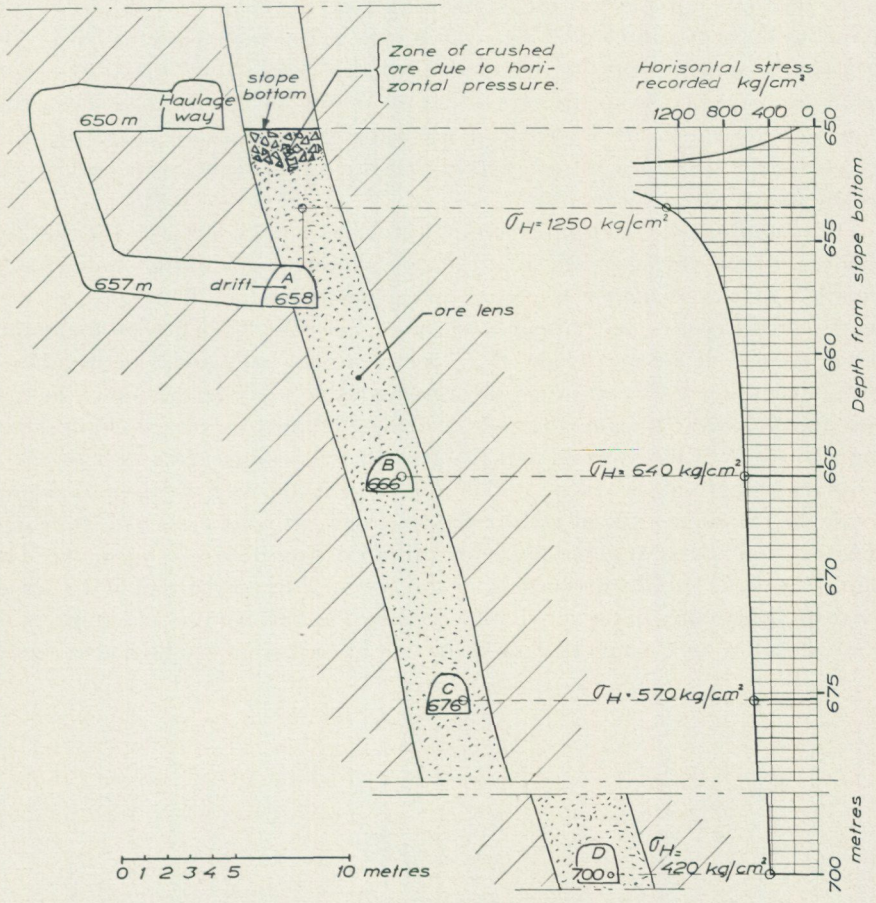

Fig. 80. A section through the working zone of the narrow ore lens (4 metres in width) in the mine of Ställbergsbolagen at Ställberg in Central Sweden. The horizontal stresses acting perpendicular to the lens have been measured in holes drilled from the 3 drifts *A*, *B* and *C*. The maximum magnitude recorded is 1,250 kg/sq.cm at a depth of 4 metres below the bottom of the stope. At a depth of only 3 metres the stress is probably higher, say 1,800—2,000 kg/sq.cm.

rock seems to increase with increasing depth. The percentage is now of a magnitude that necessitates a change in the mining methods being used.

The ore of Ställberg is magnetit and has a high breaking strength, 1,800-2,000 kg/sq.cm at places. However, the bed rock of limestone is of low strength. In the mining the shrinkage stoping method has hitherto been used. Due to the high horizontal stresses acting great frictional forces can appear between the ore and the limestone. The bed rock of limestone may rupture simultaneously with the ore during the blasting procedure. If the frictional forces are very high there is also a risk that parts of the broken ore will be fixed between the hanging and foot walls and so prevented from falling down.

Therefore, in the planning for a change in the mining method at Ställberg it is necessary to know the magnitude and distribution of the horizontal stresses in the orebody, especially at the levels of the working zone.

In Fig. 80 *A*, *B* and *C* are 3 drifts cut for the experimental mining work. The drifts were located at the 658, 666 and 676 metre levels, that is 8 to 10 metres below each other; the drifts were about 30 metres in length. The measuring holes were drilled in the ore vertically from the roof face and horizontally from the end of the drifts and to such depths that the measurments were not influenced by the presence of the drifts.

The magnitude of the virgin horizontal stress field at the levels of *A*, *B* and *C* is about 420 kg/sq.cm measured in a direction perpendicular to the ore lens. The recorded stresses at higher levels were at a maximum of 1,250 kg/sq.cm at a depth 4 metres below the bottom of the stope (see Fig. 80). The real maximum value appears at a depth below this bottom of between 2 and 4 metres. However, a recording of this value has not been made due to the separation of the core into discs 1.5 cm in thickness during the drilling of the stress release channel (see pages 51—53). It seems likely that the greatest stress values were as high as the breaking strength of the ore or 1,800—2,000 kg/cq.cm. At a depth of 12 metres below the recorded value of 1,250 kg/sq.cm the horizontal stress had decreased to 640 kg/sq.cm and at about the same distance deeper to 570 kg/sq.cm. The high stress zone in which crushing of the ore appears in the roof and walls of the drifts apparently has a very limited depth. The new method of mining must be arranged in such a way that no drifts will be located in the high stress zone.

PART SIX

HORIZONTAL ROCK PRESSURE IN SCANDINAVIA

Examples of rock pressure in Sweden and Norway

One of the most interesting and unexpected results yielded by rock pressure measurements performed by the method described in the foregoing Parts I—V is the demonstration of *large horizontal stresses in the earth's crust*. In mining it has long been the practice to reinforce by vertical supports those places in the drifts, cross-cuts etc. where destructive forces may be acting. However, in all cases where rock pressure measurements have been performed in Swedish mines the rock pressure has been found to be incomparably greater in the horizontal direction than in the vertical. In the virgin rock and at depths of about 400 metres (in one case 900 metres) measurements have revealed horizontal pressures as great as 1.5—3.5 times the dead weight of the overlying strata. Locally values as high as 8 times that of the overburden have been obtained.

Fig. 81 shows a map of the North in which the mines where stress determinations have been made are indicated by small circles numbered 1—6. At these points the magnitude and direction of the horizontal principal stresses, in most cases obtained from measurements in vertical drill holes, have been entered. The ellipse thus roughly represents a horizontal section through the stress ellipsoid for the point in question. For the determination of the ellipsoid the measuring of 6 values from 3 adjacent holes is required, one of which may conveniently be vertical and 2 horizontal and at right angles to each other. All the holes are drilled to such a depth that the local influence exerted by the drift on the stress field at the measuring point may be neglected. This complete determination of the state of stress, which, of course, involves more work than would be required for the horizontal plane alone, have been performed for points 1 and 6. The stresses acting along the axes of the ellipsoid represent the three principal stresses in magnitude and direction. The determination of the ellipsoid also gives the three principal shearing stresses and the angle-position of the surfaces in which they act. In this way it is possible to analyze the stress conditions in the earth's crust at depths reached in the mines.

Point 1 The mine of Ställbergsbolagen at Ställberg, Central Sweden.

The measurements have not yet been made available. The ore lens about 4 metres wide and one kilometre long, has a dip of 75—80°, and the ore has been mined out to a depth of 650 metres. The main shaft has been taken down to 915 metres. The horizontal pressure has been measured at several places in the foot and hanging walls, and at various distances from the ore lens. In the virgin rock at a depth of 915 metres and 150 metres from the lens the stress ellipsoid was determined. The horizontal rock pressure is about 550 kg/sq.cm

(σ_1 in the horizontal stress ellipse); at the 700 metre level it is about 100 kg/sq.cm lower. It is acting approximately NW—SE (60° W of N).

POINT 2 The mine of Trafik AB Grängesberg—Oxelösund at Grängesberg, Central Sweden, near point 1.

The larger of the horizontal principal stresses at a depth of 310 metres is acting in a direction roughly NW. However, the magnitude of the stresses varies at different places in the mine owing to the influence of the adjacent zone of excavation. New measurements are being made deep below this zone at the 515 metre level for the determination of the stress ellipsoid. The results are not yet available.

POINT 3 The mine of S.K.F. at Vingesbacke, Central Sweden, 100 kilometres from points 1 and 2.

The complete results of the stress measurements in this mine have not yet been made available. In this area there is a stress field where, at the 410 metre level, the major horizontal principal stress is 450 kg/sq. cm, and acts in a N—S direction, — actually about 10° E of N. The stresses are being measured in the granite and amphibolite, which surround the ore lens.

POINT 4 The mine of L. K. A. B. at Malmberget, northern Sweden.

The results of these stress determinations are presented in Part Four, p. 131. At a depth of 460 metres and 50 metres below the working zone there is a horizontal stress field of which the major principal stress σ_1 is 360 kg/sq.cm, and acts in an E—W direction — 10° N of W, σ_2 is 110 kg/sq. cm. The stress thus varies widely with direction. The measurements were performed in strong granite.

POINT 5 The mine of Bolidenbolaget at Laisvall, northern Sweden.

The results of the stress measurements are described in Part Two, p. 61. At a depth of 100 metres the major horizontal principal stress is about 250 kg/sq. cm and acts roughly NNE—SSW — 20° E of N. $\sigma_2 \simeq 0.5 \cdot \sigma_1$.

POINT 6 The mine of Fosdalens Bergverks Aktieselskab at Malm, Norway.

The results of these stress measurements are not yet made available. They are of particular interest because in this case the stress ellipsoid was determined as to form and angle position. The mine is located in a region where there have been numerous displacements. At many places the ore lens is interrupted and has been shifted laterally and vertically, the greatest single displacement in the latter direction being no less than 500 metres downwards. Moreover, the area contains many almost parallel planes of cleavage, which divide the rock into plates which have a dip of 58°. The stress ellipsoid has been calculated at two places in the region — in a horizontal direction 500 metres apart and at a depth of 600 metres. 3 adjacent-perpendicular measuring holes at each place give 9 recorded stress values. However, as 6 values from 3 holes are enough to determine the stress ellipsoid the 3 other values serve as a check of the results. They show that in spite of the division of the rock into plates the maximum

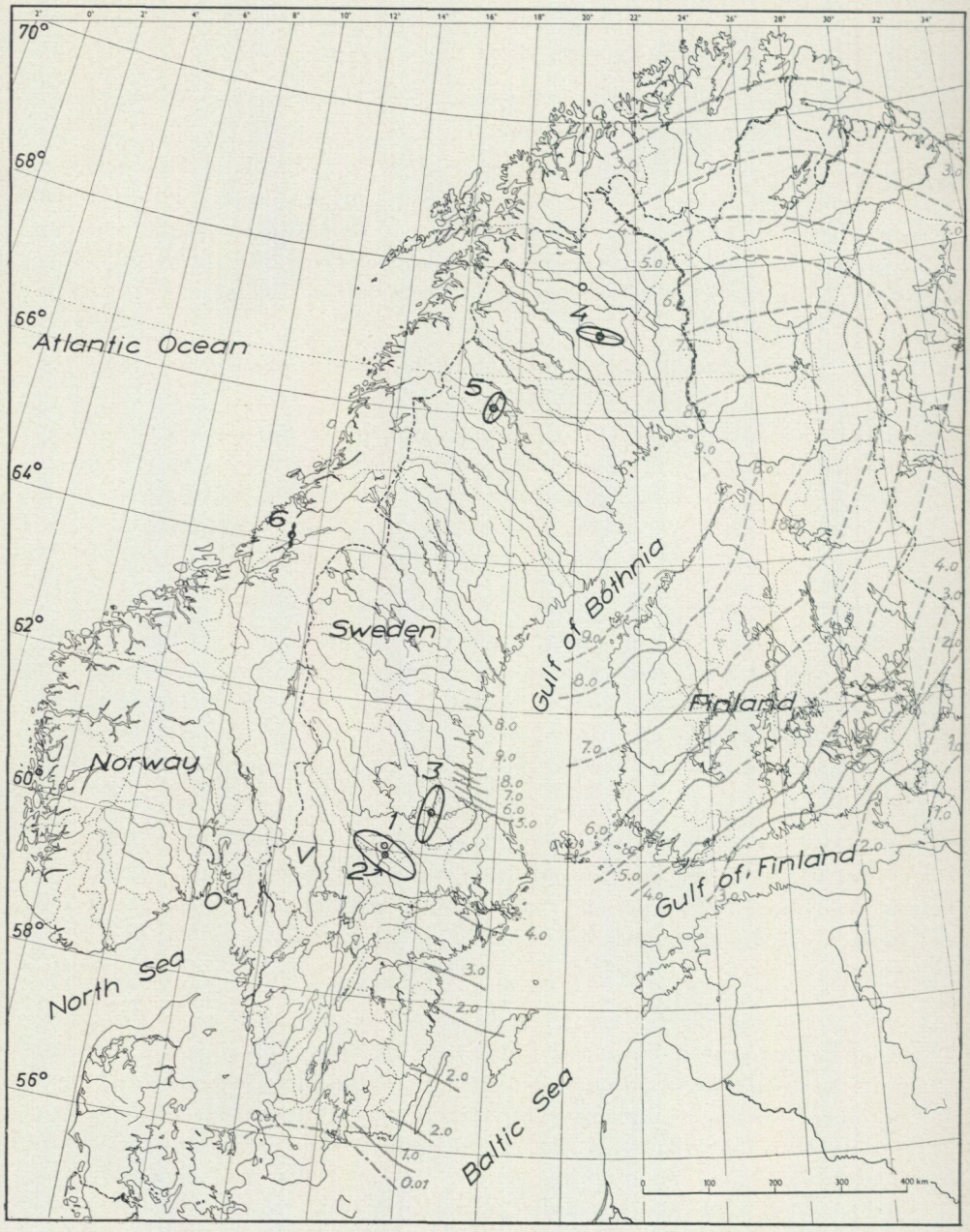

Fig. 81. Points 1—6 on the map indicate the six mines in Scandinavia where the stresses in the earth's crust have been determined. The magnitude and direction of the horizontal principal stresses are evident from the stress ellipses.

error is between 1 — 5 per cent for the values of σ_1, σ_2 and σ_3; for the two points 500 metres apart the values are in agreement.

The measurements show that the dead weight of the rock is transmitted downwards in the plane of the plates, and that in these plates, which are directed N—S, there is also a horizontal stress of 160 kg/sq. cm. Perpendicular to the plane of the plates there is a lateral stress of a magnitude sufficient to maintain the plates in a state of equilibrium. There are no other form of lateral forces.

In the Norwegian massive around Malm the earth's crust is consequently subjected to a horizontal stress of 160 kg/sq. cm in a N—S direction. In the E—W direction the horizontal stress is zero. The numerous cleavages suggest that the rock has at some time been subjected to tensile or shearing stresses. Is is possible that the tensile stresses remain at great depths where, however, they are probably superimposed by a lateral pressure in the mass set up by the high vertical load. There is evidence that the area around Malm is a region of tensile or zero-stress, just as Vingesbacke (Mp 3) is a region of compressive stress in the earth's crust. The horizontal stress ellipse in Mp 6 in Fig. 81 thus assumes the form of a line in the N—S direction.

Is the rock pressure due to bending of the earth's crust?

As has been shown in some parts of Scandinavia the bed rock down to great depths is subjected to horizontal compressive stresses that are several times greater than the dead weight of the overlying strata. At several points horizontal pressures of 400—500 kg/sq. cm have been measured. The stresses generally vary with direction and increase with depth.

It seems likely that these enormous stresses in the bed rock — a fairly common feature in Scandinavia — have a general explanation, probably of a geologic or tectonic nature. It is not inconceivable that *the stresses may be bending stresses in the solid crust of earth*, set up owing to uneven uplift and subsidence. According to measurements made at Kiruna, the thickness of the earth's crust in Scandinavia — one of the oldest areas of primitive rock in the world — is probably about 30 km[1]. However, with our present limited knowledge of the uplift and subsidence of the earth's crust in Sweden it is impossible to establish a definite link between these phenomena and the observed horizontal rock pressure. The discussion presented below should be regarded as no more than an indication of such a connection and as a basis for further discussion.

Secular movements in the North

In Fig. 81 the changes in coastline and elevation obtained from tide-gauge observations along the east coast of Sweden have been marked.[2] The changes in the level of the bed rock in Finland — also entered in the map — have been obtained from similar measurements, but they are here combined with precise levelling over the whole country.[3]

[1] These determinations were made in 1955 by Dr. Markus Båth of the Seismological Laboratory in Uppsala, Sweden.

[2] The figures have been taken from F. Model: Gegenwärtige Küstenhebung im Ostseeraum. Mitt. der geogf. Gesellsch. in Hamburg BD. XLIX 1950.

[3] These values have been taken from Erkki Kääriäinen: "On the recent uplift of the earth's crust in Finland". Suomen Geodeettisen Laitoksen Julkaisuja, No. 42. Helsinki 1953.

With the exception of the extreme south of Sweden where there is a slight subsidence, the whole country is being elevated. At the 56th parallel the change is nowhere greater than 0.1 cm per year but it increases towards the north; at 61° it is 0.5 cm and at 63° 0.9 cm per year. This value remains constant as far as the 66th parallel, after which the uplift gradually decreases until it is zero approximately at the northern extremity of the Scandinavian peninsular. If the land had originally been plane in a N—S direction the earth's crust in certain parts of the country would now curve bowl-shaped with the concave side upwards. The crust would then be acted on by a bending moment that gives compression stresses in the upper side and shearing stresses at deeper levels, just as a loaded beam or plate. In the area that is surrounded on all sides by smaller uplifts the earth's crust undergoes a convex bending, which gives rise of tensile stresses in the upper zone. Since the various types of rock in question have very low tensile strength the rock will probably have been ruptured at an early stage of the uplift movement and there will now probably be no tensile stresses at depths accessible to study.

The uplift per year in southern Finland is 0.2—0.3 cm. On the Gulf of Bothnia it increases to about 0.9 cm at the 63rd, and remains constant to the 66th parallel. It then decreases again to only 0.3 cm per year at 70°. In Sweden no such accurate measurements have been made, but there is evidence that the coast of Sweden on the Gulf of Bothnia is rising in a similar manner to that of the west coast of Finland. In an east—west section, too, the North is being elevated most rapidly around the Gulf of Bothnia (0.9 cm per year). The uplift tends to zero on the eastern frontier of Finland. Along the Atlantic coast of Norway the rise seems to be practically nil. In and around the Gulf of Bothnia there has consequently formed a plateau in the area of uplift.

Secular movements in other countries than the North

The uplift of the North that is taking place at present has been said to be a reaction to depression during the ice age. However, according to the most recent findings of scientists in this field, practically nowhere in the world does the level of the crust remain unchanged over a considerable period, irrespective of whether or not there has been a recession of ice. Bands of subsidence and uplift appear in succession in a wavelike pattern over many parts of the surface of the earth. These secular movements appear to follow a cycle of one or a few thousand years.

In parts of Europe it has been found that bands 200—300 kilometres in width are most clearly developed along the lines of longitude, but that a wave pattern of uplifts and subsidences can also be observed along the parallels of latitude; that is to say, crossing the first band system.

Crustal movements in progress at the present time have been determined only at a few places on the earth — primarily in Finland, Japan, the United States and the Soviet Union. As an example of the American measurements

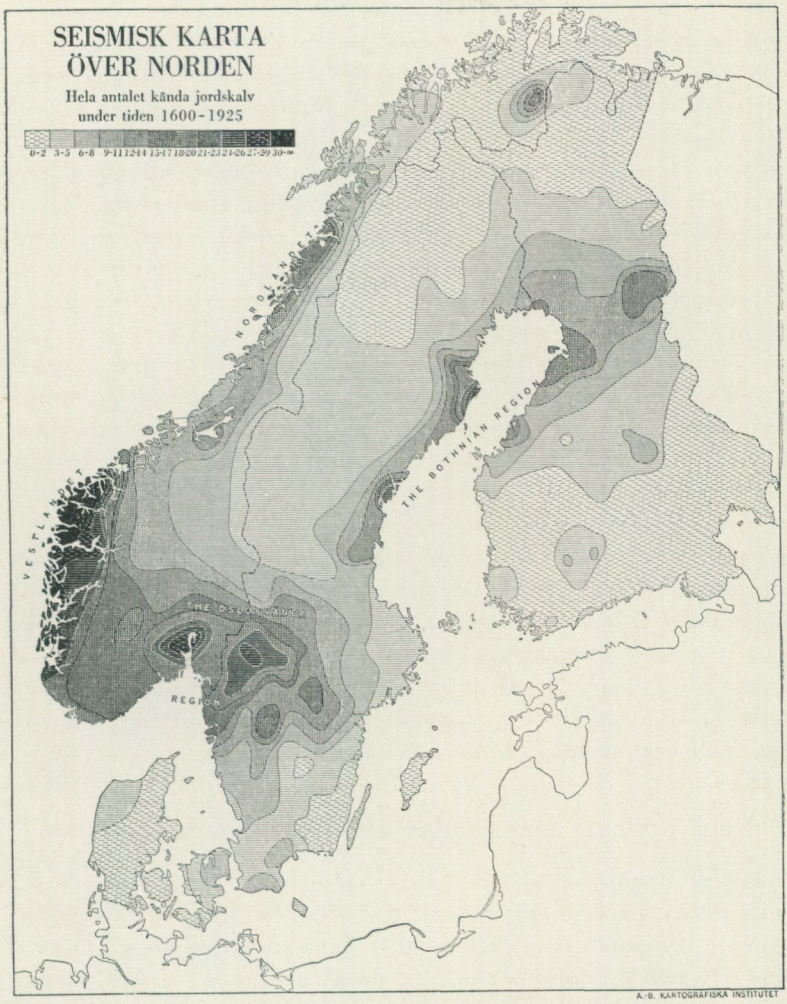

Fig. 82. Earthquake frequency in the North, given as the total number of known earthquakes during the interval 1600—1925. After K. E. Sahlström. The map was published in 1930. By courtesy of Dr. Sahlström the author has been informed of his supplementary work on the map about earthquakes after 1925. Dr. Sahlström points out that the only change in the map will be that the earthquake area of and around the Bothnian Bay extends to a some what increased distance into Sweden. The author is indebted to Dr. Sahlström for the use of his mape and for his information.

mention may be made of a study from the Great Lakes area, in which determinations were made at 106 points.[1]

Comprehensive studies have been performed by F. A. Mescherikov of the Geographical Institute of the USSR Academy of Sciences and the Central

[1] An account of this study is given by Sherman Moore in "Bulletin of Geological Society of America", 1948.

Scientific Research Institute of Geodesy, Air Survey and Cartography. The results were presented at the XIth General Assembly of the International Union of Geodesy and Geophysics in Toronto, 1957. Investigations have been made of large parts of European USSR, and part of the following data are obtained from that source.

The area of subsidence that begins east of the Bay of Finland (Fig. 81) has been found to extend southwards across the Baltic States to the Carpathians. East of this area there begins a region of uplift, which extends from the north as far as the subsidence area down to the Black Sea. East of this area of uplift there is another band, of about equal width, where the ground level is subsiding, this in turn being followed by another area of uplift.

These secular uplifts and subsidences have been attributed to volumetric changes associated with processes of crystallization in the lower zones of the earth's crust. It would seem more likely, however, that the movements are of a tectonic nature. There is, in fact, a close connection between the secular movements of the earth's crust and the seismic activity of the earth. This is evident from the fact that epicentres of earthquakes are usually located in areas of marked uplift and that the secular movements increase greatly in magnitude near epicentres. A study made in Japan has shown that while the land on an average undergoes an annual uplift of about 0.5 cm, movements locally increase to 1—5 cm near centres of seismic activity. From the Russian investigations has been found, moreover, that the marginal zone between areas of uplift and subsidence are surprisingly narrow, and that epicentres are located in the areas of uplift near these marginal zone.

Rock pressure and secular movements in Scandinavia

As has been mentioned above, the east coast of Sweden is rising at different rates in different parts of the country (Fig. 81). The greatest change in rate is taking place near the 61st parallel, where for a stretch of about 75 kilometres the rate at which the land is rising is changing from 0.5 to 0.9 cm per year. If it is assumed that these movements have been continuing at the same rate for two or three thousand years there would now be a considerable cumulative curvature of the earth's crust accumulated in these areas (concave side upwards). The rock pressure determinations in the neighbourhood at Vingesbacke (point 3, Fig. 81) demonstrate the presence of very high horizontal stresses. σ_1 of the horizontal stress field is 450 kg/sq. cm at a depth of 410 metres and acts in a N—S direction. The value of σ_2 is also high, at about 300 kg/sq. cm. It is interesting to find that this area with the high rock pressure lies in a region where the curve of the uplift is very steep. Unfortunately, the uplift is not known in the region of the other measuring points.

However, it is fairly certain that there are no appreciable vertical movements on the Atlantic coast of Norway. The earth's crust in Sweden and Norway is therefore undergoing a curving or bending in an E—W direction at the same time as there is an almost N—S curvature. The horizontal stress field in the

interior of Central Sweden — as measured at points 1 and 2 (Fig. 81) — has its major principal stress in a direction 60° W of N. As nothing is known of the secular movements in these areas, no definite relationship can be established between these and the existing rock pressure. However, Fig. 82 shows the location of epicentres of earthquakes in the Oslo Bay and in the west parts of Central Sweden (*O*, *V*, in Fig. 81) It seems possible that the present rate of uplift of the earth's crust in Central Sweden is increasing near this area — the same takes place at Vingesbacke, south of the epicentres of the Bothnian Bay. Then the NW direction at points 1 and 2 seems more reasonable.

Point 4 lies between the Gulf of Bothnia, where the uplift seems to be the highest in Scandinavia (0.9 cm per year), and the Atlantic coast of Norway, where the uplift is about nil. The greatest bending moment of the earth's crust should here be in an E—W direction. This is also the direction of the major principal stress at this point. At point 6 near the Atlantic coast, where there is no uplift the only appreciable stresses act in a N—S direction: The presence of compressive stresses at points 5 and 6 acting about N—S might be associated with the gradually increasing secular uplift from the 56th to the 65th parallel.

Calculations

No general conclusions can be drawn from the relationship between the directions of the horizontal rock pressure in Scandinavia and the secular movements, owing to insufficient knowledge of these secular movements. Nevertheless there would appear to be enough data to justify a calculation in principle of the relation between the uplift movements of the earth's crust and the magnitude of a rock pressure due to bending moments of the crust. However, the calculation will be made under the simplified assumption that the area of uplift is circular and without any adjacent areas of subsidence and that the earth's crust acts as a solid elastic plate, irrespective of the presence of forces at deeper levels due to its own weight.

It is natural to associate the presence of uplift and subsidence with an upward pressure and downward, respectively, exerted by the underlying strata locally on the under surface of the solid crust. Whether this change in pressure is a result of crystallization processes in the underlying strata, of over- and under-pressure formed during slow movements of the viscous masses on which the crust is floating, or whether it is of a tectonic nature, cannot be decided.

In Fig. 83 *C* represents the earth's crust, 25 km in thickness, supported by a uniformly distributed force of reaction from the underlying less solid strata. Locally, over a circular area of radius a there is assumed to act an over-pressure p, which acts from below and hence deforms the earth's crust of thickness h, as if it were a plate supported at the periphery at *A*. Since the earth's crust is supported on a deformable medium the deformation will be rapidly extinguished on the opposite side of the periphery *A*.

Let the bending stress in the upper side of the earth's crust at, and perpendic-

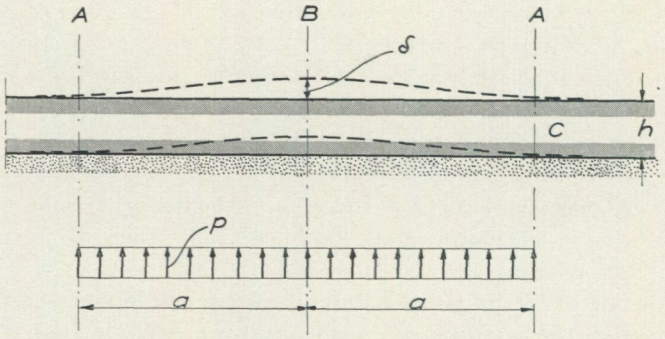

Fig. 83. Cross-section through an area of uplift in the solid earth's crust C, of thickness h. The layer is supported by the force of reaction due to its own weight. In a circular area of diameter $2a$ the earth's crust is acted on by a further upward pressure p, which is responsible for the elevation δ at B.

ular to, the periphery of the support be represented by σ_A (compression), and that at the centre by σ_B (tensile). Then, if E is the modulus of elasticity of the material of the earth's crust, the change in height of the earth's crust at the centre relative to the periphery according to the elastic theory is given by the expression

$$\delta = 0.171\, p\, \frac{a^4}{E \cdot h^3} \quad \ldots\ldots\ldots\ldots\ldots \quad (1)$$

We have

$$\sigma_A = -\,0.75\, p\, \frac{a^2}{h^2} \quad \ldots\ldots\ldots\ldots\ldots \quad (2)$$

and

$$\sigma_B = 0.488\, p\, \frac{a^2}{h^2} \quad \ldots\ldots\ldots\ldots\ldots \quad (3)$$

From Eqn. (2) we have $p = -\,\sigma_A\, \dfrac{h^2}{0.75\, a^2}$

Substituting for p in eqn. (1) we have

$$\delta = -\,\sigma_A\, \frac{0.228\, a^2}{h \cdot E}$$

Suppose, by way of example, the diameter $2a$ of the area acted on by an over-pressure is 200 km, and h, the thickness of the earth's crust, is 25 km.

Then, if $E = 10^6$ kg/sq. cm (for rock at great depth) and $\sigma_A = -\,300$ kg/sq. cm,

we have

$$\delta = \frac{300 \cdot 0.228 \cdot 10{,}000{,}000^2}{2{,}500{,}000 \cdot 1{,}000{,}000} = 27 \text{ metres.}$$

This change in level is distributed over a distance of 100 km. If the average secular movement is one centimetre per year more at B than at A, a horizontal rock pressure at A of 300 kg/sq. cm will be set up by these movements, this

being cumulative over 2,700 years. If the uplifts are greater the period will be shorter.

The over-pressure p, which is assumed to occur at a depth of 25 km below ground level, is given by the expression

$$p = -\sigma_A \frac{h^2}{0.75\, a^2} = \frac{300 \cdot 2{,}500{,}000^2}{0.75 \cdot 10{,}000{,}000^2}$$

$$p = 25 \text{ kg/sq. cm}$$

The over-pressure p is thus small compared with the pressure exerted on the underlying strata by the dead weight of the earth's crust, 25 km thick.

It has been assumed above that beneath the solid earth's crust areas of upward pressure are developed (p in Fig. 83). It may similarly be assumed that areas of under-pressure occur, these being responsible for local subsidence of the earth's surface. At these sites the earth's crust then assumes a curved form with its upper surface concave; the stresses so formed will be compressive at the crust surface. Alternating over- and under-pressure would thus give rise to upward and downward movements of the earth's crust and hence a wave pattern.

In the case of the loading conditions illustrated in Fig. 83 compressive stresses are acting in a marginal zone along the periphery A. At the center B of the circular plate the stresses are tensile and at some point between A and B they are zero. Shearing stresses are also acting.

In the central part of an area of uplift the upper zone of the bed rock will be under tension and badly fissured. *Due to this fissuring the moment of inertia of the earth's crust will be lowered and consequently the upward movements in an uplift area will be greater than the subsidence in an area of subsidence* — for the same value of p. This is consistent with the observations made by, for instance, the Russian investigators.

If the earth's crust is subjected to deformations by bending moment, the concave side upwards, the greatest compressive stresses should occur in the upper surface and decrease to zero in the plane of the axis of bending, which should lie at very great depth.

The Swedish mines lie completely in the surface layer of the earth's crust, and it might therefore be supposed that the horizontal pressure does not vary appreciably with depth. However, this pressure appears to be so great that near the earth's upper face the surface zone is broken at some points — with small local uplifts, and the surface stresses are lowered. The stresses might not reach their maximum magnitude until at depths where the dead weight of the overlying rock prevents rupture and such upheavals.

At such depths it seems likely that the horizontal rock pressure is fully developed and may at places be dangerous to the stability of some parts of the mine. In other countries than Sweden there are mines 3,000—4,000 metres in depth. Extensive rock bursts have recently appeared in such mines at very deep levels. *The horizontal stresses in the earth's crust may in these cases have been the destructive forces.*

Relationship between the horizontal rock pressure and earthquakes

The presence of high horizontal pressure in the rock suggests that practically all earthquakes may have their origin in a local release of such latent stresses, which have accumulated over a period through movement of the earth's crust. *The displacements and faults that occurred frequently in some geological eras may have been similar phenomena*, though much more powerful ones owing to the much greater stresses that were then acting in the earth's crust.

At many places earthquakes occur in the form of displacements along existing deep planes of slip (faults). Experience from, for instance, San Francisco (San Andreas fault) has shown that earthquakes have repeatedly occurred along the same fault. The presence of high horizontal stresses in the earth's crust, which itself is everywhere undergoing secular uplift or subsidence, would suggest the following mechanism for earthquakes.

A horizontal stress field, which after an earthquake may be assumed to have diminished considerably in magnitude, gradually increases again owing to further movement of the earth's crust. If there is a fault passing through the bed rock of the area, new, principally horizontal, stresses will gradually be set up around it. If the coefficient of friction and the pressure acting perpendicular to the face of the fault are known, the frictional forces required for setting up a state of equilibrium with the forces of displacement along the fault may be calculated. Only when these latter forces which can be determined by direct measurement have reached such values that the friction in the fault can no longer maintain equilibrium, does slipping occur along the fault, this being felt as an earthquake.

As soon as the movement in the fault has begun the static friction changes to dynamic friction with a consequent fall in magnitude since the coefficient of dynamic friction is lower than that of static friction. The movement continues until a state of equilibrium has been reached between the residual forces of displacement and the product of the normal force and the coefficient of dynamic friction. *As soon as earth movement has stopped the dynamic friction changes again to the appreciably greater static friction*, after which the forces of displacement must increase considerably before there is any new risk of movement in the fault — that is to say, before another earthquake occours.

If, in the bed rock near a fault, *the absolute values of the stresses are followed over a period, it should evidently be possible to determine when there is a great risk of an earthquake* — that is to say, when the increase in stress has become such that a release movement in the fissure zone can be expected. This assumes, however, that the value of the coefficient of friction has been found by measuring the stress conditions immediately before the occasion of an earlier movement in the fault.

By measuring the absolute magnitude and the direction of the stresses also at a distance from the fault, it should be possible to determine the areas in which the stresses are increasing and those in which there are no stresses and where there is consequently less likelihood of earthquakes.

SUMMARY

The importance of being able to determine the absolute value of the rock pressure must be evident to all concerned with mining. If the absolute stress and its distribution in the virgin rock around the ore were known, these factors could be taken into account when deciding on the working methods and the procedure to be followed in the mining. Changes in stress distribution in the pillars or in the walls and roof of the drifts during the course of the mining operations could also be followed. From the absolute stresses it would be possible, moreover, to judge whether the limiting load on a pillar is being approached.

Application of the method described in the paper for obtaining absolute stress values has led to the discovery of hitherto unsuspected horizontal stresses, the magnitude of which far exceeds the vertical load at the same points. In cases where the ore lenses are of considerable length the stability of the whole mine opening might be prejudiced by these horizontal stresses, and at very deep levels a knowledge of the absolute value and the direction of the horizontal rock pressure is essential for the extension of the mining to still greater depths.

In the measuring method described in this paper a hole 26 mm in diameter is drilled straight into the rock — a wall or a roof of a drift, for instance — through and beyond the point where the stress is to be ascertained. Into this hole is inserted a cell by means of which the stress is to be measured. This cell is brought into contact with diametrically opposite points of the drill hole surface and is pre-stressed to a desired value by a special procedure. In the case where the absolute value of the stress is required, a continuous annular channel is cut in the rock co-axially with the hole containing the cell, so that a rock cylinder is formed, this normally having a diameter of 87 mm. When the channel has been cut a few centimetres beyond the cell, any stresses in the cylinder will be released, as a result of which its diameter will increase or decrease, according to whether the stresses are compressive or tensile; there will then be a corresponding change in the stress in the cell.

By the aid of a calibration curve for the cell the absolute stress at the point in question can be derived from the recorded values. The stress value so obtained will apply to that particular direction in which the cell is oriented. From readings taken with the cell in three directions in the plane perpendicular to the axis of the drill hole, the principal stresses in this plane can be computed from given formulae.

The laboratory experiments relating to the measuring technique were finished in 1951, the method first being applied in the iron mines of Trafik AB

Grängesberg—Oxelösund at Grängesberg, and later on in the lead mines of Bolidens Gruvaktiebolag at Laisvall.

In the Laisvall mine the underground working level is at a depth of 100 metres and consists of a wide room about 10 metres in height. The rock pillars are about 7 metres in diameter and are spaced about 20 metres apart. The stresses in the pillars have been measured in the vertical and horizontal directions. Moreover, it was found that their load-bearing capacity diminishes with age. Measurements have also shown how the load bearing capacity is influenced by the presence of fissures and cracks.

Another problem that has been studied is whether a narrow pillar can be relieved of any of its load by one or more wider adjacent pillars. Calculations have shown that any such distribution that may occur is negligible.

The horizontal stresses in the plane sandstone roof between the pillars in the Laisvall mine were measured near the surface and at depths of up to two metres. The existence of a horizontal stress system extending over the whole mine was established from measurements performed in the roof, floor and large pillars, the maximum value of this stress being almost in an N—S direction and coinciding with the main direction of fissuring in the mine.

In Grängesberg the rock pressure has been measured at many points in the roof and walls of drifts. Most of the measuring points were located in or near vertical cross-sections through the mine at the Central Shaft and the Jacobina Shaft, and were within the ore lens as well as in the foot wall. It was ascertained that the highest stresses in the mine are horizontal. However, in the upper part of the ore lens — that is to say, inside or near the working zone — the stresses are generally small, the natural high horizontal stresses concentrated at this point having compressed the ore at this level until it was crushed. Less than 50 metres below this, the stresses increase to a maximum value. At greater depth, there is first a decrease and then a steady rise.

The measurements have revealed the regions in the foot wall where the stresses have the greatest influence on its stability. Some calculations are included that show the probable origin of the stress concentrations in the ore lens.

During 1957 measurements of the stress conditions were performed in the Malmberget mines. An orebody 800 metres in length and 20—40 metres wide was mined out to a depth of about 250 metres below ground level. To protect an inclined shaft located in the foot wall a 50-metre stretch of the orebody was left. This part, which remains as a pillar between the foot and hanging walls, transmits very high horizontal forces, which constitute a complicating factor in the stabilization of the foot wall and its shaft. It was necessary to determine the stress in the pillar and neighbouring parts of the foot wall to see whether it might be possible to remove the pillar for its valuable ore without risk of the foot wall caving.

The fifth part of the book deals with the stress conditions in block caving. An indication of whether block caving is a suitable method for a particular mine or part of a mine would seem to be given by rock pressure measure-

ments. These may also be used to estimate the appropriate size of the blocks to ensure a short maturing period and efficient disintegration of the ore. A fall of too large pieces of ore immediately after undercutting may be due to an unsuitable shape of the under-cut zone. Stress measurements performed in 1958 in the mines of Ställberg revealed horizontal stresses of 550 kg/sq.cm acting in the virgin rock at a depth of 915 metres and concentrations of stresses in the working zone $>$ 1250 kg/sq.cm, as high as the breaking strength of the ore or about 2000 kg/sq.cm.

Part VI is devoted to a survey of the horizontal rock pressure determined at six mines in Scandinavia. There would seem to be some connection between the origin of the horizontal rock pressure and the secular movements in this area. Earthquakes may well be manifestations of the local release of cumulative stresses set up in the earth's crust over long periods by such secular movements. In certain areas where earthquakes use to recur along the same line of rupture in the earth's crust the accumulation of stresses along such a fault may be followed by periodic measurement of the rock pressure. By this means it should be possible to ascertain when there is a serious risk of an earthquake.

Sveriges Geologiska Undersöknings senast utkomna publikationer äro:

Ser. Aa Geologiska kartblad i skalan 1:50 000 med beskrivningar.

Priset för karta i Ser. Aa med beskrivning är 10:— kr, för karta enbart 8:— kr.
(Price: map sheet + descriptive text Sw. cr. 10:—, map sheet Sw. cr. 8:—)

N:o 197 *Laholm* av W. Larsson och C. Caldenius T. v. utan beskrivning
» 198 *Halmstad* av W. Larsson och C. Caldenius » » »
» 199 *Uppsala* av P. H. Lundegårdh och G. Lundqvist. With English summaries. 1956

Ser. Ad. Agrogeologiska kartblad i skalan 1:20 000 med beskrivningar

Priset för karta i Ser. Ad med beskrivning är 8:— kr, för karta enbart 6:— kr.
(Price: map sheet + descriptive text Sw. cr. 8:—, map sheet Sw. cr. 6:—)

N:o 1 *Hardeberga* av G. Ekström. 1947, karta med beskrivning
» 2 *Lund* » » 1953, » » »
» 3 *Revinge* » » » t. v. utan beskrivning
» 4 *Löberöd* » » » t. v. » »
» 5 *Örtofta* » » » t. v. » »
» 6 *Kävlinge* » » 1955 t. v. » »
» 7 *Teckomatorp* » » 1955 t. v. » »
» 8 *Trollenäs* » » 1955 t. v. » »
» 9 *Bosjökloster* » » 1956 t. v. » »

Årsbok 51 (1957)

N:o 550 Lundqvist, J., Övre Klarälvsdalens kvartärgeologi. — With English summary. Med 3 planscher. 1957 5,00
» 551 Lundqvist, J. Geokronologiska undersökningar i Värmland. Med en plansch. — With English summary. 1957 2,50
» 552 Sund, R. B., Nyare undersökningar inom nordöstra Upplands berggrund. — With English abstract. Med en plansch. 1957 3,00
» 553 Lundegårdh, P. H., Göteborgstraktens berggrund. Med en plansch.— English summary: Petrology of the Göteborg (Gothenburg) — Kungälv region, Western Sweden. 1958 7,50
» 554 Lundqvist, J., C^{14}-dateringar av rekurrensytor i Värmland. — English summary: C^{14}-determinations of recurrence surfaces in Värmland, Western Sweden. 1957 2,00
» 555 Åhman, E., Degerberget, Baggen och Kluntarna. Några drag ur Piteområdets berggrundsgeologi. —With English abstract. 1957. 2,50
» 556 Assarsson, G., Kristallisationserscheinungen und Paragenese in den Systemen der Alkalichloride — Erdalkalichloride — Wasser. 1957 2,00
» 557 Lundqvist, G., C^{14}-analyser i svensk kvartärgeologi. — With English summary. 1957 2,00

Årsbok 52 (1958)

N:o 558 Stålhös, G., Rackebymassivet; ett västsvenskt norit-gabbromassiv. — English summary: The Rackeby norite-gabbro massif; W. Sweden. - 1958 4,00
» 559 Lundqvist, J., Studies of the Quaternary history and deposits of Värmland, Sweden. Experiences made while preparing a survey map. 1958 . . . 6,00
» 560 Hast, N., The measurement of rock pressure in mines. 1958 15,00

Forts. å omslagets 4: de sida

N:o 561 LUNDQVIST, G., Kvartärgeologisk forskning i Sverige under ett sekel. 1958. . 4,00

» 562 SAHLSTRÖM, K. E. och BÅTH, M., Jordskalv i Sverige 1951 — 1957. Zusammenfassung: Erbeben in Schweden 1951 — 1957. — 1958 1,50

Årsbok 53 (1959)

N:o 563 SANDEGREN, R., Register över Sveriges geologiska undersöknings publikationer 1858—1957. - Under tryckning. (In preparation).

» 564 OFFERBERG, J. Rocks and stratigraphy of the Ledfat area. - Under tryckning. (In preparation).

» 565 LUNDQVIST, G., C^{14}-daterade tallstubbar i fjällen. - Under tryckning. (In preparation).

Ser. Ba.

N:o 14 Jordartskarta över södra och mellersta Sverige. Efter de geologiska kartbladen sammandragen vid S. G. U. av K. E. SAHLSTRÖM. Skala 1:400000
Mellersta bladet, tryckt 1947 15,00
Södra bladet, tryckt 1948 15,00
Norra bladet, tryckt 1949 15,00

» 15 Beskrivning till Jordartskarta över Uppsalatrakten (Quaternary deposits in the Uppsala region.) Av B. JÄRNEFORS. 1958 5,00
Jordartskarta över Uppsalatrakten. Av N. G. HÖRNER och B. JÄRNEFORS. Berggrunden sammanställd av P. H. LUNDEGÅRDH.—1956 8,00

» 16 Karta över Sveriges berggrund. (Pre-Quaternary rocks of Sweden). Skala 1:1 milj. Sammanställd av N. H. MAGNUSSON m. fl. 1958. Karta i tre blad; pris per blad 15,00

» 17 Karta över Sveriges jordarter. (Quaternary deposits of Sweden). Skala 1:1 milj. Sammanställd av G. LUNDQVIST m. fl. 1958. Karta i tre blad; pris per blad 15,00
Beskrivning till Jordartskarta över Sverige. Av G. LUNDQVIST. 1958. . . . 5,00

Ser. Ca.

» 37 GAVELIN, S. och KULLING, O., Beskrivning till berggrundskarta över Västerbottens län. (Description to Map of the Pre-Quaternary rocks of the Västerbotten County, N. Sweden.) Karta i skala 1:400000. — With English summary. 1955. Beskrivning med karta 45,00
Karta 18,00

» 38 LUNDQVIST, J., Beskrivning till jordartskarta över Värmlands län. (Quaternary deposits of the County of Värmland.) Karta i skala 1:200000. 1958.
Beskrivning med karta 65,00
Karta, i två blad 30,00

» 41 ÖDMAN, O. H., Beskrivning till berggrundskarta över urberget i Norrbottens län. English summary: Description to Map of the Pre-Cambrian rocks of the Norrbotten County, N. Sweden, excl. the Caledonian mountain range. Karta i skala 1:400000. 1957. Beskrivning med karta 45,00
Karta, i två blad 20,00

Distribueras genom

Generalstabens Litografiska Anstalts Förlag, Drottninggatan 20, Stockholm 16

STOCKHOLM 1959. KUNGL. BOKTRYCKERIET P. A. NORSTEDT & SÖNER PRINTED IN SWEDEN